Title
Design of regenerative stormwater biofilters for long term removal of legacy and emerging pollutants

Author
Borthakur, Annesh

Publication Date
2022

Peer reviewed|Thesis/dissertation

UNIVERSITY OF CALIFORNIA

Los Angeles

Design of regenerative stormwater biofilters for long term removal of legacy and emerging pollutants

A dissertation submitted in partial satisfaction of the requirements for the degree of Doctor of Philosophy in Civil Engineering

by

Annesh Borthakur

2022

ABSTRACT OF THE DISSERTATION

Design of regenerative stormwater biofilters

for long term removal of legacy and emerging pollutants

by

Annesh Borthakur

Doctor of Philosophy in Civil Engineering

University of California, Los Angeles, 2022

Professor Sanjay K. Mohanty, Chair

Stormwater biofilters are low-impact development systems that are typically designed to quickly remove stormwater from surfaces for flood control with limited capacity to remove dissolved pollutants. Although certain amendments such as biochar, iron filings, and compost are added to biofilters to increase removal of pollutants, their pollutant removal capacity is unreliable due to various reasons including variable removal capacity of adsorbent media, exhaustion of adsorption sites, and environmental conditions. Adsorbed pollutants accumulate in the biofilter media and reduce the further removal of pollutants in stormwater. Replacement of exhausted biofilter media is cost-prohibitive. An alternate strategy is in-situ regeneration of the biofilters as a non-intrusive method to replenish exhausted biofilter media. This dissertation aims to improve the understanding of the fate and transport of emerging pollutants such as perfluoroalkyl substances (PFAS) and legacy pollutants such as heavy metals and pathogens in subsurface

systems and use the improved understanding to develop methods to artificially or naturally regenerate the pollutant removal capacity of filter media to limit their exhaustion rate in stormwater biofilters.

The dissertation consists of 5 research chapters. Chapter 2 critically examines the PFAS concentrations in suspended particles or colloids in the environment and shows that the suspended particles can adsorb and transport significant amounts of PFAS in surface water, subsurface soil, and even air. Chapter 3 proves that the fluctuations in groundwater flow can release colloids from PFAS-contaminated aquifer soil, which can carry PFAS. Therefore, removing soil colloids from groundwater samples through filtration or centrifugation can underestimate the PFAS concentration in groundwater. Chapter 4 examines the role of weathering cycles in the transport of PFAS in the subsurface and shows that dry-wet and freeze-thaw cycles can increase the release of colloids and associated PFAS from the subsurface into the groundwater. Chapter 5 demonstrates that in-situ injection of cationic polymers could regenerate exhausted biofilter media and improve their ability to remove PFAS from stormwater without clogging the biofilter. Chapter 6 offers a more natural method for regenerating the pathogen removal capacity of biofilters by utilizing the inherent toxicity of heavy metals to pathogens. Overall, the dissertation improves the understanding of the interactions between pollutants, microorganisms, and natural colloids in the solid-liquid interfaces and the effect of environmental conditions on these interactions in subsurface systems such as stormwater biofilters. The knowledge is useful to design biofilters, which are more efficient in removing legacy and emerging pollutants.

The dissertation of Annesh Borthakur is approved.

Shaily Mahendra

Eric M. V. Hoek

Richard F. Ambrose

Sanjay K. Mohanty, Committee Chair

University of California, Los Angeles

2022

Dedication

I would like to dedicate my dissertation to my mother, who fully dedicated her whole life for me. Without her love, her values, her reproach, and, most of all, her sacrifices, I would never have been the person that I am today. All my success and my growth are all dedicated to her and I hope I made you proud today মা |

I would also like to dedicate my dissertation to the state of Assam. I decided to pursue a career in environmental engineering to help the people of Assam and this dissertation is the first step in fulfilling my promise to my motherland. জয় আই অসম |

Table of Contents

List of Figures

List of Tables

Acknowledgments

Firstly, I would like to thank my advisor, Professor Sanjay Mohanty. As someone who really cares about his mentees and is willing to put their needs over his own, he is the best advisor I could ask for as a Ph.D. student. I am very fortunate that I could grow under his care into the researcher that I am today and I hope that I can work with him in the future as colleagues as well.

I would also like to thank my esteemed committee members, Professors Shaily Mahendra, Eric Hoek, and Richard Ambrose. Thank you so much for your guidance and all your help throughout my Ph.D. journey. It was a great learning experience and I will remember it throughout my life.

I would also like to thank the staff in the Department of Civil and Environmental Engineering Department, especially Vanessa Thulsiraj and Mimi Baik, for all their help and support all these 4 years. You are the unsung heroes that help keep the department functioning well and I am eternally indebted to you.

I would also like to thank the Expanded Shale, Clay and Slate Institute, United Contractors and the Environmental Research & Education Foundation for understanding the value of my research and supporting me. Your support ensured that I did not encounter any financial hardships and could concentrate on my research.

I would also like to thank all the members of the SEALab. It was a really fun experience working with you and I will treasure it throughout my life. I will really miss this lab after I leave. We are truly the best lab group in the world.

I would like to thank the undergraduate and graduate students that helped me throughout my research: Meng He, Patience Olsen, Katia Ascencio, Kristida Chhour, Hannah Gayle, Samantha Prehn, Yuhui Zhang, Silvi Libbert and Emma Golub. Without your help, I would not

have been able to complete my research and I deeply thank you for the long hours you spent at the lab for my sake.

I would also like to thank the amazing friends I made in UCLA: Jamie Leonard, Vera Smirnova Koutnik, Tonoy Das, and Huong Le. You brought the “life” into my Ph.D. life. We worked together, laughed together, had fun together but most of all, supported each other throughout this journey and I am so happy that I came across you guys.

Finally, I would like to thank my family for all their love, affection, and their support for me: My mother, Ajanta Borthakur, my father, Nilim Kumar Borthakur, and my sister, Dr. Pratyasha Borthakur. As the first person in my family to come to the US for higher studies, it was a scary experience trying fit in a completely new country. However, you were always there for me especially when I was at the lowest point of my life. You taught me that everything gets better, I just can’t lose hope. মা- দেউতা, you now have two doctors in the family!

VITA

EDUCATION

2018 M.S. in Civil and Environmental Engineering, University of California, Los Angeles

2016 B.E. in Civil and Environmental Engineering, BITS Pilani, India

AWARDS

2021 Environmental Research Education Foundation Scholarship Award

2021 United Contractors Scholarship Award

2019 John Reis Scholarship, Expanded Shale, Clay, and Slate Institute

PUBLICATIONS

Borthakur, A., Chhour, K., Gayle, H., Prehn, S., Stenstrom, M.K., and Mohanty, S.K. (2022) Natural aging of expanded shale, clay, and slate (ESCS) amendment with heavy metals in stormwater increases its antibacterial properties: Implications on biofilter design. Journal of Hazardous Materials. 128309. https://doi.org/10.1016/j.jhazmat.2022.128309.

Koutnik, V.S., **Borthakur, A.**, Leonard, J., Alkidim, S., Koydemir, H.C., Tseng, D., Ozcan, A., and Mohanty, S.K. (2022) Mobility of polypropylene microplastics in stormwater biofilters under freeze-thaw cycles. Journal of Hazardous Materials Letters. 100048. https://doi.org/10.1016/j.hazl.2022.100048.

Ramos, P., Kalra, S.S, Johnson, N.W., Khor, C.M, **Borthakur, A.**, Cranmer,B., Dooley, G., Mohanty, S.K., Jassby, D., Blotevogel, J., Mahendra, S. (2022) Enhanced Removal of Per- and Polyfluoroalkyl Substances in Complex Matrices by polyDADMAC-Coated Regenerable Granular Activated Carbon Environmental Pollution. 118603. https://doi.org/10.1016/j.envpol.2021.118603.

Borthakur, A., Leonard, J., Koutnik. V.S., Ravi, S., and Mohanty, S.K. (2022) Inhalation risks from wind-blown dust in biosolid-applied agricultural lands: Are they enriched with microplastics and PFAS? Current Opinion in Environmental Science & Health. 100309. https://doi.org/10.1016/j.coesh.2021.100309.

Borthakur, A., Olsen, P., Dooley, G., Cranmer, B.K., Rao, U., Hoek, E.M.V., Blotevogel, J., Mahendra, S., and Mohanty, S.K. (2021) Dry-wet and freeze thaw cycles enhance PFOA leaching

from subsurface soils. Journal of Hazardous Materials Letters. 2. 100029. https://doi.org/10.1016/j.hazl.2021.100029.

Borthakur, A., Wang, M., He, M., Ascensio, K., Adamson, D., and Blotevogel, J., Mahendra, S., and Mohanty, S.K. (2021) Perfluoroalkyl acids on suspended particles: Unexplored transport pathways in surface water and subsurface soils. Journal of Hazardous Materials. 417. 126159. https://doi.org/10.1016/j.jhazmat.2021.126159.

Borthakur, A., Cranmer, B.K., Dooley, G., Blotevogel, J., Mahendra, S., and Mohanty, S.K. (2021) Release of soil colloids during flow interruption increases the pore-water PFAS concentration in saturated soil. Environmental Pollution. 286, 117297. https://doi.org/10.1016/j.envpol.2021.117297.

Dubey, A.A., **Borthakur, A.**, and ∗Ravi, K. (2021) Investigation of Soil Suction Characteristics Induced by the Degradation of Organic Matter Geotechnical and Geological Engineering.1-8. https://doi.org/10.1007/s10706-021-01986-7.

Ghavanloughajar, M., **Borthakur, A.**, Valenca, R., McAdam, M., Khor, C., Dittrich, T.M., Stenstrom, M., and ∗Mohanty, S.K. (2021) Iron amendment minimizes the first-flush release of pathogens from stormwater biofilters. Environmental Pollution. 116989. https://doi.org/10.1016/j.envpol.2021.116989.

Alam, S., **Borthakur, A.**, Ravi, S., Gebremichael, M., and Mohanty, S.K. (2021) Managed aquifer recharge implementation criteria to achieve water sustainability Science of the Total Environment. 768, 144992. https://doi.org/10.1016/j.scitotenv.2021.144992.

Valenca, R., **Borthakur, A.**, Zu, Y., Stenstrom, M. K., and Mohanty, S.K. (2021) Biochar selection for Escherichia coli removal in stormwater biofilters. Journal of Environmental Engineering. https://doi.org/10.1061/(ASCE)EE.1943-7870.0001843.

Ghavanloughajar, M., Le, H., Rahman, M.D., Valenca, R., **Borthakur, A.**, Ravi, S., Stenstrom, M., and Mohanty, S.K. (2020) Compaction conditions affect the capacity of biochar-amended sand filters to treat road runoff. Science of the Total Environment. 735, 139180. https://doi.org/10.1016/j.scitotenv.2020.139180.

Dubey, A.A., Ravi, K., Devrani, R., Rathore, S., and **Borthakur, A.** (2020) Characterization of Steel Slag as Geo-material, in: Latha Gali, M., P., R.R. (Eds.), Geotechnical Characterization and Modelling, Lecture Notes in Civil Engineering. Springer, Singapore,. 113–122.

1. CHAPTER 1: REGENERATIVE STORMWATER TREATMENT SYSTEMS – CHALLENGES AND RESEARCH NEEDS

1.1. Background

1.1.1. Stormwater and urban water sustainability

Water scarcity is one of the biggest challenges of this century (Liu et al., 2017). Nearly one-fifth of the world's population lives in water-stressed areas, and one-fourth of the world's population faces water shortages at least one month out of a year (Ma et al., 2020; Saha and Ray, 2019). Although there is a sufficient amount of fresh water on Earth, it is not frequently available where it is needed the most, in urban areas (McDonald et al., 2014). Urban areas are currently home to more than half of the world's population and are projected to increase to 70% by 2050 (Ejaz and Anpalagan, 2019). This growth indicates that the water scarcity issue in urban areas will almost certainly get worse unless alternative water resources such as stormwater are utilized (Oppenheimer et al., 2017). However, stormwater often contains many contaminants including pathogens, heavy metals, motor oils, nutrients, pesticides, herbicides, polyaromatic hydrocarbons (PAHs), and polychlorinated biphenyls (PCBs), and other emerging contaminants including antibiotics resistance genes and bacteria (Grebel et al., 2013). As these contaminants are typically originated from non-point sources in urban areas, treatment at the source by low-impact development systems is generally more cost-effective than the use of traditional wastewater treatment systems. An efficient and durable stormwater treatment system can transform stormwater, a traditional waste, into an alternative water resource in urban areas, while providing other ecosystem functions as well as social benefits of green space in urban areas.

1.1.2. Contaminant removal processes in stormwater biofilters

Stormwater treatment systems (also known as Best Management Practices or BMPs) are typically designed to quickly remove stormwater from surfaces for flood control, but they are often inadequate to remove many emerging contaminants, such as PFASs (Grebel et al., 2013; LeFevre et al., 2015). Among different types of BMPs, biofilters have the lowest footprint (Karakurt-Fischer et al., 2020). Biofilters are typically designed by replacing native soil with a mixture of sand, soil, and compost, where plants are grown (Figure 1-1). This compact design allows rapid infiltration of stormwater into the ground or the stormwater drain. Thus, biofilters can be retrofitted at many urban sites, particularly where allocating space for stormwater treatment is challenging. Conventional biofilter media has limited contaminant removal capacity. However, previous studies showed that adsorbents such as biochars and iron fillings could increase the attachment of contaminants (Ochoa-Herrera and Sierra-Alvarez, 2008; Ulrich et al., 2015), promote biodegradation by supporting bacterial and fungal biofilms (Lee et al., 2010), and help the biofilter media remain saturated so that remobilization of particulate-associated contaminants is minimal (Mohanty and Boehm, 2015). Furthermore, by controlling the position of stormwater drain valves (or saturated layer), the biofilters can be redesigned to promote reducing conditions in the bottom layers (Rippy, 2015). Saturated conditions allow greater diffusion of oxygen in pore water and increasing depletion of oxygen by biotic processes. Specific redox conditions can also be achieved abiotically by applying a small amount of current via electrodes. These designs could enhance the removal of various contaminants whose removal is sensitive to pH and redox conditions (Ololade et al., 2016).

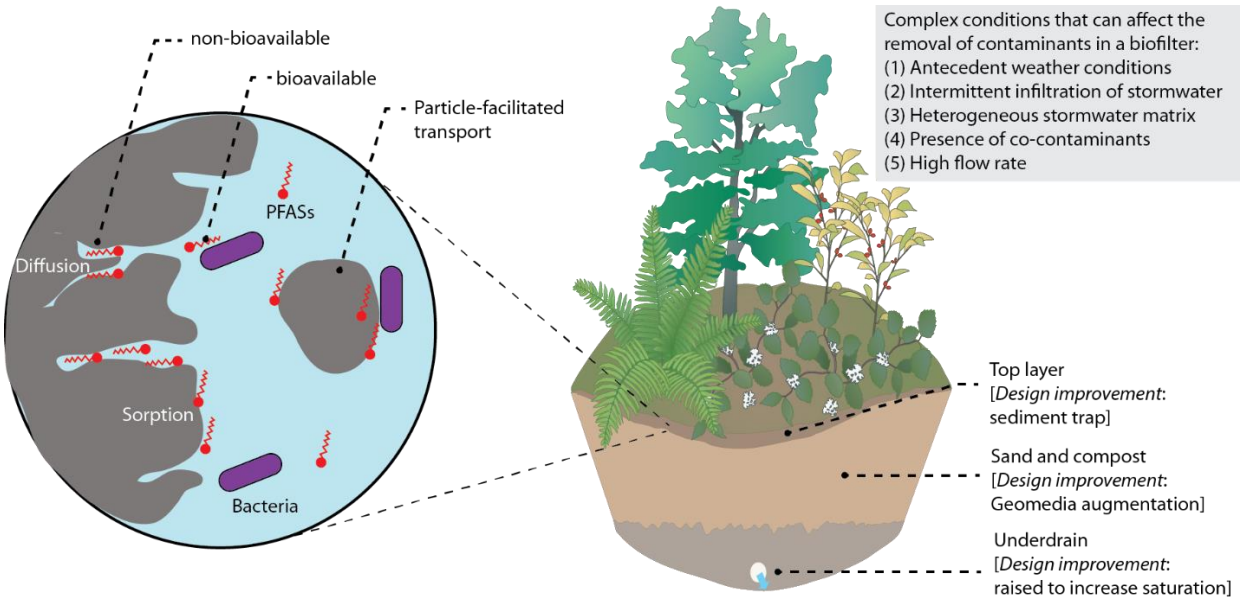

Figure 1-1: Design of typical biofilter where native soil is replaced with a mixture of sand and compost (with plants grown atop) for rapid infiltration of stormwater. Some contaminants are removed due to physiochemical filtration, sorption, and biotransformation during intermittent infiltration of contaminated stormwater. The removal capacity of biofilters can be improved by adding adsorbents.

1.1.3. Limited and unreliable pollutant removal capacity

Traditional biofilter media such as sand have a low pollutant removal capacity. To increase the capacity, biofilters can be augmented with adsorbents and redesigned for specific hydraulic and geochemical control (Grebel et al., 2013). Although many adsorbents have been demonstrated to remove contaminants from drinking water (Merino et al., 2016), most of them are not suitable for stormwater treatment because of the cost, effect on clogging (or low hydraulic conductivity), and their ineffectiveness in the presence of a high concentration of DOC, particulates, and co-contaminants (Grebel et al., 2013). Although certain adsorbents such as biochar, iron filings, and compost remove pollutants from stormwater, their ability to remove pollutants is unreliable due to various reasons. Firstly, the pollutant removal capacity of the adsorbents is highly variable depending on the production methods and the presence of other adsorbents widely (Ghavanloughajar et al., 2021; Valenca et al., 2021). Moreover, even the adsorbents, which can

remove large amounts of pollutants, lose their pollutant removal capacity with time due to exhaustion of adsorption sites. Recalcitrant pollutants such as perfluoroalkyl substances (PFAS) accumulate in the biofilter media and prevent further adsorption of pollutants from stormwater. Moreover, adsorbed pathogens can grow in the biofilter media and further accelerate this exhaustion of adsorption sites (Borthakur et al., 2022). This is exacerbated by competition from other constituents of stormwater. Stormwater matrix is complex due to the presence of a high concentration of particulate matter or suspended solids, DOC, dissolved salts, nutrients, and other co-contaminants (Grebel et al., 2013). The presence of these co-contaminants in water can decrease the adsorption of organic pollutants to soil or sorbent due to competition for attachment sites (Wang et al., 2015; Yu et al., 2012). Since hydrophobic interactions are sensitive to organic carbon, the presence of DOC and hydrophobic co-contaminants are expected to compete with organic pollutants such as PFAS for attachment sites and decrease their retention. Thus, it is critical to design stormwater BMP where the adsorption capacity can be regenerated in situ.

The exhaustion rate of filter media depends on contaminant removal processes in the stormwater biofilter. Contaminant removal in unsaturated stormwater biofilters is complex due to the presence of air and variation in typical weather conditions such as wetting, drying, and freeze-thaw cycles. The complex hydrological and geochemical conditions that a stormwater treatment system experiences in nature could affect the removal of contaminants from stormwater. The advancement of the wetting front during intermittent flow increases the release of fine particles and mobilizes particle-associated contaminants (Mohanty et al., 2015a). The amount of particles released due to this process depends on antecedent weather conditions such as drying duration and freeze-thaw cycles (Mohanty et al., 2015a, 2015b, 2014, 2013). The same processes could also affect the release of contaminants, particularly those that exhibit a high affinity toward soil

particles (Ryan and Elimelech, 1996; Xing et al., 2016). Furthermore, the presence of air or air-water interfaces in subsurface soil could affect the removal and transport of contaminants. Air-water interface is hydrophobic; thus, it can affect the distribution of hydrophobic contaminants in soil pores during wetting and drying events, and consequently affect the removal and transport of pollutants in subsurface soil. Thus, the variable removal capacity of adsorbent media, exhaustion of adsorption sites, and environmental conditions reduce the reliability of stormwater biofilters.

1.1.4. Regeneration of stormwater biofilters

Exhaustion of biofilter media is one of the major reasons for biofilter's unreliable performance. Adsorbed pollutants accumulate in the biofilter media and reduce the further removal of pollutants in stormwater. Although the biofilter microbiome can replenish some adsorption sites by degrading the pollutants, this process is very slow and impractical for stormwater treatment applications, especially in regions of heavy precipitation. Moreover, certain emerging pollutants such as PFAS are recalcitrant. Therefore, these recalcitrant pollutants could accumulate in the biofilter media and exhaust the adsorption sites. Once exhausted, biofilter media needs to be replaced, an operation that is expensive. An alternate strategy is in-situ regeneration of the biofilters as a non-intrusive method to replenish exhausted biofilter media. Chemicals can be injected into the biofilters that can regenerate or even improve the pollutant removal capacity of the biofilter media. For instance, a previous study showed that injecting HOCl into manganese oxide-coated sand amended biofilters and replenished their ability to remove organic pollutants similar to the virgin geomedia (Charbonnet et al., 2018). Another method will be to inject polymers such as Polydiallyldimethylammonium chloride (PDADMAC) into the biofilters. These injected polymers can coat the biofilter media and replenish or even increase the pollutant removal capacity of the biofilter. Coating PDADMAC onto geomedia significantly improves their ability to remove

legacy and emerging pollutants such as heavy metals, PFAS, and pesticides from stormwater (Ray et al., 2019), indicating their potential on enhancing the ability of biofilter media to remove pollutants from stormwater. However, the in-situ injection of the polymers into biofilters to regenerate their pollutant removal capacity has not been investigated.

1.2. Research gaps

1.2.1. Analysis of particle role in the transport of PFAS through surface water and air

Advection of dissolved perfluoroalkyl acids (PFAAs) is currently assumed to be the dominant mechanism of transport in surface waters and subsurface (Dauchy et al., 2019b, 2019a; Xiao et al., 2012), whereas sorption to soil or sediment is considered the primary retention mechanism. Surface runoff also often contains high concentrations of suspended particles, which are generated by the erosion of the soil surface or resuspension of sediments (Hatfield and Maher, 2009; Jia et al., 2014). These particles can bind PFAAs and carry them to surface and subsurface environments (Ahrens et al., 2010a; Llorca et al., 2018; T. V. Nguyen et al., 2016). If the suspended particles originated from the erosion of impacted lands, they may contain much higher concentrations of PFAAs than explained based on the equilibrium adsorption (Y. Q. Liu et al., 2019; Xiao et al., 2012). These particles can be mixed with suspended particles created in streams and rivers due to the turbulence of fast-moving water (Chanson et al., 2011). In addition, dust particles in the air can contain significant concentrations of PFAAs as well. However, the relative contribution of these particles to the transport of PFAA in the environment has not been adequately explored, although their role in enhancing the transport of other organic chemicals such as polycyclic aromatic hydrocarbons (Guo et al., 2007), chlorinated solvents (Tanabe and Tatsukawa, 1983), and heavy metals (Zhang, 1999) has been well established. Although some of the legacy pollutants are more hydrophobic than PFAS, thereby increasing their association with suspended

particles, the advisory limit for PFAS in water is low parts per trillion, which is an order of magnitude lower than the limit for the legacy pollutants. Thus, a relatively low concentration of PFAS on particles can lead to an exceedance of the water quality criteria. In general, it is expected that PFAAs with a long carbon chain could bind strongly to soil (Higgins and Luthy, 2006a; Yanju Liu et al., 2020; Nguyen et al., 2020) due to an increase in hydrophobicity. However, the relevance of suspended particles on PFAA distribution in the environment has not been critically analyzed.

1.2.2. Colloid facilitated transport of PFAS due to fluctuations in groundwater flow

Nearly 72% of PFAS contaminated drinking water facilities use groundwater as the water source, indicating that groundwater is a major source of PFAS contaminated drinking water (Guelfo & Adamson, 2018). Groundwater gets contaminated when surface runoff from PFAS contamination sources infiltrates into the subsurface to the groundwater. Upon mixing with the groundwater, PFAS is transported through the aquifer PFAS moves through the porous media by advection, dispersion, or diffusion (Armitage et al., 2009; Brusseau et al., 2019; Wang et al., 2005). During transport, PFAS can adsorb onto solids such as soil, sediments, or carbonaceous matter such as activated carbon (Campos-Pereira et al., 2020; Higgins and Luthy, 2006b; Johnson et al., 2007; Mejia-Avendaño et al., 2020; Xiao et al., 2017) by hydrophobic or electrostatic interactions due to their surfactant nature (Pereira et al., 2018; Zhang et al., 2014). However, flow rates in porous media can fluctuate for various practical and natural reasons. The flow of groundwater through soil can fluctuate depending on the precipitation rate, hydraulic gradient, hydraulic conductivity, and human, plant, and animal activities (Beretta and Terrenghi, 2017; Gribovszki et al., 2010; Suzuki and Higashi, 2001). Flow may be paused for several days during the operation of groundwater extraction or treatment through pack-bed reactors. Changes in flow rate or flow

interruption may affect the available time for sorption or diffusive transport to occur in the porous media (Gellrich et al., 2012a; Høisæter et al., 2019).

Flow fluctuations or interruptions can also release natural soil colloids from porous media (Gao et al., 2004; Schelde et al., 2002a; Zhou et al., 2017), which may contain previously adsorbed pollutants (Zhu et al., 2013). Natural soil colloids have been shown to facilitate the transport of other hydrophobic pollutants (Ryan and Elimelech, 1996; Xing et al., 2016). The same process may occur for PFAS. Colloids were found to carry a significant amount of PFAS in surface waters (Ahrens et al., 2010b; Y. Liu et al., 2019; Tung V. Nguyen et al., 2016; Zhao et al., 2016), indicating they could do the same in groundwater aquifer. Suspended sediment-associated PFAS can exacerbate their toxicity in surface water organisms as well (Yan Liu et al., 2020). However, studies on the transport of PFAS typically estimate the dissolved PFAS (Seo et al., 2019), assuming the concentration of PFAS associated with colloids is insignificant. Groundwater samples are typically filtered or centrifuged to remove all colloids before analyzing for PFAS. This can also underestimate the total PFAS concentration in water samples if colloids are present and they carry a significant amount of PFAS. Future studies should examine the role of colloids in PFAS concentration in pore water after flow interruption.

1.2.3. The effect of dry-wet and freeze-thaw cycles on the colloid-facilitated transport of PFAS

Surface runoff carries poly- and perfluoroalkyl substances (PFAS) from PFAS-impacted areas such as firefighting training facilities (Baduel et al., 2015), wastewater biosolids (Washington et al., 2010), and waste piles with PFAS-containing products (Laitinen et al., 2014; Trudel et al., 2008). The runoff exports PFAS to surface waters and infiltrates through subsurface soils to groundwater aquifer. During the infiltration of the PFAS-impacted runoff, short-chained PFAS can move through the subsurface because of limited adsorption on soil whereas most of the

long-chained PFAS can be removed by adsorption to soil and air-water interfaces (Brusseau, 2018; Qian et al., 2017; Zhang et al., 2014b). However, under certain conditions, the previously removed PFAS can leach into groundwater from impacted subsurface soil (Gellrich et al., 2012b). PFAS can be desorbed from impacted subsurface soils by physical, chemical, and biological processes. Previously sorbed PFAS can desorb from soil (Milinovic et al., 2015; Xiao et al., 2019) based on environmental conditions such as pH, ionic strength, and dissolved organic carbon in pore water (Jeon et al., 2011; Pereira et al., 2018; Wang et al., 2012). Furthermore, the transformation of precursors can enhance PFAS leaching (Chen et al., 2020). PFAS trapped in the soil matrix can diffuse into the flow path (Schaefer et al., 2019). Thus, back diffusion during the pause between rainfall events could increase the concentration of PFAS in porewater (Adamson et al., 2020; Brusseau, 2020; Carey et al., 2019; Guo et al., 2020). As air-water interfaces retain a significant amount of PFAS (Brusseau, 2019, 2018; Lyu et al., 2018), the collapse of the air-water interfaces during intermittent infiltration events could also release PFAS. Therefore, the development and collapse of air-water interfaces in the subsurface during intermittent rainfall events (dry-wet cycles) can leach PFAS from the subsurface soil (Gellrich et al., 2012b).

Similar to the desorption of dissolved PFAS, colloid-associated PFAS can be released in the subsurface by three steps: (1) release or mobilization of colloids from macropore flow walls by hydrodynamic fluctuations, or water phase transitions during dry-wet (Majdalani et al., 2007) or freeze-thaw cycles (Mohanty et al., 2014); (2) diffusion of released colloids from pore wall to bulk liquid via a rate-limiting step (Schelde et al., 2002b); (3) transport of colloids in bulk liquid downward via infiltrating water. Colloids have been shown to contain significantly high concentrations of PFAS in surface waters (Ahrens et al., 2010a; Chen et al., 2019; T. V. Nguyen

et al., 2016) and saturated soil (Borthakur et al., 2021a). Yet, no study to date has quantified the colloid-facilitated release of PFAS in impacted subsurface subjected to weathering cycles.

1.2.4. Using cationic polymers to regenerate PFAS removal capacity of biofilters

Infiltration-based treatment systems such as stormwater biofilters can be used to remove PFAS from stormwater (Spahr et al., 2020). However, conventional bio-filter media such as sand and compost have low adsorption capacity for PFAS (Aly et al., 2018; Hale et al., 2017). In this case, the filter media can be amended or replaced with adsorbents such as biochar, activated carbon, or clay that can adsorb PFAS using hydrophobic, electrostatic, or chemisorption interactions (Askeland et al., 2020; Mukhopadhyay et al., 2021; Park et al., 2020). Since biofilter media is mostly negatively charged, hydrophobic interactions are the major force driving the adsorption of PFAS by the media. However, this reduces the capacity of biofilters to adsorb short-chain PFAS compounds. Moreover, due to their recalcitrant nature, adsorbed long-chain PFAS compounds accumulate in the biofilter which exhausts the adsorption sites and reduces further removal of PFAS. Therefore, a method to replenish exhausted PFAS sites in biofilters and also improve their ability to remove short-chain PFAS is required.

To recharge the PFAS removal capacity of biofilters, the surface charge of the filter media can be modified in situ. (Lukasik et al., 1999) The electrostatic interactions between PFAS and oppositely charged media surfaces can increase the adsorption capacity and result in faster adsorption kinetics, thereby potentially improving PFAS removal in high flow conditions.(Li et al., 2014a, 2014b). Coating commonly used PFAS adsorbents with cationic polymers such as polydiallyldimethylammonium chloride (PDADMAC) could improve their PFAS removal capacity (Aly et al., 2019, 2018; Chen Liu et al., 2020; Ramos et al., 2022; Ray et al., 2019). Organic polymers can easily adsorb onto clay (Ray et al., 2019), activated carbon (Chen Liu et al.,

2020; Ramos et al., 2022), and aquifer soil (Aly et al., 2019, 2018) and adsorb PFAS through hydrophobic interactions. In addition, being cationic, these polymers can electrostatically adsorb PFAS as well, increasing their removal efficiency. Direct injection of PDADMAC into biofilter media provides a non-intrusive method of replenishing exhausted PFAS adsorption sites. However, being a coagulant, injection of liquid PDADMAC solutions can flocculate suspended sediments in stormwater which can clog the biofilters, rendering them unusable. Thus, the effect of injecting PDADMAC solution into biofilters to improve their PFAS removal capacity must be studied and any unintended consequences due to coagulation of sediments need to be explored. Yet, no study to date has explored the possibility of direct injection of cationic polymers into stormwater biofilters to create regenerative PFAS-removing biofilters.

1.2.5. The positive effect of aging of biofilter media on replenishing pathogen removal capacity of biofilters has not been studied

Biofilter media can age naturally due to physical, chemical, and biological processes. Physical aging occurs due to temperature fluctuation resulting in the drying of media, which has been shown to decrease the overall pathogen removal capacity (Chandrasena et al., 2014b; Fowdar et al., 2021; Li et al., 2012; Nabiul Afrooz and Boehm, 2017). In contrast, another study observed an improved removal capacity of biochar-amended biofilters after aging under dry-wet cycles due to replenished attachment sites (Mohanty and Boehm, 2015). Biological aging occurs due to the growth of biofilms (Nabiul Afrooz and Boehm, 2017), which could also decrease pathogen removal (Chandrasena et al., 2014a). In contrast, another study observed improved *E. coli* removal over time due to the growth of protozoa, a natural predator of bacteria (Zhang et al., 2011). Chemical aging occurs when chemical constituents such as natural organic matter (NOM) in stormwater adsorb on media, alter their surface properties, and reduce bacterial removal

(Ghavanloughajar et al., 2021; Mohanty and Boehm, 2015). However, previous studies rarely account for other co-contaminants such as dissolved metals in the aging of biofilter media.

Metals are ubiquitous in urban stormwater (Lau et al., 2009; Stein and Tiefenthaler, 2005), and they can be attached to amendments (Tirpak et al., 2021). The amount of metal adsorbed on amendments can increase with aging, which could affect pathogen removal due to metal toxicity (Li et al., 2016). Exposure to heavy metal contaminated stormwater could increase the concentration of heavy metals in the media (Al-Ameri et al., 2018; Hermawan et al., 2021). The same process could contribute to the positive effect of aging on pathogen removal. However, it is not clear whether naturally adsorbed metals in biofilters can sufficiently alter the surface properties to have any effect on pathogen removal. As the biofilters are designed to last more than 15-20 years, the total exposure of metals after a few years could be sufficient to alter the surface properties of amendments. However, after installation, biofilters media are typically never monitored for their changes in surface properties, or their performance is rarely evaluated beyond the first 2 years (Tirpak et al., 2021). Laboratory studies typically examined the exhaustion in attachment capacity of amendments with aging (Li et al., 2012). Rarely, the positive effect of aging such as increased removal of the pathogen by adsorbed metal is considered.

1.3. Objectives

This dissertation examines the role of colloids on the transport of pollutants such as PFAS and metals in subsurface and groundwater systems. Using this understanding, methods are developed to artificially or naturally regenerate the pollutant removal ability of filter media in stormwater biofilters. Chapters 2, 3, and 4 investigate the potential of colloids and other suspended particles in transporting PFAS through surface water, groundwater, subsurface soil, and air. Chapter 5 studies a way to regenerate exhausted stormwater biofilters and increase their capacity

to remove PFAS from stormwater by in-situ injection of cationic polymers such as PDADMAC. Chapter 6 examines the role of metals present in stormwater to naturally regenerate the pathogen removal capacity of biofilters. Specific goals are described below.

Chapter 2 critically analyzes and reviews how suspended particles are increasing the transport of PFAAs, especially long-chain PFAA compounds, in surface water. It also shows that even though PFAAs are non-volatile, dust particles can adsorb significant amounts of PFAAs and transport them in the air, posing an inhalation risk. The outcomes of Chapter 2 are:

> **Borthakur, A.,** Leonard, J., Koutnik, V.S., Ravi, S., Mohanty, S.K., 2022. Inhalation risks of wind-blown dust from biosolid-applied agricultural lands: Are they enriched with microplastics and PFAS? Current Opinion in Environmental Science & Health 25, 100309. https://doi.org/10.1016/j.coesh.2021.100309
>
> **Borthakur, A.,** Wang, M., He, M., Ascencio, K., Blotevogel, J., Adamson, D.T., Mahendra, S., Mohanty, S.K., 2021. Perfluoroalkyl acids on suspended particles: Significant transport pathways in surface runoff, surface waters, and subsurface soils. Journal of Hazardous Materials 417, 126159. https://doi.org/10.1016/j.jhazmat.2021.126159

Chapter 3 studies the flow of PFAS through groundwater and observed that fluctuations in groundwater flow can release colloids from aquifer soil that contain adsorbed PFAS. Thus, removing soil colloids from groundwater samples through filtration or centrifugation can underestimate the PFAS concentration in groundwater. The outcome of Chapter 3 is:

Borthakur, A., Cranmer, B.K., Dooley, G.P., Blotevogel, J., Mahendra, S., Mohanty, S.K., 2021. Release of soil colloids during flow interruption increases the pore-water PFAS concentration in saturated soil. Environmental Pollution 117297. https://doi.org/10.1016/j.envpol.2021.117297

Chapter 4 studies the leaching of PFAS from subsurface soil under weathering conditions and shows that dry-wet and freeze-thaw cycles can increase the release of colloids and associated PFAS from the subsurface into the groundwater. The outcome of Chapter 4 is:

Borthakur, A., Olsen, P., Dooley, G.P., Cranmer, B.K., Rao, U., Hoek, E.M.V., Blotevogel, J., Mahendra, S., Mohanty, S.K., 2021. Dry-wet and freeze-thaw cycles enhance PFOA leaching from subsurface soils. Journal of Hazardous Materials Letters 2, 100029. https://doi.org/10.1016/j.hazl.2021.100029

Chapter 5 develops a way to regenerate exhausted biofilter media and improve their ability to remove PFAS from stormwater without clogging the biofilter via in-situ injection of PDADMAC into the biofilters. The outcome of Chapter 5 is:

Borthakur, A., Das, T., Zhang, Y., Prehn, S., Libbert, S, Ramos, P., Dooley, G.P., Blotevogel, J., Mahendra, S., Mohanty, S.K. Rechargeable stormwater biofilters using cationic polymers for PFAS removal. *Manuscript Under Preparation.*

Chapter 6 develops a way for biofilters to naturally regenerate their pathogen removal capacity by utilizing the inherent toxicity of heavy metals toward pathogens. Thus, adsorbents with high

heavy metal retention capacity can be used to create these self-regenerating biofilters. The outcome of Chapter 6 is:

Borthakur, A., Chhour, K.L., Gayle, H.L., Prehn, S.R., Stenstrom, M.K., Mohanty, S.K., 2022. Natural aging of expanded shale, clay, and slate (ESCS) amendment with heavy metals in stormwater increases its antibacterial properties: Implications on biofilter design. Journal of Hazardous Materials 429, 128309. https://doi.org/10.1016/j.jhazmat.2022.128309

1.4. References

Adamson, D.T., Nickerson, A., Kulkarni, P.R., Higgins, C.P., Popovic, J., Field, J., Rodowa, A., Newell, C., DeBlanc, P., Kornuc, J.J., 2020. Mass-Based, Field-Scale Demonstration of PFAS Retention within AFFF-Associated Source Areas. Environ. Sci. Technol. 54, 15768–15777. https://doi.org/10.1021/acs.est.0c04472

Ahrens, L., Taniyasu, S., Yeung, L.W.Y., Yamashita, N., Lam, P.K.S., Ebinghaus, R., 2010a. Distribution of polyfluoroalkyl compounds in water, suspended particulate matter and sediment from Tokyo Bay, Japan. Chemosphere 79, 266–272. https://doi.org/10.1016/j.chemosphere.2010.01.045

Ahrens, L., Taniyasu, S., Yeung, L.W.Y., Yamashita, N., Lam, P.K.S., Ebinghaus, R., 2010b. Distribution of polyfluoroalkyl compounds in water, suspended particulate matter and sediment from Tokyo Bay, Japan. Chemosphere 79, 266–272. https://doi.org/10.1016/j.chemosphere.2010.01.045

Al-Ameri, M., Hatt, B., Le Coustumer, S., Fletcher, T., Payne, E., Deletic, A., 2018. Accumulation of heavy metals in stormwater bioretention media: A field study of temporal and spatial variation. Journal of Hydrology 567, 721–731. https://doi.org/10.1016/j.jhydrol.2018.03.027

Aly, Y.H., Liu, C., McInnis, D.P., Lyon, B.A., Hatton, J., McCarty, M., Arnold, W.A., Pennell, K.D., Simcik, M.F., 2018. In Situ Remediation Method for Enhanced Sorption of Perfluoro-Alkyl Substances onto Ottawa Sand. Journal of Environmental Engineering 144. https://doi.org/10.1061/(asce)ee.1943-7870.0001418

Aly, Y.H., McInnis, D.P., Lombardo, S.M., Arnold, W.A., Pennell, K.D., Hatton, J., Simcik, M.F., 2019. Enhanced adsorption of perfluoro alkyl substances for in situ remediation. Environmental Science-Water Research & Technology 5, 1867–1875. https://doi.org/10.1039/c9ew00426b

Armitage, J.M., MacLeod, M., Cousins, I.T., 2009. Modeling the Global Fate and Transport of Perfluorooctanoic Acid (PFOA) and Perfluorooctanoate (PFO) Emitted from Direct

Sources Using a Multispecies Mass Balance Model. Environ. Sci. Technol. 43, 1134–1140. https://doi.org/10.1021/es802900n

Askeland, M., Clarke, B.O., Cheema, S.A., Mendez, A., Gasco, G., Paz-Ferreiro, J., 2020. Biochar sorption of PFOS, PFOA, PFHxS and PFHxA in two soils with contrasting texture. Chemosphere 249, 126072. https://doi.org/10.1016/j.chemosphere.2020.126072

Baduel, C., Paxman, C.J., Mueller, J.F., 2015. Perfluoroalkyl substances in a firefighting training ground (FTG), distribution and potential future release. Journal of Hazardous Materials 296, 46–53. https://doi.org/10.1016/j.jhazmat.2015.03.007

Beretta, G.P., Terrenghi, J., 2017. Groundwater flow in the Venice lagoon and remediation of the Porto Marghera industrial area (Italy). Hydrogeology Journal 25, 847–861. https://doi.org/10.1007/s10040-016-1517-5

Borthakur, A., Chhour, K.L., Gayle, H.L., Prehn, S.R., Stenstrom, M.K., Mohanty, S.K., 2022. Natural aging of expanded shale, clay, and slate (ESCS) amendment with heavy metals in stormwater increases its antibacterial properties: Implications on biofilter design. Journal of Hazardous Materials 429, 128309. https://doi.org/10.1016/j.jhazmat.2022.128309

Borthakur, A., Cranmer, B.K., Dooley, G.P., Blotevogel, J., Mahendra, S., Mohanty, S.K., 2021a. Release of soil colloids during flow interruption increases the pore-water PFAS concentration in saturated soil. Environmental Pollution 117297. https://doi.org/10.1016/j.envpol.2021.117297

Borthakur, A., Olsen, P., Dooley, G.P., Cranmer, B.K., Rao, U., Hoek, E.M.V., Blotevogel, J., Mahendra, S., Mohanty, S.K., 2021b. Dry-wet and freeze-thaw cycles enhance PFOA leaching from subsurface soils. Journal of Hazardous Materials Letters 2, 100029. https://doi.org/10.1016/j.hazl.2021.100029

Borthakur, A., Wang, M., He, M., Ascencio, K., Blotevogel, J., Adamson, D.T., Mahendra, S., Mohanty, S.K., 2021c. Perfluoroalkyl acids on suspended particles: Significant transport pathways in surface runoff, surface waters, and subsurface soils. Journal of Hazardous Materials 417, 126159. https://doi.org/10.1016/j.jhazmat.2021.126159

Brusseau, M.L., 2020. Simulating PFAS transport influenced by rate-limited multi-process retention. Water Res 168, 115179. https://doi.org/10.1016/j.watres.2019.115179

Brusseau, M.L., 2019. Estimating the relative magnitudes of adsorption to solid-water and air/oil-water interfaces for per- and poly-fluoroalkyl substances. Environ Pollut 254, 113102. https://doi.org/10.1016/j.envpol.2019.113102

Brusseau, M.L., 2018. Assessing the potential contributions of additional retention processes to PFAS retardation in the subsurface. Sci Total Environ 613–614, 176–185. https://doi.org/10.1016/j.scitotenv.2017.09.065

Brusseau, M.L., Khan, N., Wang, Y., Yan, N., Van Glubt, S., Carroll, K.C., 2019. Nonideal Transport and Extended Elution Tailing of PFOS in Soil. Environ. Sci. Technol. 53, 10654–10664. https://doi.org/10.1021/acs.est.9b02343

Campos Pereira, H., Ullberg, M., Kleja, D.B., Gustafsson, J.P., Ahrens, L., 2018. Sorption of perfluoroalkyl substances (PFASs) to an organic soil horizon – Effect of cation composition and pH. Chemosphere 207, 183–191. https://doi.org/10.1016/j.chemosphere.2018.05.012

Campos-Pereira, H., Kleja, D.B., Sjöstedt, C., Ahrens, L., Klysubun, W., Gustafsson, J.P., 2020. The Adsorption of Per- and Polyfluoroalkyl Substances (PFASs) onto Ferrihydrite Is Governed by Surface Charge. Environ. Sci. Technol. 54, 15722–15730. https://doi.org/10.1021/acs.est.0c01646

Carey, G.R., McGregor, R., Pham, A.L.-T., Sleep, B., Hakimabadi, S.G., 2019. Evaluating the longevity of a PFAS in situ colloidal activated carbon remedy. Remediation Journal 29, 17–31. https://doi.org/10.1002/rem.21593

Chandrasena, G.I., Deletic, A., McCarthy, D.T., 2014a. Survival of Escherichia coli in stormwater biofilters. Environ Sci Pollut Res 21, 5391–5401. https://doi.org/10.1007/s11356-013-2430-2

Chandrasena, G.I., Pham, T., Payne, E.G., Deletic, A., McCarthy, D.T., 2014b. E. coli removal in laboratory scale stormwater biofilters: Influence of vegetation and submerged zone. Journal of Hydrology 519, 814–822. https://doi.org/10.1016/j.jhydrol.2014.08.015

Chanson, H., Reungoat, D., Simon, B., Lubin, P., 2011. High-frequency turbulence and suspended sediment concentration measurements in the Garonne River tidal bore. Estuarine, Coastal and Shelf Science 95, 298–306. https://doi.org/10.1016/j.ecss.2011.09.012

Charbonnet, J.A., Duan, Y., van Genuchten, C.M., Sedlak, D.L., 2018. Chemical Regeneration of Manganese Oxide-Coated Sand for Oxidation of Organic Stormwater Contaminants. Environ. Sci. Technol. 52, 10728–10736. https://doi.org/10.1021/acs.est.8b03304

Chen, H., Liu, M., Munoz, G., Duy, S.V., Sauvé, S., Yao, Y., Sun, H., Liu, J., 2020. Fast Generation of Perfluoroalkyl Acids from Polyfluoroalkyl Amine Oxides in Aerobic Soils. Environ. Sci. Technol. Lett. https://doi.org/10.1021/acs.estlett.0c00543

Chen, H.T., Reinhard, M., Yin, T.R., Nguyen, T.V., Tran, N.H., Gin, K.Y.H., 2019. Multi-compartment distribution of perfluoroalkyl and polyfluoroalkyl substances (PFASs) in an urban catchment system. Water Research 154, 227–237. https://doi.org/10.1016/j.watres.2019.02.009

Dauchy, X., Boiteux, V., Colin, A., Bach, C., Rosin, C., Munoz, J.F., 2019a. Poly- and Perfluoroalkyl Substances in Runoff Water and Wastewater Sampled at a Firefighter Training Area. Archives of Environmental Contamination and Toxicology 76, 206–215. https://doi.org/10.1007/s00244-018-0585-z

Dauchy, X., Boiteux, V., Colin, A., Hemard, J., Bach, C., Rosin, C., Munoz, J.F., 2019b. Deep seepage of per- and polyfluoroalkyl substances through the soil of a firefighter training site and subsequent groundwater contamination. Chemosphere 214, 729–737. https://doi.org/10.1016/j.chemosphere.2018.10.003

Ejaz, W., Anpalagan, A., 2019. Internet of Things for Smart Cities: Overview and Key Challenges, in: Ejaz, W., Anpalagan, A. (Eds.), Internet of Things for Smart Cities: Technologies, Big Data and Security, SpringerBriefs in Electrical and Computer Engineering. Springer International Publishing, Cham, pp. 1–15. https://doi.org/10.1007/978-3-319-95037-2_1

Fowdar, H., Payne, E., Schang, C., Zhang, K., Deletic, A., McCarthy, D., 2021. How well do stormwater green infrastructure respond to changing climatic conditions? Journal of Hydrology 603, 126887. https://doi.org/10.1016/j.jhydrol.2021.126887

Gao, B., Saiers, J., Ryan, J., 2004. Deposition and mobilization of clay colloids in unsaturated porous media. Water Resour. Res 40. https://doi.org/10.1029/2004WR003189

Gellrich, V., Stahl, T., Knepper, T.P., 2012a. Behavior of perfluorinated compounds in soils during leaching experiments. Chemosphere 87, 1052–1056. https://doi.org/10.1016/j.chemosphere.2012.02.011

Gellrich, V., Stahl, T., Knepper, T.P., 2012b. Behavior of perfluorinated compounds in soils during leaching experiments. Chemosphere 87, 1052–6. https://doi.org/10.1016/j.chemosphere.2012.02.011

Ghavanloughajar, M., Borthakur, A., Valenca, R., McAdam, M., Khor, C.M., Dittrich, T.M., Stenstrom, M.K., Mohanty, S.K., 2021. Iron amendments minimize the first-flush release of pathogens from stormwater biofilters. Environmental Pollution 281, 116989. https://doi.org/10.1016/j.envpol.2021.116989

Grebel, J.E., Mohanty, S.K., Torkelson, A.A., Boehm, A.B., Higgins, C.P., Maxwell, R.M., Nelson, K.L., Sedlak, D.L., 2013. Engineered Infiltration Systems for Urban Stormwater Reclamation. Environmental Engineering Science 30, 437–454. https://doi.org/10.1089/ees.2012.0312

Gribovszki, Z., Szilágyi, J., Kalicz, P., 2010. Diurnal fluctuations in shallow groundwater levels and streamflow rates and their interpretation – A review. Journal of Hydrology 385, 371–383. https://doi.org/10.1016/j.jhydrol.2010.02.001

Guelfo, J.L., Adamson, D.T., 2018. Evaluation of a national data set for insights into sources, composition, and concentrations of per- and polyfluoroalkyl substances (PFASs) in U.S. drinking water. Environ Pollut 236, 505–513. https://doi.org/10.1016/j.envpol.2018.01.066

Guo, B., Zeng, J., Brusseau, M.L., 2020. A Mathematical Model for the Release, Transport, and Retention of Per- and Polyfluoroalkyl Substances (PFAS) in the Vadose Zone. Water Resources Research 56, e2019WR026667. https://doi.org/10.1029/2019wr026667

Guo, W., He, M., Yang, Z., Lin, C., Quan, X., Wang, H., 2007. Distribution of polycyclic aromatic hydrocarbons in water, suspended particulate matter and sediment from Daliao River watershed, China. Chemosphere 68, 93–104. https://doi.org/10.1016/j.chemosphere.2006.12.072

Hale, S.E., Arp, H.P.H., Slinde, G.A., Wade, E.J., Bjorseth, K., Breedveld, G.D., Straith, B.F., Moe, K.G., Jartun, M., Hoisaeter, A., 2017. Sorbent amendment as a remediation strategy to reduce PFAS mobility and leaching in a contaminated sandy soil from a Norwegian firefighting training facility. Chemosphere 171, 9–18. https://doi.org/10.1016/j.chemosphere.2016.12.057

Hatfield, R.G., Maher, B.A., 2009. Fingerprinting upland sediment sources: particle size-specific magnetic linkages between soils, lake sediments and suspended sediments. Earth Surface Processes and Landforms 34, 1359–1373. https://doi.org/10.1002/esp.1824

Hermawan, A.A., Teh, K.L., Talei, A., Chua, L.H.C., 2021. Accumulation of heavy metals in stormwater biofiltration systems augmented with zeolite and fly ash. Journal of Environmental Management 297, 113298. https://doi.org/10.1016/j.jenvman.2021.113298

Higgins, C.P., Luthy, R.G., 2006a. Sorption of Perfluorinated Surfactants on Sediments †. Environ. Sci. Technol. 40, 7251–7256. https://doi.org/10.1021/es061000n

Higgins, C.P., Luthy, R.G., 2006b. Sorption of Perfluorinated Surfactants on Sediments. Environ. Sci. Technol. 40, 7251–7256. https://doi.org/10.1021/es061000n

Høisæter, Å., Pfaff, A., Breedveld, G.D., 2019. Leaching and transport of PFAS from aqueous film-forming foam (AFFF) in the unsaturated soil at a firefighting training facility under cold climatic conditions. J Contam Hydrol 222, 112–122. https://doi.org/10.1016/j.jconhyd.2019.02.010

Jeon, J., Kannan, K., Lim, B.J., An, K.G., Kim, S.D., 2011. Effects of salinity and organic matter on the partitioning of perfluoroalkyl acid (PFAs) to clay particles. Journal of Environmental Monitoring 13, 1803–1810. https://doi.org/10.1039/c0em00791a

Jia, Y., Zhang, L., Zheng, J., Liu, X., Jeng, D.-S., Shan, H., 2014. Effects of wave-induced seabed liquefaction on sediment re-suspension in the Yellow River Delta. Ocean Engineering 89, 146–156. https://doi.org/10.1016/j.oceaneng.2014.08.004

Johnson, R.L., Anschutz, A.J., Smolen, J.M., Simcik, M.F., Penn, R.L., 2007. The Adsorption of Perfluorooctane Sulfonate onto Sand, Clay, and Iron Oxide Surfaces. J. Chem. Eng. Data 52, 1165–1170. https://doi.org/10.1021/je060285g

Karakurt-Fischer, S., Sanz-Prat, A., Greskowiak, J., Ergh, M., Gerdes, H., Massmann, G., Ederer, J., Regnery, J., Hübner, U., Drewes, J.E., 2020. Developing a novel biofiltration treatment system by coupling high-rate infiltration trench technology with a plug-flow porous-media bioreactor. Science of The Total Environment 722, 137890. https://doi.org/10.1016/j.scitotenv.2020.137890

Laitinen, J.A., Koponen, J., Koikkalainen, J., Kiviranta, H., 2014. Firefighters' exposure to perfluoroalkyl acids and 2-butoxyethanol present in firefighting foams. Toxicology Letters, Advances in Biological Monitoring for Occupational and Environmental Health - II 231, 227–232. https://doi.org/10.1016/j.toxlet.2014.09.007

Lau, S.-L., Han, Y., Kang, J.-H., Kayhanian, M., Stenstrom, M.K., 2009. Characteristics of Highway Stormwater Runoff in Los Angeles: Metals and Polycyclic Aromatic Hydrocarbons. Water Environment Research 81, 308–318. https://doi.org/10.2175/106143008X357237

Lee, H., D'eon, J., Mabury, S.A., 2010. Biodegradation of Polyfluoroalkyl Phosphates as a Source of Perfluorinated Acids to the Environment. Environ. Sci. Technol. 44, 3305–3310. https://doi.org/10.1021/es9028183

LeFevre, G.H., Paus, K.H., Natarajan, P., Gulliver, J.S., Novak, P.J., Hozalski, R.M., 2015. Review of Dissolved Pollutants in Urban Storm Water and Their Removal and Fate in Bioretention Cells. Journal of Environmental Engineering 141, 04014050. https://doi.org/10.1061/(ASCE)EE.1943-7870.0000876

Li, Y., McCarthy, D.T., Deletic, A., 2016. Escherichia coli removal in copper-zeolite-integrated stormwater biofilters: Effect of vegetation, operational time, intermittent drying weather. Ecological Engineering 90, 234–243. https://doi.org/10.1016/j.ecoleng.2016.01.066

Li, Y.L., Deletic, A., Alcazar, L., Bratieres, K., Fletcher, T.D., McCarthy, D.T., 2012. Removal of Clostridium perfringens, Escherichia coli and F-RNA coliphages by stormwater biofilters. Ecological Engineering 49, 137–145. https://doi.org/10.1016/j.ecoleng.2012.08.007

Li, Y.L., Deletic, A., McCarthy, D.T., 2014a. Removal of E. coli from urban stormwater using antimicrobial-modified filter media. Journal of Hazardous Materials 271, 73–81. https://doi.org/10.1016/j.jhazmat.2014.01.057

Li, Y.L., McCarthy, D.T., Deletic, A., 2014b. Stable copper-zeolite filter media for bacteria removal in stormwater. Journal of Hazardous Materials 273, 222–230. https://doi.org/10.1016/j.jhazmat.2014.03.036

Liu, Chen, Hatton, J., Arnold, W.A., Simcik, M.F., Pennell, K.D., 2020. In Situ Sequestration of Perfluoroalkyl Substances Using Polymer-Stabilized Powdered Activated Carbon. Environ. Sci. Technol. 54, 6929–6936. https://doi.org/10.1021/acs.est.0c00155

Liu, J., Yang, H., Gosling, S.N., Kummu, M., Flörke, M., Pfister, S., Hanasaki, N., Wada, Y., Zhang, X., Zheng, C., Alcamo, J., Oki, T., 2017. Water scarcity assessments in the past, present, and future. Earth's Future 5, 545–559. https://doi.org/10.1002/2016EF000518

Liu, Yan, Junaid, M., Xu, P., Zhong, W., Pan, B., 2020. Suspended sediment exacerbates perfluorooctane sulfonate mediated toxicity through reactive oxygen species generation in freshwater clam Corbicula fluminea. Environmental Pollution. https://doi.org/10.1016/j.envpol.2020.115671

Liu, Yanju, Qi, F., Fang, C., Naidu, R., Duan, L., Dharmarajan, R., Annamalai, P., 2020. The effects of soil properties and co-contaminants on sorption of perfluorooctane sulfonate (PFOS) in contrasting soils. Environmental Technology & Innovation 19, 100965. https://doi.org/10.1016/j.eti.2020.100965

Liu, Y., Zhang, Y., Li, J., Wu, N., Li, W., Niu, Z., 2019. Distribution, partitioning behavior and positive matrix factorization-based source analysis of legacy and emerging polyfluorinated alkyl substances in the dissolved phase, surface sediment and suspended particulate matter around coastal areas of Bohai Bay, China. Environmental Pollution 246, 34–44. https://doi.org/10.1016/j.envpol.2018.11.113

Liu, Y.Q., Zhang, Y., Li, J.F., Wu, N., Li, W.P., Niu, Z.G., 2019. Distribution, partitioning behavior and positive matrix factorization-based source analysis of legacy and emerging polyfluorinated alkyl substances in the dissolved phase, surface sediment and suspended particulate matter around coastal areas of Bohai Bay, China. Environmental Pollution 246, 34–44. https://doi.org/10.1016/j.envpol.2018.11.113

Llorca, M., Schirinzi, G., Martínez, M., Barceló, D., Farré, M., 2018. Adsorption of perfluoroalkyl substances on microplastics under environmental conditions. Environmental Pollution 235, 680–691. https://doi.org/10.1016/j.envpol.2017.12.075

Lukasik, J., Cheng, Y.-F., Lu, F., Tamplin, M., Farrah, S.R., 1999. Removal of microorganisms from water by columns containing sand coated with ferric and aluminum hydroxides. Water Research 33, 769–777. https://doi.org/10.1016/S0043-1354(98)00279-6

Lyu, Y., Brusseau, M.L., Chen, W., Yan, N., Fu, X., Lin, X., 2018. Adsorption of PFOA at the Air-Water Interface during Transport in Unsaturated Porous Media. Environ Sci Technol 52, 7745–7753. https://doi.org/10.1021/acs.est.8b02348

Ma, T., Sun, S., Fu, G., Hall, J.W., Ni, Y., He, L., Yi, J., Zhao, N., Du, Y., Pei, T., Cheng, W., Song, C., Fang, C., Zhou, C., 2020. Pollution exacerbates China's water scarcity and its regional inequality. Nat Commun 11, 650. https://doi.org/10.1038/s41467-020-14532-5

Majdalani, S., Michel, E., Di Pietro, L., Angulo-Jaramillo, R., Rousseau, M., 2007. Mobilization and preferential transport of soil particles during infiltration: A core-scale modeling approach. Water Resources Research 43. https://doi.org/10.1029/2006wr005057

McDonald, R.I., Weber, K., Padowski, J., Flörke, M., Schneider, C., Green, P.A., Gleeson, T., Eckman, S., Lehner, B., Balk, D., Boucher, T., Grill, G., Montgomery, M., 2014. Water on an urban planet: Urbanization and the reach of urban water infrastructure. Global Environmental Change 27, 96–105. https://doi.org/10.1016/j.gloenvcha.2014.04.022

Mejia-Avendaño, S., Zhi, Y., Yan, B., Liu, J., 2020. Sorption of Polyfluoroalkyl Surfactants on Surface Soils: Effect of Molecular Structures, Soil Properties, and Solution Chemistry. Environ. Sci. Technol. 54, 1513–1521. https://doi.org/10.1021/acs.est.9b04989

Merino, N., Qu, Y., Deeb, R.A., Hawley, E.L., Hoffmann, M.R., Mahendra, S., 2016. Degradation and Removal Methods for Perfluoroalkyl and Polyfluoroalkyl Substances in Water. Environ. Eng. Sci. 33, 615–649. https://doi.org/10.1089/ees.2016.0233

Milinovic, J., Lacorte, S., Vidal, M., Rigol, A., 2015. Sorption behaviour of perfluoroalkyl substances in soils. Science of The Total Environment 511, 63–71. https://doi.org/10.1016/j.scitotenv.2014.12.017

Mohanty, S.K., Boehm, A.B., 2015. Effect of weathering on mobilization of biochar particles and bacterial removal in a stormwater biofilter. Water Research 85, 208–215. https://doi.org/10.1016/j.watres.2015.08.026

Mohanty, S.K., Bulicek, M.C.D., Metge, D.W., Harvey, R.W., Ryan, J.N., Boehm, A.B., 2015a. Mobilization of Microspheres from a Fractured Soil during Intermittent Infiltration Events. Vadose Zone Journal 14, vzj2014.05.0058. https://doi.org/10.2136/vzj2014.05.0058

Mohanty, S.K., Saiers, J.E., Ryan, J.N., 2015b. Colloid mobilization in a fractured soil during dry–wet cycles: role of drying duration and flow path permeability. Environmental Science & Technology 49, 9100–9106. https://doi.org/10.1021/acs.est.5b00889

Mohanty, S.K., Saiers, J.E., Ryan, J.N., 2014. Colloid-facilitated mobilization of metals by freeze–thaw cycles. Environmental Science & Technology 48, 977–984. https://doi.org/10.1021/es403698u

Mohanty, S.K., Torkelson, A.A., Dodd, H., Nelson, K.L., Boehm, A.B., 2013. Engineering Solutions to Improve the Removal of Fecal Indicator Bacteria by Bioinfiltration Systems during Intermittent Flow of Stormwater. Environ. Sci. Technol. 47, 10791–10798. https://doi.org/10.1021/es305136b

Mukhopadhyay, R., Sarkar, B., Palansooriya, K.N., Dar, J.Y., Bolan, N.S., Parikh, S.J., Sonne, C., Ok, Y.S., 2021. Natural and engineered clays and clay minerals for the removal of poly- and perfluoroalkyl substances from water: State-of-the-art and future perspectives. Advances in Colloid and Interface Science 297, 102537. https://doi.org/10.1016/j.cis.2021.102537

Nabiul Afrooz, A.R.M., Boehm, A.B., 2017. Effects of submerged zone, media aging, and antecedent dry period on the performance of biochar-amended biofilters in removing fecal indicators and nutrients from natural stormwater. Ecological Engineering 102, 320–330. https://doi.org/10.1016/j.ecoleng.2017.02.053

Nguyen, T.M.H., Bräunig, J., Thompson, K., Thompson, J., Kabiri, S., Navarro, D.A., Kookana, R.S., Grimison, C., Barnes, C.M., Higgins, C.P., McLaughlin, M.J., Mueller, J.F., 2020. Influences of Chemical Properties, Soil Properties, and Solution pH on Soil–Water Partitioning Coefficients of Per- and Polyfluoroalkyl Substances (PFASs). Environ. Sci. Technol. https://doi.org/10.1021/acs.est.0c05705

Nguyen, Tung V., Reinhard, M., Chen, H., Gin, K.Y.-H., 2016. Fate and transport of perfluoro- and polyfluoroalkyl substances including perfluorooctane sulfonamides in a managed urban water body. Environ Sci Pollut Res Int 23, 10382–10392. https://doi.org/10.1007/s11356-016-6788-9

Nguyen, T. V., Reinhard, M., Chen, H.T., Gin, K.Y.H., 2016. Fate and transport of perfluoro- and polyfluoroalkyl substances including perfluorooctane sulfonamides in a managed urban water body. Environmental Science and Pollution Research 23, 10382–10392. https://doi.org/10.1007/s11356-016-6788-9

Ochoa-Herrera, V., Sierra-Alvarez, R., 2008. Removal of perfluorinated surfactants by sorption onto granular activated carbon, zeolite and sludge. Chemosphere 72, 1588–1593. https://doi.org/10.1016/j.chemosphere.2008.04.029

Ololade, I.A., Zhou, Q., Pan, G., 2016. Influence of oxic/anoxic condition on sorption behavior of PFOS in sediment. Chemosphere 150, 798–803. https://doi.org/10.1016/j.chemosphere.2015.08.068

Oppenheimer, J., Da Silva, A., Yu, Z.L.T., Hanna, M., Susilo, K., 2017. Total Water Solutions—Capturing Alternative Water Sources to Supplement Drinking Water Supply. Journal AWWA 109, 18–25. https://doi.org/10.5942/jawwa.2017.109.0017

Park, M., Wu, S.M., Lopez, I.J., Chang, J.Y., Karanfil, T., Snyder, S.A., 2020. Adsorption of perfluoroalkyl substances (PFAS) in groundwater by granular activated carbons: Roles of hydrophobicity of PFAS and carbon characteristics. Water Research 170. https://doi.org/10.1016/j.watres.2019.115364

Patrick Wang, P., Zheng, C., Gorelick, S.M., 2005. A general approach to advective–dispersive transport with multirate mass transfer. Advances in Water Resources 28, 33–42. https://doi.org/10.1016/j.advwatres.2004.10.003

Pereira, H.C., Ullberg, M., Kleja, D.B., Gustafsson, J.P., Ahrens, L., 2018. Sorption of perfluoroalkyl substances (PFASs) to an organic soil horizon – Effect of cation composition and pH. Chemosphere 207, 183–191. https://doi.org/10.1016/j.chemosphere.2018.05.012

Qian, J., Shen, M., Wang, P., Wang, C., Hou, J., Ao, Y., Liu, J., Li, K., 2017. Adsorption of perfluorooctane sulfonate on soils: Effects of soil characteristics and phosphate competition. Chemosphere 168, 1383–1388. https://doi.org/10.1016/j.chemosphere.2016.11.114

Ramos, P., Singh Kalra, S., Johnson, N.W., Khor, C.M., Borthakur, A., Cranmer, B., Dooley, G., Mohanty, S.K., Jassby, D., Blotevogel, J., Mahendra, S., 2022. Enhanced removal of per- and polyfluoroalkyl substances in complex matrices by polyDADMAC-coated regenerable granular activated carbon. Environmental Pollution 294, 118603. https://doi.org/10.1016/j.envpol.2021.118603

Ray, J.R., Shabtai, I.A., Teixidó, M., Mishael, Y.G., Sedlak, D.L., 2019. Polymer-clay composite geomedia for sorptive removal of trace organic compounds and metals in urban stormwater. Water Research 157, 454–462. https://doi.org/10.1016/j.watres.2019.03.097

Rippy, M.A., 2015. Meeting the criteria: linking biofilter design to fecal indicator bacteria removal. WIREs Water 2, 577–592. https://doi.org/10.1002/wat2.1096

Ryan, J.N., Elimelech, M., 1996. Colloid mobilization and transport in groundwater. Colloids and Surfaces A: Physicochemical and Engineering Aspects, A collection of papers presented at the Symposium on Colloidal and Interfacial Phenomena in Aquatic Environments 107, 1–56. https://doi.org/10.1016/0927-7757(95)03384-X

Saha, D., Ray, R.K., 2019. Groundwater Resources of India: Potential, Challenges and Management, in: Sikdar, P.K. (Ed.), Groundwater Development and Management: Issues and Challenges in South Asia. Springer International Publishing, Cham, pp. 19–42. https://doi.org/10.1007/978-3-319-75115-3_2

Schaefer, C.E., Drennan, D.M., Tran, D.N., Garcia, R., Christie, E., Higgins, C.P., Field, J.A., 2019. Measurement of Aqueous Diffusivities for Perfluoroalkyl Acids. Journal of Environmental Engineering 145, 06019006. https://doi.org/doi:10.1061/(ASCE)EE.1943-7870.0001585

Schelde, K., Moldrup, P., Jacobsen, O., Jonge, H., de Jonge, L., Komatsu, T., 2002a. Diffusion-Limited Mobilization and Transport of Natural Colloids in Macroporous Soil. Vadose Zone Journal - VADOSE ZONE J 1, 125–136. https://doi.org/10.2113/1.1.125

Schelde, K., Moldrup, P., Jacobsen, O.H., de Jonge, H., de Jonge, L.W., Komatsu, T., 2002b. Diffusion-Limited Mobilization and Transport of Natural Colloids in Macroporous Soil. Vadose Zone Journal 1, 125–136. https://doi.org/10.2113/1.1.125

Seo, S.-H., Son, M.-H., Shin, E.-S., Choi, S.-D., Chang, Y.-S., 2019. Matrix-specific distribution and compositional profiles of perfluoroalkyl substances (PFASs) in multimedia environments. Journal of Hazardous Materials 364, 19–27. https://doi.org/10.1016/j.jhazmat.2018.10.012

Spahr, S., Teixidó, M., L. Sedlak, D., G. Luthy, R., 2020. Hydrophilic trace organic contaminants in urban stormwater: occurrence, toxicological relevance, and the need to enhance green stormwater infrastructure. Environmental Science: Water Research & Technology 6, 15–44. https://doi.org/10.1039/C9EW00674E

Stein, E.D., Tiefenthaler, L.L., 2005. Dry-Weather Metals and Bacteria Loading in an Arid, Urban Watershed: Ballona Creek, California. Water Air Soil Pollut 164, 367–382. https://doi.org/10.1007/s11270-005-4041-0

Suzuki, K., Higashi, S., 2001. Groundwater flow after heavy rain in landslide-slope area from 2-D inversion of resistivity monitoring data. Geophysics 66. https://doi.org/10.1190/1.1444963

Tanabe, S., Tatsukawa, R., 1983. Vertical transport and residence time of chlorinated hydrocarbons in the open ocean water column. Journal of the Oceanographical Society of Japan 39, 53–62. https://doi.org/10.1007/BF02210759

Tirpak, R.A., Afrooz, A.N., Winston, R.J., Valenca, R., Schiff, K., Mohanty, S.K., 2021. Conventional and amended bioretention soil media for targeted pollutant treatment: A critical review to guide the state of the practice. Water Research 189, 116648. https://doi.org/10.1016/j.watres.2020.116648

Trudel, D., Horowitz, L., Wormuth, M., Scheringer, M., Cousins, I.T., Hungerbühler, K., 2008. Estimating Consumer Exposure to PFOS and PFOA. Risk Analysis 28, 251–269. https://doi.org/10.1111/j.1539-6924.2008.01017.x

Ulrich, B.A., Im, E.A., Werner, D., Higgins, C.P., 2015. Biochar and Activated Carbon for Enhanced Trace Organic Contaminant Retention in Stormwater Infiltration Systems. Environ. Sci. Technol. 49, 6222–6230. https://doi.org/10.1021/acs.est.5b00376

Valenca, R., Borthakur, A., Zu, Y., Matthiesen, E.A., Stenstrom, M.K., Mohanty, S.K., 2021. Biochar Selection for *Escherichia coli* Removal in Stormwater Biofilters. Journal of Environmental Engineering 147, 06020005. https://doi.org/10.1061/(ASCE)EE.1943-7870.0001843

Wang, F., Liu, C., Shih, K., 2012. Adsorption behavior of perfluorooctanesulfonate (PFOS) and perfluorooctanoate (PFOA) on boehmite. Chemosphere 89, 1009–14. https://doi.org/10.1016/j.chemosphere.2012.06.071

Wang, F., Shih, K., Leckie, J.O., 2015. Effect of humic acid on the sorption of perfluorooctane sulfonate (PFOS) and perfluorobutane sulfonate (PFBS) on boehmite. Chemosphere 118, 213–8. https://doi.org/10.1016/j.chemosphere.2014.08.080

Washington, J.W., Yoo, H., Ellington, J.J., Jenkins, T.M., Libelo, E.L., 2010. Concentrations, Distribution, and Persistence of Perfluoroalkylates in Sludge-Applied Soils near Decatur, Alabama, USA. Environ. Sci. Technol. 44, 8390–8396. https://doi.org/10.1021/es1003846

Xiao, F., Jin, B., Golovko, S.A., Golovko, M.Y., Xing, B., 2019. Sorption and Desorption Mechanisms of Cationic and Zwitterionic Per- and Polyfluoroalkyl Substances in Natural Soils: Thermodynamics and Hysteresis. Environ Sci Technol 53, 11818–11827. https://doi.org/10.1021/acs.est.9b05379

Xiao, F., Simcik, M.F., Gulliver, J.S., 2012. Perfluoroalkyl acids in urban stormwater runoff: Influence of land use. Water Research 46, 6601–6608. https://doi.org/10.1016/j.watres.2011.11.029

Xiao, X., Ulrich, B.A., Chen, B., Higgins, C.P., 2017. Sorption of Poly- and Perfluoroalkyl Substances (PFASs) Relevant to Aqueous Film-Forming Foam (AFFF)-Impacted Groundwater by Biochars and Activated Carbon. Environ. Sci. Technol. 51, 6342–6351. https://doi.org/10.1021/acs.est.7b00970

Xing, Y., Chen, Xijuan, Chen, Xin, Zhuang, J., 2016. Colloid-Mediated Transport of Pharmaceutical and Personal Care Products through Porous Media. Sci Rep 6, 35407. https://doi.org/10.1038/srep35407

Yu, J., Lv, L., Lan, P., Zhang, S., Pan, B., Zhang, W., 2012. Effect of effluent organic matter on the adsorption of perfluorinated compounds onto activated carbon. Journal of Hazardous Materials 225–226, 99–106. https://doi.org/10.1016/j.jhazmat.2012.04.073

Zhang, J., 1999. Heavy metal compositions of suspended sediments in the Changjiang (Yangtze River) estuary: significance of riverine transport to the ocean. Continental Shelf Research 19, 1521–1543. https://doi.org/10.1016/S0278-4343(99)00029-1

Zhang, L., Seagren, E.A., Davis, A.P., Karns, J.S., 2011. Long-Term Sustainability of *Escherichia Coli* Removal in Conventional Bioretention Media. Journal of Environmental Engineering 137, 669–677. https://doi.org/10.1061/(ASCE)EE.1943-7870.0000365

Zhang, R., Yan, W., Jing, C., 2014a. Mechanistic study of PFOS adsorption on kaolinite and montmorillonite. Colloids and Surfaces A: Physicochemical and Engineering Aspects 462, 252–258. https://doi.org/10.1016/j.colsurfa.2014.09.019

Zhang, R., Yan, W., Jing, C., 2014b. Mechanistic study of PFOS adsorption on kaolinite and montmorillonite. Colloids and Surfaces A: Physicochemical and Engineering Aspects 462, 252–258. https://doi.org/10.1016/j.colsurfa.2014.09.019

Zhao, P., Xia, X., Dong, J., Xia, N., Jiang, X., Li, Y., Zhu, Y., 2016. Short- and long-chain perfluoroalkyl substances in the water, suspended particulate matter, and surface sediment of a turbid river. Science of The Total Environment 568, 57–65. https://doi.org/10.1016/j.scitotenv.2016.05.221

Zhou, J., Liu, D., Zhang, W., Chen, X., Huan, Y., Yu, X., 2017. Colloid characterization and in situ release in shallow groundwater under different hydrogeology conditions. Environ Sci Pollut Res 24, 14445–14454. https://doi.org/10.1007/s11356-017-8856-1

Zhu, Y., Dong, X., Harris, W., Bonzongo, J.-C., Han, F., 2013. Ionic strength reduction and flow interruption enhanced colloid-facilitated Hg transport in contaminated soils. Journal of hazardous materials 264C, 286–292. https://doi.org/10.1016/j.jhazmat.2013.11.009

2. CHAPTER 2: PERFLUOROALKYL ACIDS ON SUSPENDED PARTICLES: SIGNIFICANT TRANSPORT PATHWAYS IN SURFACE RUNOFF, SURFACE WATERS, AND SUBSURFACE SOILS

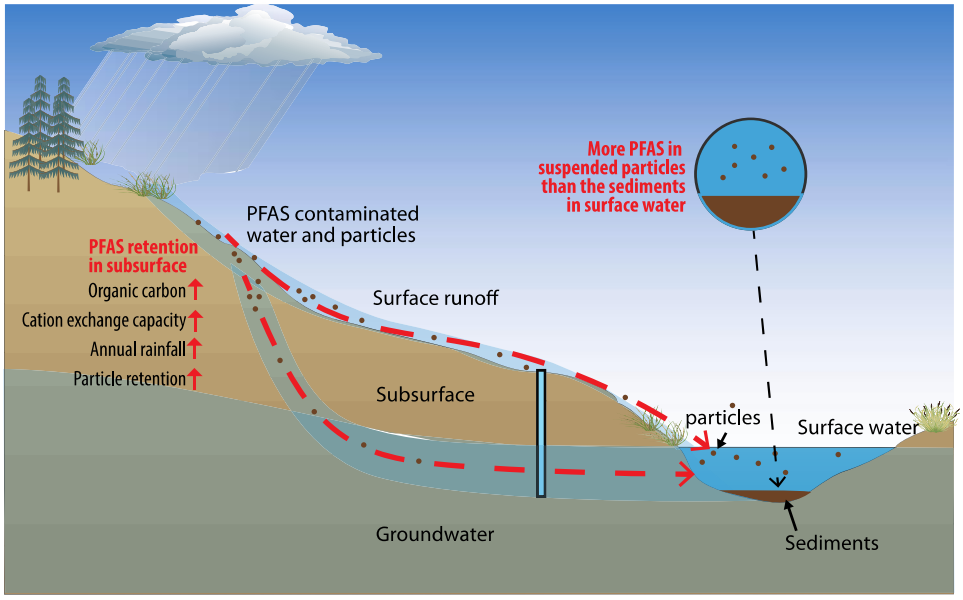

Borthakur, A., Leonard, J., Koutnik, V.S., Ravi, S., Mohanty, S.K., 2022. Inhalation risks of wind-blown dust from biosolid-applied agricultural lands: Are they enriched with microplastics and PFAS? Current Opinion in Environmental Science & Health 25, 100309. https://doi.org/10.1016/j.coesh.2021.100309

Borthakur, A., Wang, M., He, M., Ascencio, K., Blotevogel, J., Adamson, D.T., Mahendra, S., Mohanty, S.K., 2021. Perfluoroalkyl acids on suspended particles: Significant transport pathways in surface runoff, surface waters, and subsurface soils. Journal of Hazardous Materials 417, 126159. https://doi.org/10.1016/j.jhazmat.2021.126159

Abstract

Eroded particles from the source zone could transport a high concentration of perfluoroalkyl acids (PFAAs) to sediments and water bodies. Yet, the contribution of suspended particles has not been systematically reviewed. Analyzing reported studies, we quantitatively demonstrate that suspended particles in surface water can contain significantly higher concentrations of PFAAs than the sediment below, indicating the source of suspended particles are not the sediment but particles eroded and carried from the source zone upstream. The affinity of PFAAs to particles depends on the particle composition, including organic carbon fraction and iron or aluminum oxide content. In soils, most PFAAs are retained within the top 5 m below the ground surface. The distribution of PFAAs in the subsurface varies based on site properties and local weather conditions. The depth corresponding to the maximum concentration of PFAA in soil decreases with an increase in soil organic carbon or rainfall amount received in the catchment areas. We attribute a greater accumulation of PFAAs near the upper layer of the subsurface to an increase in the accumulation of particles eroded from source zones upstream receiving heavy rainfall. Precursor transformation in the aerobic zone is significantly higher than in the anaerobic zone, thereby making the aerobic subsurface zone serve as a long-term source of groundwater pollution. Collectively, these results suggest that suspended particles, often an overlooked vector for PFAAs, can be a dominant pathway for the transport of PFAAs in environments.

2.1. Introduction

Perfluoroalkyl acids (PFAAs) are the most persistent fraction of per- and polyfluoroalkyl substances (PFASs). These chemicals have been released into surface waters from sources including fluorochemical industrial sites (Wang et al., 2016, 2013), firefighting training areas (Baduel et al., 2015; Dauchy et al., 2019a), airports (de Solla et al., 2012; Filipovic et al., 2015; Milley et al., 2018), accidental spill sites (D'Agostino and Mabury, 2014; Dauchy et al., 2017; Mejia-Avendano et al., 2017), and poorly managed landfills (Benskin et al., 2012; Hepburn et al., 2019; Knutsen et al., 2019; Robey et al., 2020). The runoff near these sources can impact surface waters and infiltrate through the subsurface, which leads to impacts to groundwater or drinking water wells (Guelfo and Adamson, 2018). Exposure to PFAA-impacted drinking water can lead to several adverse health effects including elevated blood pressure (Pitter et al., 2020), lung disease (Qin et al., 2017), birth defects (Rokoff et al., 2018), immunotoxicity (Sunderland et al., 2019) and potentially cancer (Nicole, 2013). Therefore, it is critical to determine the factors that control the transport and release of PFAAs in the environments.

Fate and transport of dissolved PFAAs in surface and subsurface environments are well-established. PFAAs are dissolved into the rainwater or runoff near the source zones and conveyed by surface runoff to surface waters. Some of the runoff can infiltrate through subsurface soil and reach groundwater (Figure 2-1). Advection of dissolved PFAAs is currently assumed to be the dominant mechanism of transport in surface waters and subsurface (Dauchy et al., 2019b, 2019a; Xiao et al., 2012), whereas sorption to soil or sediment is considered the primary retention mechanism. Surface runoff also often contains high concentrations of suspended particles, which are generated by the erosion of soil surface or resuspension of sediments (Hatfield and Maher, 2009; Jia et al., 2014). These particles can bind PFAAs and carry them to surface and subsurface

environments (Ahrens et al., 2010; Llorca et al., 2018; Nguyen et al., 2016). If the suspended particles are originated from the erosion of impacted lands, they may contain much higher concentrations of PFAAs than explained based on equilibrium adsorption (Liu et al., 2019; Xiao et al., 2012). These particles can be mixed with suspended particles created in streams and rivers due to the turbulence of fast-moving water (Chanson et al., 2011). The relative contribution of these particles to the transport of PFAA to sediment is unclear. However, most studies reported PFAA concentration in surface water samples based on filtered or centrifuged samples (Qiu et al., 2010; Zhou et al., 2013). These sample processing steps ignore the contribution of PFAAs adsorbed on suspended particles, which could introduce significant error in estimating the 'true' extent of PFAA impacts to and transport in surface water.

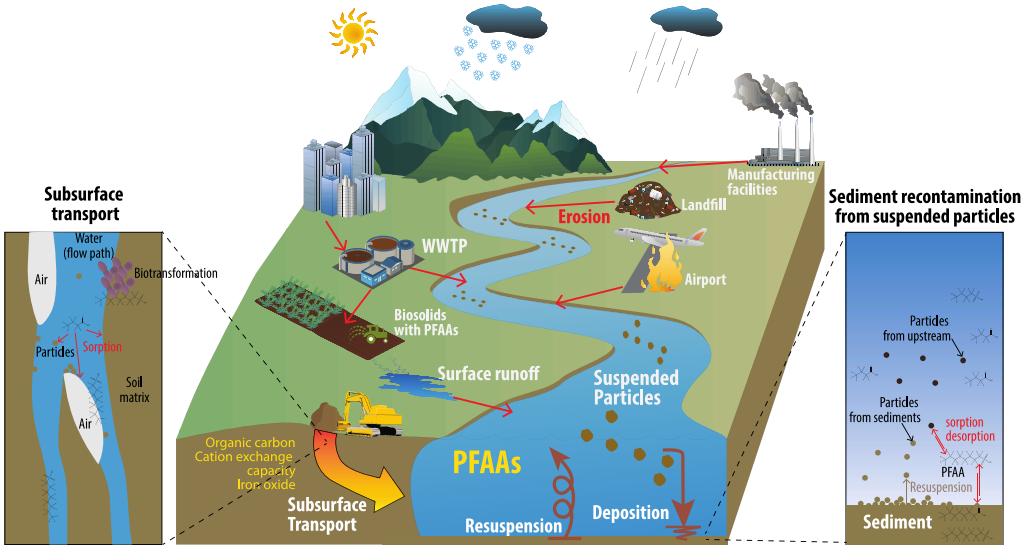

Figure 2-1: Potential role of particles on the fate and transport of PFAAs in surface waters and subsurface soil. Surface runoff carries PFAAs and eroded particles impacted with PFAAs from the source zones to surface waters. Impacted runoff can infiltrate into the subsurface soil where PFAAs can adsorb on soil or impacted particles can be deposited in topsoil, which can serve as a long-term source for groundwater pollution.

The role of suspended particles on PFAA transport is relatively unexplored, although their role in enhancing the transport of other organic chemicals such as polycyclic aromatic hydrocarbons (Guo et al., 2007), chlorinated solvents (Tanabe and Tatsukawa, 1983), and heavy metals (Zhang, 1999) has been well established. These chemicals strongly adsorb on suspended particles and move farther than the dissolved chemicals, because dissolved chemicals can be removed from the water column due to adsorption to sediment or soil. Consequently, conditions that influence the concentration of the suspended particle concentration in water such as high rainfall intensity and flow velocity could affect particle-facilitated transport of the highly adsorbing pollutants. Although some of the legacy pollutants are more hydrophobic than PFAS, thereby increasing their association with suspended particles, the advisory limit for PFAS in water is in low parts per trillion, which is an order of magnitude lower than the limit for the legacy pollutants. Thus, a relatively low concentration of PFAS on particles can lead to an exceedance of the water quality criteria. In general, it is expected that PFAAs with a long carbon chain could bind strongly to soil (Higgins and Luthy, 2006; Liu et al., 2020; Nguyen et al., 2020) due to an increase in hydrophobicity (Figure 2-2). However, the relevance of suspended particles on PFAA distribution in the environment has not been critically reviewed, although the fate and transport of aqueous PFAA in the environment have been reviewed extensively (Ahmed et al., 2020; Ahrens and Bundschuh, 2014; Armitage et al., 2009; Banzhaf et al., 2017; Brusseau et al., 2020; Lam et al., 2017; Nadal and Domingo, 2014; Prevedouros et al., 2006; Sharifan et al., 2021; Sunderland et al., 2019; Vedagiri et al., 2018).

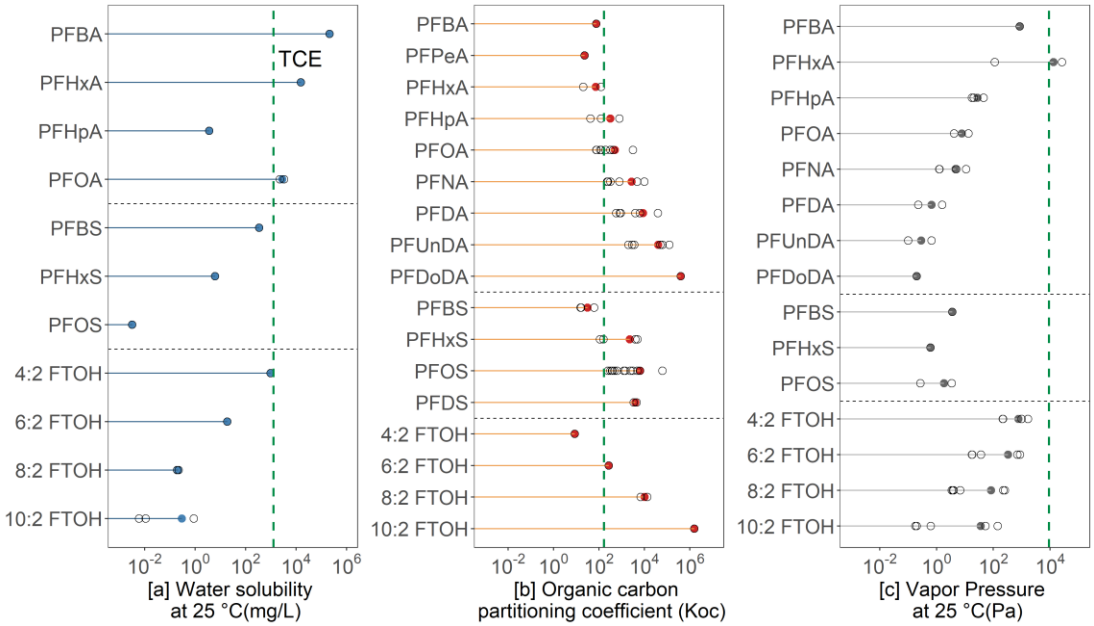

Figure 2-2: (a) Water solubility, (b) organic carbon partitioning coefficient and (c) vapor pressure of different PFAA compounds and fluorotelomer alcohol precursors. The green line denotes the value of the respective properties for trichloroethylene (TCE) as a benchmark. The white open circles indicate the individual values of the respective property for each compound while the filled circle indicates the mean value of the individual values.

In this review, we aim to assess the impact of suspended particles on the transport and accumulation of PFAAs in surface water and subsurface soil. By analyzing PFAA concentration data from surface waters and subsurface soils, we compare the concentration of PFAAs on suspended particles and sediment and correlate the concentration distribution at different depths in the subsurface with rainfall intensity and soil mineral properties at the sites. Furthermore, we evaluate how the affinity of PFAAs on particles can vary with their composition including organic carbon, iron oxide, and aluminum oxide.

2.2. Data collection and analysis

We searched the Web of Science database (https://www.webofknowledge.com/) in July 2020, to collect research articles using keyword combinations: “PFAS” with “properties”, “soil” and “water” (Table 2-1). Out of 697 articles found, 249 were selected after analyzing the title and

abstract. To compare the PFAA concentrations in suspended sediments and bed sediments, we searched for research articles that had reported PFAA concentrations in both suspended sediments and bed sediments in surface waters and at different depths of the subsurface around impacted areas. Only studies that reported PFAA concentration at depths greater than at least 25 cm were selected, and studies that reported PFAA concentrations only at the surface were excluded. Only five studies reported the organic carbon content of the soil, which was used to examine the effects of the organic carbon content in the soil. Annual precipitation value was collected based on historic precipitation data at all locations to analyze the effect of annual precipitation amount on the subsurface depth corresponding to maximum PFAA concentration. To examine the ability of soil particles to facilitate the transport of PFOA and PFOS, we analyzed 11 studies and correlated the adsorption affinity of both PFAAs with soil mineralogy including the organic carbon, cation exchange capacity, iron oxide, and aluminum oxide. It should be noted that the concentration of PFAA in soils was based on the studies that measured PFAA concentration in hotspots, and background concentrations are not often reported in these studies. Thus, the conclusion on soil is applicable to the hotspots, although particles released from these hotspots could contribute to pollution downstream. The list of studies included in the analysis is provided in an online open-access repository: Figshare (Borthakur et al., 2020).

Table 2-1: Criteria used to select studies and synthesize data reported in this study.

Keyword Combination	Total search results	Selected entries	Total entries used for analysis[a]	Figure for which data used	Selection criteria
PFAS+Properties	195	30	13	Figure 2-2	Papers reporting the solubility of PFAAs at 25 °C, the organic-carbon partitioning coefficient and the vapor pressure at 25 °C were selected.
PFAS+Water	784	63	3	Figure 2-3	Papers reporting PFAA concentrations in bed sediments and suspended sediments in surface water samples
PFAS+Soil	146	105	8	Figure 2-4	Papers reporting PFAS concentrations in different soil depths were selected
			4	Figure 2-6	Papers reporting PFAS concentrations in different soil depths along with the surface soil organic carbon content or the location of the study site were selected
			11	Figure 2-8	Papers reporting K_d for PFAA sorption onto soils and sediments. Papers reporting K_f and n values for PFAA sorption were also selected and the K_d values at 10 μg L^{-1} were determined (Set arbitrarily based on (Chen et al., 2012)) Papers should also characterize soils for their organic carbon, Cation exchange capacity iron oxide and aluminum oxide content

Note: [a]This is the final number of papers used for analysis comprising those selected from Web of Science + papers cited in our initial shortlist + new research

2.3. Contribution of suspended particles on PFAA transport

2.3.1. Surface water

Runoff from source zones typically carries dissolved PFAAs and eroded particles to surface waters. Most studies account for the contribution of dissolved PFAAs on surface water pollution, even though the eroded particles could very well contain a high concentration of pollutants as the soil in the source zone. Our analysis reveals that suspended particles in surface water bodies often contain a disproportionally higher concentration of PFAAs than the sediment below the water columns, and the suspended particles are enriched with perfluoroalkane sulfonic acids (PFSAs) to a greater extent than perfluoroalkyl carboxylic acids (PFCAs) (Figure 2-3), possibly due to the higher affinity of PFSAs to suspended sediments than that of PFCAs. The data for the Figure 2-3 is shown in Table 2-2. In suspended sediments, K_{oc} values of PFSAs is 5.1-5.8 times greater than K_{oc} of PFCAs for the same carbon chain length (Ahrens et al., 2010), whereas, in sediments, the K_{oc} values of PFSAs are 1.7 times greater than the K_{oc} values of PFCAs (Higgins and Luthy, 2006). A higher concentration of PFAAs in suspended particles could be due to many different reasons. Suspended particles have a higher specific surface area due to their small size which enhances adsorption (Li et al., 2019). In addition, bioaccumulation of PFAAs by algae and other organisms can also increase the PFAA concentrations in suspended particles (Ahrens et al., 2010). Suspended particles may also be precontaminated by PFAA before being carried by runoff into surface water sources (Chen et al., 2019; Xiao et al., 2012). However, source appropriation based on particle-associated PFAS requires a further environmental forensic approach, which has not been explored in detail. The relative concentration of PFAAs in particles or sediment could depend on their surface chemistry or mineralogy such as the fraction of organic carbon (Higgins and Luthy, 2006; Li et al., 2019, 2018). As organic carbon fraction in sediment and particle could

vary widely, this could add uncertainty in estimating the relative concentration of PFAAs in sediment and suspended particles. Nevertheless, our result indicates that suspended particles could transport a significant amount of PFAAs in surface water and recontaminate sediments. This could lower the effectiveness of remediation of impacted sediments in a surface water body and delay the cleanup effort of sediment. The concentration of suspended particles in water above sediments could depend on the rate at which the suspended particles can agglomerate and deposit on the sediments and the rate at which the deposited particles are resuspended by fluid turbulence or shear force (Turner and Millward, 2002). The resuspension of particles can increase the concentration of PFAS in the water. Thus, the best management method to prevent erosion and trap sediments in the source zones could protect surface water and sediment from particles containing PFAAs.

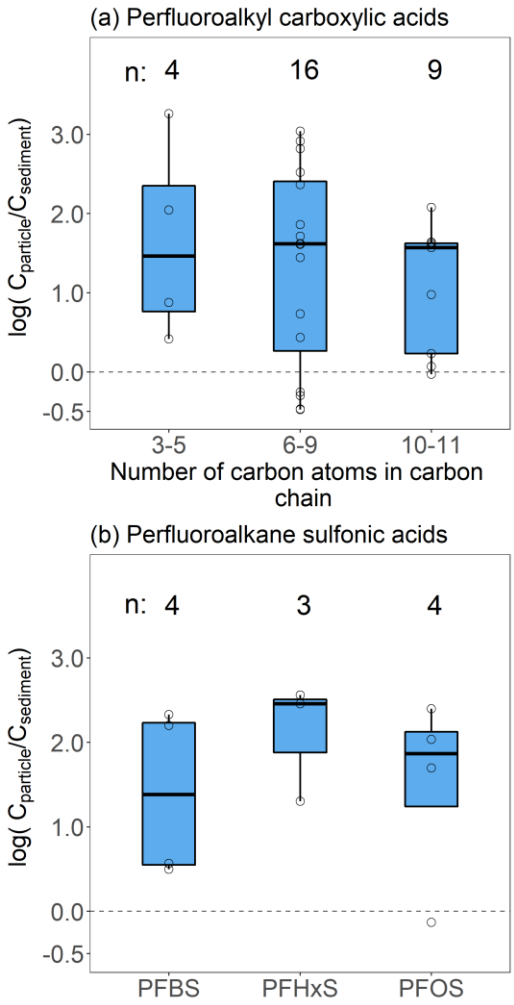

Figure 2-3: The ratio of (a) perfluoroalkyl carboxylic acid concentration and (b) perfluoroalkane sulfonic acid concentration in suspended particles and bed sediments. Each ratio value is illustrated in white circles and the boxes denote the 95% confidence interval for the overall data. Values below the 0 line indicate that the PFAA concentration in the sediments is higher than that in the suspended particles. Values above the 0 line indicate that the PFAA concentration in the suspended particles is higher than that in the sediments.

Table 2-2: Ratio of PFAA concentrations in suspended particles ($C_{particle}$) and sediments ($C_{sediments}$).

PFAA	$Log(\frac{C_{particle}}{C_{sediment}})$	Reference	DOI
PFHxA	3.26	Huiting Chen, et al. (2019)	https://doi.org/10.1016/j.watres.2019.02.009
PFBA	0.42	Zhao et al. (2016)	10.1016/j.scitotenv.2016.05.221
PFHxA	2.04	Chen et al. (2015)	https://doi.org/10.1016/j.watres.2015.04.032
PFHxA	0.88	Chen et al. (2015)	https://doi.org/10.1016/j.watres.2015.04.032
PFHpA	3.04	Huiting Chen, et al. (2019)	https://doi.org/10.1016/j.watres.2019.02.009
PFOA	2.82	Huiting Chen, et al. (2019)	https://doi.org/10.1016/j.watres.2019.02.009
PFNA	2.92	Huiting Chen, et al. (2019)	https://doi.org/10.1016/j.watres.2019.02.009
PFDA	2.52	Huiting Chen, et al. (2019)	https://doi.org/10.1016/j.watres.2019.02.009
PFHpA	-0.47	Zhao et al. (2016)	10.1016/j.scitotenv.2016.05.221
PFOA	-0.25	Zhao et al. (2016)	10.1016/j.scitotenv.2016.05.221
PFNA	-0.48	Zhao et al. (2016)	10.1016/j.scitotenv.2016.05.221
PFDA	-0.3	Zhao et al. (2016)	10.1016/j.scitotenv.2016.05.221
PFHpA	1.86	Chen et al. (2015)	https://doi.org/10.1016/j.watres.2015.04.032
PFOA	2.37	Chen et al. (2015)	https://doi.org/10.1016/j.watres.2015.04.032
PFNA	1.71	Chen et al. (2015)	https://doi.org/10.1016/j.watres.2015.04.032
PFDA	1.44	Chen et al. (2015)	https://doi.org/10.1016/j.watres.2015.04.032
PFHpA	0.73	Chen et al. (2015)	https://doi.org/10.1016/j.watres.2015.04.032
PFOA	1.62	Chen et al. (2015)	https://doi.org/10.1016/j.watres.2015.04.032
PFNA	0.44	Chen et al. (2015)	https://doi.org/10.1016/j.watres.2015.04.032
PFDA	1.61	Chen et al. (2015)	https://doi.org/10.1016/j.watres.2015.04.032
PFUnA	2.08	Huiting Chen, et al. (2019)	https://doi.org/10.1016/j.watres.2019.02.009
PFDoA	1.6	Huiting Chen, et al. (2019)	https://doi.org/10.1016/j.watres.2019.02.009
PFTrA	1.57	Huiting Chen, et al. (2019)	https://doi.org/10.1016/j.watres.2019.02.009
PFUdA	0.07	Zhao et al. (2016)	10.1016/j.scitotenv.2016.05.221
PFDoA	-0.03	Zhao et al. (2016)	10.1016/j.scitotenv.2016.05.221
PFUnA	0.98	Chen et al. (2015)	https://doi.org/10.1016/j.watres.2015.04.032
PFDoA	0.23	Chen et al. (2015)	https://doi.org/10.1016/j.watres.2015.04.032

PFUnA	1.64	Chen et al. (2015)	https://doi.org/10.1016/j.watres.2015.04.032
PFDoA	1.62	Chen et al. (2015)	https://doi.org/10.1016/j.watres.2015.04.032
PFBS	2.33	Huiting Chen, et al. (2019)	https://doi.org/10.1016/j.watres.2019.02.009
PFBS	0.5	Zhao et al. (2016)	10.1016/j.scitotenv.2016.05.221
PFBS	0.57	Chen et al. (2015)	https://doi.org/10.1016/j.watres.2015.04.032
PFBS	2.2	Chen et al. (2015)	https://doi.org/10.1016/j.watres.2015.04.032
PFHxS	2.46	Huiting Chen, et al. (2019)	https://doi.org/10.1016/j.watres.2019.02.009
PFHxS	2.56	Chen et al. (2015)	https://doi.org/10.1016/j.watres.2015.04.032
PFHxS	1.3	Chen et al. (2015)	https://doi.org/10.1016/j.watres.2015.04.032
PFOS	2.4	Huiting Chen, et al. (2019)	https://doi.org/10.1016/j.watres.2019.02.009
PFOS	-0.13	Zhao et al. (2016)	10.1016/j.scitotenv.2016.05.221
PFOS	1.7	Chen et al. (2015)	https://doi.org/10.1016/j.watres.2015.04.032
PFOS	2.03	Chen et al. (2015)	https://doi.org/10.1016/j.watres.2015.04.032

2.3.2. Subsurface soil

The subsurface zone is the unsaturated region connecting surface water and soil to groundwater aquifer. Impacted surface runoff passes through the subsurface zone before reaching groundwater, so the subsurface zone acts as a natural filter to remove particles in surface runoff and adsorb pollutants. However, accumulation of PFAA and PFAA-containing particles in subsurface soil and transformation of PFAA precursors in aerobic conditions could make subsurface soils serve as a secondary source for PFAAs to groundwater (Weber et al., 2017). A recent review (Sharifan et al., 2021) highlights the importance of all relevant processes that affect the fate of PFASs in subsurface soil. Briefly, PFAS and their precursors can be removed by adsorption to soil minerals, air-water interfaces, and microbial biomass or roots, translocated into plants, and degraded or transformed by soil microorganisms. However, it is unknown to what extent suspended particles can influence the distribution of PFAAs in the subsurface by these processes.

To compare the vertical migration of PFAAs in subsurface soils between sites, we normalized the concentration at all depths by dividing them by the maximum or peak PFAA concentration found at the site. Thus, the location with a relative concentration of 1 represents the location corresponding to peak or concentration maxima. Our analysis reveals that the concentration of most PFAAs decreased steadily with increases in depth surveyed (Figure 2-4). The data for Figure 2-4 is shown in Table 2-3. Most PFAAs are retained within 5 m below ground surface, although concentration varied widely for all types of PFAAs, except PFOS, within the top 5 m below the ground surface at all sites surveyed. There was also limited data available beyond 5 m depth, and the groundwater table locations in most sites were not reported. Our result is similar to a previous study that measured PFAS concentration in two cores up to 15 m depth (Nickerson et al., 2020). Both cores in that study showed a contrasting concentration profile within the top 5 m below the ground surface: while concentration increased in one core, it decreased in the other. The difference was attributed to high clay content and organic carbon that limit infiltration at the site (Nickerson et al., 2020). Beyond the top 5 m, the location of groundwater table, PFAS concentrations decreased at both sites. The result indicates that soil heterogeneity such as differences in pore size and organic carbon content between different sites could explain the inconsistent distribution of PFAAs within the first 5 m soil below ground surface.

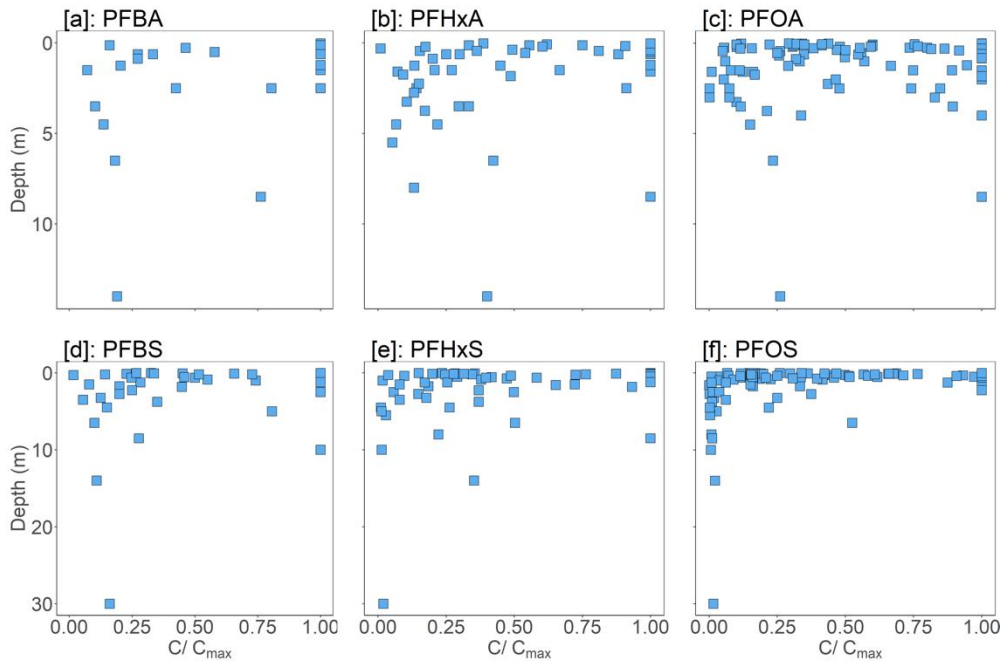

Figure 2-4: Depth profiles of (a) PFBA, (b) PFHxA, (c) PFOA, (d) PFBS, (e) PFHxS and (f) PFOS in the subsurface. Most PFAS are located near the surface indicating subsurface as a long-term reservoir of PFAS.

Table 2-3: List of references used for soil PFAA concentrations.

Reference	**Study area**	**PFAA tested**	**DOI**
Bao et al. (2018)	Well drilling site exposed to 10 years of PFAS contamination in Beijing.	PFBS, PFHxS, PFOS	https://doi.org/10.1007/s13213-018-1346-y
Dauchy et al., (2019)	Firefighting training area in France.	PFBA, PFHxA, PFOA, PFBS, PFHxS, PFOS	https://doi.org/10.1016/j.chemosphere.2018.10.003
Filipovic et al. (2015)	Air force base in Tullinge Riksten, Sweden.	PFOA	https://doi.org/10.1016/j.chemosphere.2014.09.005
Groffen et al. (2019)	Around a 3M fluorochemical plant in Antwerp, Belgium.	PFBA, PFOA, PFOS	https://doi.org/10.1016/j.chemosphere.2019.124407
Hale et al. (2017)	Firefighting training facility west of Oslo airport, Norway.	PFBA, PFOA	https://doi.org/10.1016/j.chemosphere.2016.12.057
SFT (2009)	4 firefighting training facilities.	PFHxA, PFOA, PFBS, PFHxS	https://evalueringsportalen.no/evaluering/screening-of-polyfluorinated-organic-compounds-at-four-fire-training-facilities-in-norway/ta2444.pdf/@@inline
Washington et al. (2010)	Sludge applied soils.	PFHxA, PFOA, PFHxS, PFOS	https://doi.org/10.1021/es1003846
Xiao et al. (2015)	Soil samples along US highway 10 from the location of a former PFAS manufacturing facility to City of Big Lake.	PFOA, PFOS	https://doi.org/10.1016/j.watres.2014.09.052

Except for PFOS, all other PFAAs showed high variability within the first 5 m below ground surface. There could be several reasons for the variability within the top 5 m of subsurface soil. First, PFAAs may migrate down the subsurface due to leaching and redistribution of PFAAs in the subsurface. Sorbed PFAS compounds can desorb and leach from the soil, which can lead to their downward migration through the subsurface (Gellrich et al., 2012). This is supported by the fact that the variability in data increases with the decrease in K_d of the compound, as the desorption of PFAAs increase with the decrease in K_d of the compound (Milinovic et al., 2015). Because PFOS has a high affinity and low desorption coefficient, its concentration profile in the subsurface exhibited the lowest variability. However, despite relatively high K_d of PFOA and PFHxS, there is significant variability in the concentrations at different depths of the subsurface. Therefore, in addition to desorption, the release of suspended particles from the surface soil may also be contributing to the downward migration of PFAA compounds, especially those with high K_d values. Another cause of an inconsistent location for maximum PFAA concentrations within the top 3 m in the subsurface, where conditions are likely more oxic, could be enhanced transformation of polyfluorinated precursors by microbial communities (Dasu et al., 2013; Hamid et al., 2020; Zhang et al., 2017). Analyzing 20 studies on the biotransformation of PFAA precursors, we observed that the PFAA precursor transformation rate by aerobic bacteria is an order of magnitude faster than that of anaerobic bacteria (Figure 2-5**,** Table 2-4, 2-5, 2-6). Biotransformation of cationic and zwitterionic precursors, which strongly bind to negatively charged soil, to less sorptive anionic PFAAs may enhance PFAS mobility in the subsurface. The implications are that precursor transformation and thus downward migration of PFASs in the topsoil may proceed at a faster rate. For instance, 6:2 fluorotelomer thioether propionate has been shown to transform into stable compounds that do not transform to PFAAs under anaerobic conditions (Yi et al., 2018).

The analysis also reveals that biotransformation depends on functional groups on the precursors: hydroxyl groups are highly susceptible to enzymic oxidation whereas the urethane group is least susceptible, possibly due to the unavailability of urethane oxidizing enzymes in most soil microorganisms. Similarly, precursors with an ether group are recalcitrant to microbial cleavage (Chen et al., 2018). Our analysis shows no significant difference ($p>0.05$) between the half-lives of non-ionic, anionic, and zwitterionic precursors. Adsorption of cationic and zwitterionic precursors to soil minerals could reduce their bioavailability, consequently the likelihood of them being transformed to PFAAs (Mejia-Avendano et al., 2020). In particular, cationic and zwitterionic precursors are more susceptible to particle-facilitated transport due to their strong affinity to suspended particles that have a net negative surface charge (Ahrens et al., 2010; Chen et al., 2015). Particle association could also reduce their bioavailability. Therefore, biotransformation of cationic and zwitterionic PFAA precursors in the presence of suspended particles should be examined.

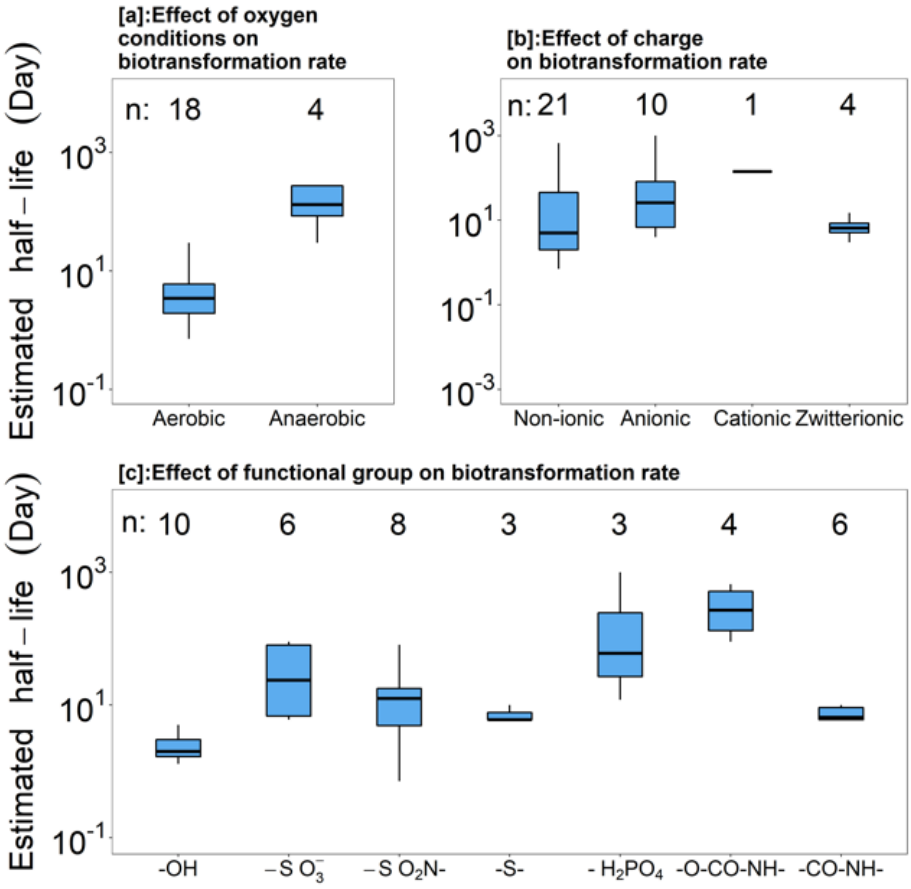

Figure 2-5: (a) Comparison of half-lives of precursors subjected to aerobic and anaerobic biodegradation (*$p < 0.02$) (b) Effects of charge on half-lives of precursors subjected to aerobic biodegradation (c) Effects of a functional group on half-lives of precursors subjected to aerobic biotransformation.

Table 2-4: Effect of oxygen conditions on transformation of PFAA precursor.

Condition	Compound	Half-life (Day)	Reference	DOI
Aerobic	6:2FTOH	1.6	Liu et al. 2010	10.1016/j.chemosphere.2009.10.044
Aerobic	6:2FTOH	1.3	Liu et al. 2010	10.1016/j.chemosphere.2009.10.044
Aerobic	6:2FTOH	3	Zhang et al. 2017a	10.1016/j.scitotenv.2016.09.214
Aerobic	6:2FTOH	3	Zhang et al. 2017a	10.1016/j.scitotenv.2016.09.214
Aerobic	6:2FTOH	1.9	Zhao et al. 2013a	10.1016/j.chemosphere.2012.06.035
Aerobic	6:2FTOH	1.5	Zhao et al. 2013b	10.1016/j.chemosphere.2013.02.032
Aerobic	6:2FTOH	28	Tseng et al. 2014	10.1021/es4057483
Aerobic	8:2FTOH	2	Dinglasan et al. 2004	10.1021/es0350177
Aerobic	8:2FTOH	5	Wang et al. 2005	10.1021/es0506760
Aerobic	8:2FTOH	2	Dasu et al. 2012	10.1021/es203978g
Aerobic	8:2FTOH	45	Hamid et al. 2020a	10.1016/j.scitotenv.2020.136547
Aerobic	4:2 FtTAoS	6	Harding-Marjanovic et al. 2015	10.1021/acs.est.5b01219
Aerobic	6:2 FtTAoS	6	Harding-Marjanovic et al. 2015	10.1021/acs.est.5b01219
Aerobic	8:2 FtTAoS	10	Harding-Marjanovic et al. 2015	10.1021/acs.est.5b01219
Aerobic	EtFOSE	4	Zhang et al. 2017b	10.1016/j.envpol.2017.05.074
Aerobic	EtFOSE	30	Zhang et al. 2017b	10.1016/j.envpol.2017.05.074
Aerobic	EtFOSE	5.23	Avendano and Liu 2015	10.1016/j.chemosphere.2014.09.059
Aerobic	EtFOSE	0.71	Rhoads et al. 2008	10.1021/es702866c
Anaerobic	6:2FTOH	30	Zhang et al. 2013	10.1021/es4000824
Anaerobic	8:2FTOH	145	Zhang et al. 2013	10.1021/es4000824
Anaerobic	6:2 FtTAoS	120	Yi et al. 2018	10.1021/acs.estlett.8b00148
Anaerobic	EtFOSE	1860	Lange 2018	10.1002/etc.4014

Table 2-5: Effect of functional group on PFAA precursor transformation.

Functional Group	Compound	Half-life (Day)	Reference	DOI
-OH Hydroxyl Group	6:2FTOH	1.6	Liu et al. 2010	10.1016/j.chemosphere.2009.10.044
-OH Hydroxyl Group	6:2FTOH	1.3	Liu et al. 2010	10.1016/j.chemosphere.2009.10.044
-OH Hydroxyl Group	6:2FTOH	3	Zhang et al. 2017a	10.1016/j.scitotenv.2016.09.214
-OH Hydroxyl Group	6:2FTOH	3	Zhang et al. 2017a	10.1016/j.scitotenv.2016.09.214
-OH Hydroxyl Group	6:2FTOH	1.9	Zhao et al. 2013a	10.1016/j.chemosphere.2012.06.035
-OH Hydroxyl Group	6:2FTOH	1.5	Zhao et al. 2013b	10.1016/j.chemosphere.2013.02.032
-OH Hydroxyl Group	8:2FTOH	2	Dinglasan et al. 2004	10.1021/es0350177
-OH Hydroxyl Group	8:2FTOH	5	Wang et al. 2005	10.1021/es0506760
-OH Hydroxyl Group	8:2FTOH	2	Dasu et al. 2012	10.1021/es203978g
-OH Hydroxyl Group	8:2FTOH	45	Hamid et al. 2020a	10.1016/j.scitotenv.2020.136547
-SO3H Sulfonic Acid Group	6:2 FTSA	56	Chen et al. 2019	10.1360/TB-2019-0126
-SO3H Sulfonic Acid Group	6:2 FTSA	90	Hamid et al. 2020a	10.1016/j.scitotenv.2020.136547
-SO3H Sulfonic Acid Group	6:2 FTSA	90	Wang et al. 2011	10.1016/j.chemosphere.2010.11.003
-SO3H Sulfonic Acid Group	4:2 FtTAoS	6	Harding-Marjanovic et al. 2015	10.1021/acs.est.5b01219
-SO3H Sulfonic Acid Group	6:2 FtTAoS	6	Harding-Marjanovic et al. 2015	10.1021/acs.est.5b01219
-SO3H Sulfonic Acid Group	8:2 FtTAoS	10	Harding-Marjanovic et al. 2015	10.1021/acs.est.5b01219
-SO2-N-Sulfonamide Group	EtFOSA linear	11.2	Liu et al. 2019	10.1016/j.scitotenv.2018.09.214
-SO2-N-Sulfonamide Group	EtFOSA branch	80.8	Liu et al. 2019	10.1016/j.scitotenv.2018.09.214
-SO2-N-Sulfonamide Group	N-EtFOSA	13.9	Avendano and Liu 2015	10.1016/j.chemosphere.2014.09.059
-SO2-N-Sulfonamide Group	EtFOSE	4	Zhang et al. 2017b	10.1016/j.envpol.2017.05.074
-SO2-N-Sulfonamide Group	EtFOSE	30	Zhang et al. 2017b	10.1016/j.envpol.2017.05.074
-SO2-N-Sulfonamide Group	EtFOSE	5.23	Avendano and Liu 2015	10.1016/j.chemosphere.2014.09.059

-SO2-N- Sulfonamide Group	PFOSNO	15	Chen et al., 2020	10.1021/acs.estlett.0c00543
-SO2-N- Sulfonamide Group	EtFOSE	0.71	Rhoads et al. 2008	10.1021/es702866c
-S- Sulfide Group	4:2 FtTAoS	6	Harding-Marjanovic et al. 2015	10.1021/acs.est.5b01219
-S- Sulfide Group	6:2 FtTAoS	6	Harding-Marjanovic et al. 2015	10.1021/acs.est.5b01219
-S- Sulfide Group	8:2 FtTAoS	10	Harding-Marjanovic et al. 2015	10.1021/acs.est.5b01219
Phosphate ester	6:2 diPAP	12	Liu and Liu 2016	10.1016/j.envpol.2016.01.069
Phosphate ester	6:2 diPAP	60	Lee et al. 2014	10.1021/es403949z
Phosphate ester	8:2 diPAP	1000	Liu and Liu 2016	10.1016/j.envpol.2016.01.069
-O-CO-NH- Urethane Group	FTU	90	Dasu and Lee 2016	10.1016/j.chemosphere.2015.11.021
-O-CO-NH- Urethane Group	FTU	150	Dasu and Lee 2016	10.1016/j.chemosphere.2015.11.021
-O-CO-NH- Urethane Group	HMU	477	Dasu and Lee 2016	10.1016/j.chemosphere.2015.11.021
-O-CO-NH- Urethane Group	HMU	666	Dasu and Lee 2016	10.1016/j.chemosphere.2015.11.021
-CO-NH- Peptide Group	4:2 FtTAoS	6	Harding-Marjanovic et al. 2015	10.1021/acs.est.5b01219
-CO-NH- Peptide Group	6:2 FtTAoS	6	Harding-Marjanovic et al. 2015	10.1021/acs.est.5b01219
-CO-NH- Peptide Group	8:2 FtTAoS	10	Harding-Marjanovic et al. 2015	10.1021/acs.est.5b01219
-CO-NH- Peptide Group	PFOAAmS	142	Mejia-Avendano et al. 2016	10.1021/acs.est.6b00140
-CO-NH- Peptide Group	PFOANO	3	Chen et al., 2020	10.1021/acs.estlett.0c00543
-CO-NH- Peptide Group	PFOANO	7	Chen et al., 2020	10.1021/acs.estlett.0c00543

Table 2-6: Effect of charge on PFAA transformation.

Charge	Compound	Half-life (Day)	Reference	DOI
Non-ionic	6:2FTOH	1.6	Liu et al. 2010	10.1016/j.chemosphere.2009.10.044
Non-ionic	6:2FTOH	1.3	Liu et al. 2010	10.1016/j.chemosphere.2009.10.044
Non-ionic	6:2FTOH	3	Zhang et al. 2017a	10.1016/j.scitotenv.2016.09.214
Non-ionic	6:2FTOH	3	Zhang et al. 2017a	10.1016/j.scitotenv.2016.09.214
Non-ionic	6:2FTOH	1.9	Zhao et al. 2013a	10.1016/j.chemosphere.2012.06.035
Non-ionic	6:2FTOH	1.5	Zhao et al. 2013b	10.1016/j.chemosphere.2013.02.032
Non-ionic	8:2FTOH	2	Dinglasan et al. 2004	10.1021/es0350177
Non-ionic	8:2FTOH	5	Wang et al. 2005	10.1021/es0506760
Non-ionic	8:2FTOH	2	Dasu et al. 2012	10.1021/es203978g
Non-ionic	8:2FTOH	45	Hamid et al. 2020a	10.1016/j.scitotenv.2020.136547
Non-ionic	EtFOSA linear	11.2	Liu et al. 2019	10.1016/j.scitotenv.2018.09.214
Non-ionic	EtFOSA branch	80.8	Liu et al. 2019	10.1016/j.scitotenv.2018.09.214
Non-ionic	N-EtFOSA	13.9	Avendano and Liu 2015	10.1016/j.chemosphere.2014.09.059
Non-ionic	EtFOSE	4	Zhang et al. 2017b	10.1016/j.envpol.2017.05.074
Non-ionic	EtFOSE	30	Zhang et al. 2017b	10.1016/j.envpol.2017.05.074
Non-ionic	EtFOSE	5.23	Avendano and Liu 2015	10.1016/j.chemosphere.2014.09.059
Non-ionic	EtFOSE	0.71	Rhoads et al. 2008	10.1021/es702866c
Non-ionic	FTU	90	Dasu and Lee 2016	10.1016/j.chemosphere.2015.11.021
Non-ionic	FTU	150	Dasu and Lee 2016	10.1016/j.chemosphere.2015.11.021
Non-ionic	HMU	477	Dasu and Lee 2016	10.1016/j.chemosphere.2015.11.021
Non-ionic	HMU	666	Dasu and Lee 2016	10.1016/j.chemosphere.2015.11.021
Anionic	6:2 FTSA	56	Chen et al. 2019	10.1360/TB-2019-0126

Anionic	6:2 FTSA	90	Hamid et al. 2020a	10.1016/j.scitotenv.2020.136547
Anionic	6:2 FTSA	90	Wang et al. 2011	10.1016/j.chemosphere.2010.11.003
Anionic	4:2 FtTAoS	6	Harding-Marjanovic et al. 2015	10.1021/acs.est.5b01219
Anionic	6:2 FtTAoS	6	Harding-Marjanovic et al. 2015	10.1021/acs.est.5b01219
Anionic	8:2 FtTAoS	10	Harding-Marjanovic et al. 2015	10.1021/acs.est.5b01219
Anionic	6:2 diPAP	12	Liu and Liu 2016	10.1016/j.envpol.2016.01.069
Anionic	6:2 diPAP	60	Lee et al. 2014	10.1021/es403949z
Anionic	8:2 diPAP	1000	Liu and Liu 2016	10.1016/j.envpol.2016.01.069
Cationic	PFOAAmS	142	Mejia-Avendano et al. 2016	10.1021/acs.est.6b00140
Zwitterionic	PFOANO	3	Chen et al., 2020	10.1021/acs.estlett.0c00543
Zwitterionic	PFOANO	7	Chen et al., 2020	10.1021/acs.estlett.0c00543
Zwitterionic	PFOSNO	15	Chen et al., 2020	10.1021/acs.estlett.0c00543

The subsurface can also adsorb aqueous PFAAs and filter PFAA-impacted particles from infiltrating water, and the impacted region can subsequently release the PFAAs over longer periods. Moreover, the advancement of air-water interfaces during intermittent rainfall cycles can also dislodge particles from the soil trapped at these interfaces (Flury and Aramrak, 2017). In particular, natural environmental conditions such as dry-wet and freeze-thaw cycles have been shown to accelerate the release of mobile particles in the subsurface (Mohanty et al., 2015, 2014). If the particles contain sorbed PFAAs, they can transport the PFAAs as well. Several studies have examined the retention mechanisms of aqueous PFAAs in the subsurface soil (Brusseau, 2018; Guelfo and Higgins, 2013; Silva et al., 2019), but they rarely included particle-mediated transport and release. Aqueous PFAAs in infiltrating water have been shown to adsorb on pore walls, infiltrate into the soil matrix, or accumulate at air-water interfaces (Brusseau, 2019; Lyu et al., 2018; Meng et al., 2014). Thus, the relative contribution of these processes on PFAS retention could vary with several factors: (a) soil organic carbon that affects adsorption on pore walls, (b)

the pore-size distribution that affects infiltration rate through the subsurface, and (c) the relative saturation of the soil that affects total air-water interface areas available for PFAA retention. Thus, these factors are expected to affect the soil depth corresponding to maximum PFAA concentration.

Analyzing the vertical distribution of PFOA and PFOS in subsurface soils within 4 m from ground surface reported in five studies (Table 2-7), we found that depth corresponding to their concentration maxima increases with decreases in the organic carbon content of soil (Figure 2-6a). The result indicates that organic carbon is an important factor that can affect peak depth. Thus, particles eroded from organic-rich soil could facilitate the transport of PFAAs in water and subsurface, similar to how they enhance the transport of other organic pollutants (Grolimund et al., 1996). It should be noted that other soil properties such as hydraulic conductivity, soil chemical heterogeneity, air-water interface, and protein, iron oxide, and manganese oxide content may also contribute to variable PFAA transport in subsurface soil (Gellrich et al., 2012; Guelfo et al., 2020; Hoisaeter et al., 2019; Longstaffe et al., 2012; Lyu et al., 2018; Ololade et al., 2016). A previous study (Anderson et al., 2019) observed an increase in PFAA sorption onto the soil with an increase in organic carbon content and decreasing clay content. Moreover, they also observed an increase in PFAA transport with the degree of flushing. Future studies can similarly try to correlate the transport of PFAAs through the subsurface with different soil and environmental parameters.

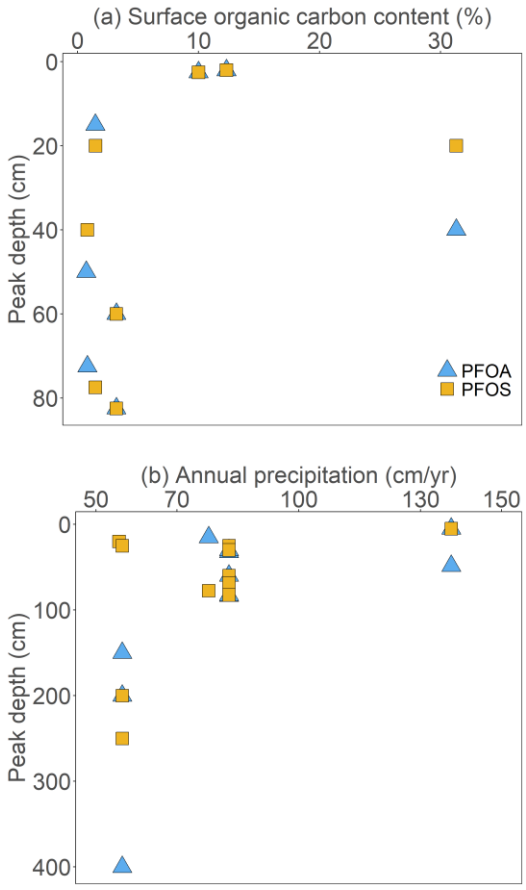

Figure 2-6: Change in the depth of maximum PFAA concentrations in the subsurface with (a) soil organic carbon content (%) and (b) annual precipitation (cm year^{-1}). Note a difference in the y-axis range.

Table 2-7: Effect of organic carbon content on the soil surface on the depth of maximum PFAA concentration.

PFAA	Surface organic carbon (%)	Peak depth (cm)	Reference	DOI
PFOA	3.2	60	Xiao et al (2015)	https://doi.org/10.1016/j.watres.2014.09.052
PFOA	3.2	82.5	Xiao et al (2015)	https://doi.org/10.1016/j.watres.2014.09.052
PFOA	1.47	15	Groffen et al. (2019)	https://doi.org/10.1016/j.chemosphere.2019.124407
PFOA	31.3	40	SFT (2009)	https://evalueringsportalen.no/evaluering/screening-of-polyfluorinated-organic-compounds-at-four-fire-training-facilities-in-norway/ta2444.pdf/@@inline
PFOA	0.8	72.5	SFT (2009)	https://evalueringsportalen.no/evaluering/screening-of-polyfluorinated-organic-compounds-at-four-fire-training-facilities-in-norway/ta2444.pdf/@@inline
PFOA	12.3	2	SFT (2009)	https://evalueringsportalen.no/evaluering/screening-of-polyfluorinated-organic-compounds-at-four-fire-training-facilities-in-norway/ta2444.pdf/@@inline
PFOA	10	2.5	SFT (2009)	https://evalueringsportalen.no/evaluering/screening-of-polyfluorinated-organic-compounds-at-four-fire-training-facilities-in-norway/ta2444.pdf/@@inline
PFOA	0.72	50	Hale et al. (2017)	https://doi.org/10.1016/j.chemosphere.2016.12.057
PFOS	3.2	60	Xiao et al (2015)	https://doi.org/10.1016/j.watres.2014.09.052
PFOS	3.2	82.5	Xiao et al (2015)	https://doi.org/10.1016/j.watres.2014.09.052
PFOS	1.47	77.5	Groffen et al. (2019)	https://doi.org/10.1016/j.chemosphere.2019.124407
PFOS	1.48	20	Bao et al (2018)	https://doi.org/10.1007/s13213-018-1346-y
PFOS	31.3	20	SFT (2009)	https://evalueringsportalen.no/evaluering/screening-of-polyfluorinated-organic-compounds-at-four-fire-training-facilities-in-norway/ta2444.pdf/@@inline
PFOS	0.8	40	SFT (2009)	https://evalueringsportalen.no/evaluering/screening-of-polyfluorinated-organic-compounds-at-four-fire-training-facilities-in-norway/ta2444.pdf/@@inline
PFOS	12.3	2	SFT (2009)	https://evalueringsportalen.no/evaluering/screening-of-polyfluorinated-organic-compounds-at-four-fire-training-facilities-in-norway/ta2444.pdf/@@inline
PFOS	10	2.5	SFT (2009)	https://evalueringsportalen.no/evaluering/screening-of-polyfluorinated-organic-compounds-at-four-fire-training-facilities-in-norway/ta2444.pdf/@@inline

Table 2-8. Effect of precipitation rate on the depth of maximum PFAA concentration.

PFAA	Precipitation (cm/yr)	Peak depth (cm)	Reference	doi
PFOAA	137.6	5	Washington (2010)	https://doi.org/10.1021/es1003846
PFOA	137.6	48.5	Washington (2010)	https://doi.org/10.1021/es1003846
PFOA	137.6	5	Washington (2010)	https://doi.org/10.1021/es1003846
PFOA	82.8	32.5	Xiao et al (2015)	https://doi.org/10.1016/j.watres.2014.09.052
PFOA	82.8	30	Xiao et al (2015)	https://doi.org/10.1016/j.watres.2014.09.052
PFOA	82.8	60	Xiao et al (2015)	https://doi.org/10.1016/j.watres.2014.09.052
PFOA	82.8	83.5	Xiao et al (2015)	https://doi.org/10.1016/j.watres.2014.09.052
PFOA	82.8	82.5	Xiao et al (2015)	https://doi.org/10.1016/j.watres.2014.09.052
PFOA	77.8	15	Groffen et al. (2019)	https://doi.org/10.1016/j.chemosphere.2019.124407
PFOA	56.5	150	Filipovic et al (2015)	https://doi.org/10.1016/j.chemosphere.2014.09.005
PFOA	56.5	200	Filipovic et al (2015)	https://doi.org/10.1016/j.chemosphere.2014.09.005
PFOA	56.5	400	Filipovic et al (2015)	https://doi.org/10.1016/j.chemosphere.2014.09.005
PFOS	137.6	5	Washington (2010)	https://doi.org/10.1021/es1003846
PFOS	137.6	5	Washington (2010)	https://doi.org/10.1021/es1003846
PFOS	137.6	5	Washington (2010)	https://doi.org/10.1021/es1003846
PFOS	82.8	25	Xiao et al (2015)	https://doi.org/10.1016/j.watres.2014.09.052
PFOS	82.8	30	Xiao et al (2015)	https://doi.org/10.1016/j.watres.2014.09.052
PFOS	82.8	60	Xiao et al (2015)	https://doi.org/10.1016/j.watres.2014.09.052
PFOS	82.8	68.5	Xiao et al (2015)	https://doi.org/10.1016/j.watres.2014.09.052

PFOS	82.8	82.5	Xiao et al (2015)	https://doi.org/10.1016/j.watres.2014.09.052
PFOS	77.8	77.5	Groffen et al. (2019)	https://doi.org/10.1016/j.chemosphere.2019.124407
PFOS	55.7	20	Bao et al (2018)	https://doi.org/10.1007/s13213-018-1346-y
PFOS	56.5	25	Filipovic et al (2015)	https://doi.org/10.1016/j.chemosphere.2014.09.005
PFOS	56.5	250	Filipovic et al (2015)	https://doi.org/10.1016/j.chemosphere.2014.09.005
PFOS	56.5	200	Filipovic et al (2015)	https://doi.org/10.1016/j.chemosphere.2014.09.005

Generally, it is expected that an increase in precipitation in an area could increase the amount of water flushed through subsurface soil, which could increase the desorption of PFAS from subsurface soil to groundwater (Anderson et al., 2019). For instance, subsurface leaching of PFAS during intermittent infiltration of water was shown to increase with flow rate (Gellrich et al., 2012; Hoisaeter et al., 2019). Thus, the concentration maxima of PFAS compounds should move to deeper layers in subsurface soil with an increased precipitation rate. However, our analysis reveals that the depth corresponding to PFAA concentration maxima decreased with an increase in annual precipitation received at the sites assessed (Figure 2-6b, Table 2-8). In other words, PFAAs are accumulated near the surface in areas receiving high annual precipitation. We attributed the cause of this trend to an increase in erosion in the source zone by high rainfall and a corresponding increase in loading of impacted particles to the area surveyed. Consequently, areas receiving high rainfall amounts can deposit more impacted particles downstream, most of which are filtered out in topsoil (Tondera et al., 2013). Thus, erosion control measures should be implemented in the source zone, and green infrastructures should be used to capture impacted particles. It should be noted that the soil types, not only the precipitation amount, determine the

amount of runoff that infiltrates into the ground. However, hydraulic conductivity data was not provided in the assessed studies to confirm this hypothesis. Another possibility of the high accumulation of PFAAs near the surface compared to deeper soil in wet climates is that deeper soils in wetter climates remain submerged most of the time, thereby developing anoxic conditions. In contrast, near-surface soil could drain and become oxic. Thus, the biotransformation rate of precursors at the deeper depths will be lower in wetter climates than drier climates. Thus, further study should examine the effect of climate conditions on precursor transformation in subsurface soils.

2.3.3. Air

As most PFAS are non-volatile, with an exception of volatile precursors, PFAS concentration in the air could be dominated by PFAS associated with dust or microplastics. Analyzing 8 studies that measured the PFAS concentration in dust samples from indoor environments, we show that a significant fraction of total PFAS measured in the air are associated with dust, aerosol, and other particulate matter, and the long-chained PFAS are enriched in the dust (Figure 2-7 a). Our analysis also reveals that an increase in PFAS chain length increases their association with dust. Increased affinity of long-chained PFAS with solid surfaces explained this observation (Chaemfa et al., 2010). The PFAS concentrations observed in these studies are comparable to other legacy organic pollutants typically found in the dust (Figure 2-7 b): polycyclic aromatic hydrocarbons (PAH), polybrominated diphenyl ethers (PBDE), and polychlorinated biphenyls (PCBs) (Basaran and Yılmaz Civan, 2021; Simonetti et al., 2020). The analysis indicates that PFAS has a similar potential of aerial transport as other organic pollutants, even though PFAS exposure via inhalation did not receive a similar level of attention as other organic pollutants.

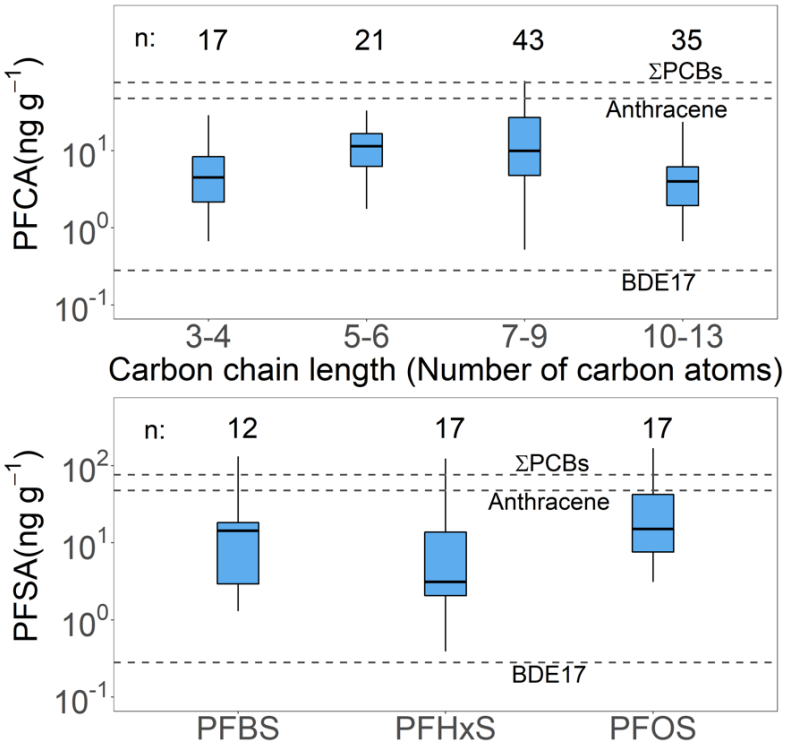

Figure 2-7: PFAS concentrations in dust emitted from land-based on 8 studies (Supplementary Material). The dashed lines refer to concentrations of ΣPCB, Anthracene and BDE-17 reported in the literature (Basaran and Yılmaz Civan, 2021; Simonetti et al., 2020).

Table 2-9: Data for PFCA concentration in air dust.

Compound	PFAS	Value(ng/g)	Author	doi
3-4 carbon	PFBA	28.8	(Besis et al., 2019)	https://doi.org/10.1016/j.ecoenv.2019.109559
3-4 carbon	PFBA	13.1	(Eriksson et al., 2015)	https://doi.org/10.1021/acs.est.5b00679
3-4 carbon	PFBA	2.16	(Eriksson et al., 2015)	https://doi.org/10.1021/acs.est.5b00679
3-4 carbon	PFBA	8.37	(Eriksson et al., 2015)	https://doi.org/10.1021/acs.est.5b00679
3-4 carbon	PFBA	12.9	(Eriksson et al., 2015)	https://doi.org/10.1021/acs.est.5b00679
3-4 carbon	PFBA	1.17	(Eriksson et al., 2015)	https://doi.org/10.1021/acs.est.5b00679
3-4 carbon	PFPeA	2.4	(Karaskova et al., 2016)	https://doi.org/10.1016/j.envint.2016.05.031
3-4 carbon	PFPeA	4.5	(Karaskova et al., 2016)	https://doi.org/10.1016/j.envint.2016.05.031
3-4 carbon	PFPeA	5.4	(Karaskova et al., 2016)	https://doi.org/10.1016/j.envint.2016.05.031
3-4 carbon	PFPeA	1.51	(Besis et al., 2019)	https://doi.org/10.1016/j.ecoenv.2019.109559
3-4 carbon	PFPeA	7.05	(Eriksson et al., 2015)	https://doi.org/10.1021/acs.est.5b00679
3-4 carbon	PFPeA	1.5	(Eriksson et al., 2015)	https://doi.org/10.1021/acs.est.5b00679
3-4 carbon	PFPeA	2.24	(Eriksson et al., 2015)	https://doi.org/10.1021/acs.est.5b00679
3-4 carbon	PFPeA	3.9	(Haug et al., 2011)	https://doi.org/10.1021/es103456h
3-4 carbon	PFPeA	5.07	(Eriksson et al., 2015)	https://doi.org/10.1021/acs.est.5b00679
3-4 carbon	PFPeA	0.67	(Eriksson et al., 2015)	https://doi.org/10.1021/acs.est.5b00679
3-4 carbon	PFPeA	8.94	(Knobeloch et al., 2012)	https://doi.org/10.1016/j.chemosphere.2012.03.082
5-6 carbon	PFHxA	12.8	(Karaskova et al., 2016)	https://doi.org/10.1016/j.envint.2016.05.031
5-6 carbon	PFHxA	14.5	(Karaskova et al., 2016)	https://doi.org/10.1016/j.envint.2016.05.031
5-6 carbon	PFHxA	20.9	(Karaskova et al., 2016)	https://doi.org/10.1016/j.envint.2016.05.031
5-6 carbon	PFHxA	11.1	(Besis et al., 2019)	https://doi.org/10.1016/j.ecoenv.2019.109559
5-6 carbon	PFHxA	17.7	(Eriksson et al., 2015)	https://doi.org/10.1021/acs.est.5b00679
5-6 carbon	PFHxA	6.24	(Eriksson et al., 2015)	https://doi.org/10.1021/acs.est.5b00679
5-6 carbon	PFHxA	17.5	(Eriksson et al., 2015)	https://doi.org/10.1021/acs.est.5b00679

5-6 carbon	PFHxA	33	(Haug et al., 2011)	https://doi.org/10.1021/es103456h
5-6 carbon	PFHxA	31.8	(Eriksson et al., 2015)	https://doi.org/10.1021/acs.est.5b00679
5-6 carbon	PFHxA	3.16	(Eriksson et al., 2015)	https://doi.org/10.1021/acs.est.5b00679
5-6 carbon	PFHpA	3.1	(Karaskova et al., 2016)	https://doi.org/10.1016/j.envint.2016.05.031
5-6 carbon	PFHpA	7.1	(Karaskova et al., 2016)	https://doi.org/10.1016/j.envint.2016.05.031
5-6 carbon	PFHpA	11.8	(Karaskova et al., 2016)	https://doi.org/10.1016/j.envint.2016.05.031
5-6 carbon	PFHpA	12.6	(Besis et al., 2019)	https://doi.org/10.1016/j.ecoenv.2019.109559
5-6 carbon	PFHpA	16.58	(ao et al., 2019)	https://doi.org/10.1016/j.envpol.2019.07.041
5-6 carbon	PFHpA	11.4	(Eriksson et al., 2015)	https://doi.org/10.1021/acs.est.5b00679
5-6 carbon	PFHpA	4.63	(Eriksson et al., 2015)	https://doi.org/10.1021/acs.est.5b00679
5-6 carbon	PFHpA	5.71	(Eriksson et al., 2015)	https://doi.org/10.1021/acs.est.5b00679
5-6 carbon	PFHpA	10	(Haug et al., 2011)	https://doi.org/10.1021/es103456h
5-6 carbon	PFHpA	6.73	(Eriksson et al., 2015)	https://doi.org/10.1021/acs.est.5b00679
5-6 carbon	PFHpA	1.76	(Eriksson et al., 2015)	https://doi.org/10.1021/acs.est.5b00679
7-9 carbon	PFOA	8.9	(Karaskova et al., 2016)	https://doi.org/10.1016/j.envint.2016.05.031
7-9 carbon	PFOA	17.7	(Karaskova et al., 2016)	https://doi.org/10.1016/j.envint.2016.05.031
7-9 carbon	PFOA	38.6	(Karaskova et al., 2016)	https://doi.org/10.1016/j.envint.2016.05.031
7-9 carbon	PFOA	80	(Besis et al., 2019)	https://doi.org/10.1016/j.ecoenv.2019.109559
7-9 carbon	PFOA	4.7	(Harrad et al., 2019)	https://doi.org/10.1021/acs.est.9b04604
7-9 carbon	PFOA	3.2	(Harrad et al., 2019)	https://doi.org/10.1021/acs.est.9b04604
7-9 carbon	PFOA	23	(Harrad et al., 2019)	https://doi.org/10.1021/acs.est.9b04604
7-9 carbon	PFOA	2.2	(Harrad et al., 2019)	https://doi.org/10.1021/acs.est.9b04604
7-9 carbon	PFOA	75.49	(ao et al., 2019)	https://doi.org/10.1016/j.envpol.2019.07.041
7-9 carbon	PFOA	55.6	(Eriksson et al., 2015)	https://doi.org/10.1021/acs.est.5b00679
7-9 carbon	PFOA	26.7	(Eriksson et al., 2015)	https://doi.org/10.1021/acs.est.5b00679
7-9 carbon	PFOA	29.1	(Eriksson et al., 2015)	https://doi.org/10.1021/acs.est.5b00679
7-9 carbon	PFOA	20	(Haug et al., 2011)	https://doi.org/10.1021/es103456h

7-9 carbon	PFOA	48	(Eriksson et al., 2015)	https://doi.org/10.1021/acs.est.5b00679
7-9 carbon	PFOA	13.9	(Eriksson et al., 2015)	https://doi.org/10.1021/acs.est.5b00679
7-9 carbon	PFOA	70.9	(Knobeloch et al., 2012)	https://doi.org/10.1016/j.chemosphere.2012.03.082
7-9 carbon	PFDA	5.2	(Karaskova et al., 2016)	https://doi.org/10.1016/j.envint.2016.05.031
7-9 carbon	PFDA	8.5	(Karaskova et al., 2016)	https://doi.org/10.1016/j.envint.2016.05.031
7-9 carbon	PFDA	6.9	(Karaskova et al., 2016)	https://doi.org/10.1016/j.envint.2016.05.031
7-9 carbon	PFDA	3.41	(Besis et al., 2019)	https://doi.org/10.1016/j.ecoenv.2019.109559
7-9 carbon	PFDA	9.15	(Eriksson et al., 2015)	https://doi.org/10.1021/acs.est.5b00679
7-9 carbon	PFDA	6.24	(Eriksson et al., 2015)	https://doi.org/10.1021/acs.est.5b00679
7-9 carbon	PFDA	5.64	(Eriksson et al., 2015)	https://doi.org/10.1021/acs.est.5b00679
7-9 carbon	PFDA	4.1	(Haug et al., 2011)	https://doi.org/10.1021/es103456h
7-9 carbon	PFDA	16.8	(Eriksson et al., 2015)	https://doi.org/10.1021/acs.est.5b00679
7-9 carbon	PFDA	15.9	(Eriksson et al., 2015)	https://doi.org/10.1021/acs.est.5b00679
7-9 carbon	PFNA	3	(Karaskova et al., 2016)	https://doi.org/10.1016/j.envint.2016.05.031
7-9 carbon	PFNA	19.4	(Karaskova et al., 2016)	https://doi.org/10.1016/j.envint.2016.05.031
7-9 carbon	PFNA	10.9	(Karaskova et al., 2016)	https://doi.org/10.1016/j.envint.2016.05.031
7-9 carbon	PFNA	2.52	(Besis et al., 2019)	https://doi.org/10.1016/j.ecoenv.2019.109559
7-9 carbon	PFNA	0.52	(Harrad et al., 2019)	https://doi.org/10.1021/acs.est.9b04604
7-9 carbon	PFNA	0.55	(Harrad et al., 2019)	https://doi.org/10.1021/acs.est.9b04604
7-9 carbon	PFNA	8.6	(Harrad et al., 2019)	https://doi.org/10.1021/acs.est.9b04604
7-9 carbon	PFNA	27.01	(ao et al., 2019)	https://doi.org/10.1016/j.envpol.2019.07.041
7-9 carbon	PFNA	58.6	(Eriksson et al., 2015)	https://doi.org/10.1021/acs.est.5b00679
7-9 carbon	PFNA	5.28	(Eriksson et al., 2015)	https://doi.org/10.1021/acs.est.5b00679
7-9 carbon	PFNA	3.48	(Eriksson et al., 2015)	https://doi.org/10.1021/acs.est.5b00679
7-9 carbon	PFNA	29	(Haug et al., 2011)	https://doi.org/10.1021/es103456h
7-9 carbon	PFNA	76.6	(Eriksson et al., 2015)	https://doi.org/10.1021/acs.est.5b00679

7-9 carbon	PFNA	9.92	(Eriksson et al., 2015)	https://doi.org/10.1021/acs.est.5b00679
7-9 carbon	PFNA	24.44	(Knobeloch et al., 2012)	https://doi.org/10.1016/j.chemosphere.2012.03.082
10-13 carbon	PFUnDA	4.3	(Karaskova et al., 2016)	https://doi.org/10.1016/j.envint.2016.05.031
10-13 carbon	PFUnDA	8.7	(Karaskova et al., 2016)	https://doi.org/10.1016/j.envint.2016.05.031
10-13 carbon	PFUnDA	3.6	(Karaskova et al., 2016)	https://doi.org/10.1016/j.envint.2016.05.031
10-13 carbon	PFUnDA	1.5	(Besis et al., 2019)	https://doi.org/10.1016/j.ecoenv.2019.109559
10-13 carbon	PFUnDA	20.8	(Eriksson et al., 2015)	https://doi.org/10.1021/acs.est.5b00679
10-13 carbon	PFUnDA	2.92	(Eriksson et al., 2015)	https://doi.org/10.1021/acs.est.5b00679
10-13 carbon	PFUnDA	1.88	(Eriksson et al., 2015)	https://doi.org/10.1021/acs.est.5b00679
10-13 carbon	PFUnDA	23.5	(Eriksson et al., 2015)	https://doi.org/10.1021/acs.est.5b00679
10-13 carbon	PFUnDA	6.02	(Eriksson et al., 2015)	https://doi.org/10.1021/acs.est.5b00679
10-13 carbon	PFDoA/PFDoDA	2.5	(Karaskova et al., 2016)	https://doi.org/10.1016/j.envint.2016.05.031
10-13 carbon	PFDoA/PFDoDA	6.3	(Karaskova et al., 2016)	https://doi.org/10.1016/j.envint.2016.05.031
10-13 carbon	PFDoA/PFDoDA	2	(Karaskova et al., 2016)	https://doi.org/10.1016/j.envint.2016.05.031
10-13 carbon	PFDoA/PFDoDA	4.92	(Besis et al., 2019)	https://doi.org/10.1016/j.ecoenv.2019.109559
10-13 carbon	PFDoA/PFDoDA	5.45	(Eriksson et al., 2015)	https://doi.org/10.1021/acs.est.5b00679
10-13 carbon	PFDoA/PFDoDA	3.98	(Eriksson et al., 2015)	https://doi.org/10.1021/acs.est.5b00679
10-13 carbon	PFDoA/PFDoDA	4.2	(Eriksson et al., 2015)	https://doi.org/10.1021/acs.est.5b00679
10-13 carbon	PFDoA/PFDoDA	22	(Haug et al., 2011)	https://doi.org/10.1021/es103456h
10-13 carbon	PFDoA/PFDoDA	5.42	(Eriksson et al., 2015)	https://doi.org/10.1021/acs.est.5b00679
10-13 carbon	PFDoA/PFDoDA	9.7	(Eriksson et al., 2015)	https://doi.org/10.1021/acs.est.5b00679
10-13 carbon	PFTrDA	3.5	(Karaskova et al., 2016)	https://doi.org/10.1016/j.envint.2016.05.031
10-13 carbon	PFTrDA	8.2	(Karaskova et al., 2016)	https://doi.org/10.1016/j.envint.2016.05.031
10-13 carbon	PFTrDA	1.8	(Karaskova et al., 2016)	https://doi.org/10.1016/j.envint.2016.05.031
10-13 carbon	PFTrDA	2.3	(Eriksson et al., 2015)	https://doi.org/10.1021/acs.est.5b00679
10-13 carbon	PFTrDA	1.29	(Eriksson et al., 2015)	https://doi.org/10.1021/acs.est.5b00679

10-13 carbon	PFTrDA	0.99	(Eriksson et al., 2015)	https://doi.org/10.1021/acs.est.5b00679
10-13 carbon	PFTrDA	8.8	(Haug et al., 2011)	https://doi.org/10.1021/es103456h
10-13 carbon	PFTrDA	8.3	(Eriksson et al., 2015)	https://doi.org/10.1021/acs.est.5b00679
10-13 carbon	PFTrDA	2.33	(Eriksson et al., 2015)	https://doi.org/10.1021/acs.est.5b00679
10-13 carbon	PFTeDA	3.6	(Karaskova et al., 2016)	https://doi.org/10.1016/j.envint.2016.05.031
10-13 carbon	PFTeDA	4.8	(Karaskova et al., 2016)	https://doi.org/10.1016/j.envint.2016.05.031
10-13 carbon	PFTeDA	1.4	(Karaskova et al., 2016)	https://doi.org/10.1016/j.envint.2016.05.031
10-13 carbon	PFTeDA	5.3	(Haug et al., 2011)	https://doi.org/10.1021/es103456h
7-9 carbon	PFOA	4.8	(Xu et al., 2020)	https://doi.org/10.1016/j.envres.2020.110243
7-9 carbon	PFDA	1.2	(Xu et al., 2020)	https://doi.org/10.1016/j.envres.2020.110243
10-13 carbon	PFUdA	1.2	(Xu et al., 2020)	https://doi.org/10.1016/j.envres.2020.110243
10-13 carbon	PFDoA	0.67	(Xu et al., 2020)	https://doi.org/10.1016/j.envres.2020.110243
10-13 carbon	PFTeDA	0.24	(Xu et al., 2020)	https://doi.org/10.1016/j.envres.2020.110243

Table 2-10: Data for PFSA concentrations in dust.

PFAS	Value (ng/g)	Author	doi
PFBS	3.6	(Karaskova et al., 2016)	https://doi.org/10.1016/j.envint.2016.05.031
PFBS	1.6	(Karaskova et al., 2016)	https://doi.org/10.1016/j.envint.2016.05.031
PFBS	1.4	(Karaskova et al., 2016)	https://doi.org/10.1016/j.envint.2016.05.031
PFBS	22.9	(Besis et al., 2019)	https://doi.org/10.1016/j.ecoenv.2019.109559
PFBS	17	(Harrad et al., 2019)	https://doi.org/10.1021/acs.est.9b04604
PFBS	12	(Harrad et al., 2019)	https://doi.org/10.1021/acs.est.9b04604
PFBS	19	(Harrad et al., 2019)	https://doi.org/10.1021/acs.est.9b04604
PFBS	17	(Harrad et al., 2019)	https://doi.org/10.1021/acs.est.9b04604
PFBS	131.57	(ao et al., 2019)	https://doi.org/10.1016/j.envpol.2019.07.041
PFBS	1.3	(Haug et al., 2011)	https://doi.org/10.1021/es103456h
PFBS	4.03	(Knobeloch et al., 2012)	https://doi.org/10.1016/j.chemosphere.2012.03.082
PFHxS	2.8	(Karaskova et al., 2016)	https://doi.org/10.1016/j.envint.2016.05.031
PFHxS	3.1	(Karaskova et al., 2016)	https://doi.org/10.1016/j.envint.2016.05.031
PFHxS	13.8	(Karaskova et al., 2016)	https://doi.org/10.1016/j.envint.2016.05.031
PFHxS	2.06	(Besis et al., 2019)	https://doi.org/10.1016/j.ecoenv.2019.109559
PFHxS	1.4	(Harrad et al., 2019)	https://doi.org/10.1021/acs.est.9b04604
PFHxS	6.2	(Harrad et al., 2019)	https://doi.org/10.1021/acs.est.9b04604
PFHxS	2.7	(Harrad et al., 2019)	https://doi.org/10.1021/acs.est.9b04604
PFHxS	5.1	(Harrad et al., 2019)	https://doi.org/10.1021/acs.est.9b04604
PFHxS	491.07	(ao et al., 2019)	https://doi.org/10.1016/j.envpol.2019.07.041
PFHxS	51	(Eriksson et al., 2015)	https://doi.org/10.1021/acs.est.5b00679
PFHxS	2.54	(Eriksson et al., 2015)	https://doi.org/10.1021/acs.est.5b00679
PFHxS	65.2	(Eriksson et al., 2015)	https://doi.org/10.1021/acs.est.5b00679
PFHxS	8.4	(Haug et al., 2011)	https://doi.org/10.1021/es103456h
PFHxS	0.65	(Eriksson et al., 2015)	https://doi.org/10.1021/acs.est.5b00679
PFHxS	0.39	(Eriksson et al., 2015)	https://doi.org/10.1021/acs.est.5b00679
PFHxS	123.36	(Knobeloch et al., 2012)	https://doi.org/10.1016/j.chemosphere.2012.03.082

PFOS	20.7	(Karaskova et al., 2016)	https://doi.org/10.1016/j.envint.2016.05.031
PFOS	10.8	(Karaskova et al., 2016)	https://doi.org/10.1016/j.envint.2016.05.031
PFOS	42.4	(Karaskova et al., 2016)	https://doi.org/10.1016/j.envint.2016.05.031
PFOS	23.5	(Besis et al., 2019)	https://doi.org/10.1016/j.ecoenv.2019.109559
PFOS	6	(Harrad et al., 2019)	https://doi.org/10.1021/acs.est.9b04604
PFOS	7.6	(Harrad et al., 2019)	https://doi.org/10.1021/acs.est.9b04604
PFOS	91	(Harrad et al., 2019)	https://doi.org/10.1021/acs.est.9b04604
PFOS	3.1	(Harrad et al., 2019)	https://doi.org/10.1021/acs.est.9b04604
PFOS	15.13	(ao et al., 2019)	https://doi.org/10.1016/j.envpol.2019.07.041
PFOS	87.3	(Eriksson et al., 2015)	https://doi.org/10.1021/acs.est.5b00679
PFOS	27.3	(Eriksson et al., 2015)	https://doi.org/10.1021/acs.est.5b00679
PFOS	42.2	(Eriksson et al., 2015)	https://doi.org/10.1021/acs.est.5b00679
PFOS	11	(Haug et al., 2011)	https://doi.org/10.1021/es103456h
PFOS	9.83	(Eriksson et al., 2015)	https://doi.org/10.1021/acs.est.5b00679
PFOS	4.93	(Eriksson et al., 2015)	https://doi.org/10.1021/acs.est.5b00679
PFOS	168.23	(Knobeloch et al., 2012)	https://doi.org/10.1016/j.chemosphere.2012.03.082
PFBS	18	(Xu et al., 2020)	https://doi.org/10.1016/j.envres.2020.110243
PFHxS	0.68	(Xu et al., 2020)	https://doi.org/10.1016/j.envres.2020.110243
PFOS	4.2	(Xu et al., 2020)	https://doi.org/10.1016/j.envres.2020.110243

2.3.4. The relative importance of particle mineralogy on PFAA affinity

All suspended particles may not facilitate the transport of PFAAs similarly. In general, suspended particles that exhibit a high affinity to chemicals are responsible for particle-facilitated transport in the subsurface (DeNovio et al., 2004). The compositional properties of particles can affect the affinity of PFAAs to suspended particles (Li et al., 2018). Analyzing 6 studies (Li et al., 2019; Mejia-Avendano et al., 2020; Miao et al., 2017; Milinovic et al., 2015; Nguyen et al., 2020; Wei et al., 2017) where sorption of PFAAs to soils and the soil properties were reported, we found that the dominant compositional properties affecting PFAA sorption include organic carbon (OC), iron oxide, and aluminum oxides (Figure 2-8). However, it should be noted that the correlation is weak, potentially because of the interactive effect between these minerals. For instance, organic carbon can coat iron oxides and block sorption sites (Borggaard et al., 1990). Nevertheless, studies using specific soil minerals validated our finding. For instance, several studies show that PFAAs may sorb onto metal oxides such as iron and aluminum oxides including hematite, goethite, and boehmite (Gao and Chorover, 2012; Tang et al., 2010; Wang et al., 2012; Zhao et al., 2014) particularly because many iron oxides, may have a net positive surface charge around neutral pH (Hsia et al., 1994). It should be noted that some other iron oxides such as magnetite can be negatively charged in neutral pH conditions (Aredes et al., 2013; Carlson and Kawatra, 2013). Thus, specific iron oxide types and soil pH should be determined to examine their role in the adsorption of PFAAs. Adsorption of dissolved organic carbon (DOC) on these mineral oxides can also reduce their affinity to PFAAs (Wang et al., 2015). In all cases, PFOS adsorption is higher than PFOA adsorption for the same mineralogical properties, indicating PFOS are more likely to be transported in association with particles, compared with PFOA.

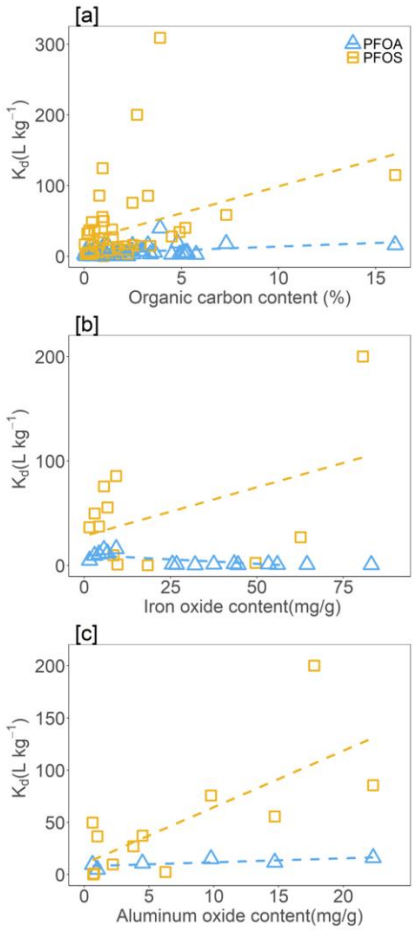

Figure 2-8. Correlation of soil partitioning constant (K_d) of PFOA and PFOS with soil properties including (a) organic carbon, (b) iron oxide content, and (c) aluminum oxide content. The dashed lines indicate a linear correlation. Data source in Table 2-11, Table 2-12 and Table 2-13.

Table 2-11: Soil-water partitioning coefficients (K_d) of PFOA and PFOS with organic carbon content.

Source	K_d (L/kg)	Organic carbon (%)	Reference	doi
PFOA	2.3	0.52	Chen et al (2013)	https://doi.org/10.1080/19443994.2013.792145
PFOA	3.1	2.1	Chen et al (2013)	https://doi.org/10.1080/19443994.2013.792145
PFOA	3.5	2.5	Chen et al (2013)	https://doi.org/10.1080/19443994.2013.792145
PFOA	5.1	5.2	Chen et al (2013)	https://doi.org/10.1080/19443994.2013.792145
PFOA	16.1	16	Chen et al (2013)	https://doi.org/10.1080/19443994.2013.792145
PFOA	16.1	3.28	Li et al (2019)	https://doi.org/10.1016/j.scitotenv.2018.08.209
PFOA	10.9	0.52	Li et al (2019)	https://doi.org/10.1016/j.ecoenv.2017.01.022
PFOA	4.8	0.258	Li et al (2019)	https://doi.org/10.1016/j.scitotenv.2018.08.209
PFOA	11.7	0.928	Li et al (2019)	https://doi.org/10.1016/j.scitotenv.2018.08.209
PFOA	15.1	2.48	Li et al (2019)	https://doi.org/10.1016/j.scitotenv.2018.08.209
PFOA	9.6	0.993	Li et al (2019)	https://doi.org/10.1016/j.scitotenv.2018.08.209
PFOA	3.2	0.02	Milinovic et al (2015)	https://doi.org/10.1016/j.scitotenv.2014.12.017
PFOA	2.5	0.16	Milinovic et al (2015)	https://doi.org/10.1016/j.scitotenv.2014.12.017
PFOA	3.2	0.39	Milinovic et al (2015)	https://doi.org/10.1016/j.scitotenv.2014.12.017
PFOA	2.5	0.77	Milinovic et al (2015)	https://doi.org/10.1016/j.scitotenv.2014.12.017
PFOA	7.0	0.94	Milinovic et al (2015)	https://doi.org/10.1016/j.scitotenv.2014.12.017
PFOA	40.0	3.9	Milinovic et al (2015)	https://doi.org/10.1016/j.scitotenv.2014.12.017
PFOA	3.4	3.4	Mejia-Avendaño et al (2020)	https://doi.org/10.1021/acs.est.9b04989
PFOA	3.0	1.7	Mejia-Avendaño et al (2020)	https://doi.org/10.1021/acs.est.9b04989
PFOA	6.9	2.9	Mejia-Avendaño et al (2020)	https://doi.org/10.1021/acs.est.9b04989
PFOA	17.9	7.3	Mejia-Avendaño et al (2020)	https://doi.org/10.1021/acs.est.9b04989
PFOA	0.6	1.8	Mejia-Avendaño et al (2020)	https://doi.org/10.1021/acs.est.9b04989
PFOA	2.6	5.76	Maio et al (2017)	https://doi.org/10.1016/j.ecoenv.2017.01.022
PFOA	4.8	5.06	Maio et al (2017)	https://doi.org/10.1016/j.ecoenv.2017.01.022
PFOA	18.9	4.8	Maio et al (2017)	https://doi.org/10.1016/j.ecoenv.2017.01.022
PFOA	5.5	3.61	Maio et al (2017)	https://doi.org/10.1016/j.ecoenv.2017.01.022

PFOA	7.0	3.02	Maio et al (2017)	https://doi.org/10.1016/j.ecoenv.2017.01.022
PFOA	7.0	2.47	Maio et al (2017)	https://doi.org/10.1016/j.ecoenv.2017.01.022
PFOA	6.4	1.7	Maio et al (2017)	https://doi.org/10.1016/j.ecoenv.2017.01.022
PFOA	4.8	1.48	Maio et al (2017)	https://doi.org/10.1016/j.ecoenv.2017.01.022
PFOA	2.3	1.05	Maio et al (2017)	https://doi.org/10.1016/j.ecoenv.2017.01.022
PFOA	1.4	0.52	Maio et al (2017)	https://doi.org/10.1016/j.ecoenv.2017.01.022
PFOA	8.3	0.1	Xiao et al (2019)	https://doi.org/10.1021/acs.est.9b05379
PFOA	15.3	1.2	Xiao et al (2019)	https://doi.org/10.1021/acs.est.9b05379
PFOA	4.0	0.1	Xiao et al (2019)	https://doi.org/10.1021/acs.est.9b05379
PFOA	9.7	0.9	Xiao et al (2019)	https://doi.org/10.1021/acs.est.9b05379
PFOA	5.4	5.3	Xiao et al (2019)	https://doi.org/10.1021/acs.est.9b05379
PFOA	0.6	1.7	Guelfo et al (2013)	https://doi.org/10.1021/es3048043
PFOA	3.0	4.5	Guelfo et al (2013)	https://doi.org/10.1021/es3048043
PFOA	0.7	0.8	Guelfo et al (2013)	https://doi.org/10.1021/es3048043
PFOS	7.3	0.52	Chen et al (2013)	https://doi.org/10.1080/19443994.2013.792145
PFOS	14.2	2.1	Chen et al (2013)	https://doi.org/10.1080/19443994.2013.792145
PFOS	16.1	2.5	Chen et al (2013)	https://doi.org/10.1080/19443994.2013.792145
PFOS	40.3	5.2	Chen et al (2013)	https://doi.org/10.1080/19443994.2013.792145
PFOS	115.0	16	Chen et al (2013)	https://doi.org/10.1080/19443994.2013.792145
PFOS	85.6	3.28	Li et al (2019)	https://doi.org/10.1016/j.scitotenv.2018.08.209
PFOS	37.3	0.52	Li et al (2019)	https://doi.org/10.1016/j.scitotenv.2018.08.209
PFOS	36.6	0.258	Li et al (2019)	https://doi.org/10.1016/j.scitotenv.2018.08.209
PFOS	55.7	0.928	Li et al (2019)	https://doi.org/10.1016/j.scitotenv.2018.08.209
PFOS	75.8	2.48	Li et al (2019)	https://doi.org/10.1016/j.scitotenv.2018.08.209
PFOS	49.9	0.993	Li et al (2019)	https://doi.org/10.1016/j.scitotenv.2018.08.209
PFOS	38.0	1.43	Chen et al (2012)	https://doi.org/10.1016/j.marpolbul.2012.03.012
PFOS	25.7	0.99	Chen et al (2012)	https://doi.org/10.1016/j.marpolbul.2012.03.012
PFOS	25.1	0.81	Chen et al (2012)	https://doi.org/10.1016/j.marpolbul.2012.03.012
PFOS	20.0	0.75	Chen et al (2012)	https://doi.org/10.1016/j.marpolbul.2012.03.012

PFOS	15.8	0.42	Chen et al (2012)	https://doi.org/10.1016/j.marpolbul.2012.03.012
PFOS	17.0	0.02	Milinovic et al (2015)	https://doi.org/10.1016/j.scitotenv.2014.12.017
PFOS	32.6	0.16	Milinovic et al (2015)	https://doi.org/10.1016/j.scitotenv.2014.12.017
PFOS	48.5	0.39	Milinovic et al (2015)	https://doi.org/10.1016/j.scitotenv.2014.12.017
PFOS	86.0	0.77	Milinovic et al (2015)	https://doi.org/10.1016/j.scitotenv.2014.12.017
PFOS	124.7	0.94	Milinovic et al (2015)	https://doi.org/10.1016/j.scitotenv.2014.12.017
PFOS	309.0	3.9	Milinovic et al (2015)	https://doi.org/10.1016/j.scitotenv.2014.12.017
PFOS	14.8	3.4	Mejia-Avendaño et al (2020)	https://doi.org/10.1021/acs.est.9b04989
PFOS	13.1	1.7	Mejia-Avendaño et al (2020)	https://doi.org/10.1021/acs.est.9b04989
PFOS	14.7	2.9	Mejia-Avendaño et al (2020)	https://doi.org/10.1021/acs.est.9b04989
PFOS	58.7	7.3	Mejia-Avendaño et al (2020)	https://doi.org/10.1021/acs.est.9b04989
PFOS	9.6	1.8	Mejia-Avendaño et al (2020)	https://doi.org/10.1021/acs.est.9b04989
PFOS	2.5	1.27	Wei et al (2017)	https://doi.org/10.1016/j.ecoenv.2017.03.040
PFOS	9.8	2.25	Wei et al (2017)	https://doi.org/10.1016/j.ecoenv.2017.03.040
PFOS	1.0	0.87	Wei et al (2017)	https://doi.org/10.1016/j.ecoenv.2017.03.040
PFOS	0.2	0.99	Wei et al (2017)	https://doi.org/10.1016/j.ecoenv.2017.03.040
PFOS	200.2	2.71	Wei et al (2017)	https://doi.org/10.1016/j.ecoenv.2017.03.040
PFOS	27.1	1.46	Wei et al (2017)	https://doi.org/10.1016/j.ecoenv.2017.03.040
PFOS	4.0	1.7	Guelfo et al (2013)	https://doi.org/10.1021/es3048043
PFOS	28.2	4.5	Guelfo et al (2013)	https://doi.org/10.1021/es3048043
PFOS	4.7	0.8	Guelfo et al (2013)	https://doi.org/10.1021/es3048043
PFOA	1.0	0.7	Nguyen et al (2020)	https://doi.org/10.1021/acs.est.0c05705
PFOA	0.7	0.37	Nguyen et al (2020)	https://doi.org/10.1021/acs.est.0c05705
PFOA	0.8	0.08	Nguyen et al (2020)	https://doi.org/10.1021/acs.est.0c05705
PFOA	0.6	0.25	Nguyen et al (2020)	https://doi.org/10.1021/acs.est.0c05705
PFOA	0.7	2.23	Nguyen et al (2020)	https://doi.org/10.1021/acs.est.0c05705
PFOA	2.8	4.9	Nguyen et al (2020)	https://doi.org/10.1021/acs.est.0c05705
PFOA	1.4	0.13	Nguyen et al (2020)	https://doi.org/10.1021/acs.est.0c05705
PFOA	0.5	0.4	Nguyen et al (2020)	https://doi.org/10.1021/acs.est.0c05705

PFOA	1.2	1.19	Nguyen et al (2020)	https://doi.org/10.1021/acs.est.0c05705
PFOA	0.9	0.17	Nguyen et al (2020)	https://doi.org/10.1021/acs.est.0c05705
PFOS	5.9	0.7	Nguyen et al (2020)	https://doi.org/10.1021/acs.est.0c05705
PFOS	3.5	0.37	Nguyen et al (2020)	https://doi.org/10.1021/acs.est.0c05705
PFOS	3.2	0.08	Nguyen et al (2020)	https://doi.org/10.1021/acs.est.0c05705
PFOS	4.2	0.25	Nguyen et al (2020)	https://doi.org/10.1021/acs.est.0c05705
PFOS	3.7	2.23	Nguyen et al (2020)	https://doi.org/10.1021/acs.est.0c05705
PFOS	34.3	4.9	Nguyen et al (2020)	https://doi.org/10.1021/acs.est.0c05705
PFOS	3.5	0.13	Nguyen et al (2020)	https://doi.org/10.1021/acs.est.0c05705
PFOS	3.2	0.4	Nguyen et al (2020)	https://doi.org/10.1021/acs.est.0c05705
PFOS	8.8	1.19	Nguyen et al (2020)	https://doi.org/10.1021/acs.est.0c05705
PFOS	5.7	0.17	Nguyen et al (2020)	https://doi.org/10.1021/acs.est.0c05705

Table 2-12: Soil-water partitioning coefficients (K_d) of PFOA and PFOS with iron oxide content.

PFAA	K_d (L/kg)	Iron oxide content (mg/g)	Reference	DOI
PFOS	85.6	9.21	Li et al (2019)	https://doi.org/10.1016/j.scitotenv.2018.08.209
PFOS	37.3	4.25	Li et al (2019)	https://doi.org/10.1016/j.scitotenv.2018.08.209
PFOS	36.6	1.51	Li et al (2019)	https://doi.org/10.1016/j.scitotenv.2018.08.209
PFOS	55.7	6.69	Li et al (2019)	https://doi.org/10.1016/j.scitotenv.2018.08.209
PFOS	75.8	5.68	Li et al (2019)	https://doi.org/10.1016/j.scitotenv.2018.08.209
PFOS	49.9	2.95	Li et al (2019)	https://doi.org/10.1016/j.scitotenv.2018.08.209
PFOS	2.5	49.58	Wei et al (2017)	https://doi.org/10.1016/j.ecoenv.2017.03.040
PFOS	9.8	8.44	Wei et al (2017)	https://doi.org/10.1016/j.ecoenv.2017.03.040
PFOS	1.0	9.57	Wei et al (2017)	https://doi.org/10.1016/j.ecoenv.2017.03.040
PFOS	0.2	18.35	Wei et al (2017)	https://doi.org/10.1016/j.ecoenv.2017.03.040
PFOS	200.2	80.66	Wei et al (2017)	https://doi.org/10.1016/j.ecoenv.2017.03.040
PFOS	27.1	62.6	Wei et al (2017)	https://doi.org/10.1016/j.ecoenv.2017.03.040
PFOA	16.1	9.21	Li et al (2019)	https://doi.org/10.1016/j.scitotenv.2018.08.209
PFOA	10.9	4.25	Li et al (2019)	https://doi.org/10.1016/j.scitotenv.2018.08.209
PFOA	4.8	1.51	Li et al (2019)	https://doi.org/10.1016/j.scitotenv.2018.08.209
PFOA	11.7	6.69	Li et al (2019)	https://doi.org/10.1016/j.scitotenv.2018.08.209
PFOA	15.1	5.68	Li et al (2019)	https://doi.org/10.1016/j.scitotenv.2018.08.209
PFOA	9.6	2.95	Li et al (2019)	https://doi.org/10.1016/j.scitotenv.2018.08.209
PFOA	1.5	43.4	Miao et al (2017)	https://doi.org/10.1016/j.ecoenv.2017.01.022
PFOA	1.3	53.3	Miao et al (2017)	https://doi.org/10.1016/j.ecoenv.2017.01.022
PFOA	1.2	37.5	Miao et al (2017)	https://doi.org/10.1016/j.ecoenv.2017.01.022
PFOA	1.2	25.5	Miao et al (2017)	https://doi.org/10.1016/j.ecoenv.2017.01.022
PFOA	0.9	26.7	Miao et al (2017)	https://doi.org/10.1016/j.ecoenv.2017.01.022
PFOA	0.9	55.9	Miao et al (2017)	https://doi.org/10.1016/j.ecoenv.2017.01.022
PFOA	0.8	64.5	Miao et al (2017)	https://doi.org/10.1016/j.ecoenv.2017.01.022
PFOA	0.7	44.5	Miao et al (2017)	https://doi.org/10.1016/j.ecoenv.2017.01.022
PFOA	0.6	83.1	Miao et al (2017)	https://doi.org/10.1016/j.ecoenv.2017.01.022
PFOA	0.5	32.1	Miao et al (2017)	https://doi.org/10.1016/j.ecoenv.2017.01.022

Table 2-13: Soil-water partitioning coefficients (Kd) of PFOA and PFOS with aluminum oxide content.

PFAA	K_d (L/kg)	Aluminum oxide content (mg/g)	Reference	DOI
PFOA	16.1	22.3	Li et al (2019)	https://doi.org/10.1016/j.scitotenv.2018.08.209
PFOA	10.9	4.49	Li et al (2019)	https://doi.org/10.1016/j.scitotenv.2018.08.209
PFOA	4.8	1.01	Li et al (2019)	https://doi.org/10.1016/j.scitotenv.2018.08.209
PFOA	11.7	14.7	Li et al (2019)	https://doi.org/10.1016/j.scitotenv.2018.08.209
PFOA	15.1	9.78	Li et al (2019)	https://doi.org/10.1016/j.scitotenv.2018.08.209
PFOA	9.6	0.634	Li et al (2019)	https://doi.org/10.1016/j.scitotenv.2018.08.209
PFOS	85.6	22.3	Li et al (2019)	https://doi.org/10.1016/j.scitotenv.2018.08.209
PFOS	37.3	4.49	Li et al (2019)	https://doi.org/10.1016/j.scitotenv.2018.08.209
PFOS	36.6	1.01	Li et al (2019)	https://doi.org/10.1016/j.scitotenv.2018.08.209
PFOS	55.7	14.7	Li et al (2019)	https://doi.org/10.1016/j.scitotenv.2018.08.209
PFOS	75.8	9.78	Li et al (2019)	https://doi.org/10.1016/j.scitotenv.2018.08.209
PFOS	49.9	0.634	Li et al (2019)	https://doi.org/10.1016/j.scitotenv.2018.08.209
PFOS	2.5	6.26	Wei et al (2017)	https://doi.org/10.1016/j.ecoenv.2017.03.040
PFOS	9.8	2.19	Wei et al (2017)	https://doi.org/10.1016/j.ecoenv.2017.03.040
PFOS	1.0	0.75	Wei et al (2017)	https://doi.org/10.1016/j.ecoenv.2017.03.040
PFOS	0.2	0.69	Wei et al (2017)	https://doi.org/10.1016/j.ecoenv.2017.03.040
PFOS	200.2	17.75	Wei et al (2017)	https://doi.org/10.1016/j.ecoenv.2017.03.040
PFOS	27.1	3.78	Wei et al (2017)	https://doi.org/10.1016/j.ecoenv.2017.03.040

2.4. Recommendations for future studies

Improvement of sampling and analysis protocol to account for particle-associated PFAAs. Sample collection methods such as core sampling can introduce particles in the pore water due to disturbance. Furthermore, flow perturbation can release particles near sampling well. Most studies filter or centrifuge samples before analysis (Qiu et al., 2010; Zhou et al., 2013). These steps remove particles and could potentially lower the measured PFAA concentration in the water samples. The results of this study demonstrate the importance of using appropriate soil and groundwater characterization methods to quantify PFAA, particularly those that retain the PFAA mass associated with small particles that might be lost using conventional field and lab protocols. To quantify the particle-associated concentration of PFAA, PFAA is first desorbed from suspended particles using appropriate solvents (Higgins and Luthy, 2006; Houtz et al., 2013). However, the recovery of adsorbed PFAS from solids varies widely based on the solvent type and extraction protocol (Zhang et al., 2010). The detection limit and sensitivity of the analytical method used to identify unknown PFAAs and precursors on particles could affect the estimation of particle-associated PFAS (Coggan et al., 2019).

PFAA contaminated suspended sediments in surface runoff: Surface runoff on PFAA contaminated sites can erode particles from the soil which can contain PFAA. High concentrations of PFAA were observed on suspended particles in surface runoff (Xiao et al., 2012), but their concentration is difficult to quantify as the sorbed PFAA resist desorption for analysis (Nguyen et al., 2016). Our analysis showed that this transport of PFAA contaminated suspended particles could be responsible for the increase in surface PFAA concentrations with precipitation rate (Figure 2-6b). Therefore, surface runoff carrying these contaminated suspended particles can cause recontamination of sediments in surface water sources, creating secondary hotspots in the process.

Thus, the transport of PFAA associated with suspended particles must be considered by modeling and impact assessment studies**.**

Transport of cationic and zwitterionic PFAS. Cationic and zwitterionic PFAS have positive charges, whereas most natural soil particles have a net negative charge. Thus, these PFAS can strongly bind with soil particles compared with PFAAs. Consequently, particles could affect the transport of cationic and zwitterionic PFAS to a greater extent than the anionic PFAS. However, limited studies have examined the transport of cationic and zwitterionic PFAS (Barzen-Hanson et al., 2017; Mejia-Avendano et al., 2020; Nickerson et al., 2021; Xiao et al., 2019), and none of these studies considered particle-mediated transport.

Effect of weathering cycles on the release of particle-associated PFAAs in the subsurface. Subsurface soils naturally experience dry-wet and freeze-thaw cycles, which can accelerate the mobilization of particles and particle-associated pollutants (Mohanty et al., 2014). However, the contribution of these transient weather conditions on the leaching of PFAA from subsurface soil has not been evaluated. PFAAs can also bind to air-water interfaces (Brusseau, 2019), where the hydrophobic tail sticks into the air phase (Meng et al., 2014). However, the air-water interface is dynamic and collapses during rewetting. Perturbation of air-water interfaces during dry-wet and freeze-thaw cycles could release PFAA attached to air-water interfaces. The same processes release soil particulates (Mohanty et al., 2015, 2014). Future studies should evaluate the role of the environmentally relevant conditions on PFAS transport and distribution in soil.

Effect of the air-water interface on the transport of suspended particle-associated PFAA: The air-water interface can retain significant amounts of PFAAs and has been found to be the major retention mechanism of PFAAs in the subsurface (Brusseau, 2018). However, the

suspended particles have a high affinity to the air-water interface as well (Flury and Aramrak, 2017). Therefore, the air-water interface can also retain PFAA which is adsorbed to suspended sediments. On the other hand, the air-water interface can also leach sorbed PFAAs from the soil when the subsurface is exposed to intermittent rainfall, increasing its mobility through the subsurface to the groundwater (Gellrich et al., 2012). In such cases, the release of suspended particles by the air-water interface can also enhance the mobility of the associated PFAAs. PFAAs sorbed to the colloids can then be transported to the groundwater. Therefore, the effect of the air-water interface in the transport of PFAAs and particle-associated PFAAs through the subsurface needs further study.

2.5. Conclusions

Risk assessment studies often overlook the transport of PFAAs in association with suspended particles eroded from the source zones. Analyzing 43 studies, we reveal a significant role of suspended particles on the transport of PFAAs in surface waters, subsurface soils and air. Suspended particles in surface waters often contain 1-3 orders of magnitude higher PFAA concentration than bed sediments, indicating the source of suspended parties in surface water may not be the sediments but eroded particles from source zones upstream. The concentration of PFAAs in subsurface soil is typically high within the top 5 m below ground surface, but the concentration decreased thereafter rapidly, indicating subsurface soil could serve as a secondary source for long-term release of PFAAs into groundwater. The subsurface soil depth corresponding to the concentration maxima decreases rapidly with increases in soil organic carbon content. Thus, organic-rich suspended sediment could facilitate the transport of PFAAs. Surprisingly, the depth corresponding to the concentration maxima is lower in areas receiving higher rainfall intensity. We attribute this result to an increase in erosion of soil from the source zone during high-intensity

rainfall, which could increase the loading of suspended particles and their deposition in the subsurface zone near the ground surface. Analyzing the mineralogy of soils in the reported studies, we found that increase in organic carbon and iron or aluminum oxides content in particles could enhance PFAA adsorption on particles and consequently their ability to serve as a PFAA vector in environments. Collectively, the results indicate that suspended particles, which are often ignored in previous assessment studies, can be a significant pathway for the transport of PFAAs in the environment. Therefore, future studies should measure particle associated PFAAs in the samples instead of just measuring the aqueous concentration of PFAAs.

2.6. References

Ahmed, M.B., Johir, M.A.H., McLaughlan, R., Nguyen, L.N., Xu, B., Nghiem, L.D., 2020. Per- and polyfluoroalkyl substances in soil and sediments: Occurrence, fate, remediation and future outlook. Science of The Total Environment 748, 141251. https://doi.org/10.1016/j.scitotenv.2020.141251

Ahrens, L., Bundschuh, M., 2014. Fate and effects of poly- and perfluoroalkyl substances in the aquatic environment: a review. Environmental Toxicology and Chemistry 33, 1921–1929. https://doi.org/10.1002/etc.2663

Ahrens, L., Taniyasu, S., Yeung, L.W.Y., Yamashita, N., Lam, P.K.S., Ebinghaus, R., 2010. Distribution of polyfluoroalkyl compounds in water, suspended particulate matter and sediment from Tokyo Bay, Japan. Chemosphere 79, 266–272. https://doi.org/10.1016/j.chemosphere.2010.01.045

Anderson, R.H., Adamson, D.T., Stroo, H.F., 2019. Partitioning of poly- and perfluoroalkyl substances from soil to groundwater within aqueous film-forming foam source zones. Journal of Contaminant Hydrology 220, 59–65. https://doi.org/10.1016/j.jconhyd.2018.11.011

Aredes, S., Klein, B., Pawlik, M., 2013. The removal of arsenic from water using natural iron oxide minerals. Journal of Cleaner Production, Special Volume: Water, Women, Waste, Wisdom and Wealth 60, 71–76. https://doi.org/10.1016/j.jclepro.2012.10.035

Armitage, J.M., MacLeod, M., Cousins, I.T., 2009. Comparative Assessment of the Global Fate and Transport Pathways of Long-Chain Perfluorocarboxylic Acids (PFCAs) and Perfluorocarboxylates (PFCs) Emitted from Direct Sources. Environ. Sci. Technol. 43, 5830–5836. https://doi.org/10.1021/es900753y

Baduel, C., Paxman, C.J., Mueller, J.F., 2015. Perfluoroalkyl substances in a firefighting training ground (FTG), distribution and potential future release. Journal of Hazardous Materials 296, 46–53. https://doi.org/10.1016/j.jhazmat.2015.03.007

Banzhaf, S., Filipovic, M., Lewis, J., Sparrenbom, C.J., Barthel, R., 2017. A review of contamination of surface-, ground-, and drinking water in Sweden by perfluoroalkyl and polyfluoroalkyl substances (PFASs). Ambio 46, 335–346. https://doi.org/10.1007/s13280-016-0848-8

Barzen-Hanson, K.A., Davis, S.E., Kleber, M., Field, J.A., 2017. Sorption of Fluorotelomer Sulfonates, Fluorotelomer Sulfonamido Betaines, and a Fluorotelomer Sulfonamido Amine in National Foam Aqueous Film-Forming Foam to Soil. Environ. Sci. Technol. 51, 12394–12404. https://doi.org/10.1021/acs.est.7b03452

Benskin, J.P., Li, B., Ikonomou, M.G., Grace, J.R., Li, L.Y., 2012. Per- and Polyfluoroalkyl Substances in Landfill Leachate: Patterns, Time Trends, and Sources. Environ. Sci. Technol. 46, 11532–11540. https://doi.org/10.1021/es302471n

Borggaard, O.K., Jdrgensen, S.S., Moberg, J.P., Raben-Lange, B., 1990. Influence of organic matter on phosphate adsorption by aluminium and iron oxides in sandy soils. Journal of Soil Science 41, 443–449. https://doi.org/10.1111/j.1365-2389.1990.tb00078.x

Borthakur, A., Wang, M., He, M., Ascencio, K., Blotevogel, J., Adamson, D.T., Mahendra, S., Mohanty, S.K., 2020. Dataset for the review: Perfluoroalkyl acids on suspended particles: Unexplored transport pathways in surface water and subsurface soils. https://doi.org/10.6084/m9.figshare.c.5185736

Brusseau, M.L., 2019. Estimating the relative magnitudes of adsorption to solid-water and air/oil-water interfaces for per- and poly-fluoroalkyl substances. Environ Pollut 254, 113102. https://doi.org/10.1016/j.envpol.2019.113102

Brusseau, M.L., 2018. Assessing the potential contributions of additional retention processes to PFAS retardation in the subsurface. Sci Total Environ 613–614, 176–185. https://doi.org/10.1016/j.scitotenv.2017.09.065

Brusseau, M.L., Anderson, R.H., Guo, B., 2020. PFAS concentrations in soils: Background levels versus contaminated sites. Science of The Total Environment 740, 140017. https://doi.org/10.1016/j.scitotenv.2020.140017

Carlson, J.J., Kawatra, S.K., 2013. Factors Affecting Zeta Potential of Iron Oxides. Mineral Processing and Extractive Metallurgy Review 34, 269–303. https://doi.org/10.1080/08827508.2011.604697

Chanson, H., Reungoat, D., Simon, B., Lubin, P., 2011. High-frequency turbulence and suspended sediment concentration measurements in the Garonne River tidal bore. Estuarine, Coastal and Shelf Science 95, 298–306. https://doi.org/10.1016/j.ecss.2011.09.012

Chen, H., Choi, Y.J., Lee, L.S., 2018. Sorption, Aerobic Biodegradation, and Oxidation Potential of PFOS Alternatives Chlorinated Polyfluoroalkyl Ether Sulfonic Acids. Environ. Sci. Technol. 52, 9827–9834. https://doi.org/10.1021/acs.est.8b02913

Chen, H.T., Reinhard, M., Yin, T.R., Nguyen, T.V., Tran, N.H., Gin, K.Y.H., 2019. Multi-compartment distribution of perfluoroalkyl and polyfluoroalkyl substances (PFASs) in an urban catchment system. Water Research 154, 227–237. https://doi.org/10.1016/j.watres.2019.02.009

Chen, X., Zhu, L., Pan, X., Fang, S., Zhang, Y., Yang, L., 2015. Isomeric specific partitioning behaviors of perfluoroalkyl substances in water dissolved phase, suspended particulate matters and sediments in Liao River Basin and Taihu Lake, China. Water Research 80, 235–244. https://doi.org/10.1016/j.watres.2015.04.032

Coggan, T.L., Anumol, T., Pyke, J., Shimeta, J., Clarke, B.O., 2019. A single analytical method for the determination of 53 legacy and emerging per- and polyfluoroalkyl substances (PFAS) in aqueous matrices. Analytical and Bioanalytical Chemistry 411, 3507–3520. https://doi.org/10.1007/s00216-019-01829-8

D'Agostino, L.A., Mabury, S.A., 2014. Identification of Novel Fluorinated Surfactants in Aqueous Film Forming Foams and Commercial Surfactant Concentrates. Environ. Sci. Technol. 48, 121–129. https://doi.org/10.1021/es403729e

Dasu, K., Lee, L.S., Turco, R.F., Nies, L.F., 2013. Aerobic biodegradation of 8:2 fluorotelomer stearate monoester and 8:2 fluorotelomer citrate triester in forest soil. Chemosphere 91, 399–405. https://doi.org/10.1016/j.chemosphere.2012.11.076

Dauchy, X., Boiteux, V., Bach, C., Rosin, C., Munoz, J.F., 2017. Per- and polyfluoroalkyl substances in firefighting foam concentrates and water samples collected near sites impacted by the use of these foams. Chemosphere 183, 53–61. https://doi.org/10.1016/j.chemosphere.2017.05.056

Dauchy, X., Boiteux, V., Colin, A., Bach, C., Rosin, C., Munoz, J.F., 2019a. Poly- and Perfluoroalkyl Substances in Runoff Water and Wastewater Sampled at a Firefighter Training Area. Archives of Environmental Contamination and Toxicology 76, 206–215. https://doi.org/10.1007/s00244-018-0585-z

Dauchy, X., Boiteux, V., Colin, A., Hemard, J., Bach, C., Rosin, C., Munoz, J.F., 2019b. Deep seepage of per- and polyfluoroalkyl substances through the soil of a firefighter training site and subsequent groundwater contamination. Chemosphere 214, 729–737. https://doi.org/10.1016/j.chemosphere.2018.10.003

de Solla, S.R., De Silva, A.O., Letcher, R.J., 2012. Highly elevated levels of perfluorooctane sulfonate and other perfluorinated acids found in biota and surface water downstream of an international airport, Hamilton, Ontario, Canada. Environment International 39, 19–26. https://doi.org/10.1016/j.envint.2011.09.011

DeNovio, N., Saiers, J., Ryan, J., 2004. Colloid Movement in Unsaturated Porous Media: Recent Advances and Future Directions. Vadose Zone Journal - VADOSE ZONE J 3, 338–351. https://doi.org/10.2113/3.2.338

Filipovic, M., Woldegiorgis, A., Norström, K., Bibi, M., Lindberg, M., Österås, A.-H., 2015. Historical usage of aqueous film forming foam: A case study of the widespread distribution of perfluoroalkyl acids from a military airport to groundwater, lakes, soils and fish. Chemosphere 129, 39–45. https://doi.org/10.1016/j.chemosphere.2014.09.005

Flury, M., Aramrak, S., 2017. Role of air-water interfaces in colloid transport in porous media: A review. Water Resources Research 53, 5247–5275. https://doi.org/10.1002/2017wr020597

Gao, X., Chorover, J., 2012. Adsorption of perfluorooctanoic acid and perfluorooctanesulfonic acid to iron oxide surfaces as studied by flow-through ATR-FTIR spectroscopy. Environ. Chem. 9, 148–157. https://doi.org/10.1071/EN11119

Gellrich, V., Stahl, T., Knepper, T.P., 2012. Behavior of perfluorinated compounds in soils during leaching experiments. Chemosphere 87, 1052–6. https://doi.org/10.1016/j.chemosphere.2012.02.011

Grolimund, D., Borkovec, M., Barmettler, K., Sticher, H., 1996. Colloid-Facilitated Transport of Strongly Sorbing Contaminants in Natural Porous Media: A Laboratory Column Study. Environ. Sci. Technol. 30, 3118–3123. https://doi.org/10.1021/es960246x

Guelfo, J.L., Adamson, D.T., 2018. Evaluation of a national data set for insights into sources, composition, and concentrations of per- and polyfluoroalkyl substances (PFASs) in US drinking water. Environmental Pollution 236, 505–513. https://doi.org/10.1016/j.envpol.2018.01.066

Guelfo, J.L., Higgins, C.P., 2013. Subsurface Transport Potential of Perfluoroalkyl Acids at Aqueous Film-Forming Foam (AFFF)-Impacted Sites. Environ. Sci. Technol. 47, 4164–4171. https://doi.org/10.1021/es3048043

Guelfo, J.L., Wunsch, A., McCray, J., Stults, J.F., Higgins, C.P., 2020. Subsurface transport potential of perfluoroalkyl acids (PFAAs): Column experiments and modeling. Journal of Contaminant Hydrology 233, 103661. https://doi.org/10.1016/j.jconhyd.2020.103661

Guo, W., He, M., Yang, Z., Lin, C., Quan, X., Wang, H., 2007. Distribution of polycyclic aromatic hydrocarbons in water, suspended particulate matter and sediment from Daliao River watershed, China. Chemosphere 68, 93–104. https://doi.org/10.1016/j.chemosphere.2006.12.072

Hamid, H., Li, L.Y., Grace, J.R., 2020. Formation of perfluorocarboxylic acids from 6:2 fluorotelomer sulfonate (6:2 FTS) in landfill leachate: Role of microbial communities. Environmental Pollution 259, 113835. https://doi.org/10.1016/j.envpol.2019.113835

Hatfield, R.G., Maher, B.A., 2009. Fingerprinting upland sediment sources: particle size-specific magnetic linkages between soils, lake sediments and suspended sediments. Earth Surface Processes and Landforms 34, 1359–1373. https://doi.org/10.1002/esp.1824

Hepburn, E., Madden, C., Szabo, D., Coggan, T.L., Clarke, B., Currell, M., 2019. Contamination of groundwater with per- and polyfluoroalkyl substances (PFAS) from legacy landfills in an urban re-development precinct. Environmental Pollution 248, 101–113. https://doi.org/10.1016/j.envpol.2019.02.018

Higgins, C.P., Luthy, R.G., 2006. Sorption of Perfluorinated Surfactants on Sediments †. Environ. Sci. Technol. 40, 7251–7256. https://doi.org/10.1021/es061000n

Hoisaeter, A., Pfaff, A., Breedveld, G.D., 2019. Leaching and transport of PFAS from aqueous film-forming foam (AFFF) in the unsaturated soil at a firefighting training facility under cold climatic conditions. Journal of Contaminant Hydrology 222, 112–122. https://doi.org/10.1016/j.jconhyd.2019.02.010

Houtz, E.F., Higgins, C.P., Field, J.A., Sedlak, D.L., 2013. Persistence of Perfluoroalkyl Acid Precursors in AFFF-Impacted Groundwater and Soil. Environ. Sci. Technol. 47, 8187–8195. https://doi.org/10.1021/es4018877

Hsia, T.-H., Lo, S.-L., Lin, C.-F., Lee, D.-Y., 1994. Characterization of arsenate adsorption on hydrous iron oxide using chemical and physical methods. Colloids and Surfaces A: Physicochemical and Engineering Aspects 85, 1–7. https://doi.org/10.1016/0927-7757(94)02752-8

Jia, Y., Zhang, L., Zheng, J., Liu, X., Jeng, D.-S., Shan, H., 2014. Effects of wave-induced seabed liquefaction on sediment re-suspension in the Yellow River Delta. Ocean Engineering 89, 146–156. https://doi.org/10.1016/j.oceaneng.2014.08.004

Knutsen, H., Maehlum, T., Haarstad, K., Slinde, G.A., Arp, H.P.H., 2019. Leachate emissions of short- and long-chain per- and polyfluoralkyl substances (PFASs) from various Norwegian landfills. Environmental Science-Processes & Impacts 21, 1970–1979. https://doi.org/10.1039/c9em00170k

Lam, N.H., Cho, C.-R., Kannan, K., Cho, H.-S., 2017. A nationwide survey of perfluorinated alkyl substances in waters, sediment and biota collected from aquatic environment in Vietnam: Distributions and bioconcentration profiles. Journal of Hazardous Materials 323, 116–127. https://doi.org/10.1016/j.jhazmat.2016.04.010

Li, F., Fang, X., Zhou, Z., Liao, X., Zou, J., Yuan, B., Sun, W., 2019. Adsorption of perfluorinated acids onto soils: Kinetics, isotherms, and influences of soil properties. Science of The Total Environment 649, 504–514. https://doi.org/10.1016/j.scitotenv.2018.08.209

Li, Y., Oliver, D.P., Kookana, R.S., 2018. A critical analysis of published data to discern the role of soil and sediment properties in determining sorption of per and polyfluoroalkyl

substances (PFASs). Sci Total Environ 628–629, 110–120. https://doi.org/10.1016/j.scitotenv.2018.01.167

Liu, Y., Qi, F., Fang, C., Naidu, R., Duan, L., Dharmarajan, R., Annamalai, P., 2020. The effects of soil properties and co-contaminants on sorption of perfluorooctane sulfonate (PFOS) in contrasting soils. Environmental Technology & Innovation 19, 100965. https://doi.org/10.1016/j.eti.2020.100965

Liu, Y.Q., Zhang, Y., Li, J.F., Wu, N., Li, W.P., Niu, Z.G., 2019. Distribution, partitioning behavior and positive matrix factorization-based source analysis of legacy and emerging polyfluorinated alkyl substances in the dissolved phase, surface sediment and suspended particulate matter around coastal areas of Bohai Bay, China. Environmental Pollution 246, 34–44. https://doi.org/10.1016/j.envpol.2018.11.113

Llorca, M., Schirinzi, G., Martínez, M., Barceló, D., Farré, M., 2018. Adsorption of perfluoroalkyl substances on microplastics under environmental conditions. Environmental Pollution 235, 680–691. https://doi.org/10.1016/j.envpol.2017.12.075

Longstaffe, J.G., Courtier-Murias, D., Soong, R., Simpson, M.J., Maas, W.E., Fey, M., Hutchins, H., Krishnamurthy, S., Struppe, J., Alaee, M., Kumar, R., Monette, M., Stronks, H.J., Simpson, A.J., 2012. In-Situ Molecular-Level Elucidation of Organofluorine Binding Sites in a Whole Peat Soil. Environ. Sci. Technol. 46, 10508–10513. https://doi.org/10.1021/es3026769

Lyu, Y., Brusseau, M.L., Chen, W., Yan, N., Fu, X., Lin, X., 2018. Adsorption of PFOA at the Air-Water Interface during Transport in Unsaturated Porous Media. Environ Sci Technol 52, 7745–7753. https://doi.org/10.1021/acs.est.8b02348

Mejia-Avendano, S., Munoz, G., Vo Duy, S., Desrosiers, M., Benoi, T.P., Sauve, S., Liu, J., 2017. Novel Fluoroalkylated Surfactants in Soils Following Firefighting Foam Deployment During the Lac-Megantic Railway Accident. Environ Sci Technol 51, 8313–8323. https://doi.org/10.1021/acs.est.7b02028

Mejia-Avendano, S., Zhi, Y., Yan, B., Liu, J., 2020. Sorption of Polyfluoroalkyl Surfactants on Surface Soils: Effect of Molecular Structures, Soil Properties, and Solution Chemistry. Environ Sci Technol 54, 1513–1521. https://doi.org/10.1021/acs.est.9b04989

Meng, P., Deng, S., Lu, X., Du, Z., Wang, B., Huang, J., Wang, Y., Yu, G., Xing, B., 2014. Role of Air Bubbles Overlooked in the Adsorption of Perfluorooctanesulfonate on Hydrophobic Carbonaceous Adsorbents. Environ. Sci. Technol. 48, 13785–13792. https://doi.org/10.1021/es504108u

Miao, Y., Guo, X., Dan Peng, null, Fan, T., Yang, C., 2017. Rates and equilibria of perfluorooctanoate (PFOA) sorption on soils from different regions of China. Ecotoxicol Environ Saf 139, 102–108. https://doi.org/10.1016/j.ecoenv.2017.01.022

Milinovic, J., Lacorte, S., Vidal, M., Rigol, A., 2015. Sorption behaviour of perfluoroalkyl substances in soils. Science of The Total Environment 511, 63–71. https://doi.org/10.1016/j.scitotenv.2014.12.017

Milley, S.A., Koch, I., Fortin, P., Archer, J., Reynolds, D., Weber, K.P., 2018. Estimating the number of airports potentially contaminated with perfluoroalkyl and polyfluoroalkyl substances from aqueous film forming foam: A Canadian example. Journal of Environmental Management 222, 122–131. https://doi.org/10.1016/j.jenvman.2018.05.028

Mohanty, S.K., Saiers, J.E., Ryan, J.N., 2015. Colloid mobilization in a fractured soil during dry–wet cycles: role of drying duration and flow path permeability. Environmental Science & Technology 49, 9100–9106. https://doi.org/10.1021/acs.est.5b00889

Mohanty, S.K., Saiers, J.E., Ryan, J.N., 2014. Colloid-facilitated mobilization of metals by freeze–thaw cycles. Environmental Science & Technology 48, 977–984. https://doi.org/10.1021/es403698u

Nadal, M., Domingo, J.L., 2014. Indoor Dust Levels of Perfluoroalkyl Substances (PFASs) and the Role of Ingestion as an Exposure Pathway: A Review. Current Organic Chemistry 18, 2200–2208. https://doi.org/10.2174/1385272819666140804230713

Nguyen, T.M.H., Bräunig, J., Thompson, K., Thompson, J., Kabiri, S., Navarro, D.A., Kookana, R.S., Grimison, C., Barnes, C.M., Higgins, C.P., McLaughlin, M.J., Mueller, J.F., 2020. Influences of Chemical Properties, Soil Properties, and Solution pH on Soil–Water Partitioning Coefficients of Per- and Polyfluoroalkyl Substances (PFASs). Environ. Sci. Technol. https://doi.org/10.1021/acs.est.0c05705

Nguyen, T.V., Reinhard, M., Chen, H.T., Gin, K.Y.H., 2016. Fate and transport of perfluoro- and polyfluoroalkyl substances including perfluorooctane sulfonamides in a managed urban water body. Environmental Science and Pollution Research 23, 10382–10392. https://doi.org/10.1007/s11356-016-6788-9

Nickerson, A., Maizel, A.C., Kulkarni, P.R., Adamson, D.T., Kornuc, J.J., Higgins, C.P., 2020. Enhanced Extraction of AFFF-Associated PFASs from Source Zone Soils. Environ. Sci. Technol. 54, 4952–4962. https://doi.org/10.1021/acs.est.0c00792

Nickerson, A., Rodowa, A.E., Adamson, D.T., Field, J.A., Kulkarni, P.R., Kornuc, J.J., Higgins, C.P., 2021. Spatial Trends of Anionic, Zwitterionic, and Cationic PFASs at an AFFF-Impacted Site. Environ. Sci. Technol. 55, 313–323. https://doi.org/10.1021/acs.est.0c04473

Nicole, W., 2013. PFOA and cancer in a highly exposed community: new findings from the C8 science panel. Environmental health perspectives 121, A340–A340. https://doi.org/10.1289/ehp.121-A340

Ololade, I.A., Zhou, Q., Pan, G., 2016. Influence of oxic/anoxic condition on sorption behavior of PFOS in sediment. Chemosphere 150, 798–803. https://doi.org/10.1016/j.chemosphere.2015.08.068

Pitter, G., Zare Jeddi, M., Barbieri, G., Gion, M., Fabricio, A.S.C., Daprà, F., Russo, F., Fletcher, T., Canova, C., 2020. Perfluoroalkyl substances are associated with elevated blood pressure and hypertension in highly exposed young adults. Environmental Health 19, 102. https://doi.org/10.1186/s12940-020-00656-0

Prevedouros, K., Cousins, I.T., Buck, R.C., Korzeniowski, S.H., 2006. Sources, Fate and Transport of Perfluorocarboxylates. Environ. Sci. Technol. 40, 32–44. https://doi.org/10.1021/es0512475

Qin, X.D., Qian, Z.M., Dharmage, S.C., Perret, J., Geiger, S.D., Rigdon, S.E., Howard, S., Zeng, X.W., Hu, L.W., Yang, B.Y., Zhou, Y., Li, M., Xu, S.L., Bao, W.W., Zhang, Y.Z., Yuan, P., Wang, J., Zhang, C., Tian, Y.P., Nian, M., Xiao, X., Chen, W., Lee, Y.L., Dong, G.H., 2017. Association of perfluoroalkyl substances exposure with impaired lung function in children. Environmental Research 155, 15–21. https://doi.org/10.1016/j.envres.2017.01.025

Qiu, Y., Jing, H., Shi, H., 2010. Perfluorocarboxylic acids (PFCAs) and perfluoroalkyl sulfonates (PFASs) in surface and tap water around Lake Taihu in China. Front. Environ. Sci. Eng. China 4, 301–310. https://doi.org/10.1007/s11783-010-0236-8

Robey, N.M., da Silva, B.F., Annable, M.D., Townsend, T.G., Bowden, J.A., 2020. Concentrating Per- and Polyfluoroalkyl Substances (PFAS) in Municipal Solid Waste Landfill Leachate Using Foam Separation. Environ. Sci. Technol. https://doi.org/10.1021/acs.est.0c01266

Rokoff, L.B., Rifas-Shiman, S.L., Coull, B.A., Cardenas, A., Calafat, A.M., Ye, X.Y., Gryparis, A., Schwartz, J., Sagiv, S.K., Gold, D.R., Oken, E., Fleisch, A.F., 2018. Cumulative exposure to environmental pollutants during early pregnancy and reduced fetal growth: the Project Viva cohort. Environmental Health 17. https://doi.org/10.1186/s12940-018-0363-4

Sharifan, H., Bagheri, M., Wang, D., Burken, J.G., Higgins, C.P., Liang, Y., Liu, J., Schaefer, C.E., Blotevogel, J., 2021. Fate and transport of per- and polyfluoroalkyl substances (PFASs) in the vadose zone. Science of The Total Environment 771, 145427. https://doi.org/10.1016/j.scitotenv.2021.145427

Silva, J.A.K., Martin, W.A., Johnson, J.L., McCray, J.E., 2019. Evaluating air-water and NAPL-water interfacial adsorption and retention of Perfluorocarboxylic acids within the Vadose zone. Journal of Contaminant Hydrology 223. https://doi.org/10.1016/j.jconhyd.2019.03.004

Sunderland, E.M., Hu, X.C., Dassuncao, C., Tokranov, A.K., Wagner, C.C., Allen, J.G., 2019. A review of the pathways of human exposure to poly- and perfluoroalkyl substances (PFASs)

and present understanding of health effects. Journal of Exposure Science & Environmental Epidemiology 29, 131–147. https://doi.org/10.1038/s41370-018-0094-1

Tanabe, S., Tatsukawa, R., 1983. Vertical transport and residence time of chlorinated hydrocarbons in the open ocean water column. Journal of the Oceanographical Society of Japan 39, 53–62. https://doi.org/10.1007/BF02210759

Tang, C.Y., Shiang Fu, Q., Gao, D., Criddle, C.S., Leckie, J.O., 2010. Effect of solution chemistry on the adsorption of perfluorooctane sulfonate onto mineral surfaces. Water Res 44, 2654–62. https://doi.org/10.1016/j.watres.2010.01.038

Tondera, K., Koenen, S., Pinnekamp, J., 2013. Survey monitoring results on the reduction of micropollutants, bacteria, bacteriophages and TSS in retention soil filters. Water Science and Technology 68, 1004–1012. https://doi.org/10.2166/wst.2013.340

Turner, A., Millward, G.E., 2002. Suspended Particles: Their Role in Estuarine Biogeochemical Cycles. Estuarine, Coastal and Shelf Science 55, 857–883. https://doi.org/10.1006/ecss.2002.1033

Vedagiri, U.K., Anderson, R.H., Loso, H.M., Schwach, C.M., 2018. Ambient levels of PFOS and PFOA in multiple environmental media. Remediation Journal 28, 9–51. https://doi.org/10.1002/rem.21548

Wang, F., Liu, C., Shih, K., 2012. Adsorption behavior of perfluorooctanesulfonate (PFOS) and perfluorooctanoate (PFOA) on boehmite. Chemosphere 89, 1009–14. https://doi.org/10.1016/j.chemosphere.2012.06.071

Wang, F., Shih, K., Leckie, J.O., 2015. Effect of humic acid on the sorption of perfluorooctane sulfonate (PFOS) and perfluorobutane sulfonate (PFBS) on boehmite. Chemosphere 118, 213–8. https://doi.org/10.1016/j.chemosphere.2014.08.080

Wang, P., Lu, Y., Wang, T., Meng, J., Li, Q., Zhu, Z., Sun, Y., Wang, R., Giesy, J.P., 2016. Shifts in production of perfluoroalkyl acids affect emissions and concentrations in the environment of the Xiaoqing River Basin, China. Journal of Hazardous Materials 307, 55–63. https://doi.org/10.1016/j.jhazmat.2015.12.059

Wang, P., Wang, T., Giesy, J.P., Lu, Y., 2013. Perfluorinated compounds in soils from Liaodong Bay with concentrated fluorine industry parks in China. Chemosphere 91, 751–7. https://doi.org/10.1016/j.chemosphere.2013.02.017

Weber, A.K., Barber, L.B., LeBlanc, D.R., Sunderland, E.M., Vecitis, C.D., 2017. Geochemical and Hydrologic Factors Controlling Subsurface Transport of Poly- and Perfluoroalkyl Substances, Cape Cod, Massachusetts. Environ. Sci. Technol. 51, 4269–4279. https://doi.org/10.1021/acs.est.6b05573

Wei, C., Song, X., Wang, Q., Hu, Z., 2017. Sorption kinetics, isotherms and mechanisms of PFOS on soils with different physicochemical properties. Ecotoxicol Environ Saf 142, 40–50. https://doi.org/10.1016/j.ecoenv.2017.03.040

Xiao, F., Jin, B., Golovko, S.A., Golovko, M.Y., Xing, B., 2019. Sorption and Desorption Mechanisms of Cationic and Zwitterionic Per- and Polyfluoroalkyl Substances in Natural Soils: Thermodynamics and Hysteresis. Environ Sci Technol 53, 11818–11827. https://doi.org/10.1021/acs.est.9b05379

Xiao, F., Simcik, M.F., Gulliver, J.S., 2012. Perfluoroalkyl acids in urban stormwater runoff: Influence of land use. Water Research 46, 6601–6608. https://doi.org/10.1016/j.watres.2011.11.029

Yi, S., Harding-Marjanovic, K.C., Houtz, E.F., Gao, Y., Lawrence, J.E., Nichiporuk, R.V., Iavarone, A.T., Zhuang, W.-Q., Hansen, M., Field, J.A., Sedlak, D.L., Alvarez-Cohen, L., 2018. Biotransformation of AFFF Component 6:2 Fluorotelomer Thioether Amido Sulfonate Generates 6:2 Fluorotelomer Thioether Carboxylate under Sulfate-Reducing Conditions. Environ. Sci. Technol. Lett. 5, 283–288. https://doi.org/10.1021/acs.estlett.8b00148

Zhang, J., 1999. Heavy metal compositions of suspended sediments in the Changjiang (Yangtze River) estuary: significance of riverine transport to the ocean. Continental Shelf Research 19, 1521–1543. https://doi.org/10.1016/S0278-4343(99)00029-1

Zhang, L., Lee, L.S., Niu, J., Liu, J., 2017. Kinetic analysis of aerobic biotransformation pathways of a perfluorooctane sulfonate (PFOS) precursor in distinctly different soils. Environmental Pollution 229, 159–167. https://doi.org/10.1016/j.envpol.2017.05.074

Zhang, T., Sun, H., Gerecke, A.C., Kannan, K., Müller, C.E., Alder, A.C., 2010. Comparison of two extraction methods for the analysis of per- and polyfluorinated chemicals in digested sewage sludge. Journal of Chromatography A 1217, 5026–5034. https://doi.org/10.1016/j.chroma.2010.05.061

Zhao, L., Bian, J., Zhang, Y., Zhu, L., Liu, Z., 2014. Comparison of the sorption behaviors and mechanisms of perfluorosulfonates and perfluorocarboxylic acids on three kinds of clay minerals. Chemosphere 114, 51–8. https://doi.org/10.1016/j.chemosphere.2014.03.098

Zhou, Z., Liang, Y., Shi, Y., Xu, L., Cai, Y., 2013. Occurrence and Transport of Perfluoroalkyl Acids (PFAAs), Including Short-Chain PFAAs in Tangxun Lake, China. Environ. Sci. Technol. 47, 9249–9257. https://doi.org/10.1021/es402120y

3. CHAPTER 3: RELEASE OF SOIL COLLOIDS INCREASE THE PFAS CONCENTRATION FROM SATURATED SOIL DURING FLOW INTERRUPTION

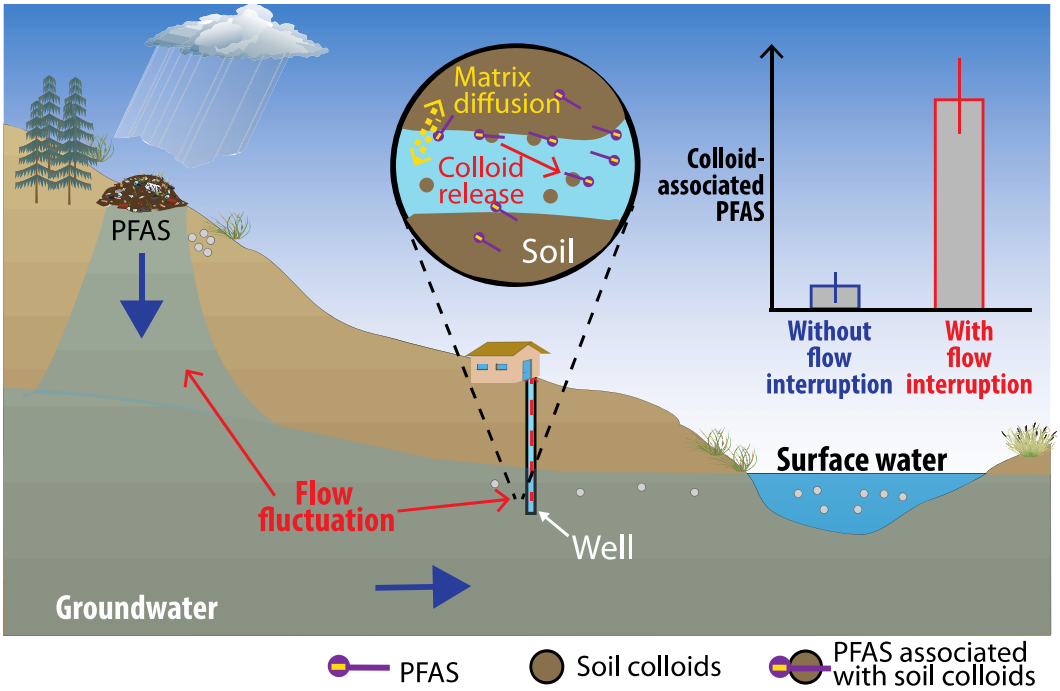

Borthakur, A., Cranmer, B.K., Dooley, G.P., Blotevogel, J., Mahendra, S., Mohanty, S.K., 2021. Release of soil colloids during flow interruption increases the pore-water PFAS concentration in saturated soil. Environmental Pollution 117297. https://doi.org/10.1016/j.envpol.2021.117297

Abstract

Groundwater flow through aquifer soils or packed bed systems can fluctuate for various reasons, which could affect the concentration of natural colloids and per- and polyfluoroalkyl substances (PFAS) in the pore water. In such cases, PFAS concentration could either decrease due to matrix diffusion of PFAS or increase by the detachment of colloids carrying PFAS. Yet, the effect of flow fluctuation on PFAS transport or release in porous media has not been examined. To examine the relative importance of either process, we interrupted the flow during an injection of groundwater spiked with perfluorobutanoic acid (PFBA), perfluorooctanoic acid (PFOA), and bromide as conservative tracer through clay-rich soil, so that diffusive transport would be prominent during flow interruption. After flow interruption, the PFAS concentration did not decrease indicating an insignificant contribution of matrix diffusion. The concentration increased, potentially due to enhanced release of colloid-associated PFAS. Analysis of samples before and after flow interruption by particle size analysis and SEM confirmed an increase in soil colloid concentration after the flow interruption. XRD analysis of soil and the colloids proved that PFAS were associated with specific sites of the colloids. Due to a higher affinity of PFOA to soil colloids, the total PFOA concentration in the effluent samples increased more than PFBA after the flow interruption process. The results indicate that colloids may have a disproportionally higher role in the transport of PFAS in conditions that release colloids from porous media. Fluctuations in groundwater flow can increase this colloid facilitated mobility of PFAS.

3.1. Introduction

Per- and polyfluoroalkyl substances (PFAS), due to their recalcitrant nature and high mobility, have been detected in various drinking water sources in concentrations ranging from 0.32 ng L^{-1} to as high as 7000 ng L^{-1} (Domingo and Nadal 2019, Guelfo and Adamson 2018, Sharma et al. 2016). Exposure to PFAS in drinking water can cause adverse health effects such as birth defects (Xu et al. 2019), liver toxicity (Zhang et al. 2016), immunotoxicity (DeWitt et al. 2019), and cancer (Grandjean and Clapp 2015). Due to the health risks associated with PFAS exposure, several agencies around the world set up very low advisory limits for PFAS concentrations in drinking water (Domingo and Nadal 2019). The US EPA has set an advisory limit of 70 ng L^{-1} for PFOA and PFOS concentrations in drinking water. Similarly, China has set health advisories of 85 ng L^{-1} for PFOA and 47 ng L^{-1} for PFOS. Swedish EPA recommends a drinking water guideline of 90 ng L^{-1} for Σ_{11}PFASes (PFBA, PFPeA, PFHxA, PFHpA, PFOA, PFNA, PFDA, PFBS, PFHxS, PFOS, and 6:2 FTSA) while the Danish EPA recommends 100 ng L^{-1} for Σ_{12}PFASes. The Italian National Health Institute (ISS) established the following maximum PFAS concentrations in drinking water: PFOS $\leq$ 30 ng L^{-1}, PFOA $\leq$ 500 ng L^{-1}, other PFAS $\leq$ 500 ng L^{-1}. The majority of PFAS impacted drinking water systems in the U.S. use groundwater as the primary water source (Guelfo and Adamson 2018). Furthermore, the transport of PFAS through porous media is also relevant for their treatment in packed activated carbon reactors (Brusseau 2020, Du et al. 2014). Thus, it is critical to understand the processes that transport PFAS through porous media that simulate aquifer soil or packed bed reactors.

Numerous studies used flow-through column experiments to examine PFAS transport processes (Dalahmeh et al. 2019, Lyu et al. 2018, McCleaf et al. 2017, McKenzie et al. 2015, Van Glubt and Brusseau 2021, Van Glubt et al. 2021). PFAS moves through the porous media by

advection, dispersion, or diffusion (Armitage et al. 2009, Brusseau et al. 2019, Wang et al. 2005). During transport, PFAS can adsorb onto solids such as soil, sediments, or carbonaceous matter such as activated carbon (Campos-Pereira et al. 2020, Higgins and Luthy 2006, Johnson et al. 2007, Mejia-Avendano et al. 2020, Xiao et al. 2017) by hydrophobic or electrostatic interactions due to their surfactant nature (Pereira et al. 2018, Zhang et al. 2014). Thus, the extent of removal depends on soil organic carbon (Johnson et al. 2007, Liu and Lee 2005, Qian et al. 2017), proteinaceous matter(Longstaffe et al. 2012), clay fraction (Zhao et al. 2014), and iron and aluminum oxide content (Wei et al. 2017, Zhao et al. 2014), groundwater pH and ionic strength (Ahrens et al. 2009, Tang et al. 2010). Additionally, removal can vary with PFAS properties such as carbon chain length (Guelfo and Higgins 2013, Milinovic et al. 2015) and functional groups including the charge and Lewis acid/base behavior (Ahrens et al. 2011, Pereira et al. 2018). Perfluorobutanoic acid (PFBA) and perfluorooctanoic acid (PFOA) are anionic PFAS compounds with a carboxylic acid functional group with a different number of carbon atoms (4 for PFBA and 8 for PFOA) in their structure. Due to the higher hydrophobicity of PFOA than PFBA, the affinity of PFOA to soils and sediments is greater than PFAS (Milinovic et al. 2015, Pereira et al. 2018). For the same reason, PFBA is more soluble in water (Gagliano et al. 2020) and has a higher diffusivity (Schaefer et al. 2019) compared to PFOA. Due to this, surface water samples mostly find PFBA in dissolved state and PFOA adsorbed to sediments and suspended sediments (Ahrens et al. 2010).

Flow rates in porous media can fluctuate for various practical and natural reasons. The flow of groundwater through soil can fluctuate depending on the precipitation rate, hydraulic gradient, hydraulic conductivity, and human, plant, and animal activities (Beretta and Terrenghi 2017, Gribovszki et al. 2010, Suzuki and Higashi 2001). Flow may be paused for several days during the

operation of groundwater extraction or treatment through pack-bed reactors. Changes in flow rate or flow interruption may affect the available time for sorption or diffusive transport to occur in the porous media (Gellrich et al. 2012, Hoisaeter et al. 2019). Diffusive transport is particularly critical in systems containing micropores, where the role of advective transport is minimal. Diffusive transport becomes prominent in the absence of advection, which occurs when the flow is completely stopped (Brusseau et al. 1997, Brusseau et al. 1989). Yet, most column studies on PFAS transport used a constant flow rate assuming equilibrium conditions in the porous media (Guelfo et al. 2020, Lyu et al. 2019).

Flow fluctuations or interruptions can release natural soil colloids from porous media (Gao et al. 2004, Schelde et al. 2002, Zhou et al. 2017), which may contain previously adsorbed pollutants (Zhu et al. 2014). Natural soil colloids have been shown to facilitate the transport of other hydrophobic pollutants (Ryan and Elimelech 1996, Xing et al. 2016). The same process may occur for PFAS. Colloids were found to carry a significant amount of PFAS in surface waters (Ahrens et al. 2010, Liu et al. 2019, Nguyen et al. 2016, Zhao et al. 2016), indicating they could do the same in groundwater aquifer. Suspended sediment-associated PFAS can exacerbate their toxicity in surface water organisms as well (Liu et al. 2020). However, studies on the transport of PFAS typically estimate the dissolved PFAS (Seo et al. 2019), assuming the concentration of PFAS associated with colloids is insignificant. Groundwater samples are typically filtered or centrifuged to remove all colloids before analyzing for PFAS. This can also underestimate the total PFAS concentration in water samples if colloids are present and they carry a significant amount of PFAS.

This study aims to examine the effect of fluctuations in flow rate on the distribution of dissolved and colloid-associated PFAS in water samples. We hypothesized that flow perturbation

could increase PFAS concentrations in pore water by increasing the release of soil colloids containing PFAS. To test this hypothesis, we injected PFAS-impacted groundwater through columns packed with soil, interrupted the flow as an extreme case scenario, and measured the change in the concentration of colloids and PFAS (dissolved and colloid) in the pore water as a result of flow perturbation. The effect of matrix diffusion on PFAS transport was evaluated by using bromide as a conservative tracer in the injected solution. Our results could improve the understanding of PFAS transport in porous media in systems where colloids may be present due to changes in flow dynamics in the system.

3.2. Experimental methods

3.2.1. Soil and groundwater

Soil and groundwater were collected upgradient of a firefighting training facility and characterized for residual PFAS. Triplicate soil and groundwater samples were analysed for the pH and electrical conductivity of the groundwater and the pH, total organic carbon and cation exchange capacity of the soil. Duplicate soil samples were analysed for the anion exchange capacity and pH of the soil. The groundwater was analysed for cation and anion concentrations using Ion exchange chromatography (ICE) and Inductively Coupled Plasma-Optical Emission Spectrometry (ICP-OES). The organic carbon content in the groundwater was measured using a total organic carbon analyser (Shimadzu TOC-LCSN). The properties and the residual PFAS concentrations in the soil and groundwater are given in Table 3-1. The soil was dried at 104 ºC for 24 h and sieved through a 2-mm sieve to remove gravel-size aggregate or grains before packing. Stock solutions of 2 g L^{-1} PFBA (99% purity, Acros Organics) and 1 g L^{-1} PFOA (96% purity, Acros Organics) was prepared in a 7:3 solution of methanol and ultrapure water. Groundwater was spiked with the stock solutions to prepare PFAS-impacted groundwater containing 200 µg L^{-}

[1] PFOA and 200 µg L^{-1} PFBA. This PFOA concentration was at least three orders of magnitude higher than any residual concentration detected in soil or groundwater (Table 3-1), which is essential to quantify the contribution of matrix diffusion or colloid-associated transport on PFAS concentration in pore water. Although the soil around firefighting training facilities should have PFBA, no PFBA was detected in the soil and groundwater samples. This is possibly due to the high mobility and low affinity of PFBA to soil (Eschauzier et al. 2013). Therefore, most PFBA was probably removed from the site by runoff. Potassium bromide (KBr > 99% purity, Alfa Aesar) was added to the solution to achieve a 20 mg L^{-1} final concentration of bromide, a conservative tracer. The final concentration of methanol in the PFAS impacted groundwater was 0.025% v/v.

Table 3-1: Groundwater and soil characteristics.

Parameters	Groundwater	Soil
pH	7.1 ± 0.01	7.3 ± 0.01[a]
Electrical Conductivity (μS cm^{-1})	423.3 ± 0.5	
Fluoride (mg L^{-1})	3.3	
Nitrate (mg L^{-1})	4	
Chloride (mg L^{-1})	55.5	
Sulfate (mg L^{-1})	19.7	
Calcium (mg L^{-1})	82.7	
Magnesium (mg L^{-1})	1.85	
Total Organic Carbon[b]	0.006	0.8 ± 0.0
Background PFBA concentration[c]	n.d	n.d
Background PFOA concentration[c]	0.108	0.881
Anion Exchange Capacity (cmol/kg)		2.8 ± 0.5
Cation Exchange Capacity (cmol/kg)		13.6 ± 0.6
Quartz[d] (%)		90.2
K-Feldspar[d] (%)		2.3
Calcite[d] (%)		6.3
Illite and Mica[d] (%)		1.2
Bulk Density (g/cm^3)		1.2 ± 0.03
Porosity (%)		38.2 ± 2.3

[a] Measured in 0.01 M $CaCl_2$
[b] Total organic carbon content is mg L^{-1} for groundwater and the percentage of the total dry weight of soil.
[c] PFAS concentration is in μg L^{-1} for groundwater and μg kg^{-1} in soil.
[d] Measured using XRD.

3.2.2. Effect of flow interruption on PFAS concentration in the effluent

The dry packing method mentioned elsewhere was used for packing the columns in this study (Mohanty et al. 2014a). The soil was packed into duplicate polypropylene columns (2.54 cm ID, 30.5 cm length) to simulate aquifer soil (Figure 3-1). The bulk density was estimated by dividing the weight of packed soil with the volume of the column. The soil columns were saturated by injecting synthetic groundwater at 0.61 cm h^{-1} from the bottom of the soil columns for 24 hours and collecting the effluent from the top of the columns. The pore volume (PV) was estimated by subtracting the dry column mass from the saturated soil column mass (Table 3-1).

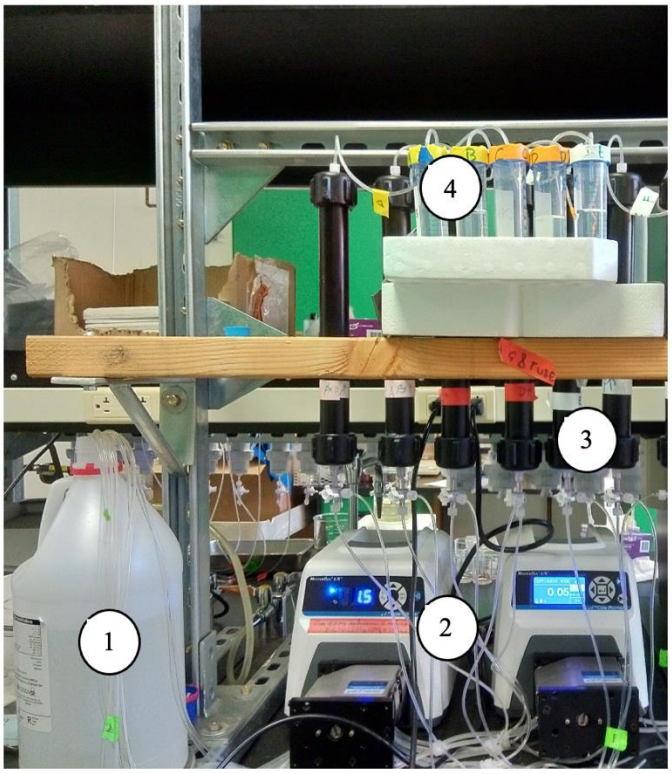

Figure 3-1: Experimental setup: PFAS-impacted groundwater (1) was injected through the bottom of the soil columns (3) using a peristaltic pump (2). The effluent was collected from the top (4).

First, PFAS-free groundwater without bromide was injected into the packed columns at 0.61 cm h^{-1} for at least 48 hours to achieve an equilibrium in pore water chemistry (pH and ionic strength) between the soil and groundwater. Then, about 16.2 PV groundwater spiked with PFAS and bromide was injected at 0.61 cm h^{-1} through the bottom end of columns before the flow was stopped for six days. The 6-day duration was used to evaluate if the diffusion of PFAS into the soil matrix would decrease their concentration in pore water. After the flow interruption, an additional 16.4 PV of the PFAS impacted groundwater was injected for 12 days at the same flux rate of 0.61 cm h^{-1}. Then, 6.9 PV of PFAS-free groundwater was injected for five days to remove PFAS from pore water. This groundwater has bromide concentrations below the detection limit (<1 ppb). To examine the contribution of any PFOA and PFBA precursor that may have been originally present in the soil, a control experiment was conducted by injecting PFAS-free groundwater through new columns. The flow regime in control columns was similar, and the effluent was monitored for PFAS that may leach out of soil due to precursor transformation during flow interruption. The maximum concentration of PFOA and PFBA in the effluent in the control columns was reported in Table 3-2.

Table 3-2: Maximum PFAS concentrations in effluent water from control columns in which PFAS-free water was injected.

PFAS Compound	Concentration (µg/L)
PFBA	n.d.
PFOA	0.47 ± 0.09

3.2.3. Water sample analysis

To determine the dissolved PFAS concentration in the pore water, effluent samples were centrifuged at 20,817 g for 15 min to settle any soil colloids greater than 0.04 μm in size. The centrifugation method, as opposed to filtration, was used to eliminate the change in concentration of PFAS due to adsorption on filter materials (Lath et al. 2019). 0.5 mL of the supernatant was mixed with 0.5 mL methanol. To measure the total PFAS concentration, the sample was mixed with methanol in a 1:1 ratio to desorb the colloid-associated PFAS. The colloids were then removed by centrifugation and the supernatant was analyzed for PFAS. Colloid-associated PFAS concentration was estimated by subtracting dissolved PFAS concentration from the total PFAS concentration. By taking the difference between the non-centrifuged and centrifuged samples, the losses of PFAS due to storage or handling were eliminated as both the samples were exposed to similar conditions. Before analysis, 50 μg L^{-1} MPFBA and MPFOA internal standards ($^{13}C_4$-PFBA and $^{13}C_4$-PFOA, Wellington Laboratories) were added to the samples to account for PFAS losses due to adsorption to the vial walls, sample processing before chemical analysis, and analytical variability. The samples were aliquoted into 200-μL polypropylene vials and analyzed for PFAS using liquid chromatography paired with triple quadrupole mass spectrometry (LC/QqQ-MS). The instrument used for PFAS analysis was an Agilent 1290 UPLC coupled to an Agilent 6460 triple quadrupole mass spectrometer, which was equipped with an electrospray ionization (ESI) source using Agilent Jet Stream Technology (Agilent, Santa Clara, CA). Analytes were separated on an Agilent Poroshell C18 column (2.1 mm x 100 mm, 2.7 μm particle size) at 40 °C. A sample volume of 15 μL was injected into a binary mixture of 5 mM ammonium acetate in water (A) and 5 mM ammonium acetate in methanol (B) at a flow rate of 0.4 mL/min. The gradient used was 20% B for 1 minute, increasing to 45% B at 2 min, and finally increased to 100% B at 5 min. The

ionization source conditions used were as follows: negative polarity, nebulizer of 15 psi, the gas flow of 4 L/min at 230°C, sheath gas flow of 12 L/min at 350 °C, nozzle voltage of 500 V, and capillary voltage at 3500 V. Analytes were identified by comparison of retention times with analytical standards, individual MRM mass transitions, and with MS/MS ion ratios. MRM transitions were 213 > 169 *m/z* for PFBA, 217 > 172 *m/z* for M4PFBA, 413 > 169 and 369 *m/z* for PFOA, and 417 > 372 and 170 *m/z* for M4PFOA. Peaks matching retention within 5% and with ion ratios at 20% of the standard ratio were considered acceptable for identification. The data collection and processing were performed by using Agilent MassHunter Quantitative software (v B.07.01). Quantitation was performed with linear regression using calibration curves from 0.05-250 ng/mL for PFBA, and 0.01-250 ng/mL for PFOA.

Several steps were taken to minimize system-related interferences or background. An Agilent Eclipse Plus C18 column (4.6 mm x 50 mm, 5 μm particle size) was installed immediately after the binary pump and before the injection port to perform as a delay column. The mobile phase degasser was bypassed allowing the mobile phase to enter the binary pump directly and avoiding contact with plastic filters. All plastic tubing in the LC-MS/MS system was replaced with PEEK tubing and plastic frits were replaced with stainless steel. All sample vials were polypropylene with polypropylene caps. Five injections of pure methanol were made before sample analysis to determine if any system background analyte levels were present. With these system changes, background levels for each analyte were not detected in blank samples.

Although EPA and ISO (BSI 2009, Shoemaker et al. 2008) recommend polypropylene containers for collecting and storing PFAS, Lath et al. (2019) observed considerable PFAS sorption by polypropylene containers. This vial sorption could underestimate the total PFAS concentration in the samples. To account for any such losses, 20 μg L^{-1} solutions of each PFAS

compound (PFBA and PFOA) were prepared in 50% methanol solution and stored in the polypropylene vials. The PFAS concentrations in the solutions were measured after 48 hours which is the average time between sampling and analysis. In this period, PFBA and PFOA concentrations decreased by only 0.3% and 1.0%, respectively. Thus, decreases in PFAS concentration due to vial sorption were considered negligible.

3.2.4. Data analysis

The area under the breakthrough curve before the flow was interrupted was calculated to determine the total amount of PFAS that exited the columns before the flow interruption. This amount was subtracted from the total amount of PFAS injected into the columns to determine the total amount of PFAS retained by the soil before the flow interruption. The increase in PFAS concentration due to flow interruption was quantified using the following equation:

$$Concentration\ change\ (\%) = \frac{C_f - C_i}{C_i} \times 100$$

where C_f = maximum increase in PFAS concentration after flow interruption and C_i = mean PFAS concentration in BTC plateau before flow interruption.

3.2.5. Colloid characterization

The turbidity of the effluent samples, an indicator of the presence of colloids, was measured by measuring the absorbance at 890 nm using a UV-vis spectrophotometer (Mohanty et al. 2014b, Sadar 2004). The size distribution of the colloids in the effluent samples was measured using an Accusizer AD Optical Particle Sizer which counts particles of size greater than 0.83 µm at 0.01 µm resolution using the Single Particle Optical Sensing (SPOS) technique. Morphology and elemental composition of the colloids were measured using a Scanning Electron Microscope with Energy Dispersive X-ray Analysis (SEM-EDS). The mineral composition of the bulk soil (grain

sizes less than 2 mm) as well as the colloid fraction (grain sizes 4 μm and less) was characterized using X-ray diffractometry. Details of the characterization methods are provided in the Supplementary Material.

3.2.6. X-ray diffraction analysis

Sample Preparation. The samples were cleaned of any obvious foreign matter and disaggregated using a mortar and pestle. A portion of the sample was taken and pulverized in a McCrone micronizing mill. The powder was dried, disaggregated and packed. This sample was used for the XRD analysis of the bulk soil (bulk soil samples).

In addition, a portion of the pulverized samples was dispersed in distilled water using a sonic probe. The samples were centrifuged to extract the particles of size less than 4 μm (<4 μm samples). The <4 μm samples were deposited on nylon membrane filters using vacuum filtration. XRD analysis of these <4 μm samples was done to determine the mineral composition of the clay fraction of the soil and the soil colloids that were released.

XRD analysis. XRD analysis of the samples was performed using a Seimens D500 automated powder diffractometer with a copper X-ray emitting source (40 kV, 30mA) and a scintillation X-ray detector. The bulk soil samples were analyzed over a range of 5 to 60 degrees 2θ at the rate of 1 degree per minute. The <4 μm samples were analyzed over a range of 2 to 36 degrees at a scan rate of 1 degree per minute. Additionally, air-dried <4μm samples were analyzed first. Then the samples were exposed to ethylene glycol vapor for 12 hours and were reanalyzed. The XRD patterns from the air-dried and ethylene glycol were compared and analyzed to determine the different types of clay minerals present in the soil.

3.2.7. SEM analysis of colloids

Glass Petri dishes were washed and cleaned with deionized water and ethanol to remove all particulate matter from them. 0.5 mL effluent samples were added to these Petri dishes and the dishes were covered with aluminum foil. The dishes were then dried overnight in a vacuum oven and the dried colloids were extracted from the dishes using carbon tape. The carbon tapes were coated with Platinum and the morphology and elemental characteristics of the colloids on the carbon tape were analyzed using SEM-EDS (Zeiss Supra 40VP).

3.3. Results

3.3.1. Retardation of PFAS in soil depended on PFAS type and soil constituents

The retardation of PFAS compounds through the soil depended on the PFAS type (Figure 3-2). The concentration of bromide, a conservative tracer, reached half the injected bromide concentration ($C/C_0 = 0.5$) after injecting 57 mL of PFAS impacted groundwater, indicating that the pore volume of the soil columns was 57 mL. The breakthrough curve of PFBA was almost similar to bromide, its concentration reached the injected PFBA concentration after the injection of about 2.16 PV of PFAS impacted groundwater. On the other hand, the transport of PFOA was more retarded by the soil. The PFOA concentration equaled the injected concentration after around 5 PV of PFAS impacted groundwater was injected into the soil columns.

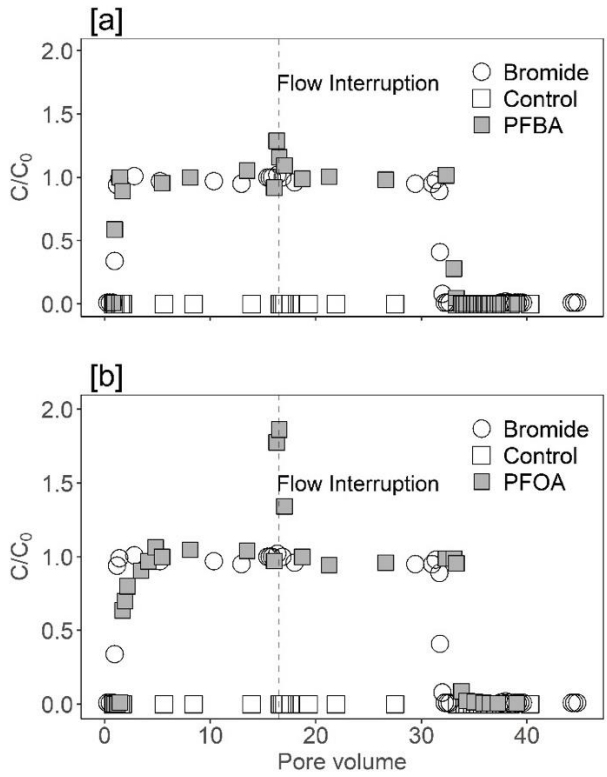

Figure 3-2: Breakthrough curves and increase in the concentration of (a) PFBA and (b) PFOA following flow interruption in soil columns. The white circles denote bromide concentration, grey circles denote PFAS concentrations in test columns where PFAS-impacted groundwater was injected through the columns and the white squares denote the PFAS concentrations in control columns where PFAS-free groundwater was injected through the columns. The dashed line denotes when the flow was interrupted for 6 days.

Mass balance analysis (Table 3-3) showed that the soil retained 5.9 ± 0.3% of the total injected PFBA and 9.1 ± 2.3% of the total injected PFOA before the flow was interrupted. During injection of PFAS-free groundwater, PFBA was flushed out from the soil relatively quickly compared with PFOA. PFBA concentration reached 1% of the injected concentration (C_0) after pumping with 1.5 PV of PFAS-free groundwater, whereas PFOA concentration reached 0.3% of C_0 after flushing with 5.8 PV of PFAS-free groundwater.

Table 3-3: Mass balance analysis of breakthrough curves.

PFAS Compound	Transported (%)[a]	Retained (%)[b]	Increase in concentration after flow interruption (%)[c]
PFBA	94.1 ± 0.3	5.9 ± 0.3	29.9 ± 2.3
PFOA	90.9 ± 2.3	9.1 ± 2.3	84.5 ± 6.4

[a] Transport percentage was estimated by dividing the area under the breakthrough curve before flow interruption by the total amount injected. [b] Retained percentage was estimated by dividing the difference between the total amount injected before flow interruption and the area under the breakthrough curve before flow interruption by the total amount injected before flow interruption. [c] Concentration increased due to flow interruption was measured by this equation: $Concentration\ change\ (\%) = \frac{C_f - C_i}{C_i} \times 100$ where C_f = Maximum increase in PFAS concentration after flow interruption and C_i = mean PFAS concentration in BTC plateau before flow interruption.

3.3.2. Flow perturbation increased colloid concentration in pore water

Size analysis of the particles confirmed the presence of soil colloids of size less than 2 μm in samples collected after flow interruption (Figure 3-3). SEM data further confirmed an increase in the number of particles in the effluent samples after the flow interruption and showed the morphology of the colloids.

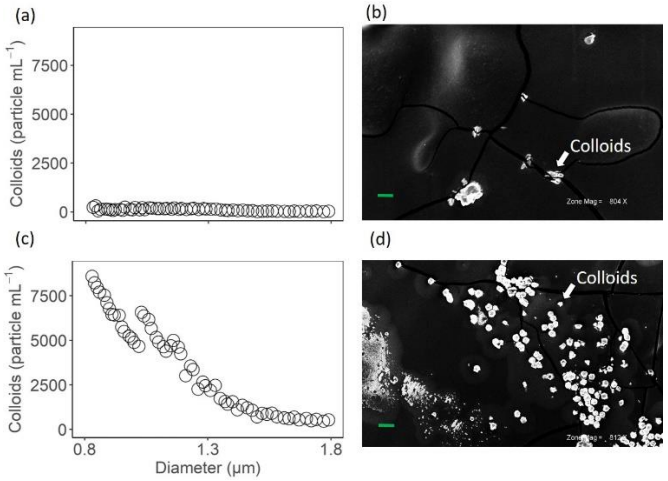

Figure 3-3: (a) Size distribution of the colloids in the effluent samples before flow interruption. (b) SEM image of the effluent sample before flow interruption showing the colloids in white against the black carbon tape background. (c) The size distribution of the colloids in the effluent samples after flow interruption. (d) SEM image of the effluent sample after flow interruption. The green line at the bottom left of the SEM image corresponds to a length of 20 μm. The colloids are marked with a white arrow in the image.

EDS analysis of the colloids revealed the presence of calcium, oxygen, silicon, magnesium, potassium, and sodium in the colloids (Figure 3-4). The turbidity concentration was near the detection limit indicating turbidity measurement is not sensitive to detect the colloids.

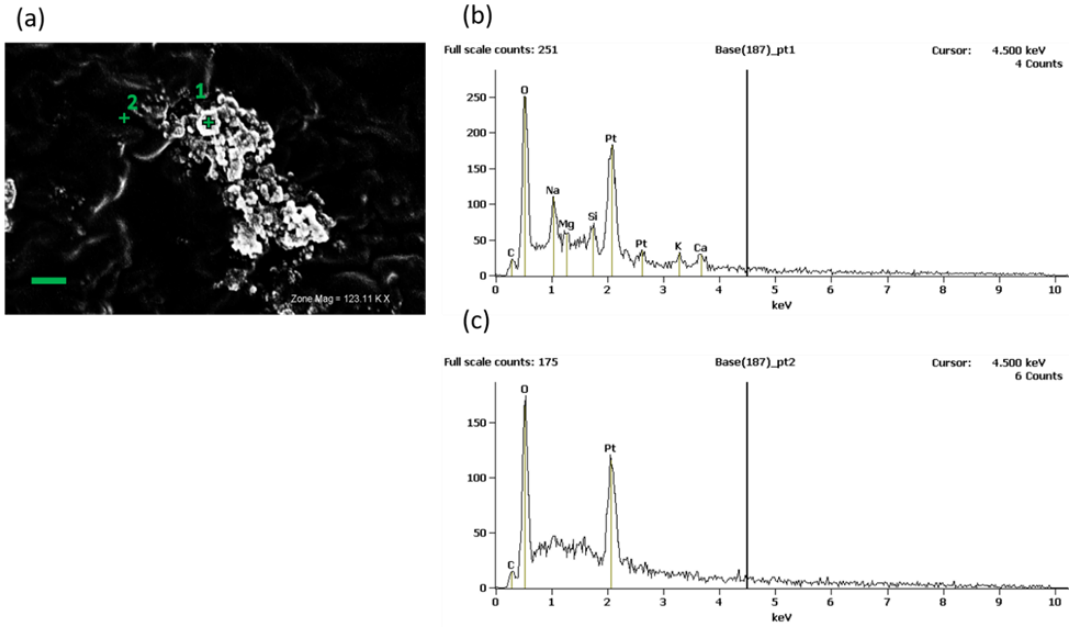

Figure 3-4: (a) SEM image of the colloid used for EDS analysis. The green line at the bottom right denotes a length of 200 nm. (b) EDS analysis of a point on the colloid surface marked as 1 in (a). (c) EDS analysis of a point outside the colloid surface marked as 2 in (a).

XRD analysis of the colloids revealed that calcite ($CaCO_3$), illite, and mica were the main minerals of the colloids, while silica (SiO_2) was the primary mineral in the bulk soil (Figure 3-5). It should be noted that XRD results provide a qualitative analysis of the difference in the mineralogy of colloids and soils that could partially explain the enrichment of PFAS on colloids.

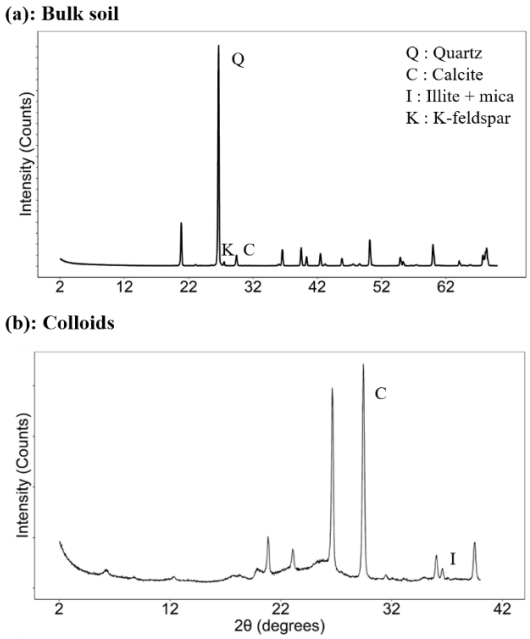

Figure 3-5: XRD analysis of (a) the bulk soil and (b) the colloid fraction of the soil.

3.3.3. Colloids contributed a significant fraction of PFAS released during or after flow interruption

We quantified the contribution of colloids on PFOA and PFBA concentration in the samples collected after flow interruption, by extracting absorbed PFOA and PFBA from colloids using methanol solution and analyzing the solution using liquid chromatography paired with triple quadrupole mass spectrometry (LC/QqQ-MS). The PFAS concentration in the effluent samples increased sharply after the flow interruption (Figure 3-2). The increase in PFOA concentration was more than that of the PFBA concentration. PFOA concentration increased by 84.5 ± 6.4%, whereas the concentration of PFBA increased by 29.9 ± 2.3% after the flow interruption (Figure 3-6). This

observation was contrary to that observed in an earlier study (Guelfo et al. 2020), where rate-limited sorption or matrix diffusion led to a decrease in PFAS concentration during flow interruption. Since PFAS-free groundwater was injected into the control columns, the concentration of PFAS in the columns did not increase during the injection period. We hypothesized that colloids released during flow interruption are the cause of the increase in PFAS concentration. This hypothesis is confirmed by our observation that removing the soil colloids by centrifugation reduced the PFAS concentration in the effluent samples. PFOA concentration decreased more than PFBA due to the removal of the soil colloids: PFOA concentration decreased by 46.9 ± 14.2% while PFBA decreased by 17.5 ± 10.8%.

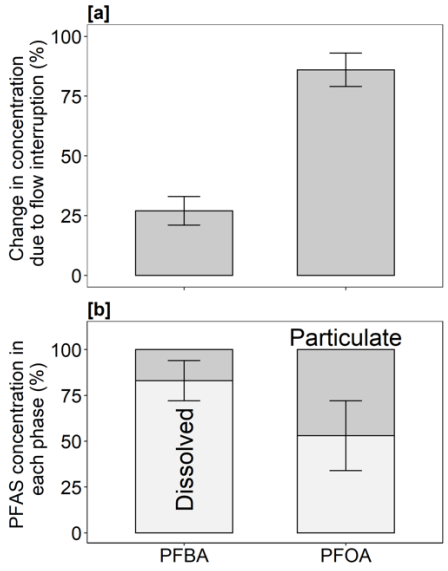

Figure 3-6: (a) Percentage increase in PFAS concentration due to flow interruption. (b) Distribution of PFAS in the dissolved and particulate phase in the effluent samples after flow interruption.

3.4. Discussion

3.4.1. The limited adsorption capacity of soil for PFAS

The low retardation of the PFAS compounds in the soil indicates that the soil had a low adsorption capacity for PFAS. This low sorption could be due to the absence of soil constituents with high PFAS affinity (Table 3-1). The organic carbon content of the soil was very low and the primary mineral in the soil was silica, which does not adsorb PFAS (Lv et al. 2018). However, despite the low sorption capacity of the soil, mass balance analysis showed that some amount of PFAS was retained by the soil in the injection phase. The soil retained more PFOA than PFBA due to increased hydrophobic interactions of PFOA to the organic carbon in the soil with an increase in the carbon chain length. This is in agreement with earlier studies (Higgins and Luthy 2006, Pereira et al. 2018), which observed higher adsorption of PFAS to soil with an increase in the carbon chain length. Collectively, the results implied that the soil had limited capacity to retard PFAS plume and that removal of the source of PFAS would quickly restore the groundwater quality for PFBA and PFOA provided the soil does not contain any PFAS precursors.

3.4.2. Increase in PFAS concentration in pore water after flow interruption

A lack of change in bromide concentration during flow interruption (Figure 3-2) indicates that the pore water concentration in the matrix was similar to pore water concentration in the macropores or flow paths (Brusseau et al. 1997). The lack of a concentration gradient limits the diffusive transport of solutes from macropore to matrix. Matrix diffusion during breakthrough plateau had been shown to decrease the PFAS concentration in another study due to rate-limited sorption (Guelfo et al. 2020). In contrast, PFAS concentrations increased after flow interruption (Figure 3-2) indicating that processes other than matrix diffusion are responsible. We surmised that colloids released after flow interruption may have increased the pore water concentration of

PFAS. The increase in colloid concentration during flow interruption was confirmed by particle size analysis and SEM images of colloids (Figure 3-3). XRD results provided evidence of colloid minerals that could adsorb PFAS (Figure 3-5). Removal of colloids from samples also decreased total PFAS concentrations (Figure 3-6), thereby confirming the role of colloids on overall PFAS concentration in the effluent samples. Guelfo et al. (2020) had removed all suspended particulate matter from the effluent samples prior to analysis, due to which the colloid facilitated an increase in PFAS concentration could not be observed.

Although the soil had some background PFOA concentration, the control columns where PFAS-free groundwater was injected did not show any increase in PFOA concentration after the flow interruption (Figure 3-2). No increase in PFAS concentration in the control columns indicates that precursor transformation is not the cause of the increase in PFAS concentration upon flow interruption. The pH and redox potential did not change as a result of a flow interruption, based on control columns without PFAS where the flow regime was similar to the treatment columns with PFAS. Therefore, the transformation rate of precursors was not affected. Therefore, the contribution of precursors was ruled out in our study.

3.4.3. Mechanism of PFAS release by colloids during flow interruption

Our results show that soil colloids enriched with PFAS elevated the pore water PFAS concentrations above the influent concentration, despite the relatively low sorption capacity of the soil (Figure 3-2). Colloid facilitated transport has been observed to increase transport of several other pollutants such as heavy metals (Grolimund et al. 1996, Ma et al. 2018) and organic pollutants (Benhabib et al. 2017, Yang et al. 2017). We primarily attribute this enhanced PFAS adsorption by colloids to the smaller size of the colloids which increases their surface area. An increase in surface area increases the sorption of PFAS onto soil particles (Li et al. 2019).

Suspended particles can carry more PFAS concentrations than benthic sediments by a factor of >100, indicating stronger sorption (Chen et al. 2019). In addition, XRD analysis of the colloids showed that colloids have distinct mineralogical properties such as enrichment of calcite, illite, and mica, which could make them preferentially adsorb PFAS compared to bulk soil, which is enriched with silica. A previous study showed that calcite can adsorb PFAS from the water, while quartz does not adsorb PFAS (Lv et al. 2018). Although the adsorption of PFAS by illite has not been studied, montmorillonite, which has a similar clay structure as illite, can adsorb anionic PFAS compounds such as PFOA and perfluorooctane sulfonic acid (PFOS) (Zhang et al. 2014, Zhao et al. 2014). Sorption of perfluorocarboxylic acids (PFCAs) such as PFOA onto clays is predominantly through hydrophobic and electrostatic interactions. However, the sulfonic acid group on perfluoroalkane sulfonic acids (PFSAs) can also chemically interact with the oxide layers on clay minerals (Zhao et al. 2014). Thus, PFSAs such as PFOS are more likely to adsorb onto montmorillonite (and possibly illite) clay surface and be transported by clay colloids.

The relative importance of colloids on facilitating the transport of PFAS could depend on the PFAS type. In particular, the contribution of colloids was more apparent for PFOA than PFBA due to the higher affinity of PFOA to the soil particles. However, PFBA, due to its small size and high diffusivity (Schaefer et al. 2019), can occupy the water in the micropores of soil and sediments (Codling et al. 2018). Release of the colloids can also release these PFBA compounds, increasing their concentrations in the effluent samples, even though they are not associated with the colloids. Nevertheless, our results collectively show that colloid-facilitated transport or release could be a significant pathway for the distribution of PFAS, especially long-chained PFAS, where the transport of long-chained PFAS is otherwise limited due to their strong affinity to soil containing a high amount of organic carbon (Higgins and Luthy 2006, Lyu et al. 2019, Pereira et al. 2018).

We provide a conceptual diagram (Figure 3-7) to show the potential mechanisms of PFAS release during flow interruption. PFAS can be transported by advection in macropores or flow paths, and some of the PFAS can diffuse into the soil matrix. The macropore walls typically enrich with PFAS due to adsorption. The macropore walls can also contain a high concentration of soil colloids that can be detached due to flow shear. Resuming flow after flow interruption perturbs the colloids attached to the macropore wall (Grolimund et al. 1996, Mohanty et al. 2014b) and releases them into flow paths. The flow of groundwater through soil can fluctuate based on several environmental factors (Gribovszki et al. 2010). Recharge of the groundwater by both natural (Suzuki and Higashi 2001) and artificial surface water infiltration (Alam et al. 2021) can increase the flow of groundwater at the recharge sites, pumping of water in the collection well (Beretta and Terrenghi 2017) can also increase the flow near vicinity of the well. Flow fluctuation at both conditions can increase colloid concentration and associated PFAS. Some of the colloids may carry a high concentration of PFAS owing to the high surface area. We speculate that the colloids are released from the soil through two mechanisms. The hydrodynamic shear force exerted by the water when the flow was restarted could release colloids from the bulk soil (Ryan and Elimelech 1996, Ryan and Gschwend 1994). In addition, colloids could also diffuse from the soil matrix during the period of flow interruption (Schelde et al. 2002). Moreover, PFAS-impacted groundwater is predominantly treated by passing through packed beds or columns containing adsorbent material. Our findings imply that fluctuation or interruptions of flow in these systems could release PFAS that was adsorbed by the adsorbents into the water. Overall, pore water may contain both dissolved PFAS and colloid-associated PFAS. Thus, removal of colloids from water samples before analysis of PFAS can underestimate the total PFAS concentration in the samples.

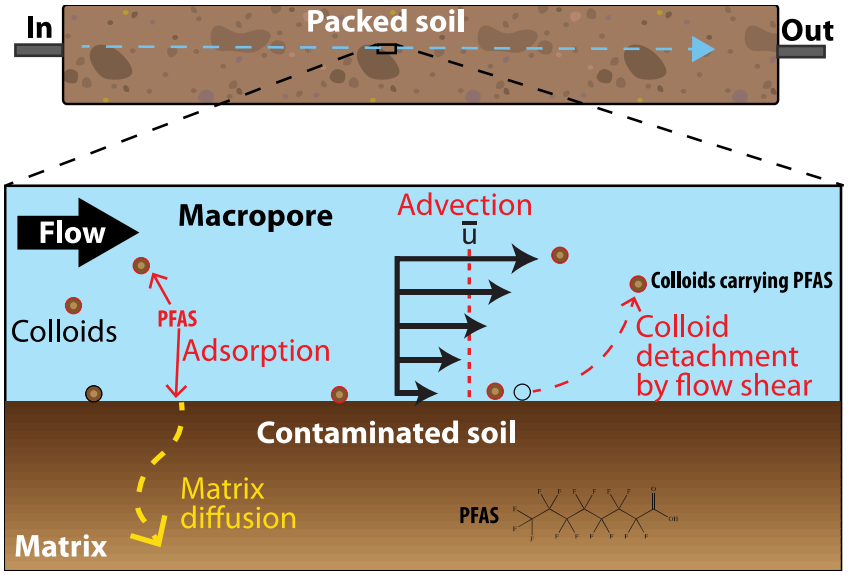

Figure 3-7. Conceptual figure depicting PFAS transport through porous media. Flow interruption can release colloids enriched with PFAS into flow paths and elevate PFAS concentration in water samples.

3.5. Conclusions

The mechanism of PFAS transport was examined when the flow regime is disrupted in porous media such as groundwater wells or packed filter media. The results show that particles released during flow interruption could significantly increase PFAS concentration in the pore water. Following flow interruption, the increases in PFOA concentrations were higher than that of PFBA, potentially due to higher affinity via the long carbon chain of PFOA than PFBA. XRD analysis reveals that colloids have different mineralogical enrichment (such as calcite) than the bulk soil from where they are mobilized, and these minerals may have a higher affinity to PFAS. This is particularly significant because the bulk soil used in this study had a low adsorption capacity. Despite its low capacity, the soil colloids contained enough PFAS to increase the PFAS concentration in pore water significantly. The result could be more pronounced if the soil had a higher adsorption capacity. We showed that the removal of colloids significantly decreased PFAS concentration, indicating studies that had not accounted for colloids might have underestimated PFAS concentration in the samples. Thus, PFAS should be desorbed from colloids before analysis

to estimate the true concentration of PFAS in eluted water, particularly in specific conditions where colloid concentration may be high. Thus, the presence of soil colloids carrying PFAS may lead to exceedances in PFAS concentrations beyond the health advisory limit set by the U.S. Environmental Protection Agency. Accounting PFAS on soil colloids may likely reveal a more accurate assessment of impaired groundwater wells.

3.6. References

Ahrens, L., Taniyasu, S., Yeung, L.W.Y., Yamashita, N., Lam, P.K.S. and Ebinghaus, R. (2010) Distribution of polyfluoroalkyl compounds in water, suspended particulate matter and sediment from Tokyo Bay, Japan. Chemosphere 79(3), 266-272. doi:https://doi.org/10.1016/j.chemosphere.2010.01.045.

Ahrens, L., Yamashita, N., Yeung, L.W.Y., Taniyasu, S., Horii, Y., Lam, P.K.S. and Ebinghaus, R. (2009) Partitioning Behavior of Per- and Polyfluoroalkyl Compounds between Pore Water and Sediment in Two Sediment Cores from Tokyo Bay, Japan. Environmental Science & Technology 43(18), 6969-6975. doi:10.1021/es901213s.

Ahrens, L., Yeung, L.W.Y., Taniyasu, S., Lam, P.K.S. and Yamashita, N. (2011) Partitioning of perfluorooctanoate (PFOA), perfluorooctane sulfonate (PFOS) and perfluorooctane sulfonamide (PFOSA) between water and sediment. Chemosphere 85(5), 731-737. doi:10.1016/j.chemosphere.2011.06.046.

Alam, S., Borthakur, A., Ravi, S., Gebremichael, M. and Mohanty, S.K. (2021) Managed aquifer recharge implementation criteria to achieve water sustainability. Science of The Total Environment 768, 144992. doi:https://doi.org/10.1016/j.scitotenv.2021.144992.

Armitage, J.M., MacLeod, M. and Cousins, I.T. (2009) Modeling the Global Fate and Transport of Perfluorooctanoic Acid (PFOA) and Perfluorooctanoate (PFO) Emitted from Direct Sources Using a Multispecies Mass Balance Model. Environmental Science & Technology 43(4), 1134-1140. doi:10.1021/es802900n.

Benhabib, K., Simonnot, M.-O., Faure, P. and Sardin, M. (2017) Evidence of colloidal transport of PAHs during column experiments run with contaminated soil samples. Environmental Science and Pollution Research 24(10), 9220-9228. doi:10.1007/s11356-017-8586-4.

Beretta, G.P. and Terrenghi, J. (2017) Groundwater flow in the Venice lagoon and remediation of the Porto Marghera industrial area (Italy). Hydrogeology Journal 25(3), 847-861. doi:10.1007/s10040-016-1517-5.

Brusseau, M.L. (2020) Simulating PFAS transport influenced by rate-limited multi-process retention. Water Res 168, 115179. doi:10.1016/j.watres.2019.115179.

Brusseau, M.L., Hu, Q. and Srivastava, R. (1997) Using flow interruption to identify factors causing nonideal contaminant transport. Journal of Contaminant Hydrology 24(3), 205-219. doi:https://doi.org/10.1016/S0169-7722(96)00009-5.

Brusseau, M.L., Khan, N., Wang, Y., Yan, N., Van Glubt, S. and Carroll, K.C. (2019) Nonideal Transport and Extended Elution Tailing of PFOS in Soil. Environ Sci Technol 53(18), 10654-10664. doi:10.1021/acs.est.9b02343.

Brusseau, M.L., Rao, P.S.C., Jessup, R.E. and Davidson, J.M. (1989) Flow interruption: A method for investigating sorption nonequilibrium. Journal of Contaminant Hydrology 4(3), 223-240. doi:https://doi.org/10.1016/0169-7722(89)90010-7.

BSI, C. (2009) Water quality− Determination of perfluorooctanesulfonate (PFOS) and perfluorooctanoate (PFOA)− Method for unfiltered samples using solid-phase extraction and liquid chromatography/mass spectrometry. BS ISO 25101: 2009.

Campos-Pereira, H., Kleja, D.B., Sjöstedt, C., Ahrens, L., Klysubun, W. and Gustafsson, J.P. (2020) The Adsorption of Per- and Polyfluoroalkyl Substances (PFASs) onto Ferrihydrite Is Governed by Surface Charge. Environmental Science & Technology 54(24), 15722-15730. doi:10.1021/acs.est.0c01646.

Chen, H., Reinhard, M., Yin, T., Nguyen, T.V., Tran, N.H. and Yew-Hoong Gin, K. (2019) Multi-compartment distribution of perfluoroalkyl and polyfluoroalkyl substances (PFASs) in an urban catchment system. Water Res 154, 227-237. doi:10.1016/j.watres.2019.02.009.

Codling, G., Sturchio, N.C., Rockne, K.J., Li, A., Peng, H., Tse, T.J., Jones, P.D. and Giesy, J.P. (2018) Spatial and temporal trends in poly- and per-fluorinated compounds in the Laurentian Great Lakes Erie, Ontario and St. Clair. Environmental Pollution 237, 396-405. doi:10.1016/j.envpol.2018.02.013.

Dalahmeh, S.S., Alziq, N. and Ahrens, L. (2019) Potential of biochar filters for onsite wastewater treatment: Effects of active and inactive biofilms on adsorption of per- and polyfluoroalkyl substances in laboratory column experiments. Environmental Pollution 247, 155-164. doi:https://doi.org/10.1016/j.envpol.2019.01.032.

DeWitt, J.C., Blossom, S.J. and Schaider, L.A. (2019) Exposure to per-fluoroalkyl and polyfluoroalkyl substances leads to immunotoxicity: epidemiological and toxicological evidence. Journal of Exposure Science & Environmental Epidemiology 29(2), 148-156. doi:10.1038/s41370-018-0097-y.

Domingo, J.L. and Nadal, M. (2019) Human exposure to per-and polyfluoroalkyl substances (PFAS) through drinking water: A review of the recent scientific literature. Environmental Research 177. doi:10.1016/j.envres.2019.108648.

Du, Z., Deng, S., Bei, Y., Huang, Q., Wang, B., Huang, J. and Yu, G. (2014) Adsorption behavior and mechanism of perfluorinated compounds on various adsorbents—A review. Journal of Hazardous Materials 274, 443-454. doi:https://doi.org/10.1016/j.jhazmat.2014.04.038.

Eschauzier, C., Raat, K.J., Stuyfzand, P.J. and De Voogt, P. (2013) Perfluorinated alkylated acids in groundwater and drinking water: Identification, origin and mobility. Science of The Total Environment 458-460, 477-485. doi:https://doi.org/10.1016/j.scitotenv.2013.04.066.

Gagliano, E., Sgroi, M., Falciglia, P.P., Vagliasindi, F.G.A. and Roccaro, P. (2020) Removal of poly- and perfluoroalkyl substances (PFAS) from water by adsorption: Role of PFAS chain length, effect of organic matter and challenges in adsorbent regeneration. Water Research 171. doi:10.1016/j.watres.2019.115381.

Gao, B., Saiers, J.E. and Ryan, J.N. (2004) Deposition and mobilization of clay colloids in unsaturated porous media. Water Resources Research 40(8). doi:https://doi.org/10.1029/2004WR003189.

Gellrich, V., Stahl, T. and Knepper, T.P. (2012) Behavior of perfluorinated compounds in soils during leaching experiments. Chemosphere 87(9), 1052-1056. doi:10.1016/j.chemosphere.2012.02.011.

Grandjean, P. and Clapp, R. (2015) Perfluorinated Alkyl Substances: Emerging Insights Into Health Risks. NEW SOLUTIONS: A Journal of Environmental and Occupational Health Policy 25(2), 147-163. doi:10.1177/1048291115590506.

Gribovszki, Z., Szilágyi, J. and Kalicz, P. (2010) Diurnal fluctuations in shallow groundwater levels and streamflow rates and their interpretation – A review. Journal of Hydrology 385(1), 371-383. doi:https://doi.org/10.1016/j.jhydrol.2010.02.001.

Grolimund, D., Borkovec, M., Barmettler, K. and Sticher, H. (1996) Colloid-Facilitated Transport of Strongly Sorbing Contaminants in Natural Porous Media: A Laboratory Column Study. Environmental Science & Technology 30(10), 3118-3123. doi:10.1021/es960246x.

Guelfo, J.L. and Adamson, D.T. (2018) Evaluation of a national data set for insights into sources, composition, and concentrations of per- and polyfluoroalkyl substances (PFASs) in US drinking water. Environmental Pollution 236, 505-513. doi:10.1016/j.envpol.2018.01.066.

Guelfo, J.L. and Higgins, C.P. (2013) Subsurface Transport Potential of Perfluoroalkyl Acids at Aqueous Film-Forming Foam (AFFF)-Impacted Sites. Environmental Science & Technology 47(9), 4164-4171. doi:10.1021/es3048043.

Guelfo, J.L., Wunsch, A., McCray, J., Stults, J.F. and Higgins, C.P. (2020) Subsurface transport potential of perfluoroalkyl acids (PFAAs): Column experiments and modeling. Journal of Contaminant Hydrology 233, 103661. doi:https://doi.org/10.1016/j.jconhyd.2020.103661.

Higgins, C.P. and Luthy, R.G. (2006) Sorption of Perfluorinated Surfactants on Sediments. Environmental Science & Technology 40(23), 7251-7256. doi:10.1021/es061000n.

Hoisaeter, A., Pfaff, A. and Breedveld, G.D. (2019) Leaching and transport of PFAS from aqueous film-forming foam (AFFF) in the unsaturated soil at a firefighting training facility under cold climatic conditions. J Contam Hydrol 222, 112-122. doi:10.1016/j.jconhyd.2019.02.010.

Johnson, R.L., Anschutz, A.J., Smolen, J.M., Simcik, M.F. and Penn, R.L. (2007) The Adsorption of Perfluorooctane Sulfonate onto Sand, Clay, and Iron Oxide Surfaces. Journal of Chemical & Engineering Data 52(4), 1165-1170. doi:10.1021/je060285g.

Lath, S., Knight, E.R., Navarro, D.A., Kookana, R.S. and McLaughlin, M.J. (2019) Sorption of PFOA onto different laboratory materials: Filter membranes and centrifuge tubes. Chemosphere 222, 671-678. doi:https://doi.org/10.1016/j.chemosphere.2019.01.096.

Li, F., Fang, X., Zhou, Z., Liao, X., Zou, J., Yuan, B. and Sun, W. (2019) Adsorption of perfluorinated acids onto soils: Kinetics, isotherms, and influences of soil properties. Sci Total Environ 649, 504-514. doi:10.1016/j.scitotenv.2018.08.209.

Liu, J. and Lee, L.S. (2005) Solubility and Sorption by Soils of 8:2 Fluorotelomer Alcohol in Water and Cosolvent Systems. Environmental Science & Technology 39(19), 7535-7540. doi:10.1021/es051125c.

Liu, Y., Junaid, M., Xu, P., Zhong, W., Pan, B. and Xu, N. (2020) Suspended sediment exacerbates perfluorooctane sulfonate mediated toxicity through reactive oxygen species generation in freshwater clam Corbicula fluminea. Environmental Pollution 267, 115671. doi:https://doi.org/10.1016/j.envpol.2020.115671.

Liu, Y.Q., Zhang, Y., Li, J.F., Wu, N., Li, W.P. and Niu, Z.G. (2019) Distribution, partitioning behavior and positive matrix factorization-based source analysis of legacy and emerging polyfluorinated alkyl substances in the dissolved phase, surface sediment and suspended particulate matter around coastal areas of Bohai Bay, China. Environmental Pollution 246, 34-44. doi:10.1016/j.envpol.2018.11.113.

Longstaffe, J.G., Courtier-Murias, D., Soong, R., Simpson, M.J., Maas, W.E., Fey, M., Hutchins, H., Krishnamurthy, S., Struppe, J., Alaee, M., Kumar, R., Monette, M., Stronks, H.J. and Simpson, A.J. (2012) In-Situ Molecular-Level Elucidation of Organofluorine Binding Sites in a Whole Peat Soil. Environmental Science & Technology 46(19), 10508-10513. doi:10.1021/es3026769.

Lv, X., Sun, Y., Ji, R., Gao, B., Wu, J., Lu, Q. and Jiang, H. (2018) Physicochemical factors controlling the retention and transport of perfluorooctanoic acid (PFOA) in saturated sand and limestone porous media. Water Res 141, 251-258. doi:10.1016/j.watres.2018.05.020.

Lyu, X., Liu, X., Sun, Y., Ji, R., Gao, B. and Wu, J. (2019) Transport and retention of perfluorooctanoic acid (PFOA) in natural soils: Importance of soil organic matter and mineral contents, and solution ionic strength. Journal of Contaminant Hydrology 225, 103477. doi:https://doi.org/10.1016/j.jconhyd.2019.03.009.

Lyu, Y., Brusseau, M.L., Chen, W., Yan, N., Fu, X. and Lin, X. (2018) Adsorption of PFOA at the Air-Water Interface during Transport in Unsaturated Porous Media. Environ Sci Technol 52(14), 7745-7753. doi:10.1021/acs.est.8b02348.

Ma, J., Guo, H., Weng, L., Li, Y., Lei, M. and Chen, Y. (2018) Distinct effect of humic acid on ferrihydrite colloid-facilitated transport of arsenic in saturated media at different pH. Chemosphere 212, 794-801. doi:https://doi.org/10.1016/j.chemosphere.2018.08.131.

McCleaf, P., Englund, S., Östlund, A., Lindegren, K., Wiberg, K. and Ahrens, L. (2017) Removal efficiency of multiple poly- and perfluoroalkyl substances (PFASs) in drinking water using granular activated carbon (GAC) and anion exchange (AE) column tests. Water Research 120, 77-87. doi:https://doi.org/10.1016/j.watres.2017.04.057.

McKenzie, E.R., Siegrist, R.L., McCray, J.E. and Higgins, C.P. (2015) Effects of Chemical Oxidants on Perfluoroalkyl Acid Transport in One-Dimensional Porous Media Columns. Environmental Science & Technology 49(3), 1681-1689. doi:10.1021/es503676p.

Mejia-Avendano, S., Zhi, Y., Yan, B. and Liu, J. (2020) Sorption of Polyfluoroalkyl Surfactants on Surface Soils: Effect of Molecular Structures, Soil Properties, and Solution Chemistry. Environ Sci Technol 54(3), 1513-1521. doi:10.1021/acs.est.9b04989.

Milinovic, J., Lacorte, S., Vidal, M. and Rigol, A. (2015) Sorption behaviour of perfluoroalkyl substances in soils. Science of The Total Environment 511, 63-71. doi:10.1016/j.scitotenv.2014.12.017.

Mohanty, S.K., Cantrell, K.B., Nelson, K.L. and Boehm, A.B. (2014a) Efficacy of biochar to remove Escherichia coli from stormwater under steady and intermittent flow. Water Research 61, 288-296. doi:https://doi.org/10.1016/j.watres.2014.05.026.

Mohanty, S.K., Saiers, J.E. and Ryan, J.N. (2014b) Colloid-facilitated mobilization of metals by freeze–thaw cycles. Environmental Science & Technology 48(2), 977-984.

Nguyen, T.V., Reinhard, M., Chen, H. and Gin, K.Y.-H. (2016) Fate and transport of perfluoro- and polyfluoroalkyl substances including perfluorooctane sulfonamides in a managed urban water body. Environmental Science and Pollution Research 23(11), 10382-10392. doi:10.1007/s11356-016-6788-9.

Pereira, H.C., Ullberg, M., Kleja, D.B., Gustafsson, J.P. and Ahrens, L. (2018) Sorption of perfluoroalkyl substances (PFASs) to an organic soil horizon - Effect of cation composition and pH. Chemosphere 207, 183-191. doi:10.1016/j.chemosphere.2018.05.012.

Qian, J., Shen, M., Wang, P., Wang, C., Hou, J., Ao, Y., Liu, J. and Li, K. (2017) Adsorption of perfluorooctane sulfonate on soils: Effects of soil characteristics and phosphate competition. Chemosphere 168, 1383-1388. doi:https://doi.org/10.1016/j.chemosphere.2016.11.114.

Ryan, J.N. and Elimelech, M. (1996) Colloid mobilization and transport in groundwater. Colloids and Surfaces A: Physicochemical and Engineering Aspects 107, 1-56. doi:https://doi.org/10.1016/0927-7757(95)03384-X.

Ryan, J.N. and Gschwend, P.M. (1994) Effects of Ionic Strength and Flow Rate on Colloid Release: Relating Kinetics to Intersurface Potential Energy. Journal of Colloid and Interface Science 164(1), 21-34. doi:https://doi.org/10.1006/jcis.1994.1139.

Sadar, M. (2004) Making sense of turbidity measurements-advantages in establishing traceability between measurements and technology.

Schaefer, C.E., Drennan, D.M., Tran, D.N., Garcia, R., Christie, E., Higgins, C.P. and Field, J.A. (2019) Measurement of Aqueous Diffusivities for Perfluoroalkyl Acids. Journal of Environmental Engineering 145(11), 06019006. doi:10.1061/(ASCE)EE.1943-7870.0001585.

Schelde, K., Moldrup, P., Jacobsen, O.H., de Jonge, H., de Jonge, L.W. and Komatsu, T. (2002) Diffusion-Limited Mobilization and Transport of Natural Colloids in Macroporous Soil. Vadose Zone Journal 1(1), 125-136. doi:10.2113/1.1.125.

Seo, S.-H., Son, M.-H., Shin, E.-S., Choi, S.-D. and Chang, Y.-S. (2019) Matrix-specific distribution and compositional profiles of perfluoroalkyl substances (PFASs) in multimedia environments. Journal of Hazardous Materials 364, 19-27. doi:https://doi.org/10.1016/j.jhazmat.2018.10.012.

Sharma, B.M., Bharat, G.K., Tayal, S., Larssen, T., Becanova, J., Karaskova, P., Whitehead, P.G., Futter, M.N., Butterfield, D. and Nizzetto, L. (2016) Perfluoroalkyl substances (PFAS) in river and ground/drinking water of the Ganges River basin: Emissions and implications for human exposure. Environmental Pollution 208, 704-713. doi:10.1016/j.envpol.2015.10.050.

Shoemaker, J., Grimmett, P. and Boutin, B. (2008) Determination of selected perfluorinated alkyl acids in drinking water by solid phase extraction and liquid chromatography/tandem mass spectrometry (LC/MS/MS). US Environmental Protection Agency, Washington, DC.

Suzuki, K. and Higashi, S. (2001) Groundwater flow after heavy rain in landslide-slope area from 2-D inversion of resistivity monitoring data. GEOPHYSICS 66(3), 733-743. doi:10.1190/1.1444963.

Tang, C.Y., Shiang Fu, Q., Gao, D., Criddle, C.S. and Leckie, J.O. (2010) Effect of solution chemistry on the adsorption of perfluorooctane sulfonate onto mineral surfaces. Water Res 44(8), 2654-2662. doi:10.1016/j.watres.2010.01.038.

Van Glubt, S. and Brusseau, M.L. (2021) Contribution of Nonaqueous-Phase Liquids to the Retention and Transport of Per and Polyfluoroalkyl Substances (PFAS) in Porous Media. Environmental Science & Technology. doi:10.1021/acs.est.0c07355.

Van Glubt, S., Brusseau, M.L., Yan, N., Huang, D., Khan, N. and Carroll, K.C. (2021) Column versus batch methods for measuring PFOS and PFOA sorption to geomedia. Environmental Pollution 268, 115917. doi:https://doi.org/10.1016/j.envpol.2020.115917.

Wang, P., Zheng, C. and Gorelick, S.M. (2005) A general approach to advective–dispersive transport with multirate mass transfer. Advances in Water Resources 28(1), 33-42. doi:https://doi.org/10.1016/j.advwatres.2004.10.003.

Wei, C., Song, X., Wang, Q. and Hu, Z. (2017) Sorption kinetics, isotherms and mechanisms of PFOS on soils with different physicochemical properties. Ecotoxicology and Environmental Safety 142, 40-50. doi:https://doi.org/10.1016/j.ecoenv.2017.03.040.

Xiao, X., Ulrich, B.A., Chen, B.L. and Higgins, C.P. (2017) Sorption of Poly- and Perfluoroalkyl Substances (PFASs) Relevant to Aqueous Film-Forming Foam (AFFF)-Impacted Groundwater by Biochars and Activated Carbon. Environmental Science & Technology 51(11), 6342-6351. doi:10.1021/acs.est.7b00970.

Xing, Y., Chen, X., Chen, X. and Zhuang, J. (2016) Colloid-Mediated Transport of Pharmaceutical and Personal Care Products through Porous Media. Scientific Reports 6.

Xu, C., Yin, S., Liu, Y., Chen, F., Zhong, Z., Li, F., Liu, K. and Liu, W. (2019) Prenatal exposure to chlorinated polyfluoroalkyl ether sulfonic acids and perfluoroalkyl acids: Potential role of maternal determinants and associations with birth outcomes. Journal of Hazardous Materials 380, 120867. doi:https://doi.org/10.1016/j.jhazmat.2019.120867.

Yang, W., Wang, Y., Sharma, P., Li, B., Liu, K., Liu, J., Flury, M. and Shang, J. (2017) Effect of naphthalene on transport and retention of biochar colloids through saturated porous media. Colloids and Surfaces A: Physicochemical and Engineering Aspects 530, 146-154. doi:https://doi.org/10.1016/j.colsurfa.2017.07.010.

Zhang, H., Cui, R., Guo, X., Hu, J. and Dai, J. (2016) Low dose perfluorooctanoate exposure promotes cell proliferation in a human non-tumor liver cell line. Journal of Hazardous Materials 313, 18-28. doi:https://doi.org/10.1016/j.jhazmat.2016.03.077.

Zhang, R., Yan, W. and Jing, C. (2014) Mechanistic study of PFOS adsorption on kaolinite and montmorillonite. Colloids and Surfaces A: Physicochemical and Engineering Aspects 462, 252-258. doi:10.1016/j.colsurfa.2014.09.019.

Zhao, L., Bian, J., Zhang, Y., Zhu, L. and Liu, Z. (2014) Comparison of the sorption behaviors and mechanisms of perfluorosulfonates and perfluorocarboxylic acids on three kinds of clay minerals. Chemosphere 114, 51-58. doi:10.1016/j.chemosphere.2014.03.098.

Zhao, P., Xia, X., Dong, J., Xia, N., Jiang, X., Li, Y. and Zhu, Y. (2016) Short- and long-chain perfluoroalkyl substances in the water, suspended particulate matter, and surface sediment of a turbid river. Science of The Total Environment 568, 57-65. doi:https://doi.org/10.1016/j.scitotenv.2016.05.221.

Zhou, J., Liu, D., Zhang, W., Chen, X., Huan, Y. and Yu, X. (2017) Colloid characterization and in situ release in shallow groundwater under different hydrogeology conditions. Environmental Science and Pollution Research 24(16), 14445-14454. doi:10.1007/s11356-017-8856-1.

Zhu, Y., Ma, L.Q., Dong, X., Harris, W.G., Bonzongo, J.C. and Han, F. (2014) Ionic strength reduction and flow interruption enhanced colloid-facilitated Hg transport in contaminated soils. Journal of Hazardous Materials 264, 286-292. doi:https://doi.org/10.1016/j.jhazmat.2013.11.009.

4. CHAPTER 4: DRY-WET AND FREEZE-THAW CYCLES ENHANCE PFOA LEACHING FROM SUBSURFACE SOILS

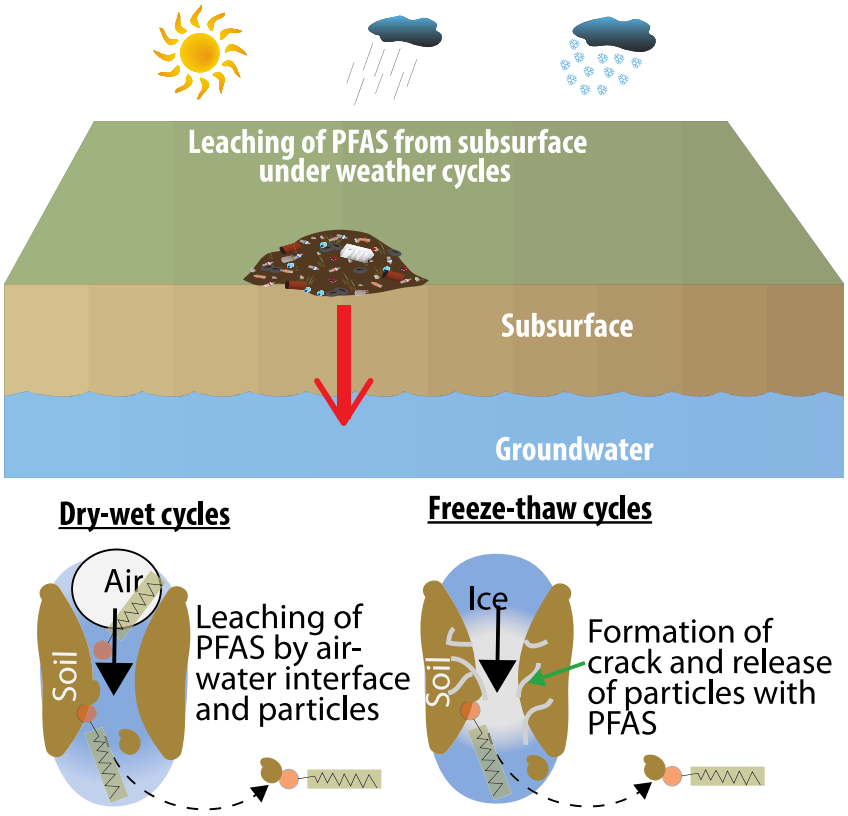

Borthakur, A., Olsen, P., Dooley, G.P., Cranmer, B.K., Rao, U., Hoek, E.M.V., Blotevogel, J., Mahendra, S., Mohanty, S.K., 2021. Dry-wet and freeze-thaw cycles enhance PFOA leaching from subsurface soils. Journal of Hazardous Materials Letters 2, 100029. https://doi.org/10.1016/j.hazl.2021.100029

Abstract

Subsurface soil naturally experiences dry-wet and freeze-thaw cycles, which could affect the leaching of previously adsorbed pollutants. A slow release of poly- and perfluoroalkyl substances (PFAS) from impacted subsurface soil may serve as a long-term diffuse source of PFAS to groundwater. Yet, the extent to which these weathering conditions may affect the subsurface release of PFAS is unknown. We subjected columns packed with soil pre-adsorbed with perfluorooctanoic acid (PFOA) to dry-wet and freeze-thaw cycles and observed a spike in PFOA concentration in leachate following each weathering treatment compared to no weathering treatment. Weathering conditions released a high concentration of soil colloids, which were confirmed by particle-size distribution analysis, SEM-EDS, and XRD. Fractionation of PFOA in the water sample reveals that up to 36% of leached PFOA was associated with soil colloids. Thus, previous studies that did not account for colloids may underestimate the leaching of PFAS from the soil. Overall, the results indicate that natural weathering conditions can enhance subsurface leaching of colloids and colloid-associated PFOA. Therefore, current conceptual site models to quantify the leaching of PFAS from source zones should account for weathering and the contribution of colloids.

4.1. Introduction

Surface runoff carries poly- and perfluoroalkyl substances (PFAS) from PFAS-impacted areas such as firefighting training facilities (Baduel et al., 2015), wastewater biosolids (Washington et al., 2010), and waste piles with PFAS-containing products (Laitinen et al., 2014; Trudel et al., 2008). The runoff exports PFAS to surface waters and infiltrates through subsurface soils to groundwater aquifer. During the infiltration of the PFAS-impacted runoff, short-chained PFAS can move through subsurface because of limited adsorption on soil whereas most of the long-chained PFAS can be removed by adsorption to soil and air-water interfaces (Brusseau, 2018; Qian et al., 2017; Zhang et al., 2014). However, under certain conditions, the previously removed PFAS can leach into groundwater from impacted subsurface soil (Gellrich et al., 2012). These conditions include infiltration of uncontaminated runoff that promote desorption, alteration of pH, presence of dissolved organic carbon in infiltrating water, or release of soil particles containing adsorbed pollutants (Borthakur et al., 2021a; Gellrich et al., 2012; Jeon et al., 2011; Kabiri et al., 2021). Additionally, long chain PFAS can displace short chain PFAS and leach them from the soil (Gellrich et al., 2012; Xiao et al., 2011). Thus, subsurface can serve as a diffused source for pollution of groundwater (Alam et al., 2021). Removal of PFAS from groundwater can be expensive and ineffective based on the treatment technologies (Crone et al., 2019; Merino et al., 2016). Exposure to PFAS-impacted drinking water has been linked to several adverse health effects including liver disorder (Zhang et al., 2016), cardiovascular diseases (Huang et al., 2018) and cancer (Grandjean and Clapp, 2015; Yeung et al., 2013). Thus, it is critical to identify the conditions that could enhance the leaching of PFAS from the PFAS-impacted subsurface soil.

PFAS can be desorbed from impacted subsurface soils by physical, chemical, and biological processes. Previously sorbed PFAS can desorb from soil (Milinovic et al., 2015; Xiao

et al., 2019) based on environmental conditions such as pH, ionic strength, and dissolved organic carbon in pore water (Jeon et al., 2011; Pereira et al., 2018; Wang et al., 2012). Furthermore, the transformation of precursors can enhance PFAS leaching (Chen et al., 2020). PFAS trapped in the soil matrix can diffuse into the flow path (Schaefer et al., 2019). Thus, back diffusion during the pause between rainfall events could increase the concentration of PFAS in porewater (Adamson et al., 2020; Brusseau, 2020; Carey et al., 2019; Guo et al., 2020). As air-water interfaces retain a significant amount of PFAS (Brusseau, 2019, 2018; Lyu et al., 2018), the collapse of the air-water interfaces during intermittent infiltration events could also release PFAS. Therefore, development and collapse of air-water interfaces in the subsurface during intermittent rainfall events (dry-wet cycles) can leach PFAS from the subsurface soil (Gellrich et al., 2012).

Similar to desorption of dissolved PFAS, colloid-associated PFAS can be released in the subsurface by three steps: (1) release or mobilization of colloids from macropore flow walls by hydrodynamic fluctuations, or water phase transitions during dry-wet (Majdalani et al., 2007) or freeze-thaw cycles (Mohanty et al., 2014); (2) diffusion of released colloids from pore wall to bulk liquid via a rate-limiting step (Schelde et al., 2002); (3) transport of colloids in bulk liquid downward via infiltrating water. Colloids have been shown to contain significantly high concentrations of PFAS in surface waters (Ahrens et al., 2010; Borthakur et al., 2021b; Chen et al., 2019) and saturated soil (Borthakur et al., 2021a). Yet, no study to date has quantified the colloid-facilitated release of PFAS in impacted subsurface subjected to weathering cycles. Most column studies on leaching have examined the leaching of pollutants during injection of water through packed columns to simulate rainfall (Ding et al., 2010; Gellrich et al., 2012; Wang and Alva, 1996), ignoring the effect of antecedent weather conditions

We aim to examine the effect of dry-wet and freeze-thaw cycles on the release of PFAS from impacted subsurface soil. We hypothesized that these weathering cycles would increase the release of PFAS from subsurface soils due to the release of soil colloids enriched with PFAS. To test the hypothesis, we injected perfluorooctanoic acid (PFOA) as a model PFAS through packed soil columns to adsorb PFOA on soil and subjected the columns to multiple cycles of weathering treatments. Analyzing leachate for colloid concentration, dissolved PFOA, and colloid-bound PFOA, we quantified and distinguished the role of colloids on PFOA release from weathered subsurface soils.

4.2. Materials and Methods

4.2.1. Soil and groundwater

Soil and groundwater were collected from an unimpacted area upgradient of a fire-fighting training facility. The soil and groundwater characteristics are provided in Table 3-1. The soil was dried in an oven at 110 °C for 24 h and sieved to remove particles greater than 2 mm to minimize preferential flow in the packed columns. To prepare PFOA-impacted groundwater, we spiked concentrated PFOA (96% purity, Acros Organics) and potassium bromide (KBr > 99% purity, Alfa Aesar) stock solution into groundwater to achieve a final concentration of 200 μg L^{-1} PFOA and 20 mg L^{-1} Br. Bromide was used as a conservative tracer to compare the transport or retardation of PFOA, to determine the pore volume of columns based on 50% breakthrough time, and to evaluate the diffusion of solute from or into the matrix (Mohanty et al., 2016).

Duplicate polypropylene columns were packed with the soil using a method described elsewhere (Borthakur et al., 2021a). The packed columns were saturated by injecting synthetic groundwater (6 mM NaCl) without PFOA through the bottom of the columns. The pH and ionic

strength of the synthetic groundwater were adjusted to match the pH (7.1 ± 0.01) and ionic strength of the collected groundwater.

4.2.2. Column experiments

To establish flow and chemical equilibrium before injection of PFOA, the synthetic groundwater was injected from bottom through soil columns at 0.61 cm h^{-1} for at least 48 hours until no change in pH and ionic strength of effluents was observed. The effluent PFOA concentration was measured to determine background PFOA concentration in the soil, which was determined to be negligible compared to the PFOA concentration in the contaminated groundwater. To uniformly contaminate packed soil with PFOA, the groundwater spiked with 200 µg L^{-1} PFOA and 20 mg L^{-1} Br^- was injected from the bottom of the soil columns at 0.61 cm h^{-1} for 25 days in total, followed by injection of PFOA-free groundwater for 5 days to flush out PFOA from pore water. Injection of contaminated water from bottom ensured saturated flow with limited opportunity for preferential flow (Kung, 1990) and uniform contamination of all columns for comparison of leaching between control (no dry-wet or freeze-thaw treatment) and treatment. This injection phase was conducted for 25 days to ensure soil is saturated with PFOA and PFOA had diffused into the soil matrix. Diffusion into the soil, particularly if it contains a high amount of clays, may take a long time (Brusseau, 2020).

After contamination phase, leaching phase was initiated by inverting the columns and draining the pore water by gravity. Then uncontaminated groundwater was injected from the top to simulate the leaching phase. Inversion of columns ensured that the flow direction during contamination and leaching phases remained same. To compare the effect of weathering treatments on PFOA release from soil columns pre-adsorbed with PFOA, the soil columns were subjected to weathering treatments. Duplicate soil columns were subjected to intermittent infiltration events,

where columns were first subjected to a cycle of treatment lasting 45 h followed by injection of PFOA-free groundwater at 6.1 cm h^{-1} for 4 h. The columns were first subjected to a total of 3 cycles of drying treatment followed by 3 cycles of freeze-thaw treatments. To simulate drying treatment, the columns were first drained by gravity while keeping them at room temperature (~23 °C) for 45 h. During each freeze-thaw treatment cycle, soil columns were kept at -15 ºC for 24 hours and then at 22 ºC for 21 hours. During the 4-h injection period following each treatment, soil columns were injected with PFOA-free groundwater from the top of the columns and effluent samples were collected from the bottom of columns every 30 minutes and analyzed to estimate dissolved and colloid-associated PFOA. The volume of water drained by gravity during drying or freeze-thaw treatment was insignificant, so no samples were collected after the injection period. To examine the release of PFOA without weathering treatment, soil columns previously injected with PFOA were flushed with PFOA-free groundwater for 24 h into without any intermediate drying or freeze-thaw treatments.

4.2.3. Water sample analysis and quality control

The dissolved PFOA concentration was determined by removing the colloids by centrifuging the samples at 20817 RCF (g-force) for 15 minutes. 0.5 mL supernatant was removed and added to 0.5 mL methanol and the mixture was analyzed for PFOA. To measure the total PFOA concentration, the PFOA adsorbed to the colloids was first desorbed by mixing the sample with an equal volume of methanol. The colloids were then removed by centrifugation and the sample was analyzed. Before analysis, 50 μg L^{-1} of $^{13}C_4$-PFOA internal standard (Wellington Laboratories) was added to all the samples to account for PFOA loss due to adsorption to the vial walls, sample processing before chemical analysis, and analytical variability. The samples were then aliquoted into 200 mL polypropylene vials and analyzed using an Agilent 1290 liquid

chromatography paired with an Agilent 6460 Triple Quadrupole Mass Spectrometer (LC/QqQ-MS) equipped with a Poroshell 120 EC-C18, 2.1x100 mm, 2.7 μm column plus C18 guard and delay columns (details in Section 3.2.3). The detection limit of the method is 0.01 μg L^{-1}. The concentration of PFOA adsorbed to the colloids was determined by estimating the difference between the total PFOA concentration and the dissolved PFOA concentration. The total concentration was measured by first desorbing PFOA from colloids in 50% methanol solution, removing colloids by centrifuging samples, and analyzing supernatant for dissolved and desorbed PFOA. The recovery of PFOA adsorbed to colloids was estimated using 50% methanol solution following a method described elsewhere (Xiao et al., 2020). Although 50% methanol is not sufficient to desorb all PFOA from colloids, we used the same solution for both recovery and samples, so that they can be analyzed. The details of the recovery steps were described in the Supplementary Materials. The recovery of PFOA from the soil in 50% methanol was found to be 75.5 ± 5.9 %. Thus, colloid associated PFOA concentration estimated in our experiment is underestimated.

PFOA can adsorb from the solution onto the walls of the polypropylene vials (vial sorption) which can lead to underestimation of the total PFOA concentration in the effluent samples (Lath et al., 2019). To account for any such losses, 20 μg L^{-1} PFOA solution was prepared in a 1:1 methanol: water solution and stored in the polypropylene vials. The PFOA concentrations in the solutions were measured after 48 hours, simulating the time between sampling and analysis. The PFOA concentration decreased by a maximum of 1% so this decrease was considered negligible. To account for PFOA adsorption by the column walls, we injected PFOA-contaminated groundwater into empty columns (no soil) and subjected the columns to same treatment as control and treatment columns. We observed no significant difference between the PFOA concentration

between the samples during injection, potentially due to saturation of limited sorption capacity of polypropylene. Furthermore, we did not observe any leaching of PFOA (or concentration below detection limit) from contaminated columns during dry-wet and freeze-thaw treatment of contaminated column walls. Therefore, we assumed that adsorbed PFOA had insignificant effect on our results.

4.2.4. Colloid characterization

The turbidity of the sample was estimated by measuring the absorbance of the samples at 890 nm wavelength using a UV/Vis spectrophotometer. The number of colloids in the effluent samples was counted using an Accusizer AD Optical Particle Sizer machine that uses the Single Particle Optical Sensing (SPOS) technique, which counts particles greater than 0.83 μm at 0.01 μm resolution. The morphology of colloids in the effluent samples was examined using a Scanning Electron Microscope with Energy Dispersive X-ray Analysis (SEM-EDS). To analyze the mineralogical properties of colloids, the soil was analyzed using X-ray diffraction analysis (XRD). Details of all characterization methods are provided in Section 3.2.6.

4.2.5. Mass balance analysis

To quantify the total amount of PFOA retained in the soil before the weathering treatment, the area under the breakthrough curve in the injection phase was calculated, which determined the total PFOA transported. The total PFOA transported was subtracted from the total injected to estimate the total amount retained. The area under the breakthrough curve during the leaching phase represented the quantity of PFOA leached. The fraction of retained PFOA leached by each weathering treatment was determined using the following equations:

$$\%\ \text{PFOA leached by Dry wet cycles} = \frac{\text{Mass of PFOA collected during dry}-\text{wet cycles}}{\text{Mass of PFOA retained in soil after injection phase}} \times 100 \qquad (1)$$

$$\%\ \text{PFOA leached by Freeze} - \text{thaw cycles} = \frac{\text{Mass of PFOA collected during freeze–thaw cycles}}{\text{Mass of PFOA retained in soil after dry–wet cycles}} \times 100 \qquad (2)$$

4.3. Results and Discussion

4.3.1. Change in PFOA concentration in the injection phase

The breakthrough profile of PFOA is similar to that of bromide indicating soil has a low capacity to retain PFOA (Figure 4-1 a). The PFOA concentration in the effluent samples quickly reached the influent concentration (C_0) in 2.1 pore volumes. When the columns were flushed with 5,8 PV of PFOA-free groundwater, the PFOA concentration decreased to 0.6% of C_0. Most of the injected PFOA (99.2%) was removed when the soil columns were flushed with PFOA-free groundwater and only a small fraction of PFOA (0.8%) was retained in the soil media (Figure 4-1 b). Thus, the leaching phase examined whether or not weathering conditions affect the release of the fraction retained in subsurface soil.

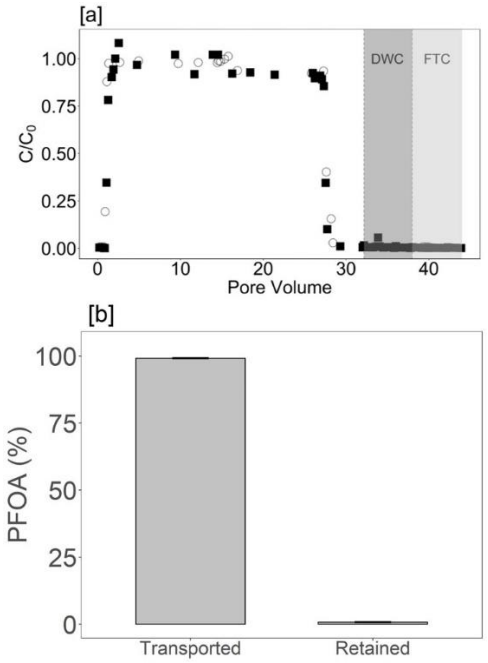

Figure 4-1: (a) Breakthrough curve of total PFOA through soil showing locations of dry-wet cycles (DWC) and freeze-thaw cycles (FTC). The black squares denote the PFOA concentration while the white circles denote the bromide concentration. (b) Mass balance analysis of the total PFOA showing the % PFOA transported outside the soil columns and % retained within the soil during injection of PFOA-containing groundwater.

4.3.2. Weathering cycles leached PFOA from the soil

Compared to the no-treatment control, the PFOA concentration increased following each weathering cycle, indicating weathering cycles can enhance the release of PFOA from the subsurface (Figure 4-2).

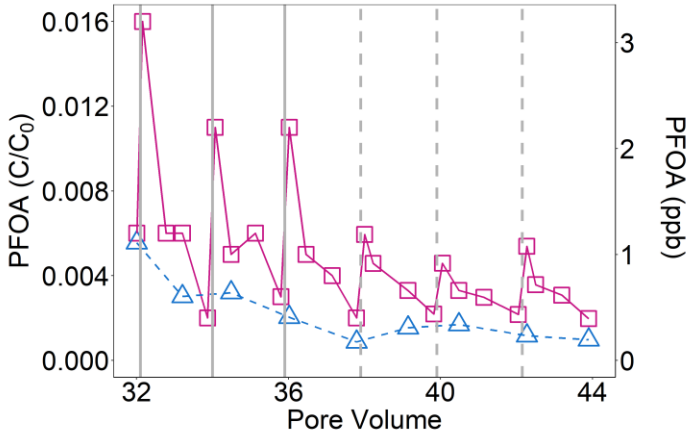

Figure 4-2: Change in PFOA concentrations during dry-wet and freeze-thaw treatments. The solid grey lines indicate the three dry-wet cycles, whereas the grey dashed lines indicate the three freeze-thaw cycles. The blue triangles show the PFOA concentration released from columns, which were not exposed to weathering treatments. The detection limit of the method is 0.01 μg L^{-1}, which is nearly 10 times lower concentration than the minimum concentration observed in the leaching study.

Mass balance analysis showed that the three dry-wet cycles released 31.3 ± 14.9 % of previously retained PFOA and three freeze-thaw cycles released 12.9 ± 1.5 % of the remaining PFOA retained after the dry-wet cycles (Figure 4-3 a). In comparison, the control columns which were not subjected to weathering conditions had much lesser PFOA concentrations in the effluent samples: they released 0.13 ± 0.03% of PFOA and 0.07 ± 0.02% of PFOA, when the same amount of groundwater was eluted without dry-wet or freeze-thaw treatments, respectively. Moreover, the PFOA concentration in the pore water increased right after the weathering treatments (Figure 4-3 b). In contrast, there was no increase in PFOA concentration observed in the control columns. The

leaching of PFOA by intermittent infiltration of water was also observed in another study (Gellrich et al., 2012). We attributed enhanced leaching of PFOA in the dry-wet cycles to back diffusion of PFOA from the soil matrix, the collapse of air-water interfaces during dry-wet cycles, and the release of colloids carrying PFOA (Adamson et al., 2020; Aramrak et al., 2011). In the case of freeze-thaw cycles, freezing could concentrate solutes in the remaining liquid film after ice formation and increase the concentration of solutes adsorbed on pore walls (Mohanty et al., 2014; Spaans and Baker, 1996; Wu et al., 2015). Additionally, the freezing of water increases its volume, increasing the pressure on the pore walls. Both these processes could crack the pore walls and generate colloids enriched with PFOA. In our study, both dry-wet and freeze-thaw cycles released similar ($p > 0.05$) amount of PFOA. It should be noted that the same columns were subjected to dry-wet cycles before freeze-thaw cycles. Thus, more PFOA were available for release before dry-wet cycles than freeze-thaw cycles. As freeze-thaw cycles released similar amount of PFOA from depleted columns, we assumed that freeze-thaw cycles were more effective in releasing PFOA.

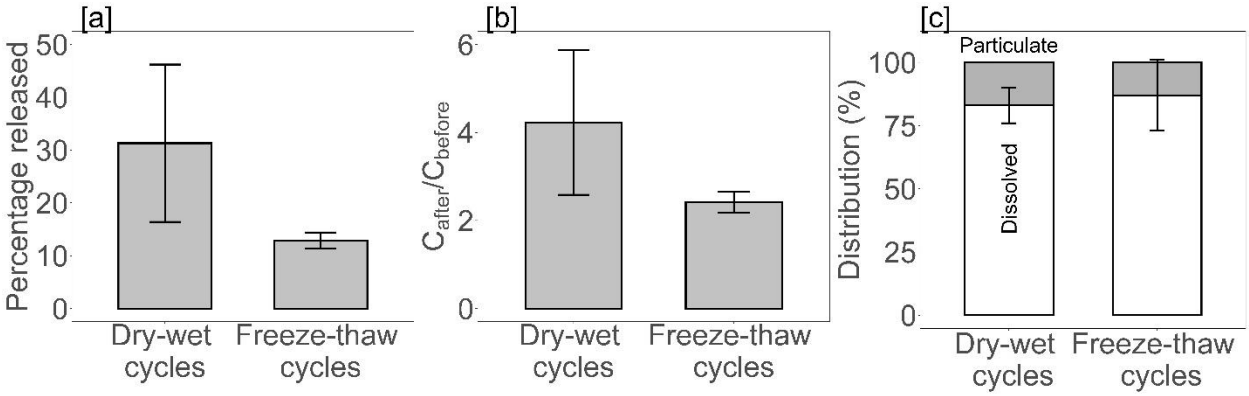

Figure 4-3: (a) Percent of total PFOA released from the impacted soil columns during dry-wet cycles and freeze-thaw cycles. (b) The ratio of PFOA concentration in the effluent samples before and just after each weathering cycle. (c) Distribution of PFOA in the dissolved phase and associated with particulates in effluent samples from dry-wet and freeze-thaw cycles.

4.3.3. Weathering conditions released soil colloids carrying PFOA

Although the turbidity in the effluent samples was below the detection limit, SEM data showed high amounts of soil colloids in the effluent samples collected following dry-wet and freeze-thaw treatments (Figure 4-4**)**. Particle size analysis of colloids in samples following weathering treatments confirmed the presence of colloids and their size distribution; nearly all mobilized colloids were smaller than 1.8 μm. The size distribution of the colloids was different based on weathering treatment type. The colloids released from the dry-wet cycles were of mode size 1.06 μm while most particles released by freeze-thaw cycles were of sizes less than 0.83 μm, which was the detection limit of the instrument. SEM analysis confirmed that most colloids in freeze-thaw cycles were lower than 0.83 μm. Thus, although freeze-thaw cycles released more colloids with sizes lower than 0.83 μm, they were not detected in the particle size analyzer. Consequently, the release of PFOA cannot be compared between dry-wet and freeze-thaw cycles based on colloid concentration measured by the particle size analyzer. Nevertheless, the results indicated that the weathering treatments could release colloids of different sizes. During dry-wet cycles, colloids are released mainly due to collapse of pore walls by capillary force during drying and collapse of the air-water interface during rewetting (Flury and Aramrak, 2017; Majdalani et al., 2007; Shang et al., 2008), whereas colloids are released during freeze-thaw cycles by fracture of pore walls by the increase in pressure from expanding ice volume (Mohanty et al., 2014; Oztas and Fayetorbay, 2003). Although previous studies confirmed the role of the weathering on colloid release, our study showed that the size of the colloid released from the soil could vary based on the treatment.

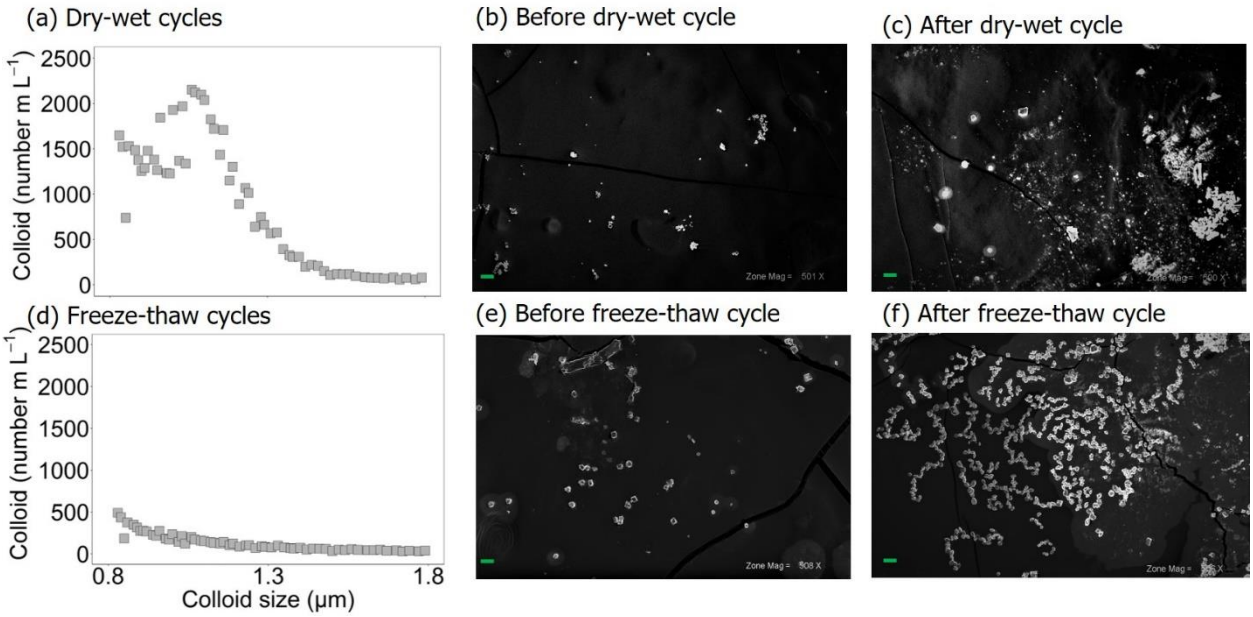

Figure 4-4: The particle size distribution of the colloids released by (a) dry-wet cycles and (d) freeze-thaw cycles. SEM image of colloids in effluent samples before (b) and after (c) dry-wet cycles, and before I and after (f) freeze-thaw cycles. The green line at the bottom left corner of the SEM images corresponds to a length of 20 μm.

XRD analysis revealed that quartz (SiO_2), K-feldspar ($KalSi_3O_8$) and calcite ($CaCO_3$) were the primary minerals in the bulk soil (**Figure 4-5**). Calcium carbonate, illite, and mica were the main minerals in the colloidal particles (Figure S4). Calcium carbonate can adsorb PFOA (Lv et al., 2018). Clay minerals could also adsorb PFOA from the water (Zhang et al., 2014). These soil colloids can carry significant amounts of PFOA even in low adsorbing subsurface soils. This adsorption can be enhanced in soils having high PFOA sorption capacities, such as soils that have a high organic matter, proteinaceous content, metal oxides, or clay minerals (Li et al., 2019; Longstaffe et al., 2012). Furthermore, compared to PFOA, PFOS has a stronger affinity to soil or colloids. Thus, the colloid-facilitated release could be more prominent for strongly adsorbing PFAS. Future study should use a series of PFAS with different affinity to the soil to examine the effect of PFAS type on colloid-facilitated leaching.

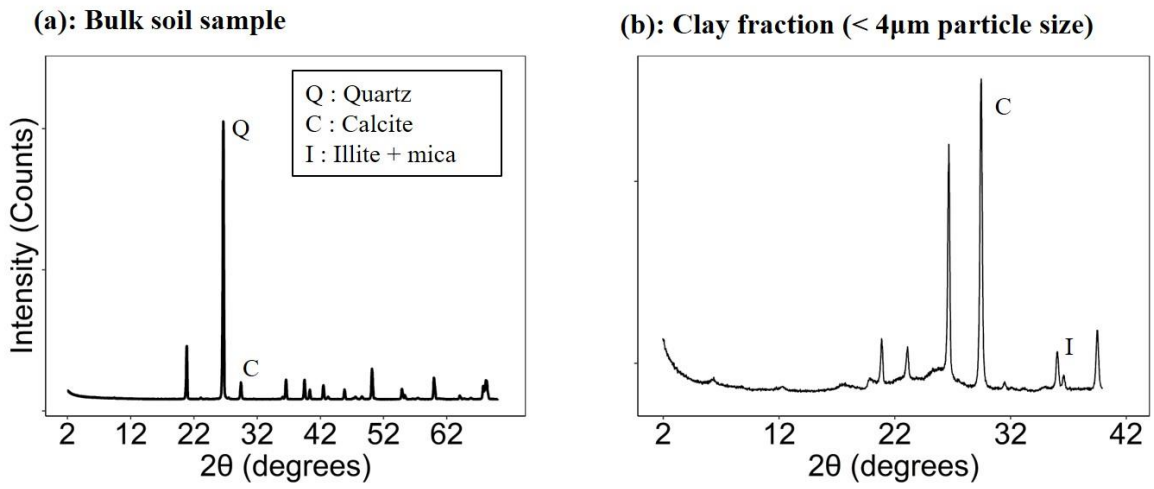

Figure 4-5: XRD analysis of (a) bulk soil and (b) clay fraction of the soil (air-dried specimens) showing the peaks corresponding to different minerals.

A significant fraction of PFOA in each effluent sample was found to be associated with soil colloids. Removing the soil colloids by centrifugation decreased the PFOA concentration in the effluent samples significantly. Removal of colloids by centrifugation decreased the PFOA concentration in the effluent samples from the dry-wet cycles by 17 ± 7% and from the freeze-thaw cycles by 13 ± 14 % (Figure 4-3 c). This was also observed in a previous study where removal of soil colloids reduced the PFOA concentrations in the effluent samples (Borthakur et al., 2021a). The colloid concentration in the effluent samples from the control columns was negligible. Therefore, centrifuging the samples did not decrease the PFOA concentration. This confirmed that the released soil colloids contributed to the total PFOA concentration in the effluent samples. As most soil colloids have a negative surface charge, they can electrostatically bind positively charged solutes. Thus, cationic or zwitterionic PFAS (Mejia-Avendano et al., 2020; Milinovic et al., 2015) could have a higher affinity to colloids, and therefore the leaching of those PFAS could be dominated by colloids. Furthermore, colloids are typically accumulated near the air-water interface in the vadose zone (Flury and Aramrak, 2017), the same location where PFAS, owing to their

surfactant properties, are relocated from bulk liquid (Brusseau, 2018; Lyu et al., 2018). Due to the proximity of both colloids and PFAS near the air-water interface, PFAS are more likely to adsorbed on colloids. Further study should be conducted to examine how surfactant behavior at interfaces affected their association with colloids.

4.4. Conclusions

We examined the effect of common weathering conditions on the leaching of PFOA from an impacted subsurface and showed that leaching of PFOA from subsurface soil increased when the soil was subjected to natural dry-wet or freeze-thaw cycles. An increase in PFOA release coincided with the release of soil colloids, indicating colloid release can be a significant pathway for PFOA release from the source zone. In this study, nearly 36% of PFOA in water samples was attributed to colloids. Thus, conceptual site models should account for the effect of natural weather cycles on the leaching of PFOA from the subsurface and concentration of colloid-bound PFOA in water samples.

4.5. References

Adamson, D.T., Nickerson, A., Kulkarni, P.R., Higgins, C.P., Popovic, J., Field, J., Rodowa, A., Newell, C., DeBlanc, P., Kornuc, J.J., 2020. Mass-Based, Field-Scale Demonstration of PFAS Retention within AFFF-Associated Source Areas. Environ. Sci. Technol. 54, 15768–15777. https://doi.org/10.1021/acs.est.0c04472

Ahrens, L., Taniyasu, S., Yeung, L.W.Y., Yamashita, N., Lam, P.K.S., Ebinghaus, R., 2010. Distribution of polyfluoroalkyl compounds in water, suspended particulate matter and sediment from Tokyo Bay, Japan. Chemosphere 79, 266–272. https://doi.org/10.1016/j.chemosphere.2010.01.045

Alam, S., Borthakur, A., Ravi, S., Gebremichael, M., Mohanty, S.K., 2021. Managed aquifer recharge implementation criteria to achieve water sustainability. Science of The Total Environment 768, 144992. https://doi.org/10.1016/j.scitotenv.2021.144992

Aramrak, S., Flury, M., Harsh, J.B., 2011. Detachment of Deposited Colloids by Advancing and Receding Air–Water Interfaces. Langmuir 27, 9985–9993. https://doi.org/10.1021/la201840q

Baduel, C., Paxman, C.J., Mueller, J.F., 2015. Perfluoroalkyl substances in a firefighting training ground (FTG), distribution and potential future release. Journal of Hazardous Materials 296, 46–53. https://doi.org/10.1016/j.jhazmat.2015.03.007

Borthakur, A., Cranmer, B.K., Dooley, G.P., Blotevogel, J., Mahendra, S., Mohanty, S.K., 2021a. Release of soil colloids during flow interruption increases the pore-water PFAS concentration in saturated soil. Environmental Pollution 117297. https://doi.org/10.1016/j.envpol.2021.117297

Borthakur, A., Wang, M., He, M., Ascencio, K., Blotevogel, J., Adamson, D.T., Mahendra, S., Mohanty, S.K., 2021b. Perfluoroalkyl acids on suspended particles: Significant transport pathways in surface runoff, surface waters, and subsurface soils. Journal of Hazardous Materials 417, 126159. https://doi.org/10.1016/j.jhazmat.2021.126159

Brusseau, M.L., 2020. Simulating PFAS transport influenced by rate-limited multi-process retention. Water Res 168, 115179. https://doi.org/10.1016/j.watres.2019.115179

Brusseau, M.L., 2019. Estimating the relative magnitudes of adsorption to solid-water and air/oil-water interfaces for per- and poly-fluoroalkyl substances. Environ Pollut 254, 113102. https://doi.org/10.1016/j.envpol.2019.113102

Brusseau, M.L., 2018. Assessing the potential contributions of additional retention processes to PFAS retardation in the subsurface. Sci Total Environ 613–614, 176–185. https://doi.org/10.1016/j.scitotenv.2017.09.065

Carey, G.R., McGregor, R., Pham, A.L.-T., Sleep, B., Hakimabadi, S.G., 2019. Evaluating the longevity of a PFAS in situ colloidal activated carbon remedy. Remediation Journal 29, 17–31. https://doi.org/10.1002/rem.21593

Chen, H., Liu, M., Munoz, G., Duy, S.V., Sauvé, S., Yao, Y., Sun, H., Liu, J., 2020. Fast Generation of Perfluoroalkyl Acids from Polyfluoroalkyl Amine Oxides in Aerobic Soils. Environ. Sci. Technol. Lett. https://doi.org/10.1021/acs.estlett.0c00543

Chen, H.T., Reinhard, M., Yin, T.R., Nguyen, T.V., Tran, N.H., Gin, K.Y.H., 2019. Multi-compartment distribution of perfluoroalkyl and polyfluoroalkyl substances (PFASs) in an urban catchment system. Water Research 154, 227–237. https://doi.org/10.1016/j.watres.2019.02.009

Crone, B.C., Speth, T.F., Wahman, D.G., Smith, S.J., Abulikemu, G., Kleiner, E.J., Pressman, J.G., 2019. Occurrence of per- and polyfluoroalkyl substances (PFAS) in source water and their treatment in drinking water. Critical Reviews in Environmental Science and Technology 49, 2359–2396. https://doi.org/10.1080/10643389.2019.1614848

Ding, Y., Liu, Y.-X., Wu, W.-X., Shi, D.-Z., Yang, M., Zhong, Z.-K., 2010. Evaluation of Biochar Effects on Nitrogen Retention and Leaching in Multi-Layered Soil Columns. Water Air Soil Pollut 213, 47–55. https://doi.org/10.1007/s11270-010-0366-4

Flury, M., Aramrak, S., 2017. Role of air-water interfaces in colloid transport in porous media: A review. Water Resources Research 53, 5247–5275. https://doi.org/10.1002/2017wr020597

Gellrich, V., Stahl, T., Knepper, T.P., 2012. Behavior of perfluorinated compounds in soils during leaching experiments. Chemosphere 87, 1052–6. https://doi.org/10.1016/j.chemosphere.2012.02.011

Grandjean, P., Clapp, R., 2015. Perfluorinated Alkyl Substances: Emerging Insights Into Health Risks. New Solutions: A Journal of Environmental and Occupational Health Policy 25, 147–163. https://doi.org/10.1177/1048291115590506

Guo, B., Zeng, J., Brusseau, M.L., 2020. A Mathematical Model for the Release, Transport, and Retention of Per- and Polyfluoroalkyl Substances (PFAS) in the Vadose Zone. Water Resources Research 56, e2019WR026667. https://doi.org/10.1029/2019wr026667

Huang, M., Jiao, J., Zhuang, P., Chen, X., Wang, J., Zhang, Y., 2018. Serum polyfluoroalkyl chemicals are associated with risk of cardiovascular diseases in national US population. Environment International 119, 37–46. https://doi.org/10.1016/j.envint.2018.05.051

Jeon, J., Kannan, K., Lim, B.J., An, K.G., Kim, S.D., 2011. Effects of salinity and organic matter on the partitioning of perfluoroalkyl acid (PFAs) to clay particles. Journal of Environmental Monitoring 13, 1803–1810. https://doi.org/10.1039/c0em00791a

Kabiri, S., Centner, M., McLaughlin, M.J., 2021. Durability of sorption of per- and polyfluorinated alkyl substances in soils immobilised using common adsorbents: 1. Effects of perturbations in pH. Science of The Total Environment 766, 144857. https://doi.org/10.1016/j.scitotenv.2020.144857

Kung, K.-J.S., 1990. Preferential flow in a sandy vadose zone: 2. Mechanism and implications. Geoderma 46, 59–71. https://doi.org/10.1016/0016-7061(90)90007-V

Laitinen, J.A., Koponen, J., Koikkalainen, J., Kiviranta, H., 2014. Firefighters' exposure to perfluoroalkyl acids and 2-butoxyethanol present in firefighting foams. Toxicology Letters, Advances in Biological Monitoring for Occupational and Environmental Health - II 231, 227–232. https://doi.org/10.1016/j.toxlet.2014.09.007

Lath, S., Knight, E.R., Navarro, D.A., Kookana, R.S., McLaughlin, M.J., 2019. Sorption of PFOA onto different laboratory materials: Filter membranes and centrifuge tubes. Chemosphere 222, 671–678. https://doi.org/10.1016/j.chemosphere.2019.01.096

Li, F., Fang, X., Zhou, Z., Liao, X., Zou, J., Yuan, B., Sun, W., 2019. Adsorption of perfluorinated acids onto soils: Kinetics, isotherms, and influences of soil properties. Science of The Total Environment 649, 504–514. https://doi.org/10.1016/j.scitotenv.2018.08.209

Longstaffe, J.G., Courtier-Murias, D., Soong, R., Simpson, M.J., Maas, W.E., Fey, M., Hutchins, H., Krishnamurthy, S., Struppe, J., Alaee, M., Kumar, R., Monette, M., Stronks, H.J., Simpson, A.J., 2012. In-Situ Molecular-Level Elucidation of Organofluorine Binding Sites

in a Whole Peat Soil. Environ. Sci. Technol. 46, 10508–10513. https://doi.org/10.1021/es3026769

Lv, X., Sun, Y., Ji, R., Gao, B., Wu, J., Lu, Q., Jiang, H., 2018. Physicochemical factors controlling the retention and transport of perfluorooctanoic acid (PFOA) in saturated sand and limestone porous media. Water Res 141, 251–258. https://doi.org/10.1016/j.watres.2018.05.020

Lyu, Y., Brusseau, M.L., Chen, W., Yan, N., Fu, X., Lin, X., 2018. Adsorption of PFOA at the Air-Water Interface during Transport in Unsaturated Porous Media. Environ Sci Technol 52, 7745–7753. https://doi.org/10.1021/acs.est.8b02348

Majdalani, S., Michel, E., Di Pietro, L., Angulo-Jaramillo, R., Rousseau, M., 2007. Mobilization and preferential transport of soil particles during infiltration: A core-scale modeling approach. Water Resources Research 43. https://doi.org/10.1029/2006wr005057

Mejia-Avendano, S., Zhi, Y., Yan, B., Liu, J., 2020. Sorption of Polyfluoroalkyl Surfactants on Surface Soils: Effect of Molecular Structures, Soil Properties, and Solution Chemistry. Environ Sci Technol 54, 1513–1521. https://doi.org/10.1021/acs.est.9b04989

Merino, N., Qu, Y., Deeb, R.A., Hawley, E.L., Hoffmann, M.R., Mahendra, S., 2016. Degradation and Removal Methods for Perfluoroalkyl and Polyfluoroalkyl Substances in Water. Environmental Engineering Science 33, 615–649. https://doi.org/10.1089/ees.2016.0233

Milinovic, J., Lacorte, S., Vidal, M., Rigol, A., 2015. Sorption behaviour of perfluoroalkyl substances in soils. Science of The Total Environment 511, 63–71. https://doi.org/10.1016/j.scitotenv.2014.12.017

Mohanty, S.K., Saiers, J.E., Ryan, J.N., 2016. Colloid mobilization in a fractured soil: effect of pore-water exchange between preferential flow paths and soil matrix. Environ. Sci. Technol. 50, 2310–2317.

Mohanty, S.K., Saiers, J.E., Ryan, J.N., 2014. Colloid-facilitated mobilization of metals by freeze–thaw cycles. Environmental Science & Technology 48, 977–984. https://doi.org/10.1021/es403698u

Oztas, T., Fayetorbay, F., 2003. Effect of freezing and thawing processes on soil aggregate stability. Catena 52, 1–8. https://doi.org/10.1016/S0341-8162(02)00177-7

Pereira, H.C., Ullberg, M., Kleja, D.B., Gustafsson, J.P., Ahrens, L., 2018. Sorption of perfluoroalkyl substances (PFASs) to an organic soil horizon – Effect of cation composition and pH. Chemosphere 207, 183–191. https://doi.org/10.1016/j.chemosphere.2018.05.012

Qian, J., Shen, M., Wang, P., Wang, C., Hou, J., Ao, Y., Liu, J., Li, K., 2017. Adsorption of perfluorooctane sulfonate on soils: Effects of soil characteristics and phosphate competition. Chemosphere 168, 1383–1388. https://doi.org/10.1016/j.chemosphere.2016.11.114

Schaefer, C.E., Drennan, D.M., Tran, D.N., Garcia, R., Christie, E., Higgins, C.P., Field, J.A., 2019. Measurement of Aqueous Diffusivities for Perfluoroalkyl Acids. Journal of Environmental Engineering 145, 06019006. https://doi.org/doi:10.1061/(ASCE)EE.1943-7870.0001585

Schelde, K., Moldrup, P., Jacobsen, O.H., de Jonge, H., de Jonge, L.W., Komatsu, T., 2002. Diffusion-Limited Mobilization and Transport of Natural Colloids in Macroporous Soil. Vadose Zone Journal 1, 125–136. https://doi.org/10.2113/1.1.125

Shang, J., Flury, M., Chen, G., Zhuang, J., 2008. Impact of flow rate, water content, and capillary forces on in situ colloid mobilization during infiltration in unsaturated sediments. Water Resources Research 44. https://doi.org/10.1029/2007wr006516

Spaans, E.J.A., Baker, J.M., 1996. The Soil Freezing Characteristic: Its Measurement and Similarity to the Soil Moisture Characteristic. Soil Science Society of America Journal 60, 13–19. https://doi.org/10.2136/sssaj1996.03615995006000010005x

Trudel, D., Horowitz, L., Wormuth, M., Scheringer, M., Cousins, I.T., Hungerbühler, K., 2008. Estimating Consumer Exposure to PFOS and PFOA. Risk Analysis 28, 251–269. https://doi.org/10.1111/j.1539-6924.2008.01017.x

Wang, F., Liu, C., Shih, K., 2012. Adsorption behavior of perfluorooctanesulfonate (PFOS) and perfluorooctanoate (PFOA) on boehmite. Chemosphere 89, 1009–14. https://doi.org/10.1016/j.chemosphere.2012.06.071

Wang, F.L., Alva, A.K., 1996. Leaching of Nitrogen from Slow-Release Urea Sources in Sandy Soils. Soil Science Society of America Journal 60, 1454–1458. https://doi.org/10.2136/sssaj1996.03615995006000050024x

Washington, J.W., Yoo, H., Ellington, J.J., Jenkins, T.M., Libelo, E.L., 2010. Concentrations, Distribution, and Persistence of Perfluoroalkylates in Sludge-Applied Soils near Decatur, Alabama, USA. Environ. Sci. Technol. 44, 8390–8396. https://doi.org/10.1021/es1003846

Wu, M., Tan, X., Huang, J., Wu, J., Jansson, P.-E., 2015. Solute and water effects on soil freezing characteristics based on laboratory experiments. Cold Regions Science and Technology 115, 22–29. https://doi.org/10.1016/j.coldregions.2015.03.007

Xiao, F., Jin, B., Golovko, S.A., Golovko, M.Y., Xing, B., 2019. Sorption and Desorption Mechanisms of Cationic and Zwitterionic Per- and Polyfluoroalkyl Substances in Natural Soils: Thermodynamics and Hysteresis. Environ Sci Technol 53, 11818–11827. https://doi.org/10.1021/acs.est.9b05379

Xiao, F., Sasi, P.C., Yao, B., Kubátová, A., Golovko, S.A., Golovko, M.Y., Soli, D., 2020. Thermal Stability and Decomposition of Perfluoroalkyl Substances on Spent Granular Activated Carbon. Environ. Sci. Technol. Lett. 7, 343–350. https://doi.org/10.1021/acs.estlett.0c00114

Xiao, F., Zhang, X., Penn, L., Gulliver, J.S., Simcik, M.F., 2011. Effects of Monovalent Cations on the Competitive Adsorption of Perfluoroalkyl Acids by Kaolinite: Experimental Studies and Modeling. Environ. Sci. Technol. 45, 10028–10035. https://doi.org/10.1021/es202524y

Yeung, L.W.Y., Guruge, K.S., Taniyasu, S., Yamashita, N., Angus, P.W., Herath, C.B., 2013. Profiles of perfluoroalkyl substances in the liver and serum of patients with liver cancer and cirrhosis in Australia. Ecotoxicology and Environmental Safety 96, 139–146. https://doi.org/10.1016/j.ecoenv.2013.06.006

Zhang, H., Cui, R., Guo, X., Hu, J., Dai, J., 2016. Low dose perfluorooctanoate exposure promotes cell proliferation in a human non-tumor liver cell line. Journal of Hazardous Materials 313, 18–28. https://doi.org/10.1016/j.jhazmat.2016.03.077

Zhang, R., Yan, W., Jing, C., 2014. Mechanistic study of PFOS adsorption on kaolinite and montmorillonite. Colloids and Surfaces A: Physicochemical and Engineering Aspects 462, 252–258. https://doi.org/10.1016/j.colsurfa.2014.09.019

5. CHAPTER 5: RECHARGEABLE STORMWATER BIOFILTERS USING CATIONIC POLYMERS FOR PFAS REMOVAL

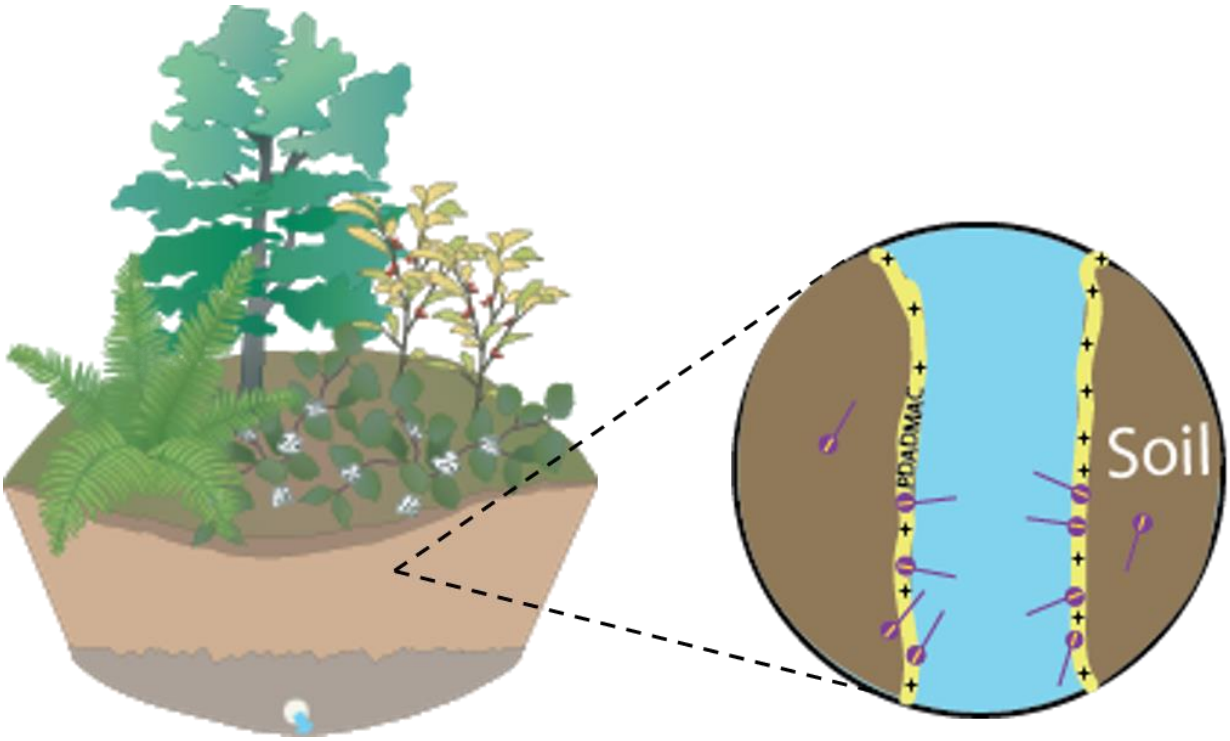

Borthakur, A., Das, T., Zhang, Y., Libbert, S., Ramos, P., Dooley, G.P., Blotevogel, J., Mahendra, S., Mohanty, S.K. Rechargeable stormwater biofilters using cationic polymers for PFAS removal. *To be submitted.*

Abstract

Conventional stormwater biofilter media such as sand and compost have limited capacity to remove PFAS. Adding amendments such as biochar or activated carbon is rarely effective in removing short-chain PFAS, and their capacity to remove PFAS could become exhausted eventually. Replacing exhausted filter media is expensive whereas in situ regeneration of filter media adsorption capacity can be an effective alternative. In this study, we show that in situ application of cationic polymers such as polydiallyldimethylammonium chloride (PDADMAC), a drinking water coagulant, not only replenishes the PFAS removal capacity of compost biofilters, but also significantly increases the adsorption capacity of conventional biofilter media. This increase is more prominent for short-chain PFAS, which are the most difficult to remove. The improvement in PFAS removal decreased exponentially with the increase in the carbon chain length. Despite being used as coagulants, the addition of PDADMAC did not increase the clogging rate of the biofilters in the presence of suspended sediments, indicating most PDADMAC were bound to filter media and not available to coagulate suspended sediments. Thus, injection of cationic polymers can be a viable option to either enhance any biofilters or regenerate any amendment's absorption capacity to remove for PFAS in situ.

5.1. Introduction

Nearly 72% of PFAS contaminated drinking water facilities use groundwater as the water source, indicating that groundwater is a major source of PFAS contaminated drinking water (Guelfo and Adamson, 2018). Groundwater gets contaminated when surface runoff from PFAS contamination sources infiltrates into the subsurface to the groundwater. Infiltration-based treatment systems such as stormwater biofilters can be used to remove PFAS from stormwater (Spahr et al., 2020). However, conventional biofilter media such as sand and compost have low adsorption capacity for PFAS (Aly et al., 2018; Hale et al., 2017). In this case, the filter media can be amended or replaced with adsorbents such as biochar, activated carbon, or clay that can adsorb PFAS using hydrophobic, electrostatic, or chemisorption interactions (Askeland et al., 2020; Mukhopadhyay et al., 2021; Park et al., 2020). Since biofilter media is mostly negatively charged, hydrophobic interactions are the major force driving the adsorption of PFAS by the media. However, this reduces the capacity of biofilters to adsorb short-chain PFAS compounds. Moreover, due to their recalcitrant nature, adsorbed long-chain PFAS compounds accumulate in the biofilter which exhausts the adsorption sites and reduces further removal of PFAS. Therefore, a method to replenish exhausted PFAS sites in biofilters and also improve their ability to remove short-chain PFAS is required.

Coating commonly used PFAS adsorbents with cationic polymers such as polydiallyldimethylammonium chloride (PDADMAC) could improve their PFAS removal capacity (Aly et al., 2019, 2018; Liu et al., 2020; Ramos et al., 2022; Ray et al., 2019). Organic polymers can easily adsorb onto clay (Ray et al., 2019), activated carbon (Liu et al., 2020; Ramos et al., 2022), and aquifer soil (Aly et al., 2019, 2018) and adsorb PFAS through hydrophobic interactions. In addition, being cationic, these polymers can electrostatically adsorb PFAS as well,

increasing their removal efficiency. PDADMAC has been used to remove PFAS either by coating adsorbents with PDADMAC (Ramos et al., 2022; Ray et al., 2019) or through direct injection of PDADMAC into adsorbents (Aly et al., 2019, 2018). Out of these methods, direct injection of PDADMAC into biofilter media provides a non-intrusive method of replenishing exhausted PFAS adsorption sites. However, being a coagulant, injection of liquid PDADMAC solutions can flocculate suspended sediments in stormwater which could clog the biofilters, rendering them unusable. Thus, the effect of injecting PDADMAC solution into biofilters to improve their PFAS removal capacity must be studied and any unintended consequences due to coagulation of sediments need to be explored. Yet, no study to date has explored the possibility of direct injection of cationic polymers into stormwater biofilters to create regenerative PFAS-removing biofilters.

This study examines the effect of PDADMAC application into biofilters on the PFAS removal capacity of biofilters and their clogging potential. Exhausted biofilter media columns were exposed to PDADMAC solution, and the improvement in PFAS removal was determined. The clogging potential of the PDADMAC injected biofilters was also determined by increased suspended sediments. The results will help develop the technology of using cationic polymers to create stormwater biofilters that can regenerate their ability to remove PFAS and other emerging pollutants from stormwater.

5.2. Materials and Methods

5.2.1. Stormwater and biofilter media preparation

Natural stormwater was used to simulate the adsorption of PFAS onto biofilter media under field conditions as organic carbon, nutrients, and other pollutants can compete with PFAS for adsorption sites in the filter media. Stormwater was collected from Ballona Creek, Los Angeles, and was spiked with 500 µg L^{-1} each of perfluorobutanoic acid (PFBA, Acros Organics),

perfluorohexanoic acid (PFHxA, Fisher Scientific), perfluorooctanoic acid (PFOA, Fisher Scientific) and perfluorodecanoic acid (PFDA, Fisher Scientific) to form PFAS-spiked stormwater. However, to ensure maximum PDADMAC adsorption onto the biofilter media, we used synthetic stormwater (10 mM NaCl) for injecting PDADMAC into the biofilter as a field injection of PDADMAC solution using synthetic stormwater is feasible. The synthetic stormwater had an electrical conductivity (900 ± 50 µS cm^{-1}) similar to natural stormwater obtained from Ballona Creek (Ghavanloughajar et al., 2020).

5.2.2. Optimum PDADMAC dose determination

To determine the optimum dose of polymer required for the highest adsorption, 4 g compost was added to triplicate 50 ml centrifuge tubes with 40 mL of 10 mM NaCl solution containing different 0, 2500, 5000, 8000, and 10000 mg L^{-1}. The tubes were then shaken in a wrist action shaker for 24 hours. The tubes were centrifuged at 5000 RPM for 15 minutes and the supernatant was extracted. The PDADMAC concentration of the supernatant was determined by measuring the total nitrogen in the water using Hach Total Nitrogen (TN) kits following the Persulfate Digestion Method as described elsewhere (Ramos et al., 2022). The optimum PDADMAC concentration was determined based on the shape of the adsorption isotherm. The optimum PDADMAC concentration was spiked into synthetic stormwater to create PDADMAC-spiked synthetic stormwater.

5.2.3. Biofilter media and column packing

Conventional biofilter media typically contain sand as a bulking agent amended with compost to remove pollutants and support vegetation. This study simulated the same biofilter design by mixing quartz sand of sizes between 0.6 to 0.85 mm and organic compost (Whittier Fertilizer, 57% organic carbon) of sizes between 0.075 mm and 2 mm at a 7: 3 ratio. Fine compost

particles (size < 0.075 mm) were removed to minimize clogging of the biofilter. Two sets of triplicate PVC columns with an inner diameter of 2.54 cm and height 30 cm were packed with the compost-sand mixture to create the model biofilters. To create a drainage layer, pea gravel was first added to the bottom of the columns up to 6 cm topped with a 100 μm nylon membrane. Then the sand-compost mixture was added to the columns in small layers up to a filter media depth of 15 cm, with each layer tamped 15 times using an iron rod. Uniform packing of the biofilter media was verified by measuring the bulk density of each layer. The bulk density, measured by dividing the weight of the dry filter media by the inner volume of the columns, was determined to be 1.36 ± 0.14 g cm^{-3}. The pore volume (PV) of the biofilters was measured by subtracting the weight of the dry biofilter media from the weight of the saturated biofilter media. The porosity of the biofilters was measured by dividing the pore volume of the biofilters by the bulk density. The porosity of the six columns was 34.8 ± 2.3%. The hydraulic conductivity of the columns was measured using the falling head method. The average hydraulic conductivity of the biofilters was 51.8 ± 9.5 cm h^{-1}.

5.2.4. Injection of PDADMAC and PFAS into biofilter columns

To check the ability of the PDADMAC in replenishing the PFAS removal capacity of the biofilters, PFAS spiked stormwater was injected into the biofilters with and without in situ application of PDADMAC. The biofilters were first conditioned with natural stormwater at 4 mL min^{-1} (47.4 cm h^{-1}) for 24 h. Then 2.2 PV PFAS spiked stormwater was injected into the biofilters at 4 mL min^{-1} until the breakthrough of each PFAS compound was observed in the effluent samples, signifying exhaustion of adsorption sites in biofilter media. After the breakthrough, the biofilters were flushed with natural stormwater without PFAS to remove unadsorbed PFAS in the pore water of the biofilters. Then, PDADMAC spiked synthetic stormwater was injected at 2 mL

min^{-1} (23.7 cm h^{-1}) into the polymer biofilters. A low flow rate was used to ensure the complete coating of PDADMAC onto biofilter media by increasing the residence time. At the same time, synthetic stormwater without PDADMAC was injected into the non-polymer biofilters. The biofilters were flushed with synthetic stormwater at 2 mL min^{-1} for 24 hours to remove unadsorbed PDADMAC followed by injection of natural stormwater at 4 mL min^{-1} to recondition the biofilters for PFAS injection. The injection and flushing of PFAS spiked water were then repeated till breakthrough. The PFAS concentration in the effluent samples before and after PDADMAC injection was measured and the removal efficiency of the biofilters was determined using the following equation:

$$Removal\ Efficiency\ (\%) = \frac{C_0 - C}{C_0} \times 100 \quad \text{(Eq. 5-1)}$$

Where C_0 is the influent PFAS concentration and C is the effluent PFAS concentration. The increase in PFAS removal due to PDADMAC addition was determined using the following equation:

$$Increase\ in\ Removal = \frac{R_P - R_{NP}}{R_{NP}} \quad \text{(Eq. 5-2)}$$

Where R_P is the removal efficiency of the biofilter after PDADMAC injection and R_{NP} is the removal efficiency before PDADMAC injection.

5.2.5. Clogging potential of PDADMAC coated biofilters

The presence of high amounts of PDADMAC in pore water could increase the coagulation of suspended particles and could result in clogging the system. To test this hypothesis, the clogging potential of the biofilters was determined following a method described in an earlier study (Le et al., 2020). Briefly, synthetic stormwater spiked with 3 g L^{-1} suspended particles of size less than 75 μm was injected into the biofilters until the hydraulic conductivity was reduced to less than

50% of the initial hydraulic conductivity. The decrease in hydraulic conductivity with increased loading of suspended particles was plotted and compared between the biofilters.

5.2.6. PFAS analysis and quality control

The PFAS concentration in the effluent samples from the columns was measured using liquid chromatography paired with triple quadrupole mass spectrometry (LC/QqQ-MS) (Borthakur et al., 2021b, 2021a). To account for PFAS removal due to adsorption onto column and tubing walls, PFAS spiked stormwater was injected into an empty column and the PFAS concentration in the effluent was compared with the influent. The difference between the concentrations was found to be negligible. PFAS samples were stored in 200 μL polypropylene vials before analyzing them for PFAS. To account for PFAS losses due to adsorption onto vial walls between the time of sampling and analysis, PFAS losses during sample processing and chemical analysis, and analytical variability, each vial containing PFAS sample was spiked with 50 μg L^{-1} MPFBA, MPFHxA, MPFOA and MPFDA ($^{13}C_4$-PFBA, $^{13}C_2$-PFHxA, $^{13}C_4$-PFOA and $^{13}C_2$-PFDA, Wellington Laboratories) before analyzing the samples. In addition, 20 μg L^{-1} solutions of each PFAS compound (PFBA, PFHxA, PFOA, and PFDA) were prepared in polypropylene vials and their concentrations were measured after 48 h, the average time between sampling and analysis. The decrease in PFAS concentration due to vial adsorption was also found to be negligible.

5.3. Results

5.3.1. Compost had high PDADMAC adsorption capacity

Batch experiments showed that compost could adsorb significant amounts of PDADMAC from the synthetic stormwater (Figure 5-1). PDADMAC adsorption increased with an increase in the initial concentration of 2500 mg L^{-1} and 5000 mg L^{-1}. Increasing the initial concentration to 8000 mg L^{-1} did not significantly increase the adsorption of PDADMAC compared to the adsorption when the initial concentration was 5000 mg L^{-1}. However, increasing the initial concentration to 10000 mg L^{-1} sharply increased the adsorption of PDADMAC by compost. Therefore, the adsorption of PDADMAC by compost increased with the increase in initial concentration, and thus the highest PDADMAC concentration (10000 mg L^{-1}) was used to create the PDADMAC spiked synthetic stormwater.

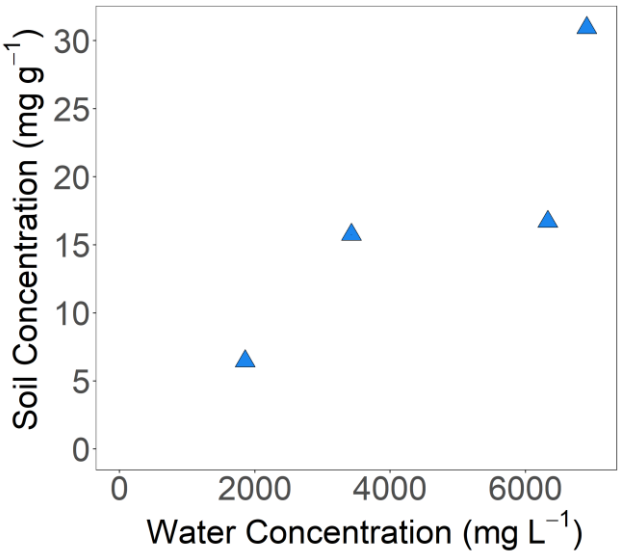

Figure 5-1: Isotherm of adsorption of PDADMAC by compost.

5.3.2. PDADMAC injection replenished the biofilter attachment sites for PFAS

Coating the biofilters with PDADMAC not only replenished the exhausted PFAS adsorption sites but also increased their PFAS adsorption capacity (Figure 5-2a). The compost amended biofilters almost completely lost their ability to remove PFBA (8.3 ± 1.3% removal) after injecting just 2 PV of PFAS-spiked stormwater into the biofilters. However, after PDADMAC injection, the same exhausted biofilters removed 87.8 ± 0.7 % PFBA. Similar improvement was also observed for PFHxA and PFOA. PDADMAC injection improved the biofilters removal capacity for PFHxA from 33.4 ± 0.2 % to 87 ± 0.5 % and for PFOA from 74.9 ± 1.6 % to 99.8 ± 0.04 %. However, PFDA removal in the biofilters was already highest (>99%), and PDADMAC injection did not affect the removal.

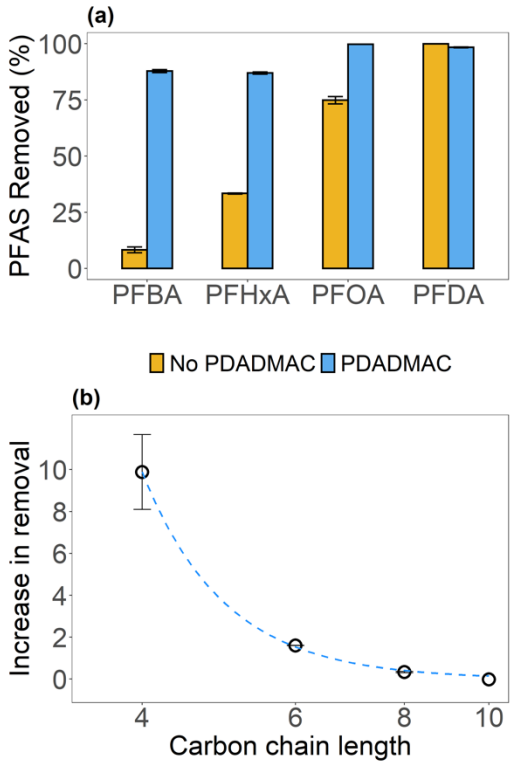

Figure 5-2 (a) PFAS removal efficiency of biofilters before (No PDADMAC) and after PDADMAC (PDADMAC) injection. The injected volume of PFAS spiked stormwater was 2.2 PV. (b) The increase in the removal of PFAS compound due to PDADMAC injection as a function of the carbon chain length.

The increase in PFAS removal due to the application of PDADMAC depended on the carbon chain length: the benefit of PDADMAC application becomes less apparent with an increase in the carbon chain length of PFAS. This was similar to that observed in a previous study (Ramos et al., 2022) where the removal of PFOA by PDADMAC modified granulated activated carbon (GAC) was higher than the removal of PFBA. However, the increase in removal due to PDADMAC injection decreased exponentially (Figure 5-2b) with an increase in the carbon chain length. The increase in PFBA removal due to PDADMAC coating was 9.9 ± 1.8 times the original PFBA removal capacity of the biofilters without PDADMAC. This increase decreased to 1.6 ± 0.002 times and 0.3 ± 0.03 times the original PFHxA and PFOA removal. Thus, adding PDADMAC to the biofilters significantly improved the removal of short-chain PFAS compounds.

5.3.3. PDADMAC coating decreased the clogging potential

Despite being a coagulant, PDADMAC injection did not increase the clogging potential of the biofilters (Figure 5-3). Instead, the hydraulic conductivity of PDADMAC applied biofilters was higher than the one without PDADMAC after the application of 2 g of solids. The hydraulic conductivity of the non-polymer biofilters decreased somewhat linearly with the increased solids loading, and its hydraulic conductivity reduced to less than 50% after just 1.7 g of sediment loading. In comparison, the hydraulic conductivity of the polymer biofilters reduced sharply by 20% after initial solid loading but then decreased at a slower linear rate than the non-polymer biofilters, requiring 2.3 g loading of solids to reduce the hydraulic conductivity to below 50%. Therefore, PDADMAC coating did not exacerbate clogging of the biofilters.

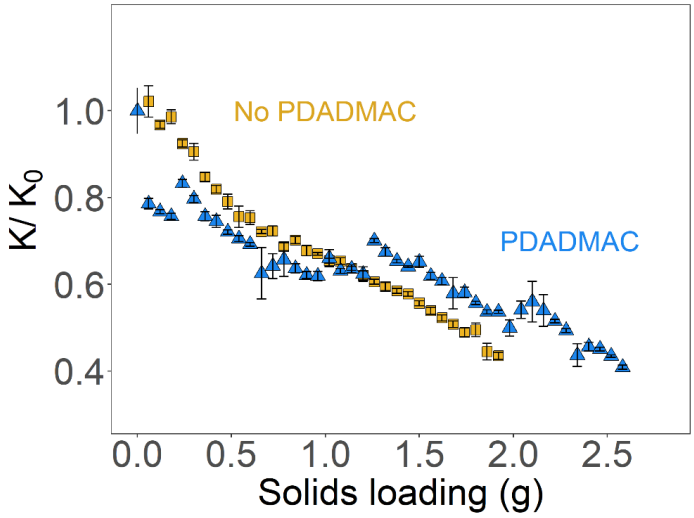

Figure 5-3: Ratio of hydraulic conductivity and initial hydraulic conductivity (K/K_0) of the polymer (PDADMAC) and non-polymer (No PDADMAC) biofilters as a function of the amount (g) of fine solid sediments added (Solids loading).

5.4. Discussion

5.4.1. PDADMAC can regenerate exhausted PFAS adsorption sites in biofilters

Compost-amended biofilters have limited ability to remove PFAS from stormwater, especially short-chain compounds as these compounds are not easily removed via the hydrophobic interactions (Fabregat-Palau et al., 2022). Removal of short-chain PFAS requires electrostatic attraction between the functional groups and the adsorbent media, which is difficult to achieve as most adsorbents have a net negative surface charge. The current study showed that injecting PDADMAC into the biofilters not only replenished the PFAS adsorption sites but also improved the PFAS removal capacity of the biofilters, and this effect was more prominent for the short-chained PFAS. The cationic polymers on compost increased the electrostatic attraction. The effect of PDADMAC was more noticeable for short-chain PFAS compounds such as PFBA as these compounds are primarily removed by electrostatic interactions. The increase in removal due to PDADMAC injection decreased logarithmically with the increase in carbon chain length as the compost was able to remove the long-chain PFAS compounds via hydrophobic interaction. Thus,

the added PDADMAC replenished the adsorption sites but did not significantly increase the adsorption capacity for PFDA. The addition of too much PDADMAC could block adsorption sites for the hydrophobic interaction (Ramos et al., 2022).

5.4.2. PDADMAC injection reduced biofilter clogging

One concern regarding the use of PDADMAC, which has been used as a drinking water coagulant, is that PDADMAC could flocculate the suspended sediments in the pore water and increase the clogging rate of the biofilter. However, our analysis showed that injecting PDADMAC did not affect clogging (Figure 5-3). This was also observed in a previous study where biofilters amended with PDADMAC coated montmorillonite clay had a higher hydraulic conductivity than biochar amended biofilters (Ray et al., 2019), despite the particles being of similar size. A possible reason for this is the coagulant properties of PDADMAC reduce the release of colloids from the biofilter media, which can contribute to the clogging of the biofilter media. Since colloids released from PFAS contaminated subsurface can contain adsorbed PFAS (Borthakur et al., 2021a, 2021b), PDADMAC could prevent the colloid facilitated the release of PFAS as well. Thus, PDADMAC injection can improve the hydraulic conductivity of biofilters and also reduce the long-term release of PFAS.

5.5. Conclusions

This study showed that injecting cationic polymers such as PDADMAC not only replenished exhausted PFAS adsorption sites but also increased PFAS adsorption, especially short-chain PFAS adsorption, through electrostatic interactions. Moreover, PDADMAC injection reduced the rate at which the biofilters clogged when loaded with suspended sediments. Therefore, injecting cationic polymers into stormwater biofilters can be a viable method to create stormwater biofilters with regenerative PFAS removal properties.

5.6. References

Aly, Y.H., Liu, C., McInnis, D.P., Lyon, B.A., Hatton, J., McCarty, M., Arnold, W.A., Pennell, K.D., Simcik, M.F., 2018. In Situ Remediation Method for Enhanced Sorption of Perfluoro-Alkyl Substances onto Ottawa Sand. Journal of Environmental Engineering 144. https://doi.org/10.1061/(asce)ee.1943-7870.0001418

Aly, Y.H., McInnis, D.P., Lombardo, S.M., Arnold, W.A., Pennell, K.D., Hatton, J., Simcik, M.F., 2019. Enhanced adsorption of perfluoro alkyl substances for in situ remediation. Environmental Science-Water Research & Technology 5, 1867–1875. https://doi.org/10.1039/c9ew00426b

Askeland, M., Clarke, B.O., Cheema, S.A., Mendez, A., Gasco, G., Paz-Ferreiro, J., 2020. Biochar sorption of PFOS, PFOA, PFHxS and PFHxA in two soils with contrasting texture. Chemosphere 249, 126072. https://doi.org/10.1016/j.chemosphere.2020.126072

Borthakur, A., Cranmer, B.K., Dooley, G.P., Blotevogel, J., Mahendra, S., Mohanty, S.K., 2021a. Release of soil colloids during flow interruption increases the pore-water PFAS concentration in saturated soil. Environmental Pollution 117297. https://doi.org/10.1016/j.envpol.2021.117297

Borthakur, A., Olsen, P., Dooley, G.P., Cranmer, B.K., Rao, U., Hoek, E.M.V., Blotevogel, J., Mahendra, S., Mohanty, S.K., 2021b. Dry-wet and freeze-thaw cycles enhance PFOA leaching from subsurface soils. Journal of Hazardous Materials Letters 2, 100029. https://doi.org/10.1016/j.hazl.2021.100029

Fabregat-Palau, J., Vidal, M., Rigol, A., 2022. Examining sorption of perfluoroalkyl substances (PFAS) in biochars and other carbon-rich materials. Chemosphere 134733. https://doi.org/10.1016/j.chemosphere.2022.134733

Ghavanloughajar, M., Valenca, R., Le, H., Rahman, M., Borthakur, A., Ravi, S., Stenstrom, M.K., Mohanty, S.K., 2020. Compaction conditions affect the capacity of biochar-amended sand filters to treat road runoff. Science of The Total Environment 735, 139180. https://doi.org/10.1016/j.scitotenv.2020.139180

Guelfo, J.L., Adamson, D.T., 2018. Evaluation of a national data set for insights into sources, composition, and concentrations of per- and polyfluoroalkyl substances (PFASs) in U.S. drinking water. Environmental Pollution 236, 505–513. https://doi.org/10.1016/j.envpol.2018.01.066

Hale, S.E., Arp, H.P.H., Slinde, G.A., Wade, E.J., Bjorseth, K., Breedveld, G.D., Straith, B.F., Moe, K.G., Jartun, M., Hoisaeter, A., 2017. Sorbent amendment as a remediation strategy to reduce PFAS mobility and leaching in a contaminated sandy soil from a Norwegian firefighting training facility. Chemosphere 171, 9–18. https://doi.org/10.1016/j.chemosphere.2016.12.057

Le, H., Valenca, R., Ravi, S., Stenstrom, M.K., Mohanty, S.K., 2020. Size-dependent biochar breaking under compaction: Implications on clogging and pathogen removal in biofilters. Environmental Pollution 266, 115195. https://doi.org/10.1016/j.envpol.2020.115195

Liu, C., Hatton, J., Arnold, W.A., Simcik, M.F., Pennell, K.D., 2020. In Situ Sequestration of Perfluoroalkyl Substances Using Polymer-Stabilized Powdered Activated Carbon. Environ. Sci. Technol. 54, 6929–6936. https://doi.org/10.1021/acs.est.0c00155

Mukhopadhyay, R., Sarkar, B., Palansooriya, K.N., Dar, J.Y., Bolan, N.S., Parikh, S.J., Sonne, C., Ok, Y.S., 2021. Natural and engineered clays and clay minerals for the removal of poly- and perfluoroalkyl substances from water: State-of-the-art and future perspectives. Advances in Colloid and Interface Science 297, 102537. https://doi.org/10.1016/j.cis.2021.102537

Park, M., Wu, S.M., Lopez, I.J., Chang, J.Y., Karanfil, T., Snyder, S.A., 2020. Adsorption of perfluoroalkyl substances (PFAS) in groundwater by granular activated carbons: Roles of hydrophobicity of PFAS and carbon characteristics. Water Research 170. https://doi.org/10.1016/j.watres.2019.115364

Ramos, P., Singh Kalra, S., Johnson, N.W., Khor, C.M., Borthakur, A., Cranmer, B., Dooley, G., Mohanty, S.K., Jassby, D., Blotevogel, J., Mahendra, S., 2022. Enhanced removal of per- and polyfluoroalkyl substances in complex matrices by polyDADMAC-coated regenerable granular activated carbon. Environmental Pollution 294, 118603. https://doi.org/10.1016/j.envpol.2021.118603

Ray, J.R., Shabtai, I.A., Teixidó, M., Mishael, Y.G., Sedlak, D.L., 2019. Polymer-clay composite geomedia for sorptive removal of trace organic compounds and metals in urban stormwater. Water Research 157, 454–462. https://doi.org/10.1016/j.watres.2019.03.097

Spahr, S., Teixidó, M., L. Sedlak, D., G. Luthy, R., 2020. Hydrophilic trace organic contaminants in urban stormwater: occurrence, toxicological relevance, and the need to enhance green stormwater infrastructure. Environmental Science: Water Research & Technology 6, 15–44. https://doi.org/10.1039/C9EW00674E

6. CHAPTER 6: AGING OF EXPANDED SHALE, CLAY, AND SLATE (ESCS) AMENDMENT WITH HEAVY METALS IN STORMWATER INCREASES ITS ANTIBACTERIAL PROPERTIES: IMPLICATIONS ON BIOFILTER DESIGN

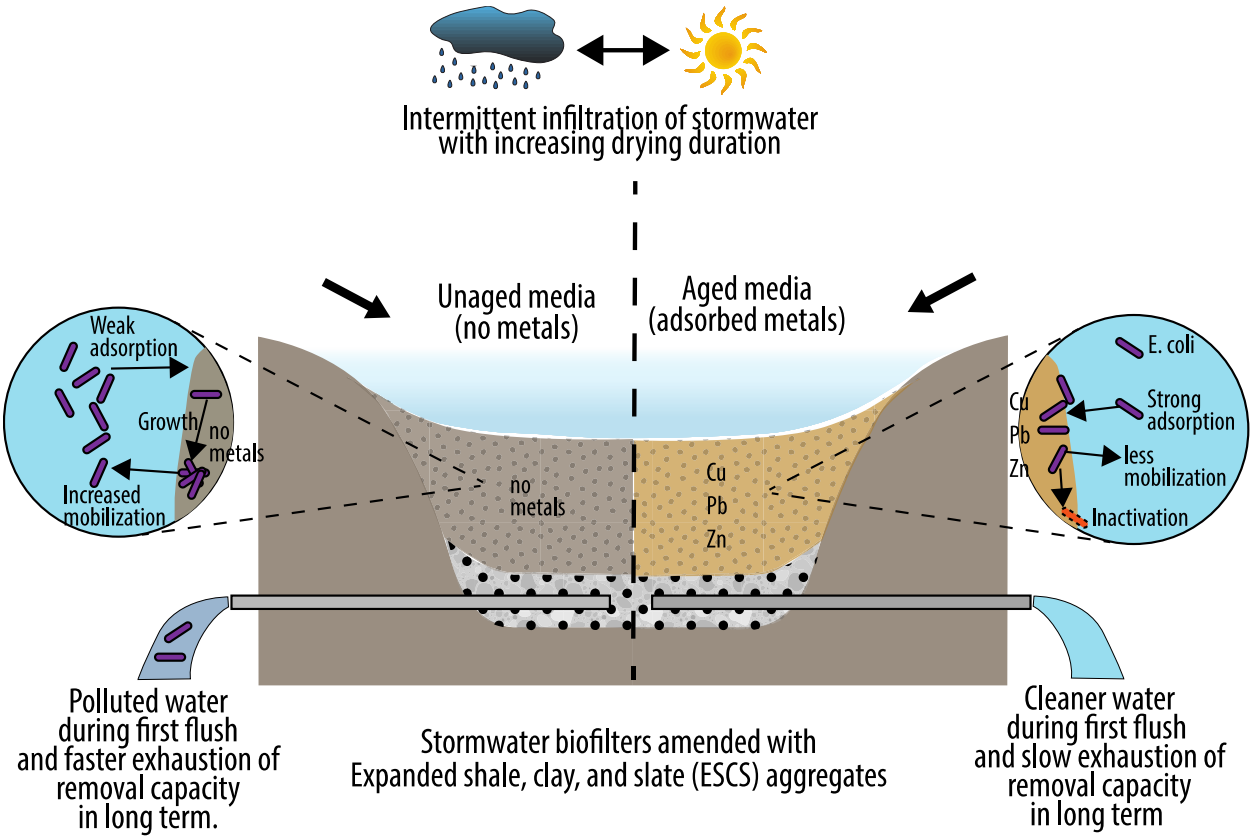

Borthakur, A., Chhour, K.L., Gayle, H.L., Prehn, S.R., Stenstrom, M.K., Mohanty, S.K., 2022. Natural aging of expanded shale, clay, and slate (ESCS) amendment with heavy metals in stormwater increases its antibacterial properties: Implications on biofilter design. Journal of Hazardous Materials 429, 128309. https://doi.org/10.1016/j.jhazmat.2022.128309

Abstract

Aging is often expected to decrease the pathogen removal capacity of media. In contrast, the adsorption of co-contaminants such as metals during aging could have a positive impact on pathogen removal. To examine the effect of adsorbed metals on pathogen removal, biofilter media amended with expanded clay, shale, and slate (ESCS) aggregates, a lightweight aggregate, was exposed by intermittently injecting natural stormwater spiked with Cu, Pb, and Zn and then compared its removal of *Escherichia coli* (*E. coli*), a pathogen indicator, with unaged media. Metal adsorption on ESCS media decreased their net negative surface charge and alter the surface properties as confirmed by zeta potential measurement and Fourier-transform infrared spectroscopy analysis. These changes increased *E. coli* adsorption on aged media compared with unaged media and decreased overall remobilization of attached *E. coli* during intermittent infiltration of stormwater. A live-dead analysis confirmed that the adsorbed heavy metals inactivated attached *E. coli*, thereby replenishing the bacterial adsorption capacity. Overall, the results confirmed that natural aging of biofilter media with adsorbed metals could indeed have a net positive effect on *E. coli* removal in biofilters and therefore should be included in the conceptual model predicting long-term removal of pathogens from stormwater containing mixed pollutants.

6.1. Introduction

Pathogens or pathogen indicators in urban stormwater is one of the leading causes of surface water and groundwater impairment (Alam et al., 2021; Galfi et al., 2016; McBride et al., 2013). To remove these biological pollutants, stormwater treatment systems such as biofilters have been used (Bratieres et al., 2008; Li et al., 2012), where biofilter media are amended with amendments (Ghavanloughajar et al., 2021; Mohanty et al., 2014; Valenca et al., 2021b). However, their removal capacity varies widely (Ghavanloughajar et al., 2021; Valenca et al., 2021b), and the cause of the variability is often attributed to the aging of the filter media (Chandrasena et al., 2016; Li et al., 2012). Biofilter media can age because of many processes. Aging occurs when biofilter media age naturally due to exposure to stormwater constituents and conditions including drying that can alter their surface properties. Understanding how aging occurs and affects the removal of pathogens can help predict the long-term performance of biofilters during their design lifetime.

Biofilter media can age naturally due to physical, chemical, and biological processes. Physical aging occurs due to temperature fluctuation resulting in drying of media, which has been shown to decrease the overall pathogen removal capacity (Chandrasena et al., 2014b; Fowdar et al., 2021; Li et al., 2012; Nabiul Afrooz and Boehm, 2017). In contrast, another study observed an improved removal capacity of biochar-amended biofilters after aging under dry-wet cycles due to replenished attachment sites (Mohanty and Boehm, 2015). Biological aging occurs due to the growth of biofilms (Nabiul Afrooz and Boehm, 2017), which could also decrease pathogen removal (Chandrasena et al., 2014a). In contrast, another study observed improved *E. coli* removal over time due to the growth of protozoa, a natural predator of bacteria (Zhang et al., 2011). Chemical aging occurs when chemical constituents such as natural organic matter (NOM) in stormwater adsorb on media, alter their surface properties, and reduce bacterial removal

(Ghavanloughajar et al., 2021; Mohanty and Boehm, 2015). However, previous studies rarely account for other co-contaminants such as dissolved metals on the aging of biofilter media.

Metals are ubiquitous in urban stormwater (Lau et al., 2009; Stein and Tiefenthaler, 2005), and they can be attached to amendments (Tirpak et al., 2021). The amount of metal adsorbed on amendments can increase with aging, which could affect pathogen removal due to the metal toxicity (Li et al., 2016). For this reason, in some studies, copper and silver nanoparticles were added to adsorbents to improve the pathogen removal (Hrenovic et al., 2012; Li et al., 2014a; Milán et al., 2001; Tuan et al., 2011). The nanoparticle metal could increase the adsorption of pathogens into the adsorbents and inactivate the adsorbed pathogens (Kennedy et al., 2008; Li et al., 2014b; Xu et al., 2019). However, these adsorbent media have limited practical relevance due to their cost and limitation on scaling up the production (Li et al., 2014a). They could also leach metals (Li et al., 2014a), which could serve as a secondary contaminant. In contrast, exposure to heavy metal contaminated stormwater could increase the concentration of heavy metals on the media (Al-Ameri et al., 2018; Hermawan et al., 2021). The same process could contribute to the positive effect of aging on pathogen removal. However, it is not clear whether naturally adsorbed metals in biofilters can sufficiently alter the surface properties to have any effect on pathogen removal. As the biofilters are designed to last more than 15-20 years, the total exposure of metals after a few years could be sufficient to alter the surface properties of amendments. However, after installation, biofilters media are typically never monitored for their changes in surface properties, or their performance is rarely evaluated beyond the first 2 years (Tirpak et al., 2021). Laboratory studies typically examined the exhaustion in attachment capacity of amendments with aging (Li et al., 2012). Rarely, the positive effect of aging such as increased removal of the pathogen by adsorbed metal is considered.

This study aims to test the antibacterial properties to biofilter media aged with heavy metals in stormwater. We hypothesized that the aging of biofilter media with heavy metals in stormwater could improve their bacterial removal capacity. To test this hypothesis, biofilters amended with expanded shale, clay, and slate (ESCS) aggregates, a novel light-weight amendment, were aged by injecting stormwater contaminated with metals and compared their capacity to remove *E. coli* with unaged biofilters. To isolate the impact of chemical aging because of metal adsorption, other processes of aging were not simulated in this study. The results will help improve the understanding of how the aging of biofilter media with co-contaminants could affect long-term pathogen removals.

6.2. Materials and Methods

6.2.1. Stormwater Preparation

Natural stormwater was used to simulate the aging of biofilter media. Natural stormwater was collected from Ballona Creek, Los Angeles, and autoclaved before use to remove any microorganisms to accurately estimate *E. coli* removal by biofilter media. The stormwater naturally contained very low concentrations of Pb (below detection limit, 0.01 µg L^{-1}), Cu (1.8 µg L^{-1}), and Zn (8.3 µg L^{-1}) (Table 6-1**)**, which was not sufficient to simulate the long-term loading of metals within the experimental time scale. Therefore, stock solutions containing $CuCl_2$, $ZnCl_2$, and $Pb(NO_3)_2$ (Fisher Scientific) were spiked into the natural stormwater to raise the influent concentration to 500 µg L^{-1} for all metals. The concentration was an order of magnitude higher than typically found in stormwater (Tirpak et al., 2021) to simulate total metal loading in a few years in the field during the laboratory experiments that had a short duration. Based on the International Stormwater Best Management Practices (BMP) database, which aggregates data globally from different locations, these three metals were selected because they are typically found

at higher concentrations than many other metals in stormwater and they exhibit a wide range of affinity to amendments (Tirpak et al., 2021). Among other metals that are present at high concentrations are Ni and Cr. While Ni exhibits similar adsorption characteristics as Zn (Tirpak et al., 2021), Cr exists as anions as metalloids. Thus, the adsorption of metalloids can have an opposite effect on a surface charge similar to other anions such as phosphate (Appenzeller et al., 2002). However, metalloid concentrations are present at a much lower concentration than metal cations (Tirpak et al., 2021), and can be outcompeted by other negatively charged species such as phosphate (Chowdhury and Yanful, 2010). Thus, we did not test the effect of metalloids on pathogen removal in this study.

Table 6-1: Properties of the stormwater.

Properties	Stormwater
pH	8.52 ± 0.005
Electrical conductivity (μS cm^{-1})	1132.7 ± 2.05
Pb (ug L^{-1})	Below detection limit
Cu (ug L^{-1})	1.8
Zn (ug L^{-1})	8.3

To test the antibacterial effect of biofilter media with adsorbed metals, a kanamycin-resistant strain of *Escherichia coli K12*, a pathogen indicator was used (Ghavanloughajar et al., 2020; Mohanty et al., 2014). *E. coli* were grown in a Luria-Bertani broth solution to a stationary phase, extracted by centrifugation, washed twice using a phosphate buffer saline (PBS) solution to remove the broth. A small volume of stock E. coli concentrated was spiked into the natural stormwater and their concentration was measured by spread plate technique. The mean concentration of *E. coli* in influent was measured to be $2.8 \pm 0.3 \times 10^5$ CFU mL^{-1}. The

concentration is high enough to test the hypothesis and within the range found in the stormwater (Grebel et al., 2013).

6.2.2. Model biofilter design

In this study, model biofilters without vegetation were used to estimate the *E. coli* removal capacity of biofilter media without interferences from the confounding factors. Plants' effect on pathogen removal is limited, and any changes in pathogen removal in vegetated biofilters have been attributed to plants' ability to alter the hydraulic retention time (Peng et al., 2016) and moisture content in the filter media (Li et al., 2012). Nevertheless, this reductionist approach without using plants has been used in numerous previous studies to examine the mechanisms of pollutant removal in the biofilters (Hatt et al., 2008; Mohanty et al., 2014; Sun et al., 2020).

Natural biofilter media typically consist of sand or sandy soil with added amendments, if needed, up to 30% by volume (Tirpak et al., 2021). Many adsorbents such as biochar, metallic iron, and zeolite were tested to increase the metal adsorption (Tirpak et al., 2021). Here, Expanded Shale, Clay, and Slate (ESCS) aggregates (<2 mm) was used as biofilter media, which have been shown to remove a wide range of stormwater pollutants due to their lightweight and high removal capacity of many stormwater pollutants (Dordio and Carvalho, 2013; Kalhori et al., 2013; Malakootian et al., 2009; Nkansah et al., 2012). The lightweight media, which can be produced at a wide grain size distribution, has the advantage over others to be used in green roofs or other stormwater infrastructure based on both infiltration and treatment needs. ESCS can replace sand, the most common amendment used for hydraulic control because the aggregate size can be chosen based on design need. They have additional advantages over sand because of lower freight and handling costs with much higher pollutant removal capacity. Thus, they can be used in rain gardens below the root zone to allow root growth, in a filter strip near the parking lot to permit rapid

drainage of water and remove pollutants, and as filtering fills above the collection pipe in the infiltration basin. Different aggregate sizes can be used in permeable pavement. The model biofilters were designed by packing a mixture of quartz sand (ASTM 20-30, Humboldt Mfg Co.) and ESCS aggregate at a ratio of 7:3 in PVC columns (2.54 cm ID x 30 cm length). Compost or soil was not used in the mixture and plants on top to distinguish the role of ESCS pathogen adsorption or removal. First, a drainage layer was created using pea gravel up to 6 cm height with a 100 µm nylon membrane on top to prevent biofilter media to get into the drainage layer. Then, sand and ESCS mixture was added in incremental layers to a total filter media depth of 15 cm. A 2-cm layer of pea gravel was added on top to prevent the resuspension or disturbance of the media particles during the stormwater application. Total six columns were packed. Of which, three columns were aged with metals and designated as aged biofilters, whereas the other three columns were exposed to stormwater without metals and designated as unaged biofilters (Figure 6-1).

Figure 6-1: Experimental setup showing the pump (1) pumping stormwater into the columns (2), the effluents were then collected in the bottles (3).

To ensure consistent packing of all biofilters, the bulk density of the packed media was estimated by dividing the weight of the media with the inner volume of the column and comparing between biofilters (Table 6-2). The pore volume (PV) was measured by subtracting the weight of the dry media biofilters from the weight of the saturated media biofilters (Borthakur et al., 2021). The residual PV was calculated by draining the saturated biofilters under gravity and subtracting the weight of the dry media biofilters from the weight of the drained biofilters. The hydraulic conductivity of the media was measured using a falling head method (Ghavanloughajar et al., 2020).

Table 6-2: Properties of the ESCS media columns.

Properties	Control Columns	Heavy metal columns
Bulk Density (g/cm^3)	1.54 ± 0.05	1.52 ± 0.03
Porosity (%)	29.8 ± 1.3	32.1 ± 0.3
Residual pore volume (mL)	7.3 ± 1.4	9.2 ± 0.4
Hydraulic conductivity (cm/sec)	0.02 ± 0.002	0.02 ± 0.002

6.2.3. Aging of ESCS media with heavy metals

The experiments were conducted in 5 phases: conditioning, aging, flushing, leaching, and *E. coli* injection. Experiments in the first four phases were designed to age biofilters by injecting stormwater with or without metals, whereas the last phase was designed to compare the *E. coli* removal capacities of aged and unaged biofilters (Table 1). All six biofilters were first conditioned by injecting stormwater at a constant flow rate of 1 mL min^{-1} (11.8 cm h^{-1}) for 24 h to equilibrate the filter media with the stormwater until the effluent pH and ionic strength did not change (Borthakur et al., 2021). To age biofilter media with metals, 500 PV of stormwater spiked with metals was applied on the top of the biofilters at 11.8 cm h^{-1} for 10 days, and the effluent samples

were collected at the bottom to measure for heavy metal concentration. It was estimated that the aging phase exposed 7.2 mg of each heavy metal to biofilter media. This amount is equivalent to 2.1 years of aging of biofilter receiving stormwater with similar metal constituents as Ballona Creek (19.9 ± 29.0 μg L^{-1} Cu, 4.4 ± 12.7 μg L^{-1} Pb, and 83.3 ± 241.2 μg L^{-1} Zn (Stein and Tiefenthaler, 2005) from an acre of catchment area in Los Angeles with an annual rainfall of 379.2 mm yr^{-1}. It should be noted that aging in field conditions can be more complex, and the speciation of adsorbed metals and metal oxides formed during aging could vary widely based on site conditions and time passed after the adsorption (Li et al., 2019; Meng et al., 2018). Nevertheless, the experimental design tested the effect of adsorbed metal in the short term without accounting for changes that may occur in natural conditions.

After injection of metal-contaminated stormwater, the contaminated biofilters were then flushed with 50 PV of the natural stormwater without spiked metals, particularly to remove any unabsorbed heavy metals from the pore water. To estimate the leachability of the adsorbed metals, the flow was stopped for 24 h to allow time for loosely bound metal to desorb back into the pore water, and then 8 PV uncontaminated stormwater was injected to estimate the percentage of the adsorbed metals leached into pore water. To prepare the unaged biofilters or biofilters without adsorbed metals, the experiment was repeated by injecting natural stormwater without adding heavy metals into other triplicate biofilters. Effluent samples in all phases were analyzed for heavy metals by using Inductively Coupled Plasma- Optical Emission Spectroscopy (ICP-OES). The samples were centrifuged at 5000 RPM for 15 minutes to remove any particles, and the supernatant was acidified with nitric acid to lower pH below 1 before analysis.

6.2.4. Effect of aging on E. coli removal in biofilters

Aged and unaged biofilters were subjected to intermittent infiltration of stormwater contaminated with *E. coli*. Heavy metals were not added to influent when the experiments were carried out for testing of *E. coli* removal capacity of aged and unaged media because dissolved metals can inhibit or inactivate the *E. coli* in stormwater and may overestimate their removal of ESCS media. In each injection, 8 PV of stormwater with $2.8 \pm 0.3 \times 10^5$ CFU mL^{-1} of *E. coli* was applied on the top of the biofilters at 11.8 cm h^{-1} for 3.3 h, and the effluent samples were collected from the bottom at two fractions following the procedure described elsewhere (Ghavanloughajar et al., 2021). The "first flush" sample fraction consisted of the first 5-10 mL of effluent sample collected, which contained the residual water from the previous infiltration event. The second fraction consisted of the stormwater injected during the infiltration events (179.9 ± 7.6 mL). Thus, the *E. coli* concentration in the first flush indicates the fate of *E. coli* in the pore water during the antecedent drying period, whereas the concentration in the second sample presents the overall bacterial removal capacity of the biofilter during the infiltration event. After each infiltration, the biofilters were drained by gravity and left at room temperature (22 °C) for a specific drying duration until the next infiltration event. The process was repeated twice to simulate removal at a specific drying duration. To simulate the effect of varying drying duration on *E. coli* removal or potential growth or inactivation of *E. coli* in biofilters, drying durations of 1, 2, 4, and 7 days were simulated, where two injection events were carried out corresponding to each drying duration. The *E. coli* concentration in the effluent samples was measured using a spread plate technique described elsewhere (Mohanty et al., 2013).

6.2.5. Heavy metal and E. coli removal by ESCS media

To examine the binding sites on ESCS media for the adsorption of heavy metals, ESCS media with and without adsorbed metals were characterized using Fourier Transform Infrared Spectroscopy (FTIR). 0.5 g of finely grounded ESCS media (size less than 75 μm) mixed with 40 mL of synthetic stormwater spiked with 25 g L^{-1} Cu, Pb, and Zn in separate 50 mL centrifuge tubes for 48 hours. An abnormally high concentration of heavy metals was used because the heavy metals need to constitute at least 5% of the total sample volume to be detectable in the FTIR spectra. 0.5 g of finely grounded ESCS media was also exposed to 40 mL synthetic stormwater without any heavy metals as a control. The ESCS media was then dried along with Potassium Bromide (KBr, Acros Organics) for 18 hours. The ESCS powders were then mixed with KBr and pelletized using a hydraulic press at 8000-10000 psi. These pellets were then analyzed using a JASCO Model 420 FTIR instrument. To evaluate any change in surface charge of the ESCS media after heavy metal adsorption, the zeta potentials of ESCS media with and without adsorbed metals were measured at the pH (8.5) of stormwater. 0.5 g of finely ground ESCS media of size less than 45 μm were added to two sets of centrifuge tubes containing 40 mL synthetic stormwater. One set was spiked with 300 mg L^{-1} of Pb, Cu, and Zn, and both the sets were shaken in a wrist action shaker for 48 hours. The tubes were then centrifuged at 1000×g for 1 min to settle all particles larger than 1 μm. The supernatant from both the tubes was then extracted and the pH of the supernatant was adjusted to 8.5 using NaOH and HCl. The zeta potential of the supernatant was measured using a Brookhaven zetaPALS instrument. Note that only particles of size less than 1 μm were analyzed because particles of size greater than 1 μm gave erroneous results in the instrument.

E. coli can be removed by aged ESCS media through various mechanisms: adsorption to aged ESCS surface, inactivation of *E. coli* by dissolved metals leached from aged ESCS, and inactivation of *E. coli* by the adsorbed metals on aged ESCS media. To distinguish the role of each process, batch sorption studies were used. To estimate removal by ESCS media without metals, 4 g of ESCS media without metals (termed as unaged media) was mixed with 40 mL of stormwater with spiked *E. coli*, and the change in concentration in water samples was measured. To estimate the removal by aged ESCS, 4 g of ESCS was mixed in triplicated 50-mL centrifuge tubes for 48 hours using a wrist action shaker with 40 mL synthetic stormwater (10 mM NaCl) spiked with 300 mg L^{-1} of Pb, Cu, and Zn and adjusted to the same pH and electrical conductivity as the natural stormwater (Ghavanloughajar et al., 2020). This simulated exposure of 12 mg of each heavy metal to 4 g of ESCS media, which corresponded to about 20 days of heavy metal injection in the biofilter experiments. The tubes were centrifuged at 5000 RPM for 15 minutes, and the supernatants were analyzed for metal concentration to estimate the dissolved and adsorbed metal concentrations. The contaminated media settled in the tube were washed thrice with synthetic stormwater to remove heavy metals in the pore water. The washed media were designated as aged ESCS and were tested to examine their *E. coli* removal capacity by exposing them to stormwater containing *E. coli* for 7 h. In this case, *E. coli* in stormwater may be inactivated by the dissolved metals leached from the aged ESCS or inactivated by the adsorbed metals on the aged ESCS media. To distinguish the contribution of each process, the aged ESCS was mixed with 40 mL synthetic stormwater using an orbital shaker for 48 hours to leach any loosely bound metals and centrifuged at 5000 RPM for 15 minutes. The settled ESCS media contained strongly adsorbed metals that were retained after the leaching test and were exposed to *E. coli* contaminated stormwater to estimate the contribution of the strongly adsorbed metals on *E. coli* inactivation or removal. The supernatant containing the

leached metals was exposed to *E. coli* to quantify the contribution of leached metals on the inactivation of *E. coli.* Live-dead analysis was performed using fluorescence microscopy to qualitatively examine the fate of the adsorbed *E. coli* on ESCS media with and without aging with metals. After exposing *E. coli* to ESCS media with and without adsorbed metals for 7 hours, *E. coli* sorbed on both media were exposed to specific dye and observed under a fluorescence microscope to distinguish live cells from the dead cells (Mandakhalikar et al., 2018; Polasko et al., 2021). 15 mL of 0.85% NaCl was added to both tubes. The tubes were then vortexed at full speed for 1 min, sonicated at 20 kHz, and 12 V amplitude for 50 s using a probe sonicator (QSonica, Newtown, CT), and vortexed again for 1 min to extract the adsorbed E. coli. The tubes were centrifuged again at 1000×g for 10 min to settle the ESCS media and supernatant was extracted. 0.5 mL of the supernatant was mixed with 0.5 mL sterile DI water mixed with propidium iodide (PI) and SYTO 9 dyes (LIVE/DEAD BacLight Bacterial Viability Kit L13152, Invitrogen). Note that 0.85% NaCl was used to extract the E. coli instead of PBS solution as PBS solution reduces the staining efficiency of the dyes. The mixture was then allowed to equilibrate in the dark for 15 minutes. 400 µL of the mixture was then added to a 35 mm glass bottom petri dish and was observed under a Leica SP8 Confocal fluorescence microscope.

6.2.6. Data analysis

The amount of heavy metals adsorbed on the ESCS media during the injection of the stormwater spiked with metals was estimated using Eq 1-1:

$$\%\, adsorbed = \frac{\sum V_e C_e}{\sum V_i C_i} \times 100 \qquad \text{(Eq. 6-1)}$$

Where V_e and V_i are the volume of the effluent and influent samples, respectively, and C_e and C_i are the heavy metal concentration in the effluent and influent samples, respectively, during

the injection and flushing stages. The amount of heavy metals leached during the leaching phase was determined using Eq. 1-2:

$$\%\ leached = \frac{\sum V_l C_l}{\sum V_i C_i - \sum V_e C_e} \times 100 \qquad \text{(Eq. 6-2)}$$

Where V_l is the volume of the effluent sample and C_l is the heavy metal concentration in the effluent samples during the leaching phase.

6.3. Results

6.3.1. Characterization of ESCS with adsorbed metal

The results reveal how the adsorbed metals change the surface properties of ESCS media. FTIR analysis shows adsorbed metals affect the characteristics of the peak 3500 cm^{-1} (Figure 6-2a), which corresponds to the hydroxyl groups ($R - OH$) in the media (Merlic et al., 2001). The peak completely disappeared in the Pb adsorbed ESCS media, while twin peaks were observed in the Cu adsorbed ESCS sample. Adsorption of Zn also showed a sharp peak in that region. Zeta potential measurements showed that the adsorbed metals decreased the net negative surface charge of the ESCS media (Figure 6-2b). The zeta potential ESCS media without adsorbed metals at 8.5 pH was -31 ± 3.3 mV, but it decreased to -7.7 ± 2.6 mV after the exposure to 300 mg L^{-1} Cu, Pb, and Zn in the batch studies. Typically, ESCS media has a net negative surface charge similar to any other clay minerals. Adsorption of metal cations could lower the negative surface charge by neutralizing the surface charges on clay minerals (Yukselen-Aksoy and Kaya, 2011). These results confirmed that the interaction of metals on ESCS media changed their surface properties, but they did not confirm the mechanisms of metal interaction. It was assumed that the mechanism of metal adsorption on ESCS media is similar to metal adsorption mechanisms on the raw material used to produce ESCS such as clay minerals, which has been extensively studied (Altın et al., 1998; Bradl,

2004). Some other studies on ESCS also focused on ESCS adsorption (Kalhori et al., 2013; Malakootian et al., 2009). Therefore, the scope of the current study is to confirm metal adsorption so that the main hypothesis to understand the effect of adsorbed metal can be tested. The added metals (~ 7.2 mg), which is less than 0.0001% of the weight of filter media, would not change the surface area or porosity of filter media.

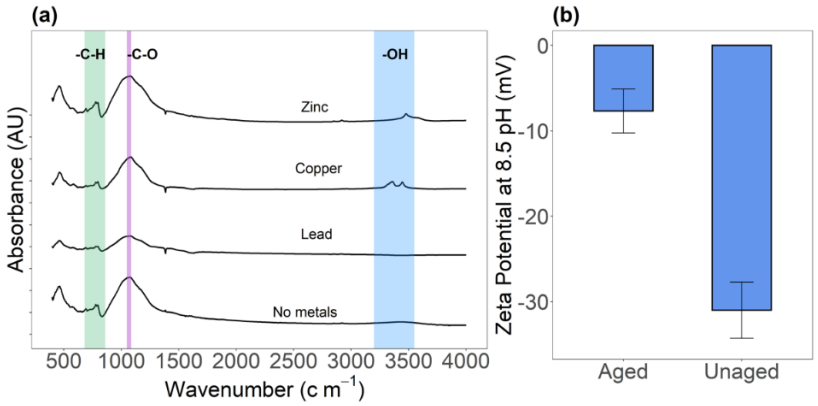

Figure 6-2: (a) FTIR analysis of unaged ESCS media (Control) and aged ESCS media with adsorbed metals. The green band refers to the wavenumber range for aromatic C-H bending, the pink band refers to the wavenumber range for C-O stretching bond of primary alcohols and the blue band refers to the wavenumber range for -OH stretch for alcohols/phenols. (b) Zeta potential of unaged ESCS (without metals) and aged ESCS media (with adsorbed metals) at a pH of 8.5 were statistically different ($p < 0.01$), where the error bars represent a standard deviation over the mean from triplicate samples.

6.3.2. ESCS has a high capacity to remove heavy metals

The goal of this study is to examine if the adsorbed metal has any effect on E. coli removal. Thus, metal adsorption is a precondition to test the hypothesis related to the aging effect on E. coli sorption. The results confirmed that the ESCS media had a high removal capacity for Pb and Zn (Figure 6-3), meaning they can be tested for their impact on E. coli removal. After injecting 500 PV of contaminated stormwater in the aging stage, the concentration of Pb and Zn remained below the detection limit ($C/C_0 = 0.1\%$), whereas the concentration of Cu in the effluent was 31.2% of the influent concentration (C_0).

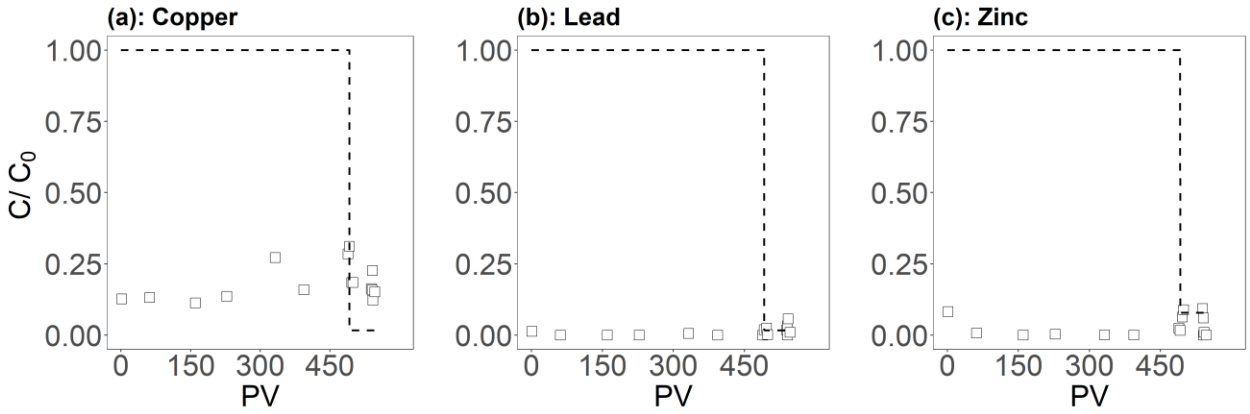

Figure 6-3: Breakthrough curves of (a) Cu, (b) Pb, and (c) Zn in the ESCS columns. The white squares denote the concentration of the respective heavy metal in the effluent samples while the dashed lines indicate the concentration of the heavy metal in the influent.

Mass balance analysis (Figure 6-4) showed biofilters adsorbed 95.5 ± 3.9 % of the injected Zn, 86.5 ± 4.4% of injected Pb, and 80.5 ± 0.3% of injected Cu. The leaching potential of the adsorbed metals was found to be minimal. During the leaching phase, only 0.17 ± 0.02 % of adsorbed Cu and 0.02 ± 0.01% of adsorbed Pb were leached. The effluent concentration of Zn was below the influent concentration in natural stormwater, which resulted in additional retention of 0.09 ± 0.005% Zn during the injection of natural stormwater without added metals. It should be noted that metal adsorption to ESCS media was tested before in the batch studies (Malakootian et al., 2009). This study confirmed that the removal is consistent with batch studies even though the hydraulic retention time in the study is an order of magnitude lower than the contact time used in previous batch studies.

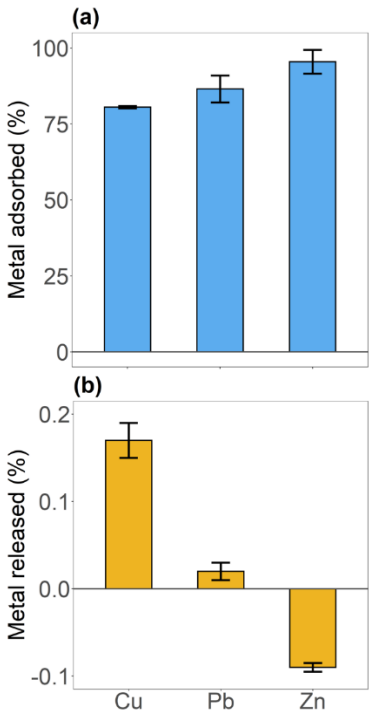

Figure 6-4: Mass balance analysis showing (a) percentage of injected metals adsorbed in biofilters after the aging and flushing stages and (b) the percentage of the adsorbed metals leached during the leaching stage. The error bars denote standard deviation over the mean values from triplicate biofilters. Negative % leaching for Zn indicates net adsorption, not leaching, because the Zn concentration in effluent was lower than the concentration in influent stormwater.

6.3.3. Aging of ESCS with heavy metals improved E. coli removal

Aged ESCS media removed more *E. coli* than unaged ECSC media (Figure 6-5). *E. coli* concentration in the second sample, which represents biofilter removal capacity during each rainfall event, increased with an increase in the drying duration in successive rainfall events, indicating that *E. coli* removal capacity of the biofilters had decreased with successive infiltration events. However, the loss in removal capacity in the unaged biofilters was higher than that of the aged biofilters.

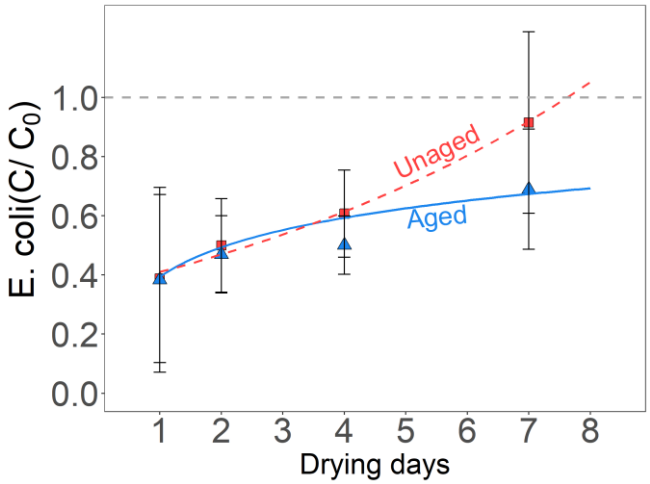

Figure 6-5: Change in mean effluent *E. coli* concentration in the effluent with an increase in drying duration for unaged biofilters and aged biofilters (with adsorbed metals). The error bars represent standard deviation over the mean value obtained from 18 samples from triplicate biofilters and duplicate experiments at a specific drying duration. The lines denote the best fits for the mean concentration in the effluents.

During infiltration events after the 4- and 7-days drying period, the effluent *E. coli* concentration in unaged biofilters without metals was significantly ($p < 0.05$) higher than the effluent concentration in aged biofilters (Figure 6-6). The effluent *E. coli* concentration in the unaged biofilters increased exponentially with the increase in drying duration ($R^2 = 0.99$): $C/Co = 0.36 \times e^{0.14 \times Drying\ days}$. However, the effluent *E. coli* concentration in aged biofilters increased logarithmically which appears to flatten out after 7 days of drying ($R^2 = 0.94$): $C/C0 = 0.14 \times \ln(Drying\ days) + 0.40$. The *E. coli* removal capacity of the aged biofilter was consistently higher than unaged biofilters, indicating faster exhaustion of unaged biofilters compared to aged biofilters.

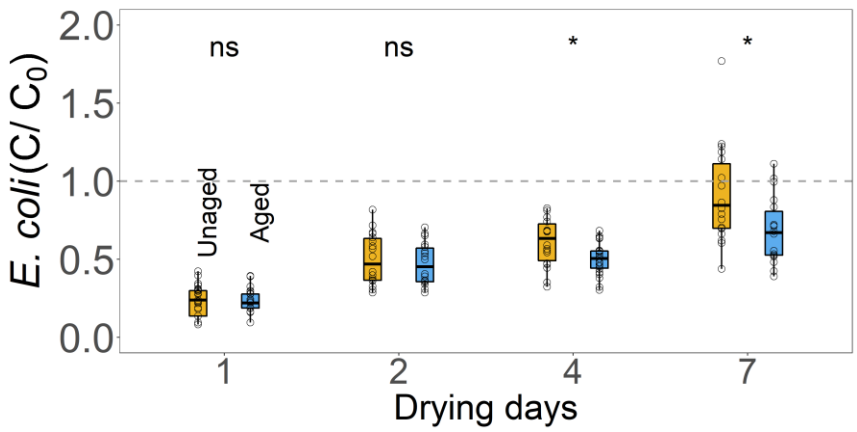

Figure 6-6: Effluent *E. coli* concentration (CFU mL^{-1}) in second samples from Unaged (No adsorbed metals) and aged biofilters (Adsorbed metals). The 'ns'notation denotes no significant difference in the *E. coli* concentration from the aged and unaged biofilters while * denotes a p value less than 0.05.

The remobilization of adsorbed *E. coli* from the biofilters during the first flush was lower in the aged biofilters than that in the unaged biofilters (Figure 6-7). The *E. coli* concentration in the first flush samples in aged biofilters decreased more rapidly than the unaged biofilters, indicating that the adsorbed metals reduced the leaching of *E. coli* from the biofilters during intermittent infiltration of stormwater.

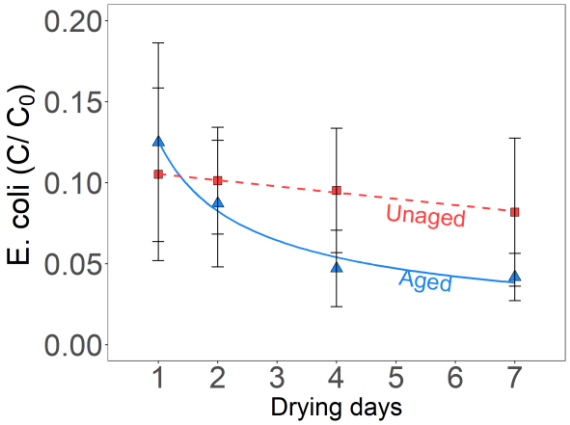

Figure 6-7: *E. coli* concentration in the first flush samples with an increase in drying duration in unaged (without adsorbed metals) and aged biofilters (with adsorbed metals). The error bars denote the standard deviation over the mean value obtained from triplicate biofilters and duplicate experiments at specific drying duration (total 18 samples per data point). The lines denote the best fits for the mean effluent concentration from biofilters.

The *E. coli* concentration in the unaged biofilters decreased linearly with the increase in drying duration (R^2 = 0.99): $C/Co = -0.0.004 \times Drying\ days + 0.109$. In contrast, the *E. coli* concentration in the aged biofilters decreased much faster by a power function (R^2 = 0.98): $C/Co = 0.125 \times (Drying\ days)^{-0.602}$. Due to this, the *E. coli* concentration in the effluent samples from the aged biofilters was significantly lower than the unaged biofilters after 4 and 7 days of drying (Figure 6-8)

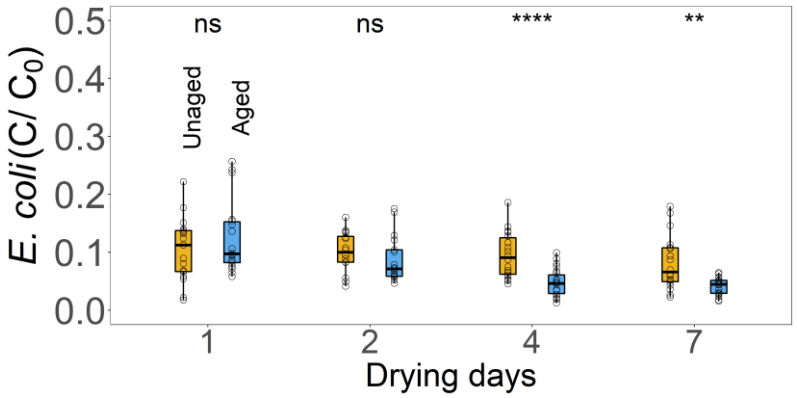

Figure 6-8: Effluent *E. coli* concentration (CFU mL^{-1}) in first flush samples from unaged (No adsorbed metals) and aged biofilters (Adsorbed metals). The 'ns'notation denotes no significant difference in the *E. coli* concentration from the aged and unaged biofilters while '**' and '****' denote a p value less than 0.01 and 0.0001.

6.3.4. Adsorbed metals, not desorbed metals, caused the inactivation of E. coli

Batch experiments validated the result of the column experiments: aged ESCS removed more *E. coli* than unaged ESCS (Figure 5). When *E. coli* was exposed to aged ESCS, all the injected *E. coli* were removed within 3 hours due to a combination of adsorption and inactivation. In contrast, *E. coli* concentration remained high in the entire 7 h of incubation study with unaged ESCS. By removing the readily leachable metals increased the time to remove all *E. coli* to 5 hours. The results from the batch experiments also revealed that removal due to leached metals was negligible compared to the removal by adsorbed metals on ESCS. Exposing the *E. coli* to the metal

concentration that was leached from the aged ESCS due to the leaching test (68 μg L^{-1} Cu, 142.8 μg L^{-1} Pb, and 61.5 μg L^{-1} Zn) did not reduce the *E. coli* concentration after 7 hours of exposure.

The batch study also confirmed that removal of *E. coli* occurred via adsorption and inactivation, and adsorbed metals, not the leached metals, increased the inactivation of *E. coli*. Fluorescence microscopy confirmed that heavy metals adsorbed to the ESCS media or aged ESCS inactivated adsorbed *E. coli* (Figure 6-9a). A high number of green fluorescent cells were observed on unaged ESCS media (Figure 6-9b), indicating that most of the adsorbed cells were alive. In contrast, a high number of red fluorescent cells was observed in samples contacted with aged ESCS media (Figure 6-9c**)**, indicating heavy metals on ESCS media increased the inactivation of the *E. coli* after adsorption.

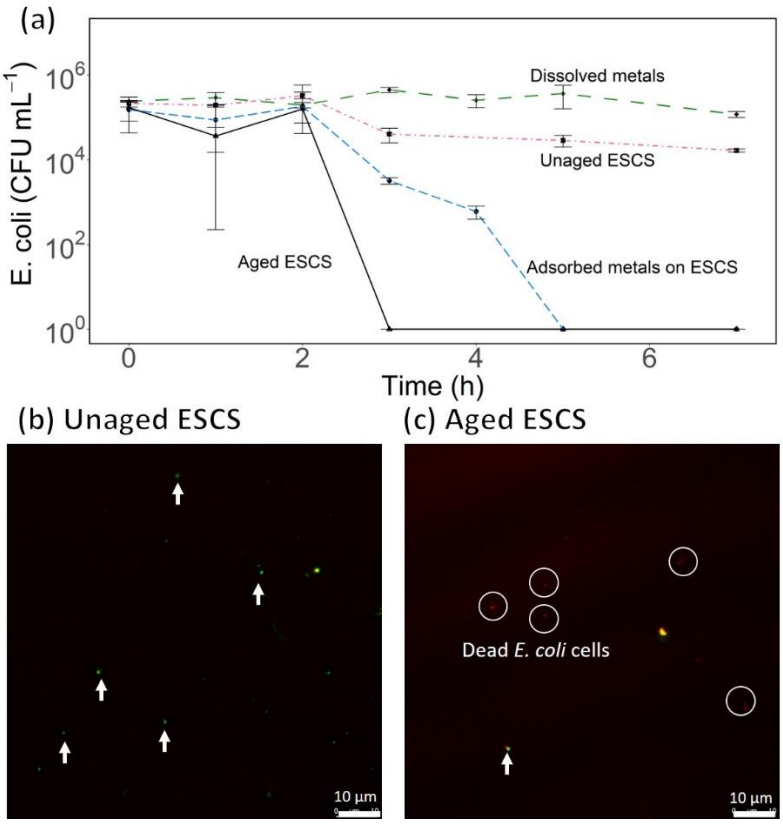

Figure 6-9: (a) Change in *E. coli* concentration batch studies after exposure to unaged ESCS (control), Dissolved metals (Metals leached from ESCS), Adsorbed metals on ESCS (ESCS with strongly adsorbed metals), and aged ESCS (ESCS media after metal adsorption). The error bars denote standard deviation over the mean value obtained from triplicate experiments. (b) Fluorescence microscopy images for *E. coli* adsorbed on unaged ESCS (no adsorbed metals). (c) Fluorescence microscopy images for *E. coli* extracted from aged ESCS (adsorbed metals). The white arrows point toward the green live cells whereas white circles enclose the red dead cells.

6.4. Discussion

6.4.1. Reasons for high metal adsorption capacity of ESCS

Heavy metals are typically found in high concentrations in urban stormwater, where their removal can be challenging, particularly when hydraulic retention time (HRT) in biofilters is low. Results in the study showed that ESCS aggregates could adsorb significant amounts of heavy metals without leaching them later. Despite the short HRT of 5-10 mins used in this study, concentrations of each metal in the effluent samples were very low, indicating the ESCS aggregates can quickly sorb heavy metals (Figure 6-2). The result is similar to a previous study on copper-coated zeolite media, which also removed significant amounts of *E. coli* with a contact time of 4.5 minutes (Li et al., 2014a). However, copper-coated zeolite is cost-prohibitive to apply on a large scale. The average HRT in field-scale biofilters can range between 20 min to as high as 13 days (Hatt et al., 2009; Zhang et al., 2021a). Since an increase in HRT can increase the removal of pollutants from stormwater (Fang et al., 2021; Zhang et al., 2021b), the metal removal capacity of the ESCS amended biofilters could be much higher in the field setting with longer HRT used in this study. Compared to other amendments such as peat, compost, fly ash, or zeolite, ESCS exhibited a comparable or higher metal removal capacity (Lim et al., 2015; Tirpak et al., 2021). Thus, studies should adopt ESCS as an alternative amendment for biofilters to remove metals from stormwater.

Although two studies tested ESCS media for stormwater treatment, they did not examine the adsorption mechanisms of heavy metals (Malakootian et al., 2009; Shojaeimehr et al., 2014). The quick removal of metals by ESCS was attributed to the strong affinity of metal to specific sites and the porous structure of the ESCS media (Kalhori et al., 2013). Based on FTIR analysis, the heavy metals primarily sorb to the ESCS media by interacting with the hydroxyl ($R-OH$) groups

on ESCS (Figure 6-2a), where the oxygen atom could act as a strong Lewis base and form complexes with the metal ions (Lim and Lee, 2015). Since the oxygen atom (O^{2-}) in the hydroxyl group is negatively charged, the adsorption of positively charged heavy metals could reduce the negative surface charge on the ESCS media. The zeta potential measurement of the ESCS media after heavy metal adsorption confirmed a net decrease in the negative surface charge of ESCS media (Figure 6-2b). Overall, these results indicate that metals bind strongly on specific sites on ESCS media, which limits the leaching of metals into clean stormwater, and the adsorbed metals reverse the net negative surface charge, which increases the removal of *E. coli*.

6.4.2. Antibacterial effect of adsorbed heavy metals in biofilters

Pathogen removal in stormwater biofilters is typically challenging because of the possibility of growth of previously removed pathogens and their release during intermittent flow (Mohanty et al., 2014, 2013). Amendments such as biochar or iron filings could improve removal, but the exhaustion of adsorption sites on those media because of bacterial growth limits their utility in long term, indicating aging of these media could lower pathogen removal (Chandrasena et al., 2014a; Valenca et al., 2021b). Using ESCS aggregate, it is shown that aging with metal-contaminated stormwater benefited bacterial removal. It was demonstrated that the aged biofilters were able to maintain their *E. coli* removal capacity when the unaged biofilters exhausted quickly. The results were attributed to the inactivation of adsorbed *E. coli* in aged biofilters. The ability of the heavy metals to limit *E. coli* growth or enhance inactivation increased with an increase in exposure time during the drying period between rainfall events. This result indicates that the growth of attached *E. coli* in between rainfall events is limited, and most adsorbed *E. coli* could be eventually inactivated during a long period between the rainfall events. Although the negative effect of aging is often highlighted in the literature (Valenca et al., 2021a), the positive effect of

aging, particularly due to adsorption of metals, on pathogen removal has not been demonstrated before. We expect that other amendments that have high adsorption capacity as ESCS should also exhibit the positive effect of adsorbed metals on the pathogen removal (Tirpak et al., 2021) as long as the adsorbed metal is sufficiently high to alter surface charge and interaction with bacteria. Future studies should confirm the finding in field studies or other amendments. We used zeta potential measurement to prove the changes in surface charge with aging, FTIR analysis to confirm possible changes in surface properties of clay minerals after metal adsorption, and live-dead analysis to confirm the inactivation of bacteria. Thus, media aged in field conditions should be measured for these changes in surface properties to confirm the finding and relevance in the actual field setting.

The remobilization of attached pathogens during intermittent infiltration of stormwater is a concern (Chandrasena et al., 2012; Li et al., 2012; Mohanty et al., 2013) because it would make the biofilter a source of pathogens. The results show that the adsorption of heavy metal on ESCS media also reduced the remobilization of adsorbed *E. coli* during intermittent infiltration of stormwater. Although unaged biofilters reduced the *E. coli* remobilization as well, the aged biofilters reduced the mobilization to a greater extent. This reduction in the remobilization of *E. coli* increased with exposure time drying periods between the rainfalls. An increase in exposure time during drying did not improve the first flush leaching of *E. coli* in other studies with biochar (Valenca et al., 2021b) and iron filings (Ghavanloughajar et al., 2021), but those studies did not use amendments aged with heavy metals. Most media are inert to pathogens, where pathogens are adsorbed on the surface without resulting in an inactivation (Peng et al., 2016; Tirpak et al., 2021). To facilitate inactivation, silver or copper nanoparticles or other metals were mixed with media (Li et al., 2016, 2014a, 2014b; Matsumura et al., 2003; Zeng et al., 2015), but these media are cost-

prohibitive for large scale applications and thus have low practical significance. In contrast, ESCS media, which is produced at an industrial scale, can develop antibacterial coating by adsorbing metals naturally present in stormwater. Thus, with an increase in the age of biofilters, the ESCS media can become better at removing pathogens due to an increase in the concentration of metals on the media surface.

6.4.3. E. coli removal processes on metal-coated ESCS media

Metals in the biofilter media could mainly remove *E. coli* by two processes: inactivation and adsorption (Hrenovic et al., 2012; Li et al., 2014a; Nan et al., 2008). First, media could leach heavy metal into pore water, which could inactivate *E. coli* due to metal toxicity. Second, media could adsorb *E. coli* and inactivate them due to interaction with the adsorbed metals (Nan et al., 2008). Batch experiments showed that leached heavy metals did not remove *E. coli* from the stormwater (Figure 6-9), indicating the contribution of leached metals on *E. coli* removal in the biofilters was negligible. In contrast, adsorbed *E. coli* were inactivated as confirmed by live-dead analysis in the study (Figure 6-9c). The heavy metals could inactivate *E. coli* by damaging the cell walls and accumulating in the *E. coli* cells (Raffi et al., 2010; Siddiqi et al., 2018; Tian et al., 2012). Overall, the results confirmed that the inactivation of *E. coli* was caused by adsorbed metals, not the leached metals from the contaminated ESCS. It should be noted that this study compared inactivation processes by adsorbed and dissolved metals, which can be present in biofilters pre-contaminated with metals. The study did not confirm the mechanism of adsorption or inactivation by the metals. Future studies should examine the mechanism by probing the oxidative stress (Engel et al., 2018; Yang et al., 2021), and observing the changes in the cell wall characteristics (Glasauer et al., 2001).

These results have practical significance in the performance lifetime of biofilters. Biofilters are constructed with a service life of at least 20 years. However, the media could become exhausted long before the design lifetime (Blecken et al., 2009; Mohanty and Boehm, 2015; Okaikue-Woodi et al., 2020; Zhang et al., 2014), particularly for bacterial pollutants due to their growth between rainfall events (Chandrasena et al., 2014a, 2012). For the same reason, unaged ESCS in the study became exhausted and lost the bacterial removal capacity after a few rainfall events. The exhaustion rate was much slower in aged ESCS with adsorbed metals, even with increasing in drying duration. Thus, the aging of ESCS could help the performance life of the biofilters amended with ESCS. However, the experiment should be repeated in the field settings to include additional complexities such as competitive adsorption by organic matter, nutrients, or ions (Charbonnet et al., 2020; Mohanty and Boehm, 2015; Okaikue-Woodi et al., 2020).

6.5. Conclusions

The study shows that aging with co-contaminants such as heavy metals, which occur naturally, could have a net positive effect on the long-term removal of *E. coli* in biofilters. Results of batch experiments and column studies reveal that biofilters amended with ESCS aggregates could adsorb significant amounts of metals such as Pb, Cu, and Zn from stormwater and decrease net negative surface charge on ESCS media, and these changes increased *E. coli* removal. Spectroscopic analysis and surface charge measurement confirmed that ESCS media irreversibly bind heavy metals from contaminated stormwater and their surface charge becomes less negative, thereby attracting more *E. coli* from stormwater. The metal coating developed with aging could help maintain the long-term *E. coli* removal capacity of the biofilter by inactivating *E. coli* or limiting their growth. The adsorbed metal could either increase adsorption or inactivation. The live-dead analysis confirmed that the adsorbed metals inactivated *E. coli* by damaging the cell

walls. Any metals that could be leached from the metal-contaminated ESCS were found to be insufficient to inactivate *E. coli*. This enhanced adsorption and inactivation of *E. coli* cells enabled the aged ESCS media to exhaust at a much slower rate than the unaged ESCS media. Thus, filter media aging with metals should be considered in predicting the long-term pathogen removal in biofilters.

6.6. Acknowledgments

We acknowledge the support of Expanded Shale, Clay, and Slate Institute (ESCSI) for providing the ESCS media. We thank Dr. Matthew J. Schibler, Ph.D. in Advanced Light Microscopy and Spectroscopy Laboratory in the California NanoSystems Institute at UCLA for his help and guidance in performing the fluorescence microscopy of the samples. The work is partially supported by the California Department of Transportation (Caltrans). The views expressed in this document are solely those of the authors and do not necessarily reflect those of the agency. Caltrans does not endorse any products mentioned in this publication.

6.7. References

Alam, S., Borthakur, A., Ravi, S., Gebremichael, M., Mohanty, S.K., 2021. Managed aquifer recharge implementation criteria to achieve water sustainability. Science of The Total Environment 768, 144992. https://doi.org/10.1016/j.scitotenv.2021.144992

Al-Ameri, M., Hatt, B., Le Coustumer, S., Fletcher, T., Payne, E., Deletic, A., 2018. Accumulation of heavy metals in stormwater bioretention media: A field study of temporal and spatial variation. Journal of Hydrology 567, 721–731. https://doi.org/10.1016/j.jhydrol.2018.03.027

Altın, O., Özbelge, H.Ö., Doğu, T., 1998. Use of General Purpose Adsorption Isotherms for Heavy Metal–Clay Mineral Interactions. Journal of Colloid and Interface Science 198, 130–140. https://doi.org/10.1006/jcis.1997.5246

Appenzeller, B.M.R., Duval, Y.B., Thomas, F., Block, J.-C., 2002. Influence of Phosphate on Bacterial Adhesion onto Iron Oxyhydroxide in Drinking Water. Environ. Sci. Technol. 36, 646–652. https://doi.org/10.1021/es010155m

Blecken, G.-T., Zinger, Y., Deletić, A., Fletcher, T.D., Viklander, M., 2009. Influence of intermittent wetting and drying conditions on heavy metal removal by stormwater biofilters. Water Research 43, 4590–4598. https://doi.org/10.1016/j.watres.2009.07.008

Borthakur, A., Cranmer, B.K., Dooley, G.P., Blotevogel, J., Mahendra, S., Mohanty, S.K., 2021. Release of soil colloids during flow interruption increases the pore-water PFAS concentration in saturated soil. Environmental Pollution 117297. https://doi.org/10.1016/j.envpol.2021.117297

Bradl, H.B., 2004. Adsorption of heavy metal ions on soils and soils constituents. Journal of Colloid and Interface Science 277, 1–18. https://doi.org/10.1016/j.jcis.2004.04.005

Bratieres, K., Fletcher, T.D., Deletic, A., Alcazar, L., Le Coustumer, S., McCarthy, D.T., 2008. Removal of nutrients, heavy metals and pathogens by stormwater biofilters, in: 11th International Conference on Urban Drainage.

Chandrasena, G.I., Deletic, A., Ellerton, J., McCarthy, D.T., 2012. Evaluating Escherichia coli removal performance in stormwater biofilters: a laboratory-scale study. Water Science and Technology 66, 1132–1138. https://doi.org/10.2166/wst.2012.283

Chandrasena, G.I., Deletic, A., McCarthy, D.T., 2016. Biofiltration for stormwater harvesting: Comparison of Campylobacter spp. and Escherichia coli removal under normal and challenging operational conditions. Journal of Hydrology 537, 248–259. https://doi.org/10.1016/j.jhydrol.2016.03.044

Chandrasena, G.I., Deletic, A., McCarthy, D.T., 2014a. Survival of Escherichia coli in stormwater biofilters. Environ Sci Pollut Res 21, 5391–5401. https://doi.org/10.1007/s11356-013-2430-2

Chandrasena, G.I., Pham, T., Payne, E.G., Deletic, A., McCarthy, D.T., 2014b. E. coli removal in laboratory scale stormwater biofilters: Influence of vegetation and submerged zone. Journal of Hydrology 519, 814–822. https://doi.org/10.1016/j.jhydrol.2014.08.015

Chowdhury, S.R., Yanful, E.K., 2010. Arsenic and chromium removal by mixed magnetite–maghemite nanoparticles and the effect of phosphate on removal. Journal of environmental management, 91(11), 2238-2247.

Charbonnet, J.A., Duan, Y., Sedlak, D.L., 2020. The use of manganese oxide-coated sand for the removal of trace metal ions from stormwater. Environ. Sci.: Water Res. Technol. 6, 593–603. https://doi.org/10.1039/C9EW00781D

Dordio, A., Carvalho, A.J.P., 2013. Constructed wetlands with light expanded clay aggregates for agricultural wastewater treatment. Science of The Total Environment 463–464, 454–461. https://doi.org/10.1016/j.scitotenv.2013.06.052

Engel, M., Hadar, Y., Belkin, S., Lu, X., Elimelech, M., Chefetz, B., 2018. Bacterial inactivation by a carbon nanotube–iron oxide nanocomposite: a mechanistic study using E. coli mutants. Environ. Sci.: Nano 5, 372–380. https://doi.org/10.1039/C7EN00865A

Fang, H., Jamali, B., Deletic, A., Zhang, K., 2021. Machine learning approaches for predicting the performance of stormwater biofilters in heavy metal removal and risk mitigation. Water Research 200, 117273. https://doi.org/10.1016/j.watres.2021.117273

Fowdar, H., Payne, E., Schang, C., Zhang, K., Deletic, A., McCarthy, D., 2021. How well do stormwater green infrastructure respond to changing climatic conditions? Journal of Hydrology 603, 126887. https://doi.org/10.1016/j.jhydrol.2021.126887

Galfi, H., Österlund, H., Marsalek, J., Viklander, M., 2016. Indicator bacteria and associated water quality constituents in stormwater and snowmelt from four urban catchments. Journal of Hydrology 539, 125–140. https://doi.org/10.1016/j.jhydrol.2016.05.006

Ghavanloughajar, M., Borthakur, A., Valenca, R., McAdam, M., Khor, C.M., Dittrich, T.M., Stenstrom, M.K., Mohanty, S.K., 2021. Iron amendments minimize the first-flush release of pathogens from stormwater biofilters. Environmental Pollution 281, 116989. https://doi.org/10.1016/j.envpol.2021.116989

Ghavanloughajar, M., Valenca, R., Le, H., Rahman, M., Borthakur, A., Ravi, S., Stenstrom, M.K., Mohanty, S.K., 2020. Compaction conditions affect the capacity of biochar-amended sand filters to treat road runoff. Science of The Total Environment 735, 139180. https://doi.org/10.1016/j.scitotenv.2020.139180

Glasauer, S., Langley, S., Beveridge, T.J., 2001. Sorption of Fe (Hydr)Oxides to the Surface of Shewanella putrefaciens: Cell-Bound Fine-Grained Minerals Are Not Always Formed De Novo. Applied and Environmental Microbiology. https://doi.org/10.1128/AEM.67.12.5544-5550.2001

Grebel, J.E., Mohanty, S.K., Torkelson, A.A., Boehm, A.B., Higgins, C.P., Maxwell, R.M., Nelson, K.L., Sedlak, D.L., 2013. Engineered Infiltration Systems for Urban Stormwater Reclamation. Environmental Engineering Science 30, 437–454. https://doi.org/10.1089/ees.2012.0312

Hatt, B.E., Fletcher, T.D., Deletic, A., 2009. Hydrologic and pollutant removal performance of stormwater biofiltration systems at the field scale. Journal of Hydrology 365, 310–321. https://doi.org/10.1016/j.jhydrol.2008.12.001

Hatt, B.E., Fletcher, T.D., Deletic, A., 2008. Hydraulic and Pollutant Removal Performance of Fine Media Stormwater Filtration Systems. Environ. Sci. Technol. 42, 2535–2541. https://doi.org/10.1021/es071264p

Hermawan, A.A., Teh, K.L., Talei, A., Chua, L.H.C., 2021. Accumulation of heavy metals in stormwater biofiltration systems augmented with zeolite and fly ash. Journal of Environmental Management 297, 113298. https://doi.org/10.1016/j.jenvman.2021.113298

Hrenovic, J., Milenkovic, J., Ivankovic, T., Rajic, N., 2012. Antibacterial activity of heavy metal-loaded natural zeolite. Journal of Hazardous Materials 201–202, 260–264. https://doi.org/10.1016/j.jhazmat.2011.11.079

Kalhori, E.M., Yetilmezsoy, K., Uygur, N., Zarrabi, M., Shmeis, R.M.A., 2013. Modeling of adsorption of toxic chromium on natural and surface modified lightweight expanded clay aggregate (LECA). Applied Surface Science 287, 428–442. https://doi.org/10.1016/j.apsusc.2013.09.175

Kennedy, L.J., Kumar, A.G., Ravindran, B., Sekaran, G., 2008. Copper impregnated mesoporous activated carbon as a high efficient catalyst for the complete destruction of pathogens in water. Environmental Progress 27, 40–50. https://doi.org/10.1002/ep.10241

Lau, S.-L., Han, Y., Kang, J.-H., Kayhanian, M., Stenstrom, M.K., 2009. Characteristics of Highway Stormwater Runoff in Los Angeles: Metals and Polycyclic Aromatic Hydrocarbons. Water Environment Research 81, 308–318. https://doi.org/10.2175/106143008X357237

Li, R., Tan, W., Wang, G., Zhao, X., Dang, Q., Yu, H., Xi, B., 2019. Nitrogen addition promotes the transformation of heavy metal speciation from bioavailable to organic bound by increasing the turnover time of organic matter: An analysis on soil aggregate level. Environmental Pollution 255, 113170. https://doi.org/10.1016/j.envpol.2019.113170

Li, Y., McCarthy, D.T., Deletic, A., 2016. Escherichia coli removal in copper-zeolite-integrated stormwater biofilters: Effect of vegetation, operational time, intermittent drying weather. Ecological Engineering 90, 234–243. https://doi.org/10.1016/j.ecoleng.2016.01.066

Li, Y.L., Deletic, A., Alcazar, L., Bratieres, K., Fletcher, T.D., McCarthy, D.T., 2012. Removal of Clostridium perfringens, Escherichia coli and F-RNA coliphages by stormwater biofilters. Ecological Engineering 49, 137–145. https://doi.org/10.1016/j.ecoleng.2012.08.007

Li, Y.L., Deletic, A., McCarthy, D.T., 2014a. Removal of E. coli from urban stormwater using antimicrobial-modified filter media. Journal of Hazardous Materials 271, 73–81. https://doi.org/10.1016/j.jhazmat.2014.01.057

Li, Y.L., McCarthy, D.T., Deletic, A., 2014b. Stable copper-zeolite filter media for bacteria removal in stormwater. Journal of Hazardous Materials 273, 222–230. https://doi.org/10.1016/j.jhazmat.2014.03.036

Lim, H.S., Lim, W., Hu, J.Y., Ziegler, A., Ong, S.L., 2015. Comparison of filter media materials for heavy metal removal from urban stormwater runoff using biofiltration systems. Journal of Environmental Management 147, 24–33. https://doi.org/10.1016/j.jenvman.2014.04.042

Lim, S.-F., Lee, A.Y.W., 2015. Kinetic study on removal of heavy metal ions from aqueous solution by using soil. Environ Sci Pollut Res 22, 10144–10158. https://doi.org/10.1007/s11356-015-4203-6

Malakootian, M., Nouri, J., Hossaini, H., 2009. Removal of heavy metals from paint industry's wastewater using Leca as an available adsorbent. Int. J. Environ. Sci. Technol. 6, 183–190. https://doi.org/10.1007/BF03327620

Mandakhalikar, K.D., Rahmat, J.N., Chiong, E., Neoh, K.G., Shen, L., Tambyah, P.A., 2018. Extraction and quantification of biofilm bacteria: Method optimized for urinary catheters. Sci Rep 8, 8069. https://doi.org/10.1038/s41598-018-26342-3

Matsumura, Y., Yoshikata, K., Kunisaki, S., Tsuchido, T., 2003. Mode of Bactericidal Action of Silver Zeolite and Its Comparison with That of Silver Nitrate. Applied and Environmental Microbiology 69, 4278–4281. https://doi.org/10.1128/AEM.69.7.4278-4281.2003

McBride, G.B., Stott, R., Miller, W., Bambic, D., Wuertz, S., 2013. Discharge-based QMRA for estimation of public health risks from exposure to stormwater-borne pathogens in recreational waters in the United States. Water Research 47, 5282–5297. https://doi.org/10.1016/j.watres.2013.06.001

Meng, J., Tao, M., Wang, L., Liu, X., Xu, J., 2018. Changes in heavy metal bioavailability and speciation from a Pb-Zn mining soil amended with biochars from co-pyrolysis of rice straw and swine manure. Science of The Total Environment 633, 300–307. https://doi.org/10.1016/j.scitotenv.2018.03.199

Merlic, C.A., Fam, B.C., Miller, M.M., 2001. WebSpectra: Online NMR and IR Spectra for Students. J. Chem. Educ. 78, 118. https://doi.org/10.1021/ed078p118

Milán, Z., de Las Pozas, C., Cruz, M., Borja, R., Sánchez, E., Ilangovan, K., Espinosa, Y., Luna, B., 2001. The Removal of Bacteria by Modified Natural Zeolites. Journal of Environmental Science and Health, Part A 36, 1073–1087. https://doi.org/10.1081/ESE-100104132

Mohanty, S.K., Boehm, A.B., 2015. Effect of weathering on mobilization of biochar particles and bacterial removal in a stormwater biofilter. Water Research 85, 208–215. https://doi.org/10.1016/j.watres.2015.08.026

Mohanty, S.K., Cantrell, K.B., Nelson, K.L., Boehm, A.B., 2014. Efficacy of biochar to remove Escherichia coli from stormwater under steady and intermittent flow. Water Research 61, 288–296. https://doi.org/10.1016/j.watres.2014.05.026

Mohanty, S.K., Torkelson, A.A., Dodd, H., Nelson, K.L., Boehm, A.B., 2013. Engineering Solutions to Improve the Removal of Fecal Indicator Bacteria by Bioinfiltration Systems during Intermittent Flow of Stormwater. Environ. Sci. Technol. 47, 10791–10798. https://doi.org/10.1021/es305136b

Nabiul Afrooz, A.R.M., Boehm, A.B., 2017. Effects of submerged zone, media aging, and antecedent dry period on the performance of biochar-amended biofilters in removing fecal indicators and nutrients from natural stormwater. Ecological Engineering 102, 320–330. https://doi.org/10.1016/j.ecoleng.2017.02.053

Nan, L., Liu, Y., Lü, M., Yang, K., 2008. Study on antibacterial mechanism of copper-bearing austenitic antibacterial stainless steel by atomic force microscopy. J Mater Sci: Mater Med 19, 3057–3062. https://doi.org/10.1007/s10856-008-3444-z

Nkansah, M.A., Christy, A.A., Barth, T., Francis, G.W., 2012. The use of lightweight expanded clay aggregate (LECA) as sorbent for PAHs removal from water. Journal of Hazardous Materials 217–218, 360–365. https://doi.org/10.1016/j.jhazmat.2012.03.038

Okaikue-Woodi, F.E.K., Cherukumilli, K., Ray, J.R., 2020. A critical review of contaminant removal by conventional and emerging media for urban stormwater treatment in the United States. Water Research 187, 116434. https://doi.org/10.1016/j.watres.2020.116434

Peng, J., Cao, Y., Rippy, M.A., Afrooz, A.R.M.N., Grant, S.B., 2016. Indicator and Pathogen Removal by Low Impact Development Best Management Practices. Water 8, 600. https://doi.org/10.3390/w8120600

Polasko, A.L., Ramos, P., Kaner, R.B., Mahendra, S., 2021. A multipronged approach for systematic in vitro quantification of catheter-associated biofilms. Journal of Hazardous Materials Letters 2, 100032. https://doi.org/10.1016/j.hazl.2021.100032

Raffi, M., Mehrwan, S., Bhatti, T.M., Akhter, J.I., Hameed, A., Yawar, W., ul Hasan, M.M., 2010. Investigations into the antibacterial behavior of copper nanoparticles against Escherichia coli. Ann Microbiol 60, 75–80. https://doi.org/10.1007/s13213-010-0015-6

Shojaeimehr, T., Rahimpour, F., Khadivi, M.A., Sadeghi, M., 2014. A modeling study by response surface methodology (RSM) and artificial neural network (ANN) on Cu2+ adsorption optimization using light expended clay aggregate (LECA). Journal of Industrial and Engineering Chemistry 20, 870–880. https://doi.org/10.1016/j.jiec.2013.06.017

Siddiqi, K.S., ur Rahman, A., Tajuddin, Husen, A., 2018. Properties of Zinc Oxide Nanoparticles and Their Activity Against Microbes. Nanoscale Research Letters 13, 141. https://doi.org/10.1186/s11671-018-2532-3

Stein, E.D., Tiefenthaler, L.L., 2005. Dry-Weather Metals and Bacteria Loading in an Arid, Urban Watershed: Ballona Creek, California. Water Air Soil Pollut 164, 367–382. https://doi.org/10.1007/s11270-005-4041-0

Sun, Y., Chen, S.S., Lau, A.Y.T., Tsang, D.C.W., Mohanty, S.K., Bhatnagar, A., Rinklebe, J., Lin, K.-Y.A., Ok, Y.S., 2020. Waste-derived compost and biochar amendments for stormwater treatment in bioretention column: Co-transport of metals and colloids. Journal of Hazardous Materials 383, 121243. https://doi.org/10.1016/j.jhazmat.2019.121243

Tian, W.-X., Yu, S., Ibrahim, M., Almonaofy, A.W., He, L., Hui, Q., Bo, Z., Li, B., Xie, G., 2012. Copper as an antimicrobial agent against opportunistic pathogenic and multidrug resistant Enterobacter bacteria. J Microbiol. 50, 586–593. https://doi.org/10.1007/s12275-012-2067-8

Tirpak, R.A., Afrooz, A.N., Winston, R.J., Valenca, R., Schiff, K., Mohanty, S.K., 2021. Conventional and amended bioretention soil media for targeted pollutant treatment: A critical review to guide the state of the practice. Water Research 189, 116648. https://doi.org/10.1016/j.watres.2020.116648

Tuan, T.Q., Son, N.V., Dung, H.T.K., Luong, N.H., Thuy, B.T., Anh, N.T.V., Hoa, N.D., Hai, N.H., 2011. Preparation and properties of silver nanoparticles loaded in activated carbon for biological and environmental applications. Journal of Hazardous Materials 192, 1321–1329. https://doi.org/10.1016/j.jhazmat.2011.06.044

Valenca, R., Borthakur, A., Le, H., Mohanty, S.K., 2021a. Chapter Seven - Biochar role in improving pathogens removal capacity of stormwater biofilters, in: Sarmah, A.K. (Ed.), Advances in Chemical Pollution, Environmental Management and Protection, Biochar: Fundamentals and Applications in Environmental Science and Remediation Technologies. Elsevier, pp. 175–201. https://doi.org/10.1016/bs.apmp.2021.08.007

Valenca, R., Borthakur, A., Zu, Y., Matthiesen, E.A., Stenstrom, M.K., Mohanty, S.K., 2021b. Biochar Selection for *Escherichia coli* Removal in Stormwater Biofilters. Journal of Environmental Engineering 147, 06020005. https://doi.org/10.1061/(ASCE)EE.1943-7870.0001843

Xu, D., Shi, X., Lee, L.Y., Lyu, Z., Ong, S.L., Hu, J., 2019. Role of metal modified water treatment residual on removal of Escherichia coli from stormwater runoff. Science of The Total Environment 678, 594–602. https://doi.org/10.1016/j.scitotenv.2019.04.207

Yang, S., Qu, C., Mukherjee, M., Wu, Y., Huang, Q., Cai, P., 2021. Soil phyllosilicate and iron oxide inhibit the quorum sensing of Chromobacterium violaceum. Soil Ecol. Lett. 3, 22–31. https://doi.org/10.1007/s42832-020-0051-5

Yukselen-Aksoy, Y., Kaya, A., 2011. A study of factors affecting on the zeta potential of kaolinite and quartz powder. Environ Earth Sci 62, 697–705. https://doi.org/10.1007/s12665-010-0556-9

Zeng, X., McCarthy, D.T., Deletic, A., Zhang, X., 2015. Silver/Reduced Graphene Oxide Hydrogel as Novel Bactericidal Filter for Point-of-Use Water Disinfection. Advanced Functional Materials 25, 4344–4351. https://doi.org/10.1002/adfm.201501454

Zhang, K., Barron, N.J., Zinger, Y., Hatt, B., Prodanovic, V., Deletic, A., 2021a. Pollutant removal performance of field scale dual-mode biofilters for stormwater, greywater, and groundwater treatment. Ecological Engineering 163, 106192. https://doi.org/10.1016/j.ecoleng.2021.106192

Zhang, K., Liu, Y., Deletic, A., McCarthy, D.T., Hatt, B.E., Payne, E.G.I., Chandrasena, G., Li, Y., Pham, T., Jamali, B., Daly, E., Fletcher, T.D., Lintern, A., 2021b. The impact of stormwater biofilter design and operational variables on nutrient removal - a statistical modelling approach. Water Research 188, 116486. https://doi.org/10.1016/j.watres.2020.116486

Zhang, K., Randelovic, A., Page, D., McCarthy, D.T., Deletic, A., 2014. The validation of stormwater biofilters for micropollutant removal using in situ challenge tests. Ecological Engineering 67, 1–10. https://doi.org/10.1016/j.ecoleng.2014.03.004

Zhang, L., Seagren, E.A., Davis, A.P., Karns, J.S., 2011. Long-Term Sustainability of *Escherichia Coli* Removal in Conventional Bioretention Media. Journal of Environmental Engineering 137, 669–677. https://doi.org/10.1061/(ASCE)EE.1943-7870.0000365

7. CHAPTER 7: CONCLUSIONS AND RECOMMENDATIONS

7.1. Conclusions

Colloids as a potential carrier of PFAS in surface water, subsurface soil, and air: An analysis of data from 43 studies reveals a significant role of suspended particles on the transport of PFAAs in surface waters and subsurface soils. Suspended particles in surface waters often contain 1-3 orders of magnitude higher PFAA concentration than bed sediments, indicating the source of suspended parties in surface water may not be the sediments but eroded particles from source zones upstream. The subsurface soil depth corresponding to the concentration maxima decreases rapidly with increases in soil organic carbon content. Thus, organic-rich suspended sediment could facilitate the transport of PFAAs. Surprisingly, the depth corresponding to the concentration maxima is lower in areas receiving higher rainfall intensity. Collectively, the results indicate that suspended particles, which are often ignored in previous assessment studies, can be a significant pathway for the transport of PFAAs in the environment. Analysis of data from 8 studies that measured the PFAS concentration in dust samples from indoor environments shows that a significant fraction of total PFAS measured in the air are associated with dust, aerosol, and other particulate matters, and the long-chained PFAS are enriched in the dust. The analysis also reveals that an increase in PFAS chain length increases their association with dust.

Flow fluctuations release colloids and associated PFAS into groundwater: Particles released during flow interruption could significantly increase PFAS concentration in the pore water. Following flow interruption, the increases in PFOA concentrations were higher than that of PFBA, potentially due to higher affinity via the long carbon chain of PFOA than PFBA. Despite the low adsorption capacity of the soil, the soil colloids contained enough PFAS to increase the PFAS

concentration in pore water significantly. The removal of colloids significantly decreased PFAS concentration, indicating studies that had not accounted for colloids might have underestimated PFAS concentration in the samples. Thus, PFAS should be desorbed from colloids before analysis to estimate the true concentration of PFAS in eluted water, particularly in specific conditions where colloid concentration may be high.

Dry-wet and freeze-thaw cycles increase the transport of colloid-associated PFAS in the subsurface: Leaching of PFOA from subsurface soil increased when the soil was subjected to natural dry-wet or freeze-thaw cycles. An increase in PFOA release coincided with the release of soil colloids, indicating colloid release can be a significant pathway for PFOA release from the source zone. In this study, nearly 36% of PFOA in water samples was attributed to colloids. Thus, conceptual site models should account for the effect of natural weather cycles on the leaching of PFOA from the subsurface and the concentration of colloid-bound PFOA in water samples.

Injection of PDADMAC regenerates and improves the PFAS removal capacity of biofilters: This study showed that injecting cationic polymers such as PDADMAC not only replenished exhausted PFAS adsorption sites but also increased PFAS adsorption, especially short-chain PFAS adsorption, through electrostatic interactions. Moreover, PDADMAC injection reduced the rate at which the biofilters clogged when loaded with suspended sediments. Therefore, injecting cationic polymers into stormwater biofilters can be a viable method to create stormwater biofilters with regenerative PFAS removal properties.

Natural aging of stormwater biofilters by heavy metals regenerates their pathogen removal capacity: The study shows that aging with co-contaminants such as heavy metals, which occur naturally, could have a net positive effect on the long-term removal of *E. coli* in biofilters. Biofilters amended with ESCS aggregates could adsorb significant amounts of metals such as Pb, Cu, and Zn from stormwater and decrease the net negative surface charge on ESCS media, and these changes increased *E. coli* removal. Adsorbed metals inactivated *E. coli* by damaging the cell walls. This enhanced adsorption and inactivation of *E. coli* cells enabled the aged ESCS media to exhaust at a much slower rate than the unaged ESCS media. Thus, filter media aging with metals should be considered in predicting the long-term pathogen removal in biofilters.

7.2. Recommendations for future research

Effect of PDADMAC injection on biofilter microbiome: PDADMAC is toxic to most microorganisms (Tran et al., 2015); however, certain bacteria such as *Bacillus subtilis* can grow in the presence of PDADMAC (John, 2008). Since *Bacillus subtilis* is involved in nitrogen fixation, it may oxidize the nitrogen in PDADMAC to form nitrate or nitrites. A previous study (SERDP report) found that microorganisms isolated from aquifer material excavated from a DoD contaminated site did not degrade PDADMAC but microbial community isolated from activated sludge did, indicating the microorganisms found in wastewater could degrade PDADMAC. Thus stormwater biofilters in cities where combine-sewer outflow could introduce this microorganism could degrade PDADMAC applied on biofilters. Nevertheless, to date, no study has examined the potential of microbial communities to degrade PDADMAC in stormwater biofilters or if the addition of PDADMAC could change the microbial activity or functions in stormwater biofilters.

Effect of heavy metal exposure on the co-selection of antibiotic resistance genes in stormwater biofilters: Although Chapter 6 showed that exposure to heavy metals can reduce *E. coli* growth in biofilters when exposed to 4 and 7 days of drying, longer periods of drying can increase the growth of the *E. coli* even in the presence of heavy metals. This is due to the growth of heavy metal-resistant bacteria by the heavy metals in the adsorbents (Rensing et al., 2000, 1997). Certain *E. coli* cells have genes such as the *copA* and the *zntA* genes which protect the microbes against heavy metal toxicity. Since heavy metals also co-select for antibiotic resistance genes as well, this could lead to greater expression of heavy metal and antibiotic resistance genes (ARGs) in the biofilter media (Seiler and Berendonk, 2012). Additionally, freezing conditions will concentrate heavy metals and pathogens in the pore water into a thin film of liquid between subsurface soil and ice by solute exclusion which will significantly increase the exposure of the pathogens to heavy metals, increasing the concentration of heavy metal and antibiotic resistance genes (DeGrandpre et al., 2021). However, the effect of heavy metal exposure on the expression of ARG in the biofilters has not been adequately explored.

7.3. References

DeGrandpre, E.L., DeGrandpre, M.D., Colman, B.P., Valett, H.M., 2021. Observations of River Solute Concentrations during Ice Formation. ACS EST Water 1, 1695–1701. https://doi.org/10.1021/acsestwater.1c00064

John, W., 2008. Synthesis, properties and analysis of polydadmac for water purification (Thesis). Stellenbosch : Stellenbosch University.

Rensing, C., Fan, B., Sharma, R., Mitra, B., Rosen, B.P., 2000. CopA: An Escherichia coli Cu(I)-translocating P-type ATPase. PNAS 97, 652–656. https://doi.org/10.1073/pnas.97.2.652

Rensing, C., Mitra, B., Rosen, B.P., 1997. The zntA gene of Escherichia coli encodes a Zn(II)-translocating P-type ATPase. Proc Natl Acad Sci U S A 94, 14326–14331.

Seiler, C., Berendonk, T., 2012. Heavy metal driven co-selection of antibiotic resistance in soil and water bodies impacted by agriculture and aquaculture. Frontiers in Microbiology 3, 399. https://doi.org/10.3389/fmicb.2012.00399

Tran, P.L., Hamood, A.N., de Souza, A., Schultz, G., Liesenfeld, B., Mehta, D., Reid, T.W., 2015. A study on the ability of quaternary ammonium groups attached to a polyurethane foam wound dressing to inhibit bacterial attachment and biofilm formation. Wound Repair and Regeneration 23, 74–81. https://doi.org/10.1111/wrr.12244